Discrete Dynamics in Nature and Society

Fintech and Financial Risk Analysis in the Era of Big Data

Lead Guest Editor: Dehua Shen
Guest Editors: Xiao Li, Xiong Xiong, and Silvano Cincotti

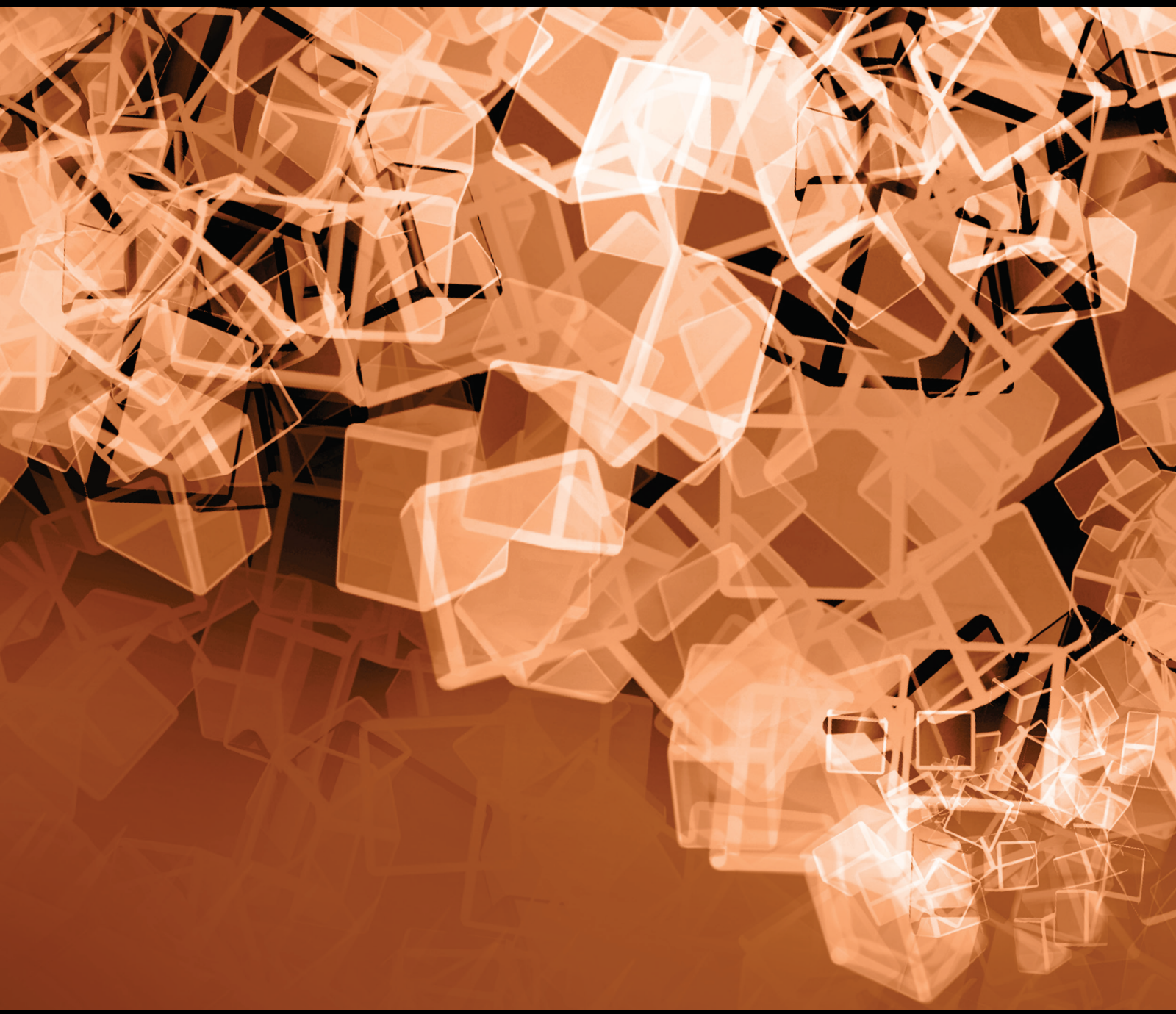

Fintech and Financial Risk Analysis in the Era of Big Data

Discrete Dynamics in Nature and Society

Fintech and Financial Risk Analysis in the Era of Big Data

Lead Guest Editor: Dehua Shen
Guest Editors: Xiao Li, Xiong Xiong, and Silvano Cincotti

Contents

A Time-Varying Multivariate Noncentral Contaminated Normal Copula Model and Its Application to the Visualized Dependence Analysis of Hong Kong Stock Markets

Zhenyu Xiao, Jie Wang, Teng Yuan Cheng, and Kuiran Shi

Research Article (23 pages), Article ID 9673623, Volume 2020 (2020)

Hindawi
Discrete Dynamics in Nature and Society
Volume 2021, Article ID 5595099, 21 pages
https://doi.org/10.1155/2021/5595099

Research Article

The Determinants of the Nondefaultable Spreads of Corporate Bonds: Evidence from China

Baochen Yang, Zijian Wu, and Yunpeng Su

College of Management and Economics, Tianjin University, Tianjin 300072, China

Correspondence should be addressed to Zijian Wu; zjwu@tju.edu.cn and Yunpeng Su; ypsu@tju.edu.cn

Received 5 February 2021; Accepted 19 June 2021; Published 1 July 2021

Academic Editor: Xiao Li

This study investigates the factors impacting the price difference between the interbank market and the exchange market for the same bond using a large transaction dataset from July 2006 to June 2016 in China. We find that market liquidity and macrofactors mainly affect the price difference between the two markets for the same bond. And individual bond liquidity explains only a small part of the price difference. We also find that the interaction between liquidity and credit risk is an important factor affecting the price difference, and the effect is greater during financial crisis.

1. Introduction

The value of China's bond market exceeded 91 trillion yuan in issues by the end of May 2019, making it the world's second-largest bond market after that of the US. China's corporate bond market is divided into an interbank market and an exchange market. In the interbank bond market, commercial banks, insurance companies, security companies, and other financial institutions buy, sell, and repurchase bonds. Participants in this bond market make inquiries to close deals with selected counterparties. On the contrary, the exchange bond market is dominated by nonbank financial institutions and individuals. Bond trading in the exchange market, such as stock trading, is conducted by many investors bidding together and negotiated by actuarial institutions.

There are two types of corporate bonds in China. One type is issued by a department of the central government or a state-owned enterprise, while the other is issued by listed companies. The first corporate bond type is traded on both the exchange market and the interbank market, whereas the second type of corporate bond is traded only on the exchange market. The first type was issued earlier and is larger in size than the second type.

China's corporate bond market began to sprout as early as the 1980s. Since then, China has transitioned from a planned economy to a market economy. In August 1993, the "corporate bond management regulations" were promulgated by the State Council, and the first type of corporate bond began to be issued. The regulations require issuers raising funds for the construction of large- and medium-sized projects in China to declare an issue of at least 1 billion yuan. From the beginning of 2006, the first type of corporate bonds grew rapidly. By the end of 2015, the first type of corporate bond issuance had grown in value to reach 16.82 trillion yuan (Chinese monetary unit), and the volume of transactions had reached 675.13 trillion yuan. By comparison, the second type of corporate bonds started late. On August 14, 2007, "the company's bond issuance pilot approach" was promulgated by China Securities Regulatory Commission, and on September 24, 2007, the 07 Yangtze Power bond was issued for the first time. The two types of corporate bonds are fixed-income securities based on an enterprise's credit and are important channels for the enterprise to raise funds directly from the public.

Most of the first type of corporate bonds in China is each traded simultaneously in both the interbank market and the exchange market. However, there are price differences when the same bond is traded in the two markets at the same time. The price difference for the same bond equals the difference in the spread between them, because the same Treasury interest rate for the same bond in both markets is subtracted

when calculating the spreads. Through detailed descriptive statistics about the pricing difference between the two markets, we find mean is 0.46% and standard deviation is 0.49%, as is shown in Figure 1. What causes the price difference? Some scholars analyze the investor structure of the two markets and argue that the different types of participants in the two markets result in different compensation for liquidity.

We adopt a different approach. From the perspective of individual bonds, we investigate the factors impacting the liquidity on bond spreads from different dimensions, including trading activity and price shocks, using a large transaction dataset for a 10-year period in China. Moreover, we introduce stock market liquidity and macrofactors and find that both of them affect bond spreads. Our study also finds that interaction between credit risk and liquidity is an important factor influencing bond spreads, and this effect is greater during financial crisis. Specifically, we investigate a large transaction dataset from July 2006 to June 2016, including the monthly data of 3716 bonds in China's bond market. We identify 1224 individual bonds that are traded simultaneously in the exchange market and the interbank market. Our sample includes the 2007-2008 crisis period and contains more comprehensive information from China's corporate bond market. We consider structural differences between the interbank market and the exchange bond market.

This study aims to provide a deeper understanding of the influencing factors of the price difference of the two markets for the same bond in China. Our research contributes to the literature in four ways.

First, we select corporate bonds traded simultaneously in both the interbank market and the exchange market as the sample and take the difference between the prices of the two markets for the same bond to eliminate the effect of credit risk on spreads. Scholars mainly adopt two methods when studying the influencing factors of spreads. The first category is based on the principle that credit risk proxies are controlled [1–4]. The second category is based on the principle of taking price differences between bonds with similar credit characteristics so that the credit risk component is approximately separated from spreads [5, 6]. Longstaff et al. [6] strip the credit risk and extract liquidity risk by using the residual in the credit default swap market. Helwege et al. [5] investigate the nondefault spread by using matched pairs of bonds based on Crabbe and Turner [7] and Dick-Nielsen et al. [1]. Our sample comprises the same bonds traded in both markets, and thus, each same bond has the same credit risk. Our method of eliminating the effect of credit risk on spreads is more accurate and reliable than those used in the existing literature.

Second, we decompose yield spreads into three parts: a liquidity component, a credit risk component, and the interaction between liquidity and credit risk, and our finding that the interaction between liquidity and credit risk significantly affects spreads is in line with that of Rossi [8]. Moreover, we study temporal effect of the interaction between liquidity and credit risk on bond spreads, especially during the global financial crisis of 2008/2009.

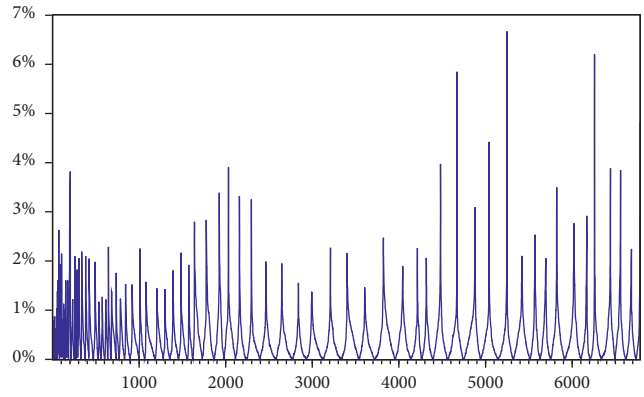

Figure 1: The price differences between the interbank market and the exchange market in China.

Third, we study the influence of bond market liquidity and stock market liquidity on spreads from the two dimensions of trading activity and price shocks. The effects of individual bond liquidity and market-level liquidity on bond spreads are compared.

Finally, we study the influence of macrofactors on the price difference of the two markets for the same bond. We use several macrovariables to explain the price differences, including inflation; GDP; monetary policy; the difference between the 10-year treasury rate, the 2-year treasury rate, and the 3-month treasury rate; and the spread between the bond market index yield and the 10-year Treasury rate.

Our main findings are as follows: market liquidity and macrofactors mainly affect the price difference between the two markets for the same bond. Stock market information can significantly explain the price difference, and the stock market has liquidity spillover effects on the bond market. Similar results are obtained by Chordia et al. [9] and Goyenko and Ukhov [10]. And individual bond liquidity explains only a small part of the price difference. The interaction between liquidity and credit risk is an important factor affecting the price difference, and the effect is greater during financial crisis.

Overall, our research provides new channels to explain the price difference of the two markets for the same bond at the same time, which is of great significance to bond pricing and risk hedging.

The rest of this paper is organized as follows. Section 2 presents a literature review. Section 3 provides the empirical model. Section 4 describes the variables, data, and sample. Section 5 elaborates on the empirical results. Section 6 outlines the results of the robustness tests. Section 7 analyzes the timing characteristics of the interaction between liquidity and credit risk. Finally, Section 8 concludes.

2. Literature Review

Many scholars have studied the impact of corporate bond spreads on different aspects, including individual liquidity, market-level liquidity, and macrofactors [11–15]. It is well documented that corporate bond spreads are explained by individual liquidity [16–24]. Roll [23] shows that under

certain assumptions, the percentage bid-ask spread of corporate bonds is double the square root of the minus covariance between consecutive returns. Amihud [16] constructs a proxy of illiquidity measure based on the theoretical model of Kyle [25], while Downing et al. [21] construct range of bond prices as a liquidity measure. Ren and Li [26] construct the pricing model of defaultable bonds under the influence of liquidity risk and find that the term structure of bond spreads is very sensitive to liquidity risk. Chen et al. [18] use zero trading days to measure liquidity. Helwege et al. [5] use many liquidity proxies to explain corporate bond spreads, including efficient individual liquidity measures.

With regard to the impact of market-level liquidity on corporate bond spreads, Brockman and Chung [27] show that commonality in liquidity includes both market and industry components. Comerton-Forde et al. [28] find that aggregate market-level and specialist firm-level spreads widen when specialists have large positions or lose money. Helwege et al. [5] use a regression model to test whether market-level liquidity measures help to explain the differences in bond spreads and find that they significantly improve explanatory power. Ji and Cao [29] find that spreads more reflect market liquidity premium rather than credit risk premium. Bongaerts et al. [30] find that the liquidity level and exposure to equity market liquidity risk affect expected bond returns, while exposure to corporate bond liquidity shocks carries an economically negligible risk premium. These studies provide evidence supporting the impact of market liquidity on corporate bond spreads. This impact cannot be ignored, because there is a systematic liquidity factor that affects corporate bond spreads by affecting market liquidity. Many scholars have found evidence of systematic liquidity factors [9, 31–36]. Chordia et al. [9] provide evidence of a systematic liquidity factor in the bond market and find that this is related to a contemporaneous systematic liquidity factor of the stock market. Brockman et al. [31] find that a systematic liquidity factor exists in the stock market. Mancini et al. [36] conclude that there is a systematic liquidity factor in the foreign exchange market, which is linked to equity market liquidity. In addition, several works in the literature provide evidence on whether the systematic liquidity risk is priced [33, 37–40]. Pástor and Stambaugh [39]; Acharya and Pedersen [37]; and Sadka [40] demonstrate that a premium of systematic liquidity risk exists. Sadka [40] provides evidence that the shocks of systematic liquidity are persistent.

The third category focuses on the causal relationship between macrofactors and corporate bond spreads. Küçük [41] studies the effects of macroeconomic variables on the nondefault component of emerging market yield spreads. Han and Zhou [42] focus on the linkage between the nondefaulting component and the macroeconomic conditions. Guo et al. [43] find that monetary policy have a more significant effect on spreads for medium-to-long-term corporate bond but have little impact on the short term. Ludvigson and Ng [44] investigate the linkages between macrofactors and bond risk premia. Vodova [45] find that monetary policy negatively impacts market liquidity. Valla et al. [46]; Dinger [47]; and Vodova [45] find a negative impact of GDP on market liquidity. In addition, Moussa [48] finds that inflation and market liquidity are closely correlated. See also Singh and Sharma [49], who propose that macrofactors affect corporate bond spreads by affecting market liquidity.

Some scholars eliminate the credit risk component in order to further study the influence of the nondefault component on spreads. In this regard, two major approaches are adopted. The first is based on the principle of controlling the credit risk component [1–4]. Longstaff [2] investigates the impact of liquidity on the spreads between Treasury and Refcorp bonds by controlling credit risk. Dick-Nielsen et al. [1] investigate the contribution of illiquidity to corporate bond spreads by controlling credit risk and bond characteristics. Shin and Kim [3] use a similar approach to study the impact of liquidity on yield spreads. These works reflect the principle of controlling credit risk. The second approach is based on the principle of approximately separating out the credit risk component from the bond spreads [5, 11]. Instead of credit controls, Dick-Nielsen et al. [1] run regressions on a matched sample of corporate bonds using pairs of bonds issued by the same firm with maturity close to each other. Helwege et al. [5] separate out the credit risk component by examining bonds that are issued by the same firm and examine the effects of liquidity in a sample of bond pairs. Ejsing et al. [11] extract liquidity premia and estimate liquidity and credit premia as latent factors in a state-space framework.

Several studies discuss the effect of liquidity and credit risk on bond spreads [50–52]. In fact, the previous literature regarding the above tends to focus on how liquidity or the credit component contributes to yield spreads independently. Thus, these works tend to overlook whether an interaction between liquidity and credit risk exists. Duffie and Singleton [51] allow for liquidity effects by introducing a stochastic process as the fractional carrying cost of the defaultable instrument. Ericsson and Renault [52] investigate the interaction between liquidity and credit risk in theory and establish the existence of a credit component, a liquidity component, and an interaction term. He and Xiong [53] develop a theoretical model to analyze the interaction between debt market liquidity and credit risk through so-called rollover risk. He and Milbradt [54] show that corporate default decisions interact with endogenous secondary market liquidity via the rollover channel. Wang and Wu [55] study the relation between trading variables and price volatility and find strong evidence of a significant interactive effect of liquidity and credit risk, magnifying during the financial crisis period. Sperna Weiland et al. [56] propose a novel way of modeling credit-liquidity interactions through mutually exciting processes and find that, on average, the credit-induced liquidity component accounts for 8% to 17% of total yield spreads, but in the most distressed periods, it can account for more than 40%. Chen et al. [50] develop a structural credit risk model to examine how the interactions of liquidity and default risk affect corporate bond pricing.

Most of these studies discuss the impact of the interaction term on corporate bond spreads by focusing on a

theoretical model, whereas this study investigates the impact of the interaction term on the nondefault spread by separating out the credit risk component from the bond spreads through different empirical methods. Our empirical analysis reveals the impact of the interaction term on the nondefault spread in China's corporate bond market. We provide evidence of the impact of the interaction between liquidity and credit risk on the nondefault spread from the cross-market perspective. Several studies show that the bond market and stock market have liquidity spillover effects [9, 57, 58]. Chordia et al. [9] investigate liquidity movements in Treasury bond and stock markets over a period of more than 1800 trading days and find that bond and stock market liquidity are significantly correlated. Goyenko and Ukhov [10] provide evidence of liquidity linkage between bond and stock markets. They propose that stock market liquidity affects the bond market. Dimic et al. [57] find that time-varying stock-bond correlation patterns vary significantly between the time horizons. However, Chordia et al. [9]; Goyenko and Ukhov [10]; and Dimic et al. [57] do not consider the interaction between liquidity and credit risk. We investigate the impact of the interaction between liquidity and credit risk on the nondefault spread from different liquidity dimensions of bond market liquidity and stock market liquidity. Our results show that the nondefault spread can be significantly explained by the interaction between liquidity and credit risk considering stock market liquidity bond market liquidity.

In summary, the previous literature provides an important foundation for this study. Few of above research study price difference between the interbank market and the exchange market, which will be studied in this paper.

3. Model

Referring to Helwege et al. [5] and Dick-Nielsen et al. [1], we select corporate bonds traded simultaneously in both the interbank market and the exchange market and take the difference between the prices of the two markets for the same bond to eliminate the effect of credit risk on spreads accurately. We study the determinants of the price difference of the two markets for the same bond in China's corporate bond market. Equation (1) presents a new model, which eliminates the credit risk:

$$\text{Price\_dif}_{jt} = \alpha_0 + \alpha_1 \times \text{Liq\_dif}_{jt} + \alpha_4 \times \text{Inter\_dif}_{jt} + \varepsilon_{jt}. \tag{1}$$

In equation (1), Price_dif_{jt} is the difference between the exchange market and the interbank market in price of the individual bond, which is equal to spread difference. And Liq_dif_{jt} is the difference between the exchange market and the interbank market in liquidity of the individual bond. Inter_dif_{jt} is the difference between the exchange market and the interbank market in the interaction between liquidity and credit risk of the individual bond.

Equations (2)–(4) present new models that include market-level liquidity and macrofactors:

$$\text{Price\_dif}_{jt} = \alpha_0 + \alpha_1 \times \text{Liq\_dif}_{jt} + \alpha_2 \times \text{Mar\_liq}_{jt} + \alpha_4 \times \text{Inter\_dif}_{jt} + \varepsilon_{jt}, \tag{2}$$

$$\text{Price\_dif}_{jt} = \alpha_0 + \alpha_1 \times \text{Liq\_dif}_{jt} + \alpha_3 \times \text{Mac}_{jt} + \alpha_4 \times \text{Inter\_dif}_{jt} + \varepsilon_{jt}, \tag{3}$$

$$\text{Price\_dif}_{jt} = \alpha_0 + \alpha_1 \times \text{Liq\_dif}_{jt} + \alpha_2 \times \text{Mar\_liq}_{jt} + \alpha_3 \times \text{Mac}_{jt} + \alpha_4 \times \text{Inter\_dif}_{jt} + \varepsilon_{jt}. \tag{4}$$

Mar_liq_{jt} are the market-level liquidity proxies, and Mac_{jt} are the macrofactor proxies.

4. Variables, Data, and Sample

4.1. Liquidity and Credit Proxies. Referring to Shin and Kim [3], we choose the following five liquidity measures in order to comprehensively measure the liquidity premium: Turnover, Vol, Day, Amihud, and Range. Turnover, the frequency with which market assets trade in a certain period, is one of the most important proxies to reflect trading activity of the market. Vol is obtained by dividing the total trading volume with the number of months during which the issue is traded. Day is defined as the number of trading days in the corresponding month. If the number of trading days is larger, the bond is more active. Amihud [16] constructs a proxy of illiquidity measure based on the theoretical model of Kyle [25]. Following the Amihud measure, this study constructs Amihud, a monthly illiquidity measure to describe liquidity. It also constructs Range, one of the illiquidity measures used by Downing et al. [21]. Amihud and Range describe the liquidity measure of the price shocks' impact dimension.

In this study, two credit risk variables are considered as explanatory variables, Rating and Coupon. Rating is the credit rating assigned to each bond. Our study adopts the coding method of Covitz and Downing [19] and Shin and Kim [3] for credit ratings: AAA = 1, AA+ = 2, . . ., and C = 14. This study assigns the credit rating of bonds below C to 15. In this way, we can quantify the credit level of the bond. Coupon refers to the coupon rate of the individual bond. Longstaff et al. [6] provide evidence that coupon is a proxy of the nondefaulting component of bond yield spreads and find that the coefficient of coupon is significant at least at the level of 10%. Bharath and Shumway [59] provide the results of

regressing bond spreads on coupon and find that coupon has a significantly positive correlation with bond spreads. See also Chen et al. [60] and Lin et al. [61].

4.2. Data and Sample Description. This study uses a sample of corporate bonds in the WIND database from July 2006 to June 2016. This study collects data on bond liquidity and credit risk from the WIND database, and bonds without transactions are removed. When bonds have less than 1 year's remaining trading time, they are often eliminated [5]. Thus, the corresponding observations are eliminated from the sample.

This study identifies 1224 individual bonds traded simultaneously in the exchange market and the interbank market in China as the sample. In addition, this study collects data for the trading volume, trading days, yield-to-maturity, highest price, lowest price, average price, remaining life, age, credit rating, coupon rate, and historical price, and the proxies of liquidity and credit risk are calculated based on the above data. This study calculates the differences of liquidity proxies. We calculate the price difference of the two markets for the same bond and analyze its determinants in China's corporate bond market.

4.3. Summary Statistics. The summary statistics for the variables and the bond characteristics of the sample used in this study are summarized in Table 1.

4.4. Pairwise Correlation Test. Table 2 shows the pairwise correlation coefficients between liquidity proxies and summarizes the differences in liquidity measures.

Bond trading activity can represent the level of liquidity of bonds. Turnover, Vol, and Day are the liquidity proxies of the bond transaction. Therefore, we need to investigate the degree of correlation between them. As confirmed from Panel A of Table 2, Turnover and Vol are highly positively correlated, with a correlation coefficient of 0.8724, while Turnover and Day seem to be quite weakly correlated, as are Vol and Day. The reason is that if the trading volume of the bond is high, the number of investments involved is large, and thus, turnover is also large in China's corporate bond market. However, trading days are determined by the market structure, for example, there are fewer trading days in the interbank market, which comprises more institutional investors than the exchange market. Similar to Panel A, in Panel B, Turnover_diff and Vol_diff are highly positively correlated, with a correlation coefficient of 0.8661. Turnover_diff and Day_diff have a very weak correlation, with a correlation coefficient of 0.2082, while the correlation coefficient of Vol_diff and Day_diff is only slightly larger at 0.2555. Amihud and Range are often used to measure the impact of trading volume on prices and are commonly used as liquidity proxies. In Table 2, Amihud is positively correlated with Range, with a correlation coefficient of 0.8343, and Amihud_diff and Range_diff are also highly positively correlated, with a correlation coefficient of 0.8307. This shows that Amihud and Range are highly correlated. Furthermore, in Panel B, Turnover_diff and Vol_diff have the highest correlation, with a correlation coefficient of 0.8661, while the correlation of Vol_diff and Range_diff is lowest, with a correlation coefficient of −0.0862.

5. Empirical Results

5.1. Summary Statistics of Liquidity Differences. This study extracts the nondefault spread, which includes the liquidity component and the interaction between liquidity and credit risk, by calculating the individual bond price difference between the exchange market and the interbank market and then analyzes its determinants. By establishing a regression model of the liquidity difference and spread difference, this study investigates the impact of liquidity on the nondefault spread. Summary statistics of liquidity differences are given in Table 3.

5.2. Impact of the Interaction between Liquidity and Credit Risk on Spreads. Our results show that individual liquidity proxies have a significant effect on the price difference of the two markets for the same bond. In Tables 4 and 5, the credit risk is eliminated, and the interaction between liquidity and credit risk is taken into account to study the marginal impact of liquidity proxies on spreads, respectively. To investigate the impact of liquidity, each regression is estimated using only one measure of liquidity and the interaction between liquidity and credit risk is controlled. Vol_diff, Day_diff, and Range_diff are used to represent individual liquidity difference, while the cross-terms represent the interaction between liquidity and credit risk, which cannot be removed due to their nonlinear functional relationship. Table 4 shows the estimated effects of liquidity on bond spreads and regressions using the Spread_dif as the dependent variable, including the subsamples and the full sample. We test all the error terms in the regressions in the paper and find that the error terms of the regression equations are normally distributed and stationary, in line with the basic assumptions of the regression model.

The results show that there is a significant interaction between liquidity and credit risk. In the full sample of Tables 4 and 5, the coefficients of the liquidity measures are smaller when credit risk is completely controlled. The estimated effects of liquidity in Table 5 are nearly always lower than those in Table 4. The reason is that the liquidity proxy explains the components of credit risk, which shows that there is a significant interaction between liquidity and credit risk. Similar results can be found from Vol and Day. In Tables 4 and 5, the coefficient of Vol decreases from −0.0018 to −0.0012, while the coefficient of Day decreases from 0.1596 to 0.0647 in the full sample. Similar results are found in the subsamples of high rating bonds and low rating bonds in Tables 4 and 5. The coefficients of the liquidity measures in Table 5 are smaller than those in Table 4. For example, the coefficient of Vol drops from −0.0022 to −0.0010 in the high rating bonds of Tables 4 and 5 while it declines from −0.0015 to −0.0014 in the low rating bonds. The coefficient of Day drops from 0.0809 to 0.0529 in the high rating bonds of

Table 1: Summary statistics of bonds in the sample.

	Mean	Median	Maximum	Minimum	Std. dev.	Jarque–Bera	Probability	Observations
Spread	2.7281	2.6652	35.5890	0.0506	1.1285	2479641.0000	0.01	13722
Turnover	0.0724	0.0311	2.1587	0.0001	0.1204	934967.7000	0.01	13722
Vol	79.2567	36.6094	2810.1350	0.0102	125.5374	1289959.0000	0.01	13722
Day	4.6155	2.0000	23.0000	1.0000	5.3099	11975.5100	0.01	13722
Amihud	0.0153	0.0004	3.5210	0.0001	0.1019	106000000.0000	0.01	13722
Range	0.0256	0.0006	5.6814	0.0001	0.1602	108000000.0000	0.01	13722
Time-to-Maturity	5.1315	5.1808	17.1973	1.0685	1.6668	4235.8130	0.01	13722
Age	2.1097	1.8603	12.5890	0.0932	1.3961	5600.3490	0.01	13722
Coupon	7.0229	7.0000	9.1000	3.5000	0.9200	259.2570	0.01	13722
Rating	3.4575	4.0000	15.0000	1.0000	1.2309	219525.1000	0.01	13722

Spread is the difference between the yield-to-maturity on the corporate bond and the corresponding Treasury rate. Turnover is the frequency of market assets traded in a certain period of time, and the calculation method is the ratio of the trading volume and the circulation market value. Vol is the average of the total trading volume (yuan), and Day is the number of trading days in the corresponding month. Amihud and Range are illiquidity measures. Time-to-Maturity denotes the remaining years of the bond. Age denotes years since issuance. Coupon is the annual coupon interest. Rating is the credit rating of each bond. The sample period is July 2006 to June 2016, and the sample includes 1224 bonds.

Table 2: Pairwise correlations between liquidity proxies.

	Turnover	Vol	Day	Amihud	Range
Panel A: liquidity proxies					
Turnover	1.0000				
Vol	0.8724	1.0000			
Day	0.0238	0.0249	1.0000		
Amihud	−0.0880	−0.0925	−0.0344	1.0000	
Range	−0.0941	−0.0989	−0.0172	0.8343	1.0000
	Turnover_diff	Vol_diff	Day_diff	Amihud_diff	Range_diff
Panel B: differences in liquidity measures					
Turnover_diff	1.0000				
Vol_diff	0.8661	1.0000			
Day_diff	0.2082	0.2555	1.0000		
Amihud_diff	−0.1425	−0.1052	−0.1270	1.0000	
Range_diff	−0.1205	−0.0862	−0.1096	0.8307	1.0000

For Panel A, the meanings of liquidity proxies are shown in Table 1. For Panel B, the variables are the differences between the exchange market and the interbank market for the corresponding variables of individual bonds. The sample period is July 2006 to June 2016; the sample includes 1224 bonds.

Table 3: Summary statistics of differences in liquidity measures.

Variable	Mean	Median	Maximum	Minimum	Std. dev.	Jarque–Bera	Probability	Observations
Panel A: all bonds								
Turnover_diff	−0.0972	−0.0568	0.6881	−2.1164	0.1529	164007.4000	0.01	6784
Vol_diff	−106.2037	−63.5312	527.2476	−2808.4630	158.4403	283567.2000	0.01	6784
Day_diff	4.9148	2.0000	22.0000	−12.0000	6.4997	964.8958	0.01	6784
Amihud_diff	0.0294	0.0012	3.5206	−0.2771	0.1424	13802006.0000	0.01	6784
Range_diff	0.0498	0.0025	5.6514	−0.1763	0.2239	14038398.0000	0.01	6784
Panel B: high rating bonds								
Turnover_diff	−0.0749	−0.0435	0.3059	−1.4227	0.1211	44359.4900	0.01	2185
Vol_diff	−96.0034	−57.8675	392.7113	−2808.4630	148.9268	318762.9000	0.01	2185
Day_diff	4.6691	2.0000	22.0000	−11.0000	6.2821	392.0431	0.01	2185
Amihud_diff	0.0239	0.0009	3.3447	−0.0378	0.1382	7660864.0000	0.01	2185
Range_diff	0.0430	0.0018	4.8422	−0.0393	0.2170	5477773.0000	0.01	2185
Panel C: low rating bonds								
Turnover_diff	−0.1079	−0.0648	0.6881	−2.1164	0.1649	97938.2000	0.01	4599
Vol_diff	−111.0498	−67.0638	527.2476	−2526.0090	162.5571	96771.0800	0.01	4599
Day_diff	5.0315	3.0000	22.0000	−12.0000	6.5980	592.4450	0.01	4599
Amihud_diff	0.0320	0.0015	3.5206	−0.2771	0.1443	7172313.0000	0.01	4599
Range_diff	0.0530	0.0028	5.6514	−0.1763	0.2270	8748478.0000	0.01	4599

The table shows the summary statistics for variables used in the study. The meanings of liquidity proxies are shown in Tables 1 and 2. The sample period is July 2006 to June 2016.

Table 4: Marginal impact of liquidity proxies on bond spreads.

	Vol	Day	Range	Vol × coupon	Day × coupon	Range × coupon
High rating	−0.0022***	0.0809***	−0.1267	0.0003***	−0.0045*	0.0387
	(−3.06)	(4.51)	(−0.26)	(2.93)	(−1.82)	(0.52)
Low rating	−0.0015**	0.2109***	1.4225**	0.0002*	−0.0197***	−0.1700**
	(−1.98)	(11.55)	(2.26)	(1.83)	(−8.06)	(−1.97)
Full sample	−0.0018***	0.1596***	0.5125	0.0002***	−0.0132***	−0.0461
	(−3.41)	(12.03)	(1.34)	(3.02)	(−7.37)	(−0.85)

The table shows the marginal impact of liquidity proxies on bond spreads, for the full sample, the subsample of high rating bonds, and the subsample of low rating bonds. Bond spreads are regressed directly on each liquidity proxy by controlling credit risk and interaction. The meanings of liquidity proxies are shown in Tables 1 and 2. The cross-terms are interactions. The sample period is July 2006 to June 2016. The t-statistics are given in parentheses, and *, **, and *** represent significance at the 10%, 5%, and 1% level, respectively.

Table 5: Marginal impact of liquidity proxies on the nondefault spread based on equation (1).

	Vol_diff	Day_diff	Range_diff	Vol_diff × coupon	Day_diff × coupon	Range_diff × coupon
High rating	−0.0010**	0.0529***	0.1678	0.0001**	−0.0075***	−0.0149
	(−2.15)	(4.75)	(0.52)	(2.11)	(−4.92)	(−0.30)
Low rating	−0.0014**	0.0764***	0.4507	0.0002**	−0.0099***	−0.0473
	(−2.36)	(5.28)	(0.87)	(2.07)	(−5.21)	(−0.66)
Full sample	−0.0012***	0.0647***	0.2682	0.0001***	−0.0086***	−0.025
	(−2.93)	(6.71)	(0.91)	(2.62)	(−6.71)	(−0.60)
Adj-R^2 (%)	0.2387	0.7718	0.1243	0.2406	0.7978	0.1445

The table shows the marginal impact of liquidity proxies on the nondefault spread based on equation (1), for the full sample, the subsample of high rating bonds, and the subsample of low rating bonds. The nondefault spread is regressed directly on each liquidity proxy by controlling interaction. The adjusted R-squares for the full sample are reported. The meanings of liquidity proxies are shown in Tables 1 and 2. The cross-terms are interactions. The sample period is July 2006 to June 2016. The t-statistics are given in parentheses, and *, **, and *** represent significance at the 10%, 5%, and 1% level, respectively.

Tables 4 and 5 while it declines from 0.2109 to 0.0764 in the low rating ones. The coefficient of Range is significant at the level of 5% in the low rating bonds in Table 4. According to the empirical results, there is a significant correlation between the nondefault spread and the interaction between liquidity and credit risk. For example, the coefficients of Vol_diff × Coupon and Day_diff × Coupon are significant at the level of 1% in the full sample in Table 5. In conclusion, our empirical results confirm that the interaction between liquidity and credit risk is priced in China's corporate bond market.

As Tables 4 and 5 show, only a small part of the nondefault spread is explained by liquidity proxies, and the interaction between liquidity and credit risk is significantly priced. To investigate these results thoroughly, the related regression results are given in Tables 6 and 7. Regression results without the interaction between liquidity and credit risk are shown in Model 1 of Tables 6 and 7. The regression result of Model 1 in Table 6 shows that the regression coefficient of Vol is significant at the level of 1%, and the sign is in line with expectations, while the regression coefficient of Range is very significant. The regression result of Model 1 in Table 7 gives the impact of liquidity differences on the nondefault spread without considering interaction. It shows that the regression coefficient of Vol_diff is significant at the level of 1%, while the regression coefficient of Range_diff is significant at the level of 10%. In addition, Adj-R^2 of Model 1 in Table 6 is 19.4355%, while Adj-R^2 of Model 1 in Table 7 is only 0.1540%, which shows that a small part of the nondefault spread is explained by liquidity proxies.

The interaction between liquidity and credit risk is considered to examine whether the interaction is priced. In Model 2 of Table 6, the coefficient of Vol × Coupon is very significant, and Adj-R^2 is 19.4831%, which is higher than 19.4355% of Model 1 in Table 6. In Model 2 of Table 7, the significance of the coefficient of Vol_diff × Coupon is 1%, and Adj-R^2 is 0.2406%, which is higher than 0.1540% of Model 1 in Table 7. This shows that the interaction between liquidity and credit risk is significantly priced. The reason is that both liquidity and credit risk are closely related to market factors and macrofactors, and when market conditions change, liquidity and credit risk must comove and induce interaction. Adj-R^2 of Model 2 in Table 6 is much larger than that of Model 2 in Table 7, which indicates that liquidity proxies explain only a small fraction of the nondefault spread. Similar conclusions are obtained in Model 3 of Tables 6 and 7.

Overall, the empirical research in Tables 6 and 7 shows that after the nondefault spread is extracted and interaction is considered, only a small part of the nondefault spread is explained by liquidity proxies, and the nondefault spread may be affected by other important factors.

5.3. Impact of Bond Market Liquidity and Stock Market Liquidity on Spreads. The impact of market liquidity on spreads cannot be ignored, because there is a systematic liquidity factor. Market liquidity affects the nondefault spread by the systematic liquidity factor.

Bond market liquidity and stock market liquidity are taken into account as market liquidity factors. This study

Table 6: Impact of liquidity proxies on bond spreads for the full sample.

Model	C	Vol	Day	Range	Vol × coupon	Day × coupon	Range × coupon	Adj-R^2 (%)
1	−0.1002	−0.0003***	0.0633***	0.1523***				19.4355
	(−1.49)	(−3.54)	(32.38)	(2.77)				
2	0.0268	−0.0019***	0.0636***	0.1530***	0.0002***			19.4831
	(0.34)	(−3.51)	(32.50)	(2.79)	(3.02)			
3	−0.5341***	−0.0003***	0.1600***	0.1429***		−0.0132***		19.7471
	(−5.97)	(−3.76)	(12.06)	(2.60)		(−7.37)		
4	−0.1094	−0.0003***	0.0632***	0.4717			−0.0461	19.4338
	(−1.60)	(−3.55)	(32.31)	(1.24)			(−0.85)	
5	−0.4169***	−0.0018***	0.1598***	0.3451	0.0002***	−0.0132***	−0.029	19.7878
	(−4.16)	(−3.39)	(12.05)	(0.90)	(2.87)	(−7.34)	(−0.53)	

The table shows the impact of liquidity proxies on bond spreads for the full sample, and bond spreads are regressed on the liquidity proxies by controlling credit risk and interaction. The meanings of liquidity proxies are shown in Tables 1 and 2. The interaction between liquidity and credit risk is represented by the cross-terms. The sample period is July 2006 to June 2016. The t-statistics are given in parentheses, and *, **, and *** represent significance at the 10%, 5%, and 1% level, respectively.

Table 7: Impact of liquidity proxies on the nondefault spread for the full sample based on equation (1).

Model	C	Vol_diff	Day_diff	Range_diff	Vol_diff × coupon	Day_diff × coupon	Range_diff × coupon	Adj-R^2 (%)
1	0.1166***	−0.0002***	0.0003	0.0804*				0.1540
	(7.77)	(−2.95)	(0.21)	(1.86)				
2	0.1214***	−0.0012***	0.0008	0.0824*	0.0001***			0.2406
	(8.04)	(−3.06)	(0.50)	(1.91)	(2.62)			
3	0.1248***	−0.0002***	0.0639***	0.0752*		−0.0086***		0.7978
	(8.32)	(−3.37)	(6.66)	(1.74)		(−6.71)		
4	0.1165***	−0.0002***	0.0003	0.2541			−0.025	0.1445
	(7.77)	(−2.97)	(0.20)	(0.86)			(−0.60)	
5	0.1270***	−0.0007*	0.0616***	0.0416	0.0001	−0.0082***	0.005	0.7942
	(8.41)	(−1.82)	(6.31)	(0.14)	(1.32)	(−6.31)	(0.12)	

The table shows the impact of liquidity proxies on the nondefault spread for the full sample based on equation (1). The nondefault spread is regressed on the liquidity proxies by controlling credit risk and interaction. The meanings of liquidity proxies are shown in Tables 1 and 2. The interaction between liquidity and credit risk is represented by the cross-terms. The sample period is July 2006 to June 2016. The t-statistics are given in parentheses, and *, **, and *** represent significance at the 10%, 5%, and 1% level, respectively.

chooses the liquidity proxies of bond market from two perspectives, transaction activity and price impact, including BML_Vol, BML_Range, and BML_Amihud to investigate the explanatory power of bond market-level liquidity on spreads. BML_Vol is the monthly trading volume of the corporate bond market. BML_Range and BML_ Amihud are illiquidity measures of the corporate bond market based on Range and Amihud, respectively.

Table 8 presents the empirical results. Vol_diff and Range_diff are liquidity differences, and they represent the transaction activity and price impact. Models 1–3 give the basic regression models. Adj-R^2 of the regression equation in Model 3 is 0.1681%. In Models 4–6, the market liquidity proxies are introduced to investigate the impact of market factors on the nondefault spread. In Model 4, the regression coefficient of BML_Vol is significant at the level of 1%, and Adj-R^2 of the regression equation increases from 0.1681% to 0.8264% when the proxy of bond market liquidity is considered. This suggests that bond market liquidity significantly improves the explanatory power of the nondefault spread and is priced. As proxies for liquidity, BML_Vol represents trading activity, while BML_Range and BML_Amihud represent price impact. In Model 6, the regression coefficient of BML_Amihud is significant at the level of 1%, and Adj-R^2 of the regression equation increases from 0.1681% to 0.3251%. This conclusion is similar to that of Model 4.

Considering the spillover and linkage effects between the bond market and stock market, the liquidity of the stock market is used to explain the nondefault spread in Model 7. Vol_diff and Range_diff are used as liquidity proxies, and SML_Range is an illiquidity measure of stock market based on Range. The Adj-R^2 of Model 7 is 0.8503% and increases more than that of Model 3. Similar conclusions are found in Models 8–10. This shows that stock market information can significantly explain the nondefault spread, and the stock market has liquidity spillover effects on the bond market. Similar results are obtained by Chordia et al. [9] and Goyenko and Ukhov [10]. Model 11 shows the regression results containing all liquidity and market liquidity proxies. The coefficient of Vol_diff is significant at the level of 1%, and the signs are in line with expectations. The coefficients of BML_Vol and SML_Range are all significant at the level of 1%, and the Adj-R^2 of Model 11 is 1.2797%. We find that the price difference of the two markets for the same bond is significantly related to stock market liquidity.

Table 8: Impact of market liquidity.

Model	1	2	3	4	5	6	7	8	9	10	11
C	−0.1116***	−0.0958***	−0.1146***	0.1865***	−0.1204***	−0.1744***	−0.0042	0.2120***	−0.0140	−0.0629**	0.0999
	(−9.65)	(−9.72)	(−9.81)	(4.06)	(−8.56)	(−8.29)	(−0.21)	(4.60)	(−0.68)	(−2.37)	(1.50)
Vol_diff	−0.0002***		−0.0002***	−0.0002***	−0.0002***	−0.0002***	−0.0002***	−0.0002***	−0.0002***	−0.0002***	−0.0002***
	(−3.16)		(−2.99)	(−3.58)	(−3.00)	(−3.02)	(−2.97)	(−3.43)	(−2.99)	(−3.00)	(−3.36)
Range_diff		0.0907**	0.0796*	0.0812*	0.0782*	0.0733*	0.0798*	0.0810*	0.0764*	0.0737*	0.0784*
		(2.11)	(1.85)	(1.89)	(1.81)	(1.70)	(1.86)	(1.89)	(1.78)	(1.71)	(1.83)
BML_Vol				−0.0070***				−0.0055***			−0.0045***
				(−6.78)				(−5.20)			(−3.89)
BML_Range					0.1158				0.2905*		−0.6361*
					(0.74)				(1.84)		(−1.79)
BML_Amihud						1.6570***				1.6061***	2.5794**
						(3.42)				(3.32)	(2.28)
SML_Range							−0.5954***	−0.4767***	−0.6203***	−0.5911***	−0.4368***
							(−6.90)	(−5.35)	(−7.11)	(−6.86)	(−4.65)
Adj-R^2 (%)	0.1326	0.0510	0.1681	0.8264	0.1614	0.3251	0.8503	1.2292	0.8849	0.9970	1.2797

The table shows the impact of market liquidity. BML_Vol is the monthly trading volume of the corporate bond market; BML_Range and BML_ Amihud are illiquidity measures of the corporate bond market based on Range and Amihud, respectively. SML_Range is an illiquidity measure of the stock market based on Range. The meanings of the other proxies are shown in Tables 1 and 2. The sample period is July 2006 to June 2016. The t-statistics are given in parentheses, and *, **, and *** represent significance at the 10%, 5%, and 1% level, respectively.

5.4. Impact of Macrofactors on Spreads. Table 9 presents the regression results.

Model 2 considers bond market and stock market liquidity. The coefficients of BML_Vol and SML_Range are significant at the level of 1%, and Adj-R^2 of Model 1 is 1.354%. The regression coefficient of BML_Vol is negative, because bond market liquidity is good and the liquidity premium is small. However, the regression coefficient of SML_Range is negative because of spillover effects between the stock market and bond market. In other words, when stock market liquidity is poor, bond market liquidity is good, and thus, the premium of bond market liquidity is small.

Models 2–7 consider macrovariables to investigate the impact of macrofactors on the price difference of the two markets for the same bond. The following three macrovariables are selected: Year102, Month3, and S10year. Year102 is the difference between the 10-year Treasury rate and the 2-year Treasury rate. Month3 is the 3-month Treasury rate, and S10year is the spread between the bond market index yield and the 10-year Treasury rate. In Models 2–4, the coefficients of Year102, Month3, and S10year are 0.1141, −0.0907, and 0.1276, respectively, at a significance level of 1%, while Adj-R^2 of Model 4 is significantly improved compared with Model 1. This shows that macrofactors have good explanatory power for the price difference of the two markets for the same bond. Similar conclusions are obtained in Models 5–7. CPI, which is the consumer price index, is used to explain the nondefault spread as the proxy of macrofactor; the coefficients of CPI are all significant at the 1% level in Models 8–12. This shows that CPI can explain the nondefault spread well, and macrofactors are the explanatory variables of the nondefault spread. GDP is a good proxy of macrofactors; the empirical results of Model 6 show that the coefficient of GDP is very significant, and Adj-R^2 is also improved compared with Model 1. The circulation of currency, represented by M_0, is an important macrovariable. The empirical result of Model 7 shows that the coefficient of M_0 is very significant, and Adj-R^2 is 1.5476%.

In Model 8, all macrofactors are considered to investigate the impact of macrofactors on spreads. Macrofactors and market factors are all considered in Model 9. In this model, the regression coefficient of Range_diff is not significant, which means that the nondefault spread is not sensitive to illiquidity proxy using extreme values in China's corporate bond market. Range_diff is replaced by Amihud_diff in Models 10–12, and the coefficients of Amihud_diff are very significant. In Model 9, the coefficient of SML_Range is not significant; a similar result is obtained from Model 10. In Model 11, the coefficient of Range_diff is significant at the level of 10%. Because the macrofactors contain stock market information, better liquidity in the stock market will result from, for example, loose monetary policy. In addition, the interaction between liquidity and credit risk is represented by the cross-terms in Models 1–12.

Because macrofactors contain stock market information, SML_Range is removed, and the regression result is given in Model 12. Adj-R^2 of Model 12 is 2.8771%, and is slightly improved, while Adj-R^2 of Model 12 is 17.12 times bigger than that of Model 1, which indicates that the proxies of liquidity explain only a small part of the nondefault spread, and the nondefault spread is also affected by the unknown factors. In other words, a systematic liquidity factor exists, and it affects the liquidity of individual bonds in the bond market.

These empirical results show that market liquidity risk and macro risk factors are the main determinants of the price difference of the two markets for the same bond.

6. Robustness Tests

6.1. Price Impact. To investigate the robustness of our results, a series of robustness tests are performed. Range is replaced by Amihud to investigate the impact of liquidity proxy on the price difference of the two markets for the same bond from the perspective of price impact in Table 10.

In Model 1, the coefficient of Vol is −0.0002 and is significant at the level of 1%, while the regression coefficient of Amihud is also significant at the level of 1%, and the sign is in line with expectations. In Model 2, the coefficient of BML_Vol is significant at the level of 1%, and Adj-R^2 is improved 3.6 times compared with Model 1, which indicates that market liquidity has explanatory power for the nondefault spread. In Model 3, the coefficients of Year102 and S10year are 0.1389 and 0.1521 and are significant at the level of 1%, while the coefficients of Year102, S10year, CPI, GDP, and M_0 are also significant at the level of 1% in Model 4. In addition, Adj-R^2 of Models 3 and 4 is 1.9262% and 2.7850%, respectively and is significantly improved over that of Model 1, which indicates that macrofactors are significant explanatory variables for the nondefault spread, and our empirical results are robust in the Chinese corporate bond market.

Model 5 shows the empirical results including the interaction between liquidity and credit risk. The coefficient of Vol × Coupon is 0.0002 and is significant at the level of 1%, while the coefficient of Day × Coupon is also significant at the level of 5%. Adj-R^2 of Model 5 is greater than that of Model 4, suggesting that the interaction between liquidity and credit risk is significantly priced in the Chinese corporate bond market. In addition, the empirical results of Models 1–5 show that the coefficients of Amihud_diff are all very significant in the Chinese corporate bond market.

6.2. Trading Activity. Trading activity is an important aspect of liquidity, and Turnover is a commonly used measure of liquidity. To investigate the robustness of our results, Vol_diff is replaced by Turnover_diff to investigate the impact of liquidity proxy on the price difference of the two markets for the same bond from the perspective of trading activity in Table 11.

The empirical results of Models 1–5 show that the coefficients of Turnover_diff are all significant at the level of 1%, and the sign is in line with expectations. Adj-R^2 of Model 1 is 0.2989%, while Adj-R^2 of Model 2 is 0.9703%, and the coefficient of BML_Vol is significant at the level of 1%. This indicates that market liquidity has good explanatory power for the nondefault spread, and this result is robust. In Model

Table 9: Impact of macrovariables.

Model	1	2	3	4	5	6	7	8	9	10	11	12
C	0.2153***	0.1716***	0.4121***	0.7383***	0.2056***	0.7311***	0.2094***	0.6477***	1.1909***	1.1874***	1.4116***	1.2038***
	(4.68)	(3.58)	(7.09)	(7.47)	(4.32)	(5.98)	(4.55)	(4.55)	(7.24)	(7.22)	(9.33)	(7.40)
Vol_diff	−0.0014***	−0.0013***	−0.0013***	−0.0013***	−0.0014***	−0.0016***	−0.0015***	−0.0013***	−0.0013***	−0.0013***	−0.0013***	−0.0013***
	(−3.59)	(−3.45)	(−3.44)	(−3.45)	(−3.54)	(−4.01)	(−3.81)	(−3.32)	(−3.43)	(−3.42)	(−3.48)	(−3.42)
Range_diff	0.0821*	0.0794*	0.0788*	0.0735*	0.0815*	0.0818*	0.0866**	0.0750*	0.0682			
	(1.92)	(1.85)	(1.84)	(1.72)	(1.90)	(1.91)	(2.02)	(1.75)	(1.60)			
Amihud_diff										0.1779***	0.1769***	0.1786***
										(2.65)	(2.64)	(2.66)
BML_Vol	−0.0056***	−0.0061***	−0.0061***	−0.0079***	−0.0057***	−0.0056***	−0.0044***		−0.0083***	−0.0083***	−0.0092***	−0.0084***
	(−5.28)	(−5.64)	(−5.72)	(−6.99)	(−5.34)	(−5.29)	(−3.90)		(−6.87)	(−6.89)	(−7.86)	(−7.02)
SML_Range	−0.4888***	−0.4637***	−0.3327***	−0.2812***	−0.5349***	−0.2313**	−0.2592**		−0.0843	−0.0810	−0.2119*	
	(−5.49)	(−5.19)	(−3.57)	(−2.95)	(−5.04)	(−2.19)	(−2.41)		(−0.72)	(−0.69)	(−1.91)	
Year102		0.1141***						0.0635	0.1262**	0.1236**	0.1138**	0.1247**
		(3.26)						(1.26)	(2.48)	(2.42)	(2.23)	(2.45)
Month3			−0.0907***					−0.0523**	−0.0369	−0.0377	−0.0473*	−0.0379
			(−5.53)					(−2.12)	(−1.50)	(−1.53)	(−1.93)	(−1.54)
S10year				0.1276***				0.1025***	0.1395***	0.1387***	0.1067***	0.1428***
				(5.97)				(4.27)	(5.51)	(5.48)	(4.53)	(5.80)
CPI					0.0111			0.0800***	0.1045***	0.1042***	0.0967***	0.1020***
					(0.80)			(4.76)	(6.03)	(6.02)	(5.62)	(5.99)
GDP						−0.0766***		−0.0397	−0.0701***	−0.0697***	−0.1168***	−0.0698***
						(−4.55)		(−1.58)	(−2.76)	(−2.75)	(−5.45)	(−2.75)
M_0							−0.0156***	−0.0308***	−0.0193***	−0.0191***		−0.0204***
							(−3.79)	(−6.11)	(−3.49)	(−3.46)		(−3.90)
Vol_diff × coupon	0.0002***	0.0002***	0.0002***	0.0002***	0.0002***	0.0002***	0.0002***	0.0002***	0.0002***	0.0002***	0.0002***	0.0002***
	(3.09)	(2.96)	(2.94)	(2.97)	(3.04)	(3.49)	(3.29)	(2.87)	(2.91)	(2.92)	(2.99)	(2.92)
Adj-R^2 (%)	1.3540	1.4942	1.7830	1.8564	1.3487	1.6405	1.5476	2.1232	2.8054	2.8696	2.7119	2.8771

The table shows the impact of macrovariables on the nondefault spread. Year102 is the difference between the 10-year Treasury rate and the 2-year Treasury rate. Month3 is the 3-month Treasury rate, and S10year is the spread between the bond market index yield and the 10-year Treasury rate. CPI is the consumer price index, and GDP is gross domestic product. M_0 is an increase in cash in circulation. The meanings of the other variables are consistent with those in Tables 2 and 8. The cross-term is the interaction between liquidity and credit risk. The sample period is July 2006 to June 2016. The t-statistics are given in parentheses, and *, **, and *** represent significance at the 10%, 5%, and 1% level, respectively.

Table 10: Robustness tests of price impact.

Model	C	Vol_diff	Amihud_diff	BML_Vol	BML_Amihud	Year102	S10year	CPI	GDP	M_0	Vol × coupon	Day × coupon	Adj-R^2 (%)
1	−0.1156***	−0.0002***	0.2063***										0.2539
	(−9.93)	(−2.83)	(3.04)										
2	0.1504 ***	−0.0002***	0.2062***	−0.0066***	0.5113								0.9137
	(2.58)	(−3.38)	(3.05)	(−5.98)	(0.99)								
3	0.7654 ***	−0.0002***	0.1840***	−0.0094***	0.0816	0.1389***	0.1521***						1.9262
	(7.43)	(−3.09)	(2.73)	(−8.14)	(0.16)	(3.97)	(7.64)						
4	1.1722***	−0.0002***	0.1678**	−0.0078***	1.0574*	0.1814***	0.1522***	0.1085***	−0.0870***	−0.0201***			2.7850
	(7.24)	(−3.45)	(2.50)	(−6.16)	(1.89)	(5.05)	(6.52)	(6.25)	(−3.19)	(−3.82)			
5	1.2203 ***	−0.0015***	0.1846***	−0.0078***	1.0654*	0.1760***	0.1487***	0.1081***	−0.0969***	−0.0205***	0.0002***	0.0004**	2.9413
	(7.51)	(−3.78)	(2.74)	(−6.23)	(1.90)	(4.91)	(6.37)	(6.23)	(−3.54)	(−3.90)	(3.23)	(2.09)	

The table shows the robustness tests of price impact on the nondefault spread. The meanings of the variables are consistent with those in Tables 2 and 9. The cross-term is the interaction between liquidity and credit risk. The sample period is July 2006 to June 2016. The t-statistics are given in parentheses, and *, **, and *** represent significance at the 10%, 5%, and 1% level, respectively.

Table 11: Robustness tests of trading activity.

Model	C	Turnover_diff	Amihud_diff	BML_Vol	BML_Amihud	Year102	S10year	CPI	GDP	M_0	Turnover × coupon	Day × coupon	Adj-R^2 (%)
1	−0.1175***	−0.2111***	0.1942***										0.2989
	(−10.27)	(−3.33)	(2.85)										
2	0.1518***	−0.2488***	0.1924***	−0.0067***	0.5053								0.9703
	(2.61)	(−3.92)	(2.83)	(−6.04)	(0.97)								
3	0.7668***	−0.2305***	0.1709*	−0.0094***	0.0772	0.1379***	0.1520***						1.9797
	(7.44)	(−3.64)	(2.53)	(−8.20)	(0.15)	(3.94)	(7.64)						
4	1.1780***	−0.2526***	0.1536**	−0.0078***	1.0611*	0.1805***	0.1519***	0.1089***	−0.0879***	−0.0200***			2.8449
	(7.28)	(−4.01)	(2.28)	(−6.21)	(1.89)	(5.03)	(6.51)	(6.27)	(−3.23)	(−3.81)			
5	1.2328***	−1.8679***	0.1659**	−0.0079***	1.0650*	0.1738***	0.1495***	0.1079***	−0.0978***	−0.0208***	0.2129***	0.0005**	3.0494
	(7.59)	(−4.35)	(2.45)	(−6.31)	(1.90)	(4.85)	(6.41)	(6.22)	(−3.58)	(−3.95)	(3.76)	(2.17)	

The table shows the robustness tests of trading activity on the nondefault spread. The meanings of the variables are consistent with those in Tables 2 and 9. The cross-term is the interaction between liquidity and credit risk. The sample period is July 2006 to June 2016. The t-statistics are given in parentheses, and *, **, and *** represent significance at the 10%, 5%, and 1% level, respectively.

3, the coefficients of Year102 and S10year are 0.1379 and 0.1520 and are significant at the level of 1%, while the coefficients of Year102, S10year, CPI, GDP, and M_0 are also significant at the level of 1% in Model 4. In addition, Adj-R^2 of Models 3 and 4 are 1.9797% and 2.8449% and are significantly improved compared with Model 1, which indicates that macrofactors are significant explanatory variables for the nondefault spread, and our empirical results are robust. The interaction between liquidity and credit risk is considered in Table 11 in order to investigate whether it is priced. Similar results are obtained to those in Model 5. The coefficient of Turnover × Coupon is 0.2129 and is significant at the level of 1%, while the coefficient of Day × Coupon is also significant at the level of 5%; Adj-R^2 of Model 5 is 3.0494% and is greater than that of Model 4. This suggests that the interaction between liquidity and credit risk is significantly priced in the Chinese corporate bond market. In addition, the empirical results of Models 1–5 show that the coefficients of Amihud_diff are all very significant. The empirical results of Table 11 show that our results are robust.

6.3. Subsamples. The robustness test results for subsamples are given in Table 12. In Panel A, the empirical results of the high credit rating subsample show that the coefficients of Turnover_diff, BML_Vol, S10year, CPI, GDP, and Turnover × Coupon are all significant at the level of 1%. This shows that market liquidity and macrofactors have explanatory power for the price difference of the two markets for the same bond and the interaction is significantly priced in the Chinese corporate bond market. In addition, the coefficient of BML_Amihud is significant at the level of 5% in the subsample of low credit rating, while the coefficient is at the level of 10% in the subsample of high credit rating, which shows that the nondefault spread of low credit rating bonds is more susceptible to market factors than that of high credit rating bonds. The coefficients of Year102 and M_0 are significant at the level of 1% in the subsample of low credit rating, while their coefficients are significant at the level of 5% in the subsample of high credit rating, which shows that the nondefault spread of low credit rating bonds is more susceptible to macrofactors than that of high credit rating bonds.

In Panel B of Table 12, the sample is divided into two parts associated with coupon. Similar results are obtained in Panel B. The empirical results of the high coupon subsample show that the coefficients of BML_Vol, Year102, S10year, CPI, GDP, and Turnover × Coupon are all significant at the level of 1%, while the empirical results of the low coupon subsample show that the coefficients of BML_Vol, Year102, S10year, CPI, and Day × Coupon are all significant at the level of 1%. This shows that market liquidity and macrofactors have explanatory power for the nondefault spread and interaction is significantly priced. In addition, the coefficient of BML_Amihud is significant at the level of 5% in the high coupon subsample, while the coefficient is at the level of 10% in the low coupon subsample, which shows that the nondefault spread of high coupon bonds is more susceptible to market factors than that of low coupon bonds.

In Panel C of Table 12, the sample is divided into two parts associated with age. The coefficients of BML_Amihud, S10year, CPI, and M_0 are not significant in the high age subsample, while their coefficients are significant at the level of 1% in the low age subsample. The reason for this is that bonds of high age are often held as asset allocation, and thus, they are less affected by macrofactors, while bonds of low age are more active and are sensitive to macrofactors. The coefficient of Day × Coupon is not significant, and the coefficient of Turnover × Coupon is significant at the level of 5% in the high age subsample, while their coefficients are significant at the level of 1% in the low age subsample. This shows that bonds of low age are sensitive to interaction.

In addition, Adj-R^2 of the subsamples is high, ranging from 1.7487% to 6.2333%, and is far higher than that considering liquidity proxies. This shows that our results are robust. Only a small part of the nondefault spread is explained by liquidity proxies, and market liquidity and macrofactors have good explanatory power for the price difference of the two markets for the same bond for the following reasons. There is a systematic liquidity factor, and it affects the liquidity of individual bonds in the bond market. Macrofactors and stock market liquidity affect the nondefault spread by affecting the systematic liquidity factor of the bond market.

In Panel A of Table 12, the coefficients of Turnover × Coupon are 0.2361 and 0.2009 and are significant at the level of 1% for the high credit rating and low credit rating subsamples. In Panel B, the coefficient of Turnover × Coupon is 0.3689 and is significant at the level of 1% in the high coupon subsample, while the coefficient of Day × Coupon is also significant at the level of 1% in the low coupon subsample. In Panel C, the coefficient of Turnover × Coupon is 0.2434 and is significant at the level of 5% in the high age subsample, while the coefficients of Turnover × Coupon and Day × Coupon are also significant at the level of 1% in the low age subsample. This shows that the interaction between liquidity and credit risk is significantly priced and has good explanatory power for the price difference of the two markets for the same bond, and our results are robust in China's corporate bond market. The reason is that although liquidity and credit risk are two different types of risk, they mutually influence each other. Ericsson and Renault [52] find that liquidity and credit risk are correlated and when market liquidity is poor, credit risk of bonds is large, which suggests that there liquidity and credit risk interact. We find that the price difference of the two markets for the same bond is significantly related to the interaction between liquidity and credit risk.

7. Interaction between Liquidity and Credit Risk during the Financial Crisis

7.1. Temporal Characteristics of Average Spreads. We study the temporal characteristics of the monthly average spreads in the Chinese corporate bond market, namely, the interbank market and the exchange market. The characteristics of average spreads are very similar, probably because they are subject to common systematic risk. From May 2007 to

Table 12: Robustness tests of subsamples.

	C	Turnover_diff	Amihud_diff	BML_Vol	BML_Amihud	Year102	S10year	CPI	GDP	M_0	Turnover × coupon	Day × coupon	Adj-R^2 (%)
Panel A: rating													
AAA/AA+/AA−	1.2343***	−2.0444***	−0.0043	−0.0061***	0.9437*	0.1036**	0.1209***	0.0895***	−0.1134***	−0.0154**	0.2361***	0.0003	4.1287
	(6.31)	(−3.28)	(−0.05)	(−3.71)	(1.93)	(2.19)	(4.04)	(4.15)	(−3.73)	(−2.20)	(2.77)	(1.10)	
Below AA−	0.9919***	−1.7687***	0.2425***	−0.0080***	3.8813**	0.2064***	0.1763***	0.1094***	−0.0682	−0.0221***	0.2009***	0.0005*	2.8918
	(3.90)	(−3.17)	(2.72)	(−4.44)	(2.35)	(4.25)	(5.40)	(4.45)	(−1.57)	(−3.07)	(2.75)	(1.75)	
Panel B: coupon													
High	1.7312***	−3.2292***	0.1344*	−0.0066***	2.9872*	0.1584***	0.1054***	0.1454***	−0.2240***	−0.0138**	0.3689***	0.0001	4.8757
	(7.02)	(−3.83)	(1.72)	(−3.71)	(1.84)	(3.33)	(3.26)	(5.92)	(−5.36)	(−2.04)	(3.51)	(0.58)	
Low	1.0946***	−1.1450	0.2120*	−0.0080***	0.4732	0.1594***	0.1699***	0.0818***	−0.0583	−0.0205**	0.1162	0.0022***	2.5693
	(4.65)	(−1.13)	(1.77)	(−4.26)	(0.72)	(2.98)	(5.00)	(3.31)	(−1.54)	(−2.48)	(0.74)	(5.28)	
Panel C: age													
High	1.3399***	−2.2194***	0.1800*	−0.0079***	0.0040	0.2025***	0.0579	0.0467	−0.1491**	−0.0094	0.2434**	0.0001	1.7487
	(3.83)	(−2.80)	(1.81)	(−3.04)	(0.00)	(3.14)	(1.13)	(1.21)	(−2.07)	(−0.91)	(2.27)	(0.35)	
Low	1.6669***	−1.4557***	0.1303	−0.0084***	1.5824***	0.1670***	0.2511***	0.1492***	−0.1065***	−0.0291***	0.1737***	0.0007***	6.2333
	(9.04)	(−3.22)	(1.42)	(−6.70)	(3.21)	(4.20)	(9.72)	(8.75)	(−4.09)	(−5.48)	(2.95)	(3.26)	

The table shows the robustness tests of subsamples. The meanings of the variables are consistent with those in Tables 2 and 9. The cross-term is the interaction between liquidity and credit risk. The sample period is July 2006 to June 2016. The t-statistics are given in parentheses, and *, **, and *** represent significance at the 10%, 5%, and 1% level, respectively.

January 2010, the average spreads gradually increase and reach the maximum value in March 2012. Then, the average spreads gradually decrease. The main reason that the spreads increase from May 2007 to January 2010 is the outbreak of the global financial crisis, leading investors to demand a higher premium for compensation. From October 2010 to March 2012, the liquidity of China's financial market is small, and liquidity risk is increasing; thus, the spreads gradually increase. Since April 2012, China has carried out a series of financial reforms, and liquidity has gradually improved; market liquidity tends toward stability, and thus, the spreads slowly become smaller.

Based on the above analysis and Dick-Nielsen et al. [1], we divide the period from July 2006 to June 2016 into two: the period of financial crisis from May 2007 to December 2009, and the normal period on either side of it.

7.2. Impact of Interaction between Liquidity and Credit Risk on Spreads. We choose the basic liquidity and credit risk proxies and use their cross-terms to represent the interaction. To study the impact of the interaction on spreads, we divide the sample into the financial crisis period and the normal period. The relevant empirical results are shown in Tables 13 and 14.

The regression results containing the interaction are given in Table 13 and those containing only liquidity and credit risk are given in Table 14. Both in the normal period and during the financial crisis, the Adj-R^2 of the regression models with the interaction significantly increases. For example, the increase of Adj-R^2 was the largest (from 0.4797 to 0.5389) in the exchange market during the financial crisis period. In addition, some variables are significant because interaction variables are considered. The t-statistic of Amihud increases from −0.18 to 2.36 owing to the consideration of interaction in the interbank market during the financial crisis. This suggests that the interaction between liquidity and credit risk is an essential explanatory variable for the spreads. We now turn to the empirical results considering the interaction.

In the whole sample, the dummy variable is introduced to test the significance of the impact of the interbank market and the exchange market on the test results. The dummy variable of the interbank market is set to 1, and that of the exchange market is set to 0. As shown in Table 14, the regression coefficient of the dummy variables has high significance, which indicates that the impact of the two trading markets on the spreads is significant in the normal period. However, the coefficient of the dummy variable is not significant in Table 13. The reason may be that liquidity and credit risk have a major impact on the spreads during the financial crisis. In the whole sample, the regression coefficients of Age, Coupon, and Age ∗ Coupon are significant at the level of 1%, and the signs are in line with expectations during the financial crisis, while the regression coefficients of Vol, Age, Volatility, Coupon, Vol ∗ Volatility, Age ∗ Volatility, and Age ∗ Coupon are significant at the level of 1%, and the signs are in line with expectations in the normal period. This shows that the impact of the interaction between liquidity and credit risk cannot be ignored. In addition, the coefficients of Age ∗ Volatility and Age ∗ Coupon increase from −0.0465 and −0.0489 to 0.0476 and −0.1432, respectively, from the normal period to the financial crisis, because the interaction between liquidity and credit risk has a greater impact on the spreads during the financial crisis. And we study samples of Chinese corporate bond markets in the normal period and crisis period, respectively, and compare and analyze the empirical results. We find that liquidity risk and credit risk have highly persistent spreads, and the liquidity risk spreads of the price shock dimension produce a break point during the crisis, which is consistent with the findings of Sibbertsen et al. [62]; Wegener et al. [63]; Wegener et al. [64]; and Phillips and Shi [65].

To ensure the robustness of the results, we perform regression analysis of the interbank market and the exchange market independently. In the interbank market, similar results are found. The regression coefficients of Age, Coupon, and Age ∗ Coupon are significant at the level of 1%, and the regression coefficients of Amihud and Amihud ∗ Coupon are significant at the level of 5% during the financial crisis. The regression coefficients of Amihud, Age, Coupon, Amihud ∗ Coupon, and Age ∗ Coupon are significant at the level of 1%, and the signs are in line with expectations in normal times. This shows that the impact of the interaction between liquidity and credit risk cannot be ignored. In addition, the coefficients of Amihud ∗ Coupon and Age ∗ Coupon increase from −15.8072 and −0.0761 to −52.4023 and −0.1476, respectively, from the normal period to the financial crisis period. On the exchange market, the regression coefficients of Day, Age, Coupon, and Age ∗ Coupon are significant at the level of 1% during the financial crisis. The regression coefficients of Vol, Volatility, Coupon, Vol ∗ Volatility, Age ∗ Coupon, and Vol ∗ Coupon are significant at the level of 1% in the normal period. This shows that the impact of the interaction between liquidity and credit risk cannot be ignored. In addition, the coefficient of Age ∗ Coupon increases from −0.0221 to −0.1832 from the normal period to the financial crisis. This shows that the interaction between liquidity and credit risk is present in China's bond market and has a greater impact on the spreads during the financial crisis.

Table 13: Effects of interaction between liquidity and credit risk on spreads during the financial crisis.

C	Dummy	Vol	Day	Amihud	Age	Volatility	Coupon	Vol*Volatility	Vol*Coupon	Amihud*Volatility	Amihud*Coupon	Age*Volatility	Age*Coupon	Adj-R^2
Panel A: interbank market														
−0.7752***		0.0002	0.0169**	−0.6452	−0.0261	0.0281	0.4414***							0.2508
(−3.76)		(1.39)	(2.19)	(−0.18)	(−1.17)	(1.05)	(11.91)							
−1.4162***		−0.0011	0.0254***	250.5998**	0.6686***	−0.0481	0.5860***	0.0000	0.0002	−17.1424	−52.4023**	0.0284	−0.1476***	0.3079
(−4.23)		(−1.01)	(3.33)	(2.36)	(4.15)	(−0.72)	(9.61)	(0.36)	(1.12)	(−1.02)	(−2.45)	(1.15)	(−4.63)	
Panel B: exchange market														
0.2122		0.0017**	−0.0159***	−0.0952	−0.0942***	−0.3329***	0.4367***							0.4797
(0.98)		(2.07)	(−3.56)	(−0.43)	(−7.72)	(−7.58)	(12.36)							
−1.6769***		0.0374***	−0.0157***	2.3959	0.7585***	−0.2697***	0.7879***	−0.0132***	−0.0051***	0.2310	−0.6000	0.0466	−0.1832***	0.5389
(−4.21)		(4.60)	(−3.68)	(1.08)	(5.48)	(−2.84)	(11.57)	(−4.46)	(−4.32)	(0.79)	(−1.18)	(1.51)	(−6.59)	
Panel C: whole sample														
(−0.7856***	−0.0942*	0.0002*	0.0048	−0.1578	−0.0399***	−0.0487**	0.4864***							0.3318
(−5.44)	(−1.74)	(1.81)	(1.29)	(−0.68)	(−3.86)	(−2.12)	(19.08)							
−1.6731***	0.0089	−0.0003	0.0077**	2.8686	0.6149***	−0.1800***	0.6666***	0.0002*	0.0000	0.0160	−0.5818	0.0476**	−0.1432***	0.3757
(−6.81)	(0.17)	(−0.33)	(2.10)	(1.23)	(6.03)	(−3.34)	(15.68)	(1.95)	(0.18)	(0.05)	(−1.08)	(2.43)	(−7.09)	

To investigate whether there is an impact of interaction on the spreads, the following regression equations are given. $\text{Spread}_{it} = \alpha + \beta_1{}^* (\text{Liquidity risk factors})_{it} + \beta_2{}^* (\text{Credit risk factors})_{it} + \beta_3{}^* (\text{Different dimension liquidity risk factors})^* (\text{Credit risk factors})_{it} + \varepsilon$. If β_3 is significantly different from zero, the impact of the interaction on the spreads is present. The term "Liquidity risk factors" represents a set of basic proxies for liquidity risk from three dimensions, namely, transaction activity (Vol, Day), price impact (Amihud), and bond survival time (Age). The term "Different dimension liquidity risk factors" represents three dimensions of liquidity, namely, Vol, Amihud, and Age. The term "Credit risk factors" represents the proxies for the default risk, namely, Coupon and Volatility. The meanings of the other variables are given in Table 2. The sample period is May 2007 to December 2009; t-statistics are shown in parentheses below each coefficient estimate, and *, **, and *** indicate significance at the 10%, 5%, and 1% level, respectively.

Table 14: Effects of interaction between liquidity and credit risk on spreads in the normal period.

C	Dummy	Vol	Day	Amihud	Age	Volatility	Coupon	Vol*Volatility	Vol*Coupon	Amihud*Volatility	Amihud*Coupon	Age*Volatility	Age*Coupon	Adj-R^2
Panel A: interbank market														
0.3152***		−0.0003***	0.0567***	12.3903***	−0.1559***	−0.1126***	0.3704***							0.2152
(7.12)		(−6.23)	(12.50)	(8.26)	(−38.74)	(−6.38)	(60.67)							
−1.0200***		0.0005**	0.0488***	56.2229***	0.3410***	−0.0332	0.5801***	0.0009***	−0.0002***	43.9458***	−15.8072***	−0.0490***	−0.0761***	0.2464
(−13.17)		(2.05)	(10.79)	(6.25)	(16.18)	(−0.76)	(50.69)	(9.78)	(−5.82)	(19.31)	(−10.52)	(−4.25)	(−22.29)	
Panel B: exchange market														
0.4332***		0.0008***	0.0591***	0.2093***	−0.1413***	0.5343***	0.2623***							0.3054
(7.83)		(5.24)	(49.95)	(3.48)	(−36.39)	(24.98)	(35.54)							
0.4403***		−0.0141***	0.0581***	0.2485	−0.0159	0.1669***	0.2952***	0.0143***	0.0011***	−0.3076**	0.0300	0.0033	−0.0221***	0.3449
(5.43)		(−12.46)	(50.05)	(0.62)	(−0.85)	(4.78)	(25.45)	(34.41)	(7.54)	(−2.26)	(0.55)	(0.34)	(−7.73)	
Panel C: whole sample														
0.2926***	0.2695***	−0.0003***	0.0623***	0.2807***	−0.1472***	0.1807***	0.3099***							0.2516
(8.25)	(22.21)	(−8.69)	(59.92)	(4.85)	(−53.04)	(13.27)	(65.54)							
−0.4970***	0.2840***	−0.0011***	0.0606***	0.9928**	0.1694***	0.2849***	0.4295***	0.0006***	0.0000	−0.1514	−0.0944*	−0.0465***	−0.0489***	0.2618
(−8.78)	(23.34)	(−4.63)	(58.34)	(2.55)	(12.41)	(10.63)	(52.72)	(6.93)	(1.39)	(−1.15)	(−1.79)	(−6.43)	(−22.87)	

To investigate whether there is an impact of interaction on the spreads, the following regression equations are given. $\text{Spread}_{it} = \alpha + \beta_1{}^* (\text{Liquidity risk factors})_{it} + \beta_2{}^* (\text{Credit risk factors})_{it} + \beta_3{}^* (\text{Different dimension liquidity risk factors})^* (\text{Credit risk factors})_{it} + \varepsilon$. If β_3 is significantly different from zero, the impact of the interaction on the spreads is present. The term "Liquidity risk factors" represents a set of basic proxies for liquidity risk from three dimensions, namely, transaction activity (Vol and Day), price impact (Amihud), and bond survival time (Age). The term "Different dimension liquidity risk factors" represents three dimensions of liquidity, namely, Vol, Amihud, and Age. The term "Credit risk factors" represents the proxies for the default risk, namely, Coupon and Volatility. The meanings of other variables are given in Table 2. The sample period is from July 2006 to April 2007 and from January 2010 to June 2016. The t-statistics are shown in parentheses below each coefficient estimate, and *, **, and *** indicate significance at the 10%, 5%, and 1% level, respectively.

8. Conclusion

This study analyzes the impact factors of the price difference between the interbank market and the exchange market for the same bond in China. We identify 1224 individual bonds based on a large transaction dataset from July 2006 to June 2016 in China's bond market. The main conclusions are as follows.

First, we study the impact of liquidity on the price difference between the two markets for the same bond from different individual liquidity dimensions, such as trading activity and price shocks, and find that individual bond liquidity is an important factor affecting bond spreads, but it explains only a small part of spreads.

Second, we introduce the interaction between liquidity and credit risk into our models. Our study finds that interaction between credit risk and liquidity is an important factor influencing bond spreads, and this effect is greater during financial crisis. Some scholars provide several reasons. He and Milbradt [54] propose that starting from the observation that bond transaction costs increase in times of distress, a decrease in bond market liquidity results in rollover losses, which in turn increases default risk. According to Sperna Weiland et al. [56], the reason that higher credit risk can imply lower liquidity is the cost of market making. Our results produce the following reason: both liquidity and credit risk are closely related to market factors and macrofactors, and when market conditions change, liquidity and credit risk must comove and induce interaction. The greater the interaction between liquidity and credit risk, the more risk premium that investors demand.

Third, we find that market liquidity and macrofactors mainly affect the price difference between the two markets for the same bond. We choose proxies of different dimensions to investigate the explanatory power of market liquidity and macrofactors on spreads. The results are all robust.

Our study contributes to the literature by providing new explanatory channels on spreads. The results of this study offer interesting insights for corporate bond investors. In this study, we do not consider the problem of how to estimate a structural model to better capture the interaction by the theoretical models, which may be an important research direction in the future.

Data Availability

This study uses the data from the WIND database.

Conflicts of Interest

The authors declare that they have no conflicts of interest.

Acknowledgments

This work was supported by the National Natural Science Foundation of China (grant nos. 71471129 and 71501140) and Tianjin Philosophy and Social Science Planning Project (grant no. TJGL19-018).

References

[1] J. Dick-Nielsen, P. Feldhütter, and D. Lando, "Corporate bond liquidity before and after the onset of the subprime crisis," *Journal of Financial Economics*, vol. 103, no. 3, pp. 471–492, 2012.

[2] F. A. Longstaff, "The flight-to-liquidity premium in U.S. treasury bond prices," *The Journal of Business*, vol. 77, no. 3, pp. 511–526, 2004.

[3] D. Shin and B. Kim, "Liquidity and credit risk before and after the global financial crisis: evidence from the Korean corporate bond market," *Pacific-Basin Finance Journal*, vol. 33, pp. 38–61, 2015.

[4] A. Warga, "Bond returns, liquidity, and missing data," *The Journal of Financial and Quantitative Analysis*, vol. 27, no. 4, pp. 605–617, 1992.

[5] J. Helwege, J.-Z. Huang, and Y. Wang, "Liquidity effects in corporate bond spreads," *Journal of Banking & Finance*, vol. 45, pp. 105–116, 2014.

[6] F. A. Longstaff, S. Mithal, and E. Neis, "Corporate yield spreads: default risk or liquidity? New evidence from the credit default swap market," *The Journal of Finance*, vol. 60, no. 5, pp. 2213–2253, 2005.

[7] L. E. Crabbe and C. M. Turner, "Does the liquidity of a debt issue increase with its size? Evidence from the corporate bond and medium-term note markets," *The Journal of Finance*, vol. 50, no. 5, pp. 1719–1734, 1995.

[8] M. Rossi, "Realized volatility, liquidity, and corporate yield spreads," *Quarterly Journal of Finance*, vol. 4, no. 1, Article ID 1450004, 2014.

[9] T. Chordia, A. Sarkar, and A. Subrahmanyam, "An empirical analysis of stock and bond market liquidity," *Review of Financial Studies*, vol. 18, no. 1, pp. 85–129, 2005.

[10] R. Y. Goyenko and A. D. Ukhov, "Stock and bond market liquidity: a long-run empirical analysis," *Journal of Financial and Quantitative Analysis*, vol. 44, no. 1, pp. 189–212, 2009.

[11] J. Ejsing, M. Grothe, and O. Grothe, "Liquidity and credit premia in the yields of highly-rated sovereign bonds," *Journal of Empirical Finance*, vol. 33, pp. 160–173, 2015.

[12] E. J. Elton, M. J. Gruber, D. Agrawal, and C. Mann, "Explaining the rate spread on corporate bonds," *The Journal of Finance*, vol. 56, no. 1, pp. 247–277, 2001.

[13] N. Friewald, R. Jankowitsch, and M. G. Subrahmanyam, "Illiquidity or credit deterioration: a study of liquidity in the US corporate bond market during financial crises," *Journal of Financial Economics*, vol. 105, no. 1, pp. 18–36, 2012.

[14] A. X. Wang, W. Z. Xie, and W. L. Yu, "Emprical research on China's corporate bond yield spread," *Journal of Management Science*, vol. 15, no. 5, pp. 32–41, 2012, in Chinese.

[15] H. Zhou, G. P. Li, W. F. Lin, and Y. Wang, "Analyze and progress of credit risk pricing model of corporate bonds," *Journal of Management Sciences in China*, vol. 18, no. 8, pp. 20–30, 2015, in Chinese.

[16] Y. Amihud, "Illiquidity and stock returns: cross-section and time-series effects," *Journal of Financial Markets*, vol. 5, no. 1, pp. 31–56, 2002.

[17] J. Bao, J. Pan, and J. Wang, "The illiquidity of corporate bonds," *The Journal of Finance*, vol. 66, no. 3, pp. 911–946, 2011.

[18] L. Chen, D. A. Lesmond, and J. Wei, "Corporate yield spreads and bond liquidity," *The Journal of Finance*, vol. 62, no. 1, pp. 119–149, 2007.

[19] D. Covitz and C. Downing, "Liquidity or credit risk? The determinants of very short-term corporate yield spreads," *The Journal of Finance*, vol. 62, no. 5, pp. 2303–2328, 2007.
[20] F. De Jong and J. Driessen, "Liquidity risk premia in corporate bond markets," *Quarterly Journal of Finance*, vol. 2, no. 2, Article ID 1250006, 2012.
[21] C. Downing, S. Underwood, and Y. Xing, *Is Liquidity Risk Priced in the Corporate Bond Market?*, Rice University, Houston, TX, USA, 2005.
[22] P. Houweling, A. Mentink, and T. Vorst, "Comparing possible proxies of corporate bond liquidity," *Journal of Banking & Finance*, vol. 29, no. 6, pp. 1331–1358, 2005.
[23] R. Roll, "A simple implicit measure of the effective bid-ask spread in an efficient market," *The Journal of Finance*, vol. 39, no. 4, pp. 1127–1139, 1984.
[24] O. Sarig and A. Warga, "Bond price data and bond market liquidity," *Journal of Financial and Quantitative Analysis*, vol. 24, no. 3, pp. 367–378, 1989.
[25] A. S. Kyle, "Continuous auctions and insider trading," *Econometrica*, vol. 53, no. 6, pp. 1315–1336, 1985.
[26] Z. Z. Ren and P. Li, "Impact of liquidity risk on the term structure of credit spreads," *Journal of Systems and Management*, vol. 15, no. 3, pp. 251–255, 2006, in Chinese.
[27] P. Brockman and D. Y. Chung, "Commonality in liquidity: evidence from an order-driven market structure," *Journal of Financial Research*, vol. 25, no. 4, pp. 521–539, 2002.
[28] C. Comerton-Forde, T. Hendershott, C. M. Jones, P. C. Moulton, and M. S. Seasholes, "Time variation in liquidity: the role of market-maker inventories and revenues," *The Journal of Finance*, vol. 65, no. 1, pp. 295–331, 2010.
[29] Z. H. Ji and Y. Y. Cao, "Credit risk premium or market liquidity premium? An empirical study on the pricing of credit bonds in China," *Financial Research*, vol. 440, no. 2, pp. 1–10, 2017, in Chinese.
[30] D. Bongaerts, F. De Jong, and J. Driessen, "An asset pricing approach to liquidity effects in corporate bond markets," *The Review of Financial Studies*, vol. 30, no. 4, pp. 1229–1269, 2017.
[31] P. Brockman, D. Y. Chung, and C. Pérignon, "Commonality in liquidity: a global perspective," *Journal of Financial and Quantitative Analysis*, vol. 44, no. 4, pp. 851–882, 2009.
[32] T. Chordia, R. Roll, and A. Subrahmanyam, "Commonality in liquidity," *Journal of Financial Economics*, vol. 56, no. 1, pp. 3–28, 2000.
[33] J. Hasbrouck and D. J. Seppi, "Common factors in prices, order flows, and liquidity," *Journal of Financial Economics*, vol. 59, no. 3, pp. 383–411, 2001.
[34] G. A. Karolyi, K.-H. Lee, and M. A. van Dijk, "Understanding commonality in liquidity around the world," *Journal of Financial Economics*, vol. 105, no. 1, pp. 82–112, 2012.
[35] R. A. Korajczyk and R. Sadka, "Pricing the commonality across alternative measures of liquidity," *Journal of Financial Economics*, vol. 87, no. 1, pp. 45–72, 2008.
[36] L. Mancini, A. Ranaldo, and J. Wrampelmeyer, "Liquidity in the foreign exchange market: measurement, commonality, and risk premiums," *The Journal of Finance*, vol. 68, no. 5, pp. 1805–1841, 2013.
[37] V. Acharya and L. Pedersen, "Asset pricing with liquidity risk," *Journal of Financial Economics*, vol. 77, no. 2, pp. 375–410, 2005.
[38] T. Chordia, R. Roll, and A. Subrahmanyam, "Market liquidity and trading activity," *The Journal of Finance*, vol. 56, no. 2, pp. 501–530, 2001.
[39] Ľ. Pástor and R. F. Stambaugh, "Liquidity risk and expected stock returns," *Journal of Political Economy*, vol. 111, no. 3, pp. 642–685, 2003.
[40] R. Sadka, "Momentum and post-earnings-announcement drift anomalies: the role of liquidity risk," *Journal of Financial Economics*, vol. 80, no. 2, pp. 309–349, 2006.
[41] U. N. Küçük, "Non-default component of sovereign emerging market yield spreads and its determinants: evidence from the credit default swap market," *The Journal of Fixed Income*, vol. 19, no. 4, pp. 44–66, 2010.
[42] S. Han and H. Zhou, "Effects of liquidity on the non-default component of corporate yield spreads: evidence from intraday transactions data," *Quarterly Journal of Finance*, vol. 6, no. 3, Article ID 1650012, 2016.
[43] Y. Guo, Z. Huang, and Y. Wang, "Unexpected monetary policy and credit spreads of corporate bonds in China: an empirical analysis using spreads of fixed and floating rate bonds," *Journal of Financial Research*, vol. 432, no. 6, pp. 67–80, 2016, in Chinese.
[44] S. C. Ludvigson and S. Ng, "Macro factors in bond risk premia," *Review of Financial Studies*, vol. 22, no. 12, pp. 5027–5067, 2009.
[45] P. Vodova, "Liquidity of Czech commercial banks and its determinants," *International Journal of Mathematical Models and Methods in Applied Sciences*, vol. 5, no. 6, pp. 1060–1067, 2011.
[46] N. Valla, B. Saes-Escorbiac, and M. Tiesset, "Bank liquidity and financial stability," *Banque de France's Financial Stability Review*, vol. 9, no. 1, pp. 89–104, 2006.
[47] V. Dinger, "Do foreign-owned banks affect banking system liquidity risk?" *Journal of Comparative Economics*, vol. 37, no. 4, pp. 647–657, 2009.
[48] M. A. B. Moussa, "The determinants of bank liquidity: case of Tunisia," *International Journal of Economics and Financial Issues*, vol. 5, no. 1, pp. 249–259, 2015.
[49] A. Singh and A. K. Sharma, "An empirical analysis of macroeconomic and bank-specific factors affecting liquidity of Indian banks," *Future Business Journal*, vol. 2, no. 1, pp. 40–53, 2016.
[50] H. Chen, R. Cui, Z. He, and K. Milbradt, "Quantifying liquidity and default risks of corporate bonds over the business cycle," *The Review of Financial Studies*, vol. 31, no. 3, pp. 852–897, 2017.
[51] D. Duffie and K. J. Singleton, "Modeling term structures of defaultable bonds," *Review of Financial Studies*, vol. 12, no. 4, pp. 687–720, 1999.
[52] J. Ericsson and O. Renault, "Liquidity and credit risk," *The Journal of Finance*, vol. 61, no. 5, pp. 2219–2250, 2006.
[53] Z. He and W. Xiong, "Rollover risk and credit risk," *The Journal of Finance*, vol. 67, no. 2, pp. 391–430, 2012.
[54] Z. He and K. Milbradt, "Endogenous liquidity and defaultable bonds," *Econometrica*, vol. 82, no. 4, pp. 1443–1508, 2014.
[55] J. Wang and C. Wu, "Liquidity, credit quality, and the relation between volatility and trading activity: evidence from the corporate bond market," *Journal of Banking & Finance*, vol. 50, pp. 183–203, 2015.
[56] R. C. Sperna Weiland, R. J. Laeven, and F. De Jong, "Feedback between credit and liquidity risk in the US corporate bond market," in *Proceedings of the 30th Australasian Finance and Banking Conference*, Sydney, Australia, 2017.
[57] N. Dimic, J. Kiviaho, V. Piljak, and J. Äijö, "Impact of financial market uncertainty and macroeconomic factors on stock-bond correlation in emerging markets," *Research in International Business and Finance*, vol. 36, pp. 41–51, 2016.

[58] W. R. Gebhardt, S. Hvidkjaer, and B. Swaminathan, "Stock and bond market interaction: does momentum spill over?" *Journal of Financial Economics*, vol. 75, no. 3, pp. 651–690, 2005.

[59] S. T. Bharath and T. Shumway, "Forecasting default with the Merton distance to default model," *Review of Financial Studies*, vol. 21, no. 3, pp. 1339–1369, 2008.

[60] T.-K. Chen, H.-H. Liao, and P.-L. Tsai, "Internal liquidity risk in corporate bond yield spreads," *Journal of Banking & Finance*, vol. 35, no. 4, pp. 978–987, 2011.

[61] H. Lin, J. Wang, and C. Wu, "Liquidity risk and expected corporate bond returns," *Journal of Financial Economics*, vol. 99, no. 3, pp. 628–650, 2011.

[62] P. Sibbertsen, C. Wegener, and T. Basse, "Testing for a break in the persistence in yield spreads of EMU government bonds," *Journal of Banking & Finance*, vol. 41, pp. 109–118, 2014.

[63] C. Wegener, T. Basse, P. Sibbertsen, and D. K. Nguyen, "Liquidity risk and the covered bond market in times of crisis: empirical evidence from Germany," *Annals of Operations Research*, vol. 282, no. 1, pp. 407–426, 2019a.

[64] C. Wegener, R. Kruse, and T. Basse, "The walking debt crisis," *Journal of Economic Behavior & Organization*, vol. 157, pp. 382–402, 2019b.

[65] P. C. B. Phillips and S. Shi, "Detecting financial collapse and ballooning sovereign risk," *Oxford Bulletin of Economics and Statistics*, vol. 81, no. 6, pp. 1336–1361, 2019.

Hindawi
Discrete Dynamics in Nature and Society
Volume 2021, Article ID 6649445, 11 pages
https://doi.org/10.1155/2021/6649445

Research Article

The Herd Behavior on Peer-To-Peer Online Lending Markets: Evidence from China

Rong Liu, Ningning Chen, and Yuelei Li

College of Management and Economics, Tianjin University, Tianjin 300072, China

Correspondence should be addressed to Rong Liu; lrong@tju.edu.cn and Ningning Chen; maria19940727@163.com

Received 15 October 2020; Revised 9 February 2021; Accepted 23 March 2021; Published 7 April 2021

Academic Editor: Seenith Sivasundaram

Based on the transaction data and related borrowers' characteristics of Renrendai.com, this study conducts an empirical study on the influencing factors of the investor's herd behavior and rationality of herd behavior on a Chinese online lending platform. We mainly find that investors' herd behavior exists significantly on Renrendai.com; there is an "inverted U-shaped" relationship between the number of bids and the herd behavior of investors. When the number of bids exceeds a certain amount, the time required for the order to obtain another bid will be prolonged, and the investors' herd behavior will be slowed down; herd behavior on Renrendai.com in Chinese market is a partly rational pursuit, but irrational in general.

1. Introduction

Internet Finance (ITFIN), the dynamic integration of Internet technology and finance, implements its function by a financial service system created by cloud computing and big data, which shows a significant difference with the traditional finance industry. By June 2019, the number of online investment users had reached 170 million, accounting for 19.9% of Chinese Internet users [1]. After nearly a decade of rapid development, the P2P online lending platform has become an important supplement to traditional financial lending industry. These figures clearly show that the research on the P2P platform has become an important part of financial market.

Traditional financial institutions do not need to act as the intermediaries between lenders and borrowers. Compared with the traditional financial lending market, the P2P online lending industry has three main characteristics in a typical lending process: Firstly, in online lending, borrowers get their money from many investors, which disperses the default risk of investors to a certain extent. Secondly, online lending provides a platform for investors on which they can check borrowers' private and loan information, besides invest behaviors of other investors. Through observation of the abovementioned information, investors then may make their own decisions. Thirdly, information asymmetry occurs between investors and borrowers, lacking related expert domain knowledge to judge a borrower's credit level and the probability of default, and investors can only use published information about borrowers and behavior of other investors. Some research has addressed such issues; for example, Freedman and Jin found the P2P online lending market Prosper has more significant problems of adverse selection and information asymmetry [2]. Consequently, the abovementioned characteristics of P2P online lending may lead to investors' behavior on the platform being easily influenced by other investors. In order to ensure the success of listing they invest in, investors may invest in a relatively popular listing, which leads to herd behavior among investors.

Herd behavior is initially a phenomenon in zoology in which groups of animals (sheep, cattle, etc.) move together to forage or seek habitat. This phenomenon was later applied in human sociology to describe the concerted action and thinking of people. In the finance field, herd behavior mainly refers to the imitation behavior of investors in the financial market who ignore their own information and follow the decisions of most people in the market. Many scholars in the finance field have given the concept and definition of herd behavior from different research perspectives [3–6]. Others also examine herd behavior of investors [7] and borrowers

[8] at the platform level in the P2P market. Recent studies conduct empirical analysis on the relationship between herd behavior and other investors' emotion [9]. From the perspective of investor decision-making rationality, herd behavior can be divided into rational herding and irrational herding. Rational herd behavior refers to the behavior that investors rationally imitate and follow the decisions of other investors under the circumstance of information asymmetry from the perspective of profit making. Irrational herd behavior refers to the investors blindly following the decisions of other investors in the investment process. Several studies have been undertaken on the decision-making process of herd behavior [10, 11]. The herd behavior often stems from the "sense of belonging" of individuals to the group, such as feeling secure when they make the same decision with the group, or individual investors directly choose to follow institutional investors' decisions due to the consideration of opportunity cost and information acquisition ability when making investment decisions. However, whether the herd behavior of investors in the Chinese P2P platform is rational is still a controversial issue. In this paper, we explore the existence and rationality of herd behavior and tries to explore the factors influencing herd behavior.

Our empirical analysis proceeds as follows: first, we explore whether the herd behavior exists in Chinese market and the relationship between the education level of borrowers and other related factors and herd behavior of lenders; second, we identify whether the herd behavior is rational. This study contributes to the current literature in two ways: first, we use a new proxy, the time it takes for an order to receive the next bid, to identify the herd behavior, which can reflect the herd behavior better; third, we study the rationality of herd behavior not only from the perspective of repayment performance but also from the perspective of the decision-making process of investors.

This study is organized as follows: Section 2 reviews the literature in herd behavior and P2P online lending market. Section 3 introduces data, variables, and methodology. Section 4 presents the empirical results. The conclusions and future research directions are summarized in Section 5.

2. Related Literature and Hypothesis

2.1. Whether There Is Herd Behavior. When an investor makes decisions in the P2P online lending market, there is some information he or she may take into consideration. The first kind of information is the borrower's and order's information, some of which are not verified. The second kind of information is the hidden information obtained by an investor through observing the behavior of previous investors. If an investor is an expert with judging ability, and he can make decisions independently; otherwise, the behavior of the "pioneer" can affect investors' decision making significantly. Under the circumstance, investors may ignore their own intelligence and imitate the behavior of others. Moreover, the rule of the P2P online lending market states only when the number of bidamount meets the ask of the order can it be completed. The abovementioned terms lead to the result that orders that have received partial bids are more likely to succeed than those that have not received any bids in the same period. If an investor bids for an order that is not fully completed finally, the money invested will be returned to their account, and they will not receive interest income in a period of time and will have to find other orders to bid again. Therefore, fail to bid an order will cause the opportunity cost (loss of interest income) and additional search costs (time lost to search for other orders); investors may be more willing to bid orders that have been partially bided in order to reduce the cost, which may lead to investors rushing to bid some order, and then, a herd behavior of investors is engendered. Studies on the herding behavior on the P2P lending platform are plentiful. Krumme and Herrero [12] discovered the herd behavior exists on Prosper, an online lending platform. Similar research is conducted by Herzenstein et al. [13]. Berkovich [14] made further research considering the cost of bidding; investors are more willing to invest in orders that have been or will be filled, which also proves the existence of herd behavior on Prosper. Others have also been undertaken on trend of herd behavior. Based on Popfunding, an online lending platform, the borrowers on which are mainly with low credit rating, Lee and Lee [15] proved the existence of herd behavior and the effect diminished with the increase of financing proportion. Yum et al. [16] found that the herd behavior of investors in Popfunding was based on information asymmetry. Not until investors had enough information to analyze and make decisions do they stop imitating others. By analyzing the data of Chinese Renrendai platform, Liao et al. [17] found that investors on the platform had a significant herding behavior, and with the increase of order completion, herd behavior marginally decreased. Moreover, the study also verified that herding behavior had a significant relationship with the information asymmetry of the platform. Li [18], Li [19], Lv [20], and other scholars have also proved the existence of herd behavior in Chinese online loan market.

Existing research on the existence of herd behavior of investors on the P2P lending market is mainly carried out from the perspective of the influence of the number of bids in the current period to the number of bids in the future or using the average time interval to measure the herd behavior. Most of the research uses the data from the unit of listings or a relative long time period, which cannot fully reflect the chasing behavior of investors. This study uses the time spent for the next bid to verify the existence of investors' herd behavior, which is more meticulous and in accordance with the premise that herd behavior decision making happens orderly. Based on the abovementioned literature, we raise the first hypothesis:

H1: Controlling the information of the borrower and the order, the higher the number of bids received by the order is, the faster the next bid will be obtained; that is, herd behavior exists in the Renrendai P2P online lending market.

In the study of Lee and Lee [15], the number of bids had a positive effect on herding behavior, but this effect decreased with the increase in the number of bids gradually; that is to say, the herding behavior of investors presented a trend of diminishing marginally with the increase of bids. For example, if there are two orders with the same loan amount

and the fundraising ratio of both orders is 50%, while order A currently has 20 bids and order B has 5, it is obvious that the average bid amount of order B is much larger than that of order A. If an investor makes a decision choice with an imitation strategy, he will not invest in order A by simply comparing the number of bids received for the two orders, but invest in order B by considering the potential risks of order A, which means order A may lose the trust of investors due to the large number of bids it has received. Therefore, if there are too many bids an order has received, investors' herd behavior may slow down to some extent. It may take more time for the order to get the next bid. The speed of order completion also slows down consequently. That is to say, there is an inverted U-shaped relationship between investors' herd behavior and the number of bids in the P2P online lending market. Based on the abovementioned analysis, hypothesis 2 is proposed.

H2: In the Renrendai P2P online lending market, the strength of herding behavior changes with the bidding state and herding behavior, and the number of bids an order has received has an "inverted U-shaped" relationship; when the number of bids is too large, investors' trust may decrease, and then, the order needs more time to obtain the next bid.

2.2. Is the Herd Behavior Rational? From the perspective of the rationality of herd behavior, herd behavior can be divided into rational herd behavior and irrational herd behavior. Rational herd behavior of investors can maximize their investment, which means investors can benefit from imitating others' investment decisions. On the contrary, irrational herd behavior is the blind herd behavior of investors. Studies on whether herd behavior in the current P2P lending platform is rational are plentiful. Using data of Prosper, Zhang and Liu [21] found that investors' herd behavior is rational after controlling unobserved heterogeneity and payoff externalities, while Luo and Lin [22] measured the rationality of herd by the potential loss benefit and found herd behavior is irrational on Prosper. Chen et al. [23] made an empirical analysis on the data of China's Paipaidai platform and found that investors in Paipaidai showed obvious herding behavior, which was irrational because investors' herding behavior did not have a positive impact on the repayment performance of orders. Zeng Jianghong and Yang Shuai [24] found that potential lenders would comprehensively consider the characteristics of the loan target and the behavior of previous lenders when making decisions, which is a manifestation of rational herd behavior. As to the definition of whether the behavior of investors is rational, Herzenstein et al. [13] use the impact of herd behavior on the reimbursement to define the rational degree of herd behavior, which means investors' rational herd behavior can reduce the loan default rates. If there is no positive relationship between herding behavior and repayment performance, investors' herd behavior will not bring benefits for themselves, and then, the herd behavior is irrational.

There is still no unanimous conclusion about whether the herd behavior in the Chinese online lending platform is rational. We follow the work of Herzenstein [13] to measure the rationality of the herd and consider the decision process of lenders and conduct the third hypothesis.

H3: Herd behavior of investors can reduce the probability of default in the Renrendai P2P online lending market.

3. Data, Variables, and Methodology

3.1. Data. The data used in this study mainly come from the P2P lending platform Renrendai in China. Founded in 2010, Renrendai is one of the earliest online lending information intermediary platforms in China. Either complexity of data fetching or the diversity of data makes Renrendai a great choice. In 2017, the Renrendai platform ranked second among the top 100 online lending platforms in China. Hence, empirical research based on large-scale data provided by the Renrendai platform made the research results of this study more meaningful. The Renrendai platform introduced automatic bidding service in 2014. In order to eliminate the impact of automatic bidding service, our sample consists of the order, borrower, and bid information of the Renrendai platform with an order ID ranging from 123500 to 173500; orders in this range occurred before the introduction of automatic bidding service. We eliminate the orders that have not received bids; at last, 11,545 orders including 494,682 bidding information are obtained, and the bid data mainly include bid time, amount, and some other information.

3.2. Variables and Methodology. Table 1 formally defines all of our main variables.

SEC is the time it takes for an order to receive the next bid, obtained by subtracting the time of this bid from the time of the next bid. We measure the herd behavior of investors using SEC. At present, the number of orders with a loan of more than 100,000 Yuan on the Renrendai platform has exceeded 35%, and the number of bids with a high loan amount is relatively high. Therefore, we use Ln (bids), the natural logarithm of the bids received by the orders, as the independent variable. Velocity represents the average bid rate of the order, obtained by dividing the total bid time of the order by the total bid amount. We measure the degree of herd behavior using velocity. The faster the orders succeed, the more significant the investor herd behavior is. Default is a dummy variable equal to 1 if the order is default and 0 otherwise. We measure the rationality of herd behavior using default.

We follow the work of Herzenstein et al. [13] to study the influence of the number of bids received for orders on investors' herd behavior. According to the characteristics of the data in Renrendai, we measure investors' herd behavior by the time it takes for orders to be bid again. The empirical model is used to analyze whether the number of bids received for the order can significantly shorten the time needed for the order to get the bid again, so as to verify the existence of herd behavior of investors in P2P online lending platforms. Our model to verify the existence of herd behavior is as follows: Control_i includes controlling variables such as BA, order information, and borrower information.

Table 1: Variable definition.

Main variables		Definition
Bid information	SEC	The time it takes for an order to receive the next bid, measured in seconds
	Ln (bids)	The natural logarithm of the number of bids an order has received
	Ln^2 (bids)	The square of the natural logarithm of the number of bids an order has received
	BA	The bid amount
Order information	PER	Current proportion of investment received for orders
	RATE	Interest rate of orders
	Default	A dummy variable equals 1 if the order is default and 0 otherwise
	Velocity	The average bid speed of the order, obtained by dividing the total bid time of the order by the total bid amount
	Lnam	The natural logarithm of the amount of an order
	DUR	Repayment term of orders
Borrower information	GEN	A dummy variable equals 1 if the borrower is a man and 0 otherwise
	AGE	The age information of the borrower ranges from 22 to 60 years
	HOU	A dummy variable equals 1 if the borrower has a real estate and 0 otherwise
	CRE	The borrower's credit rating, including AA, A, B, C, D, E, and HR, which are evaluated by the platform
	HOUSEDEBT	A dummy variable equals 1 if the borrower has a house debt and 0 otherwise
	EDU	The borrower's education level, 4 = master's degree or above; 3 = bachelor's degree; 2 = college degree; and 1 = high-school degree or below

$$\mathrm{SEC} = \beta_0 + \beta_1 \mathrm{Ln}(\mathrm{bids}) + \beta_i \mathrm{Control}_i + \varepsilon. \quad (1)$$

In our second hypothesis, we add the square of the independent variables into our model to analyze the time required to obtain another bid based on different order bidding status in an order. Model 2 is as follows:

$$\mathrm{SEC} = \beta_0 + \beta_1 \mathrm{Ln}(\mathrm{bids}) + \beta_2 \mathrm{Ln}^2(\mathrm{bids}) + \beta_i \mathrm{Control}_i + \varepsilon. \quad (2)$$

To test the rationality of investors' herd behavior, we construct the logit model to study whether orders with herd behavior have a lower default rate, that is, whether investors can better identify the risks of orders by imitating the behaviors of other investors. The independent variable of this model is the average bid rate of the order, in the whole process of a bid, the dependent variable is the order default, and the control variable mainly includes the order information and the borrower information. Model 3 is as follows:

$$\mathrm{Ln}\left[\frac{P(\mathrm{Default} = 1)}{P(\mathrm{Default} = 0)}\right] = \beta_0 + \beta_1 \mathrm{Velocity} + \beta_i \mathrm{Control}_i + \varepsilon. \quad (3)$$

4. Empirical Results

4.1. Descriptive Statistics. Table 2 reports the mean, standard deviation, minimum, and maximum for the variables used in hypotheses 1 and 2. The average bid amount is 1245.42 Yuan, the average loan interest rate is 12.81%, and the average repayment term is 29.13 months, which is basically consistent with the characteristics of high interest rate and small loan amount in the online lending market. The highest amount order has reached 500,000 ($e^{13.12}$) Yuan, which indicates that the development of Renrendai is a relatively mature platform and a relatively large amount of borrowing can be accepted by investors. The average age of the borrowers is 38.92 years, 73% of the borrowers are male borrowers, 61% of the borrowers have a real estate, and 46% of the borrowers have a house debt.

Table 2: Descriptive statistics of hypothesis 1 and hypothesis 2.

Variable	Mean	Standard deviation	Min	Max
Ln (bids)	3.339	1.312	0.000	6.607
Ln^2 (bids)	12.873	8.616	0.000	43.648
PER	0.449	0.310	0.000	1.003
BA	1245.415	3301.238	50.000	200000.000
RATE	12.814	0.806	9.500	24.000
Lnam	11.103	0.569	8.006	13.122
DUR	29.128	9.502	3.000	36.000
GEN	0.727	0.445	0.000	1.000
AGE	38.921	8.657	22.000	65.000
HOU	0.612	0.487	0.000	1.000
CRE	4.902	0.649	0.000	6.000
HOUSEDEBT	0.456	0.498	0.000	1.000
EDU	1.979	0.711	1.000	4.000

The variables involved in the model are tested for multicollinearity. We use VIF to test the multicollinearity of independent variables as we test in Table 3. As shown in Table 3, the VIF value of all independent variables does not exceed 5, so there is no multicollinearity between variables. The correlation coefficient between all independent variables is also tested, and related results are shown in Table 4. According to the test results in Table 4, the correlation between the RATE and DUR is 0.73, which conforms to the fact that the longer is the loan duration, the higher is the loan rate, so we delete DUR in our following model.

Descriptive statistics and correlation tests also were carried out for independent variables and control variables in hypothesis 3, and the test result is shown in Table 5. There

Table 3: Result of the VIF test.

Variable	VIF	1/VIF
DUR	3.529	3.529
RATE	3.061	3.061
CRE	1.635	1.635
Lnbids	1.505	1.505
HOU	1.394	1.394
Lnam	1.384	1.384
PER	1.329	1.329
BA	1.103	1.103
AGE	1.078	1.078
EDU	1.035	1.035
GEN	1.008	1.008
Mean VIF	1.642	

Table 4: Correlation between the control variables and the main independent variables.

	Second	Lnbids	PER	BA	RATE	Lnam	DUR	GEN	AGE	HOU	CRE	EDU
Second	1.000											
Lnbids	−0.036 (0.000)	1.000										
PER	−0.036 (0.000)	0.404 (0.000)	1.000									
BA	−0.003 (0.063)	−0.177 (0.000)	0.116 (0.000)	1.000								
RATE	−0.116 (0.000)	−0.027 (0.000)	−0.069 (0.000)	0.007 (0.000)	1.000							
Lnam	0.035 (0.000)	0.316 (0.000)	−0.004 (0.014)	0.040 (0.000)	−0.164 (0.000)	1.000						
DUR	−0.110 (0.000)	0.059 (0.000)	−0.113 (0.000)	0.007 (0.000)	0.732 (0.000)	0.030 (0.000)	1.000					
GEN	0.002 (0.108)	−0.023 (0.000)	0.017 (0.000)	−0.001 (0.313)	−0.035 (0.000)	−0.036 (0.000)	−0.058 (0.000)	1.000				
AGE	0.028 (0.000)	0.058 (0.000)	0.002 (0.110)	0.006 (0.000)	−0.146 (0.000)	0.208 (0.000)	−0.094 (0.000)	0.012 (0.000)	1.000			
HOU	−0.066 (0.000)	0.010 (0.000)	−0.043 (0.000)	0.028 (0.000)	0.422 (0.000)	0.115 (0.000)	0.479 (0.000)	−0.060 (0.000)	0.020 (0.000)	1.000		
CRE	0.012 (0.000)	0.140 (0.000)	−0.071 (0.000)	0.004) (0.004)	−0.124 (0.000)	0.315 (0.000)	0.300 (0.000)	−0.054 (0.000)	0.065 (0.000)	0.030 (0.000)	1.000	
EDU	0.002 (0.246)	0.020) (0.000)	0.021 (0.000)	0.006 (0.000)	−0.040) (0.000)	0.093 (0.000)	−0.020 (0.000)	−0.010 (0.000)	−0.089 (0.000)	−0.077 (0.000)	−0.014 (0.000)	1.000

Table 5: Descriptive statistics and correlation tests for hypothesis 3.

	Mean	Standard deviation	Min	Max	Velocity	Lnam	RATE	DUR	GEN	AGE	HOU	CRE	EDU
Velocity	35.561	164.531	0.000	3862.833	1.000								
Lnam	10.828	0.636	8.006	13.122	0.047	1.000							
RATE	12.905	1.041	9.500	24.000	−0.210	−0.084	1.000						
DUR	28.407	10.122	3.000	36.000	−0.206	0.418	0.421	1.000					
GEN	0.737	0.440	0.000	1.000	0.012	−0.077	0.001	−0.076	1.000				
AGE	38.092	8.607	22.000	65.000	0.050	0.196	−0.113	0.010	−0.003	1.000			
HOU	0.585	0.493	0.000	1.000	−0.121	0.337	0.238	0.402	−0.058	0.097	1.000		
CRE	4.723	1.076	0.000	6.000	0.049	0.533	−0.274	0.454	−0.077	0.138	0.080	1.000	
EDU	1.970	0.719	1.000	4.000	−0.012	0.016	−0.007	−0.001	−0.005	−0.114	−0.029	−0.020	1.000

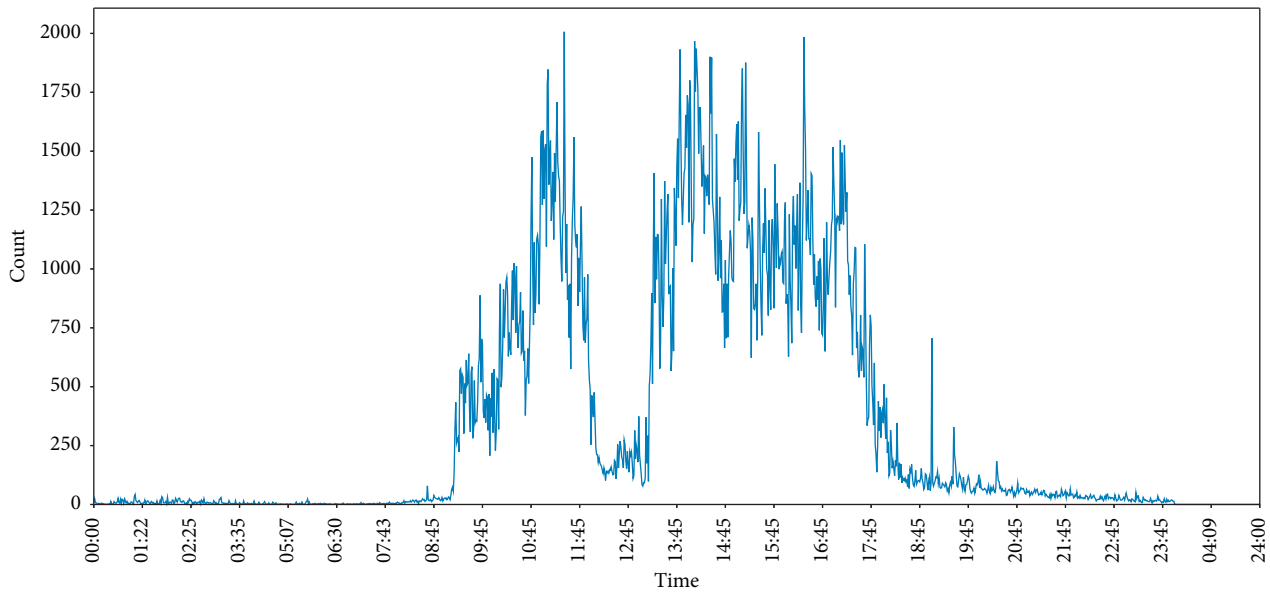

Figure 1: The time distribution of bid according to minutes. This figure illustrates the evolution of bid numbers measured in minute degree. The x-axis denotes the time, and the y-axis denotes its magnitude.

Table 6: Existence of investor herd behavior.

Variables	Model 1		Model 2	
	Model 1a	Model 1b	Model 2a	Model 2b
Lnbids	−10.611∗∗∗ (≤0.001)	−10.653∗∗∗ (≤0.001)	−22.981∗∗∗ (≤0.001)	−23.040∗∗∗ (≤0.001)
$\ln^2$ bids			1.930∗∗∗ (≤0.001)	1.933∗∗∗ (≤0.001)
PER	−33.381∗∗∗ (≤0.001)	−33.201∗∗∗ (≤0.001)	−31.657∗∗∗ (≤0.001)	−31.473∗∗∗ (≤0.001)
BA	−0.001∗∗∗ (≤0.001)	−0.001∗∗∗ (≤0.001)	−0.001∗∗∗ (≤0.001)	−0.001∗∗∗ (≤0.001)
RATE	−45.741∗∗∗ (≤0.001)	−45.739∗∗∗ (≤0.001)	−46.079∗∗∗ (≤0.001)	−46.077∗∗∗ (≤0.001)
Lnam	22.097∗∗∗ (≤0.001)	22.662∗∗∗ (≤0.001)	21.588∗∗∗ (≤0.001)	22.155∗∗∗ (≤0.001)
GEN	−2.166∗ (−0.062)	−2.222∗ (−0.055)	−1.993∗ (−0.086)	−2.050∗ (−0.077)
AGE	0.379∗∗∗ (≤0.001)	0.350∗∗∗ (≤0.001)	0.380∗∗∗ (≤0.001)	0.351∗∗∗ (≤0.001)
HOU	−21.188∗∗∗ (≤0.001)	−21.584∗∗∗ (≤0.001)	−20.703∗∗∗ (≤0.001)	−21.100∗∗∗ (≤0.001)
CRE	−4.373∗∗∗ (≤0.001)	−4.525∗∗∗ (≤0.001)	−4.024∗∗∗ (≤0.001)	−4.176∗∗∗ (≤0.001)
EDU		−3.022∗∗∗ (≤0.001)		−3.040∗∗∗ (≤0.001)
Constant	448.556∗∗∗ (≤0.001)	450.420∗∗∗ (≤0.001)	472.109∗∗∗ (≤0.001)	474.019∗∗∗ (≤0.001)
N	491502	491502	491502	491502
Adjusted R-squared	0.017	0.018	0.018	0.018

Note: ∗∗∗, ∗∗, and ∗ denote statistical significance levels at 1%, 5%, and 10%, respectively.

is no strong correlation between the variables used in model 3, which conforms to the requirements of the empirical model for variables. Among the 11,545 loan orders selected in this model, the average loan amount is 59893.05 Yuan, the average loan interest rate is 12.905%, and the average repayment term is 28.407 months, which is basically consistent

with the characteristics of high loan interest rate and small loan in the online lending market.

4.2. Results on the Existence of Investor Herd Behavior. We started with equation (1) to explore the existence of herd behavior. Then, we ran equation (2) to study the change trend of herd behavior. Figure 1 reports the time distribution of bid number according to minutes. As is shown clearly, most transactions happened in the daytime, and the number of bids happened from 8:00 to 23:00 account to 99.32% of the total number. It is obvious that rare lenders bid at night. In this section, we collect the 491502 bids in the daytime.

The results of the equations mentioned above are shown in Table 6, which shows that, with the increase of the number of bids received by the order, later investors speed up the bidding speed, and the time needed for the order to get bid again is gradually shortened. In other words, there is a significant herd behavior of investors on the Renrendai online lending platform. Model 2 in Table 6 shows that, after introducing the square of the natural logarithm of the number of bids received for an order, the result still supports model 1 and verifies hypothesis 2. The abovementioned results show that orders that have got bids need less time to get other bids, but if there are too many bids, the process may decrease. In other words, the herd behavior of investors and the number of bids orders received show an "inverted U" relationship. The decision-making process of investors is not only influenced by the number of bids orders have received but also a relatively large number of bids may decrease investors' trust. Listings with higher rates and borrowers with high credit degrees or borrowers who own houses are more attractive for lenders. Furthermore, when we introduce education degrees, results show that, for borrowers with higher education levels, herd behavior of lenders is more obvious, which means lenders trust borrowers with relatively high education degrees more.

4.3. Results on Rational Verification of Investor Herd Behavior. The regression result of model 3 is shown below in Table 7. The velocity of orders has no significant decrease on the borrower default rate; that is to say, the herd behavior of investors does not help investors to improve the investment efficiency and reduce the risk. In addition, listings with higher rates increase the default rate and borrowers with better credit degrees and higher education levels decrease the default rate, while whether borrowers owning houses have no influence on the default rates. Combining the conclusion from Section 4.2, when investors make decision, they pursue listings with higher rate and borrowers with high credit degree, high education level, and borrowers who own house. Although, some of the characteristics they pursue may decrease the default rate. Overall, their herd behavior cannot decrease the default rate. Therefore, the herd behavior of investors in the P2P online lending market is partly rational pursuit, but it is irrational in general. It is worth noting that the house variable, which has a significant impact on the herd behavior of investors, has no significant impact on the default rate of orders, indicating that real estate cannot be used as a symbol of the borrower's solvency in the P2P online lending market.

Table 7: Rational verification of investor herd behavior.

Variables	(1)	(2)	(3)
Velocity	0.001 (−0.701)	0.001 (−0.696)	0.001 (−0.769)
Lnam	0.267 (−0.19)	0.266 (−0.193)	0.316 (−0.131)
RATE	0.131∗∗ (−0.011)	0.131∗∗ (−0.01)	0.129∗∗ (−0.014)
DUR	0.083∗∗∗ (≤0.001)	0.083∗∗∗ (≤0.001)	0.083∗∗∗ (≤0.001)
GEN	−0.126 (−0.715)	−0.132 (−0.703)	−0.18 (−0.606)
AGE	0.037∗ (−0.056)	0.037∗ (−0.054)	0.033∗ (−0.096)
HOU	0.004 (−0.987)	-0.048 (−0.871)	-0.048 (−0.874)
CREDIT	−2.264∗∗∗ (≤0.001)	−2.269∗∗∗ (≤0.001)	−2.261∗∗∗ (≤0.001)
HOUSEDEBT		0.118 (−0.727)	0.226 (−0.511)
EDU			−0.461∗∗∗ (−0.004)
Constant	−7.838∗∗∗ (≤0.001)	−7.842∗∗∗ (≤0.001)	−7.244∗∗∗ (−0.001)
N Pseudo R^2	11545 0.609	11545 0.608	11545 0.616

Note: ∗∗∗, ∗∗, and ∗ denote statistical significance levels at 1%, 5%, and 10%, respectively.

4.4. Robustness Test

4.4.1. Adding Further Control Variables. To examine whether the herd behavior still exists after considering other factors that may affect the herd behavior of investors, we regress equations (1) and (2) on an expanded set of control variables such as income of borrowers, whether the borrowers owe house debt, and whether the borrowers own cars. CAR and HOUSEDEBT are dummy variables to measure whether borrowers have a car or owe a house debt. INCO is a variable to measure the borrower's income level (6 = job income equals to 50000 Yuan or above; 5 = job income between 20000 Yuan and 50000 Yuan; 4 = job income between 10000 Yuan and 20000 Yuan; 3 = job income between 5000 Yuan and 10000 Yuan; 2 = job income between 2000 Yuan and 5000 Yuan; and 1 = job income equals to 2000 Yuan or below). The results of estimation of equations (1) and (2) are reported in Table 8. Similar to the results in Table 6, we find the herd behavior still exists after adding further control variables.

4.4.2. Expanding the Samples. In this section, robustness test on our hypothesis 1 and 2 is conducted by reconsidering the analysis from Section 4.2 by including the bids that occur in the night (23:00 to the 8:00 of the next day) to our samples.

Table 8: Adding further control variables for model 1 and 2.

Variables	Model 1			Model 2		
	Model 1a	Model 1b	Model 1c	Model 2a	Model 2b	Model 2c
Lnbids	−10.677∗∗∗ (≤0.001)	−10.676∗∗∗ (≤0.001)	−10.687∗∗∗ (≤0.001)	−23.079∗∗∗ (≤0.001)	−23.140∗∗∗ (≤0.001)	−23.257∗∗∗ (≤0.001)
Ln^2 bids				1.935∗∗∗ (≤0.001)	1.945∗∗∗ (≤0.001)	1.962∗∗∗ (≤0.001)
PER	−33.076∗∗∗ (≤0.001)	−33.063∗∗∗ (≤0.001)	−33.018∗∗∗ (≤0.001)	−31.346∗∗∗ (≤0.001)	−31.323∗∗∗ (≤0.001)	−31.263∗∗∗ (≤0.001)
BA	−0.001∗∗∗ (≤0.001)	−0.001∗∗∗ (≤0.001)	−0.001∗∗∗ (≤0.001)	−0.001∗∗∗ (≤0.001)	−0.001∗∗∗ (≤0.001)	−0.001∗∗∗ (≤0.001)
RATE	−45.501∗∗∗ (≤0.001)	−45.524∗∗∗ (≤0.001)	−45.450∗∗∗ (≤0.001)	−45.839∗∗∗ (≤0.001)	−45.865∗∗∗ (≤0.001)	−45.792∗∗∗ (≤0.001)
Lnam	23.170∗∗∗ (≤0.001)	23.079∗∗∗ (≤0.001)	21.383∗∗∗ (≤0.001)	22.665∗∗∗ (≤0.001)	22.568∗∗∗ (≤0.001)	20.821∗∗∗ (≤0.001)
GEN	−2.411∗∗ (−0.038)	−2.719∗∗ (−0.019)	−2.603∗∗ (−0.025)	−2.239∗ (−0.054)	−2.555∗∗ (−0.028)	−2.435∗∗ (−0.036)
AGE	0.305∗∗∗ (≤0.001)	0.300∗∗∗ (≤0.001)	0.278∗∗∗ (≤0.001)	0.305∗∗∗ (≤0.001)	0.301∗∗∗ (≤0.001)	0.278∗∗∗ (≤0.001)
HOU	−16.847∗∗∗ (≤0.001)	−17.691∗∗∗ (≤0.001)	−18.548∗∗∗ (≤0.001)	−16.342∗∗∗ (≤0.001)	−17.209∗∗∗ (≤0.001)	−18.085∗∗∗ (≤0.001)
CRE	−4.329∗∗∗ (≤0.001)	−4.211∗∗∗ (≤0.001)	−3.691∗∗∗ (≤0.001)	−3.979∗∗∗ (≤0.001)	−3.855∗∗∗ (≤0.001)	−3.318∗∗∗ (≤0.001)
EDU	−3.002∗∗∗ (≤0.001)	−2.993∗∗∗ (≤0.001)	−3.121∗∗∗ (≤0.001)	−3.020∗∗∗ (≤0.001)	−3.012∗∗∗ (≤0.001)	−3.143∗∗∗ (≤0.001)
HOUSEDEBT	−6.675∗∗∗ (≤0.001)	−6.516∗∗∗ (≤0.001)	−7.506∗∗∗ (≤0.001)	−6.704∗∗∗ (≤0.001)	−6.541∗∗∗ (≤0.001)	−7.559∗∗∗ (≤0.001)
CAR		4.100∗∗∗ (−0.001)	2.533∗∗ (−0.041)		4.223∗∗∗ (≤0.001)	2.614∗∗ (−0.035)
INCO			2.225∗∗∗ (≤0.001)			2.286∗∗∗ (≤0.001)
Constant	442.821∗∗∗ (≤0.001)	443.279∗∗∗ (≤0.001)	452.218∗∗∗ (≤0.001)	466.414∗∗∗ (≤0.001)	467.004∗∗∗ (≤0.001)	476.390∗∗∗ (≤0.001)
N	491502	491502	491502	491502	491502	491502
Adjusted R-squared	0.018	0.018	0.018	0.018	0.018	0.018

Note: ∗∗∗, ∗∗, and ∗ denote statistical significance levels at 1%, 5%, and 10%, respectively.

Table 9: Expanding the bids occurred at night.

Variables	Model 1		Model 2	
	Model 1a	Model 1b	Model 2a	Model 2b
Lnbids	−9.554∗∗∗ (≤0.001)	−9.605∗∗∗ (≤0.001)	−16.008∗∗∗ (≤0.001)	−16.080∗∗∗ (≤0.001)
ln^2 bids			1.007∗∗∗ −0.002	1.010∗∗∗ −0.002
PER	−47.040∗∗∗ (≤0.001)	−46.823∗∗∗ (≤0.001)	−46.156∗∗∗ (≤0.001)	−45.936∗∗∗ (≤0.001)
BA	−0.001∗∗∗ (≤0.001)	−0.001∗∗∗ (≤0.001)	−0.001∗∗∗ (≤0.001)	−0.001∗∗∗ (≤0.001)
RATE	−58.092∗∗∗ (≤0.001)	−58.088∗∗∗ (≤0.001)	−58.274∗∗∗ (≤0.001)	−58.271∗∗∗ (≤0.001)
Lnam	29.646∗∗∗ (≤0.001)	30.319∗∗∗ (≤0.001)	29.374∗∗∗ (≤0.001)	30.048∗∗∗ (≤0.001)
GEN	−1.408 (−0.385)	−1.475 (−0.363)	−1.316 (−0.417)	−1.383 (−0.394)

Table 9: Continued.

Variables	Model 1		Model 2	
	Model 1a	Model 1b	Model 2a	Model 2b
AGE	0.541∗∗∗ (≤0.001)	0.508∗∗∗ (≤0.001)	0.542∗∗∗ (≤0.001)	0.508∗∗∗ (≤0.001)
HOU	−25.011∗∗∗ (≤0.001)	−25.479∗∗∗ (≤0.001)	−24.754∗∗∗ (≤0.001)	−25.223∗∗∗ (≤0.001)
CRE	−7.009∗∗∗ (≤0.001)	−7.190∗∗∗ (≤0.001)	−6.826∗∗∗ (≤0.001)	−7.006∗∗∗ (≤0.001)
EDU		−3.597∗∗∗ (≤0.001)		−3.607∗∗∗ (≤0.001)
Constant	543.391∗∗∗ (≤0.001)	545.576∗∗∗ (≤0.001)	555.828∗∗∗ (≤0.001)	558.060∗∗∗ (≤0.001)
N	494854	494854	494854	494854
Adjusted R-squared	0.014	0.014	0.014	0.014

Note: ∗∗∗, ∗∗, and ∗ denote statistical significance levels at 1%, 5%, and 10%, respectively.

Table 10: Using alternative dependent variable and independent variable.

	BA	BA	BA	BA
Bids	−4.847∗∗∗ (≤0.001)	−6.206∗∗∗ (≤0.001)	−11.468∗∗∗ (≤0.001)	−14.016∗∗∗ (≤0.001)
Cum		0.007∗∗∗ (≤0.001)		0.008∗∗∗ (≤0.001)
$Bids^2$			0.019∗∗∗ (≤0.001)	0.021∗∗∗ (≤0.001)
RATE	−15.332∗∗ (−0.017)	54.121∗∗∗ (≤0.001)	−18.486∗∗∗ (−0.004)	62.783∗∗∗ (≤0.001)
GEN	−23.121∗∗ (−0.023)	−29.457∗∗∗ (−0.004)	−18.482∗ (−0.069)	−25.272∗∗ (−0.013)
AGE	3.936∗∗∗ (≤0.001)	0.748 (−0.163)	5.021∗∗∗ (≤0.001)	1.426∗∗∗ (−0.008)
HOU	202.361∗∗∗ (≤0.001)	207.980∗∗∗ (≤0.001)	187.658∗∗∗ (≤0.001)	192.159∗∗∗ (≤0.001)
CRE	68.253∗∗∗ (≤0.001)	67.464∗∗∗ (≤0.001)	96.594∗∗∗ (≤0.001)	99.732∗∗∗ (≤0.001)
EDU	49.256∗∗∗ (≤0.001)	19.182∗∗∗ (−0.003)	57.611∗∗∗ (≤0.001)	23.423∗∗∗ (≤0.001)
Constant	995.712∗∗∗ (≤0.001)	140.726 (−0.157)	1049.379∗∗∗ (≤0.001)	51.063 (−0.606)
N	483770	483770	483770	483770
Adjusted R-squared	0.016	0.022	0.023	0.029

Note: ∗∗∗, ∗∗, and ∗ denote statistical significance levels at 1%, 5%, and 10%, respectively.

The results are reported in Table 9, and the results still support our hypothesis 1 and 2 that investors on the Renrendai platform showed a significant herd behavior and there is an "inverted U-shaped" relationship between herd behavior and the number of bids orders have received.

4.4.3. Using an Alternative Dependent Variable and Independent Variable. We also reestimate our model by using alternative dependent variables to measure the herd behavior. As to the independent variables, we add the cumulated bid amount as our main independent. As shown in Table 10, with the increase of cumulated bid amount, investors increase their bid amount, while with the increase of the number of bids an order has received, investors decrease their bid amount. It is reasonable. Other things being equal, the more bids an order has got, the less the average amount of bids would be and lenders may believe other investors do not trust the orders. These results also support our hypothesis that herd behavior exist in Chinese P2P Online Lending Markets.

4.4.4. Robustness Test for Hypothesis 3. In this section, the robustness test on our hypothesis 3 is conducted by reconsidering the analysis from Section 4.3 by introducing

Table 11: Robustness test for hypothesis 3.

Variables	(1)	(2)	(3)
Velocity	0.001	0.001	0.001
	(−0.705)	(−0.7)	(−0.768)
Lnam	0.164	0.164	0.23
	(−0.471)	(−0.471)	(−0.328)
RATE	0.136∗∗∗	0.136∗∗∗	0.133∗∗
	(−0.009)	(−0.008)	(−0.011)
DUR	0.089∗∗∗	0.089∗∗∗	0.088∗∗∗
	(≤0.001)	(≤0.001)	(≤0.001)
GEN	−0.133	−0.138	−0.18
	(−0.701)	(−0.69)	(−0.607)
AGE	0.034∗	0.034∗	0.031
	(−0.083)	(−0.08)	(−0.124)
HOU	0.005	−0.043	−0.046
	(−0.984)	(−0.884)	(−0.88)
CREDIT	−2.269∗∗∗	−2.273∗∗∗	−2.264∗∗∗
	(≤0.001)	(≤0.001)	(≤0.001)
INCO	0.107	0.106	0.085
	(−0.307)	(−0.312)	(−0.427)
HOUSEDEBT		0.109	0.213
		(−0.748)	(−0.536)
EDU			−0.452∗∗∗
			(−0.004)
Constant	−7.259∗∗∗	−7.269∗∗∗	−6.782∗∗∗
	(−0.001)	(−0.001)	(−0.002)
N	11545	11545	11545
Pseudo R^2	0.610	0.609	0.617

Note: ∗∗∗, ∗∗, and ∗ denote statistical significance levels at 1%, 5%, and 10%, respectively.

INCO (the definition of INCO is the same as in 4.4.1) as the control variable. As shown in Table 11, we find the herd behavior of investors in the P2P online lending market is the blind pursuit behavior after adding further control variables, which is similar compared to the results in Table 7.

5. Conclusions

The primary aim of this study is to investigate the existence of herd behavior in Chinese online lending market Renrendai and whether the herd behavior is rational. Specifically, we conduct an empirical test and come to the following conclusions:

Firstly, there is a significant herd behavior of investors on the Renrendai online lending platform, which is consistent with studies of other scholars. Secondly, there is an "inverted U-shaped" relationship between investor herd behavior and the number of bids. With the increase of the number of bids, the time required for the order to be bid again increases, and investor herd behavior decreases. Thirdly, we get the conclusion that the herd behavior in Renrendai is partly rational, but is irrational in general. This is different from the results of American online lending platform Prosper. Furthermore, our study includes real estate and real estate debt as control variables, which is of great significant for herd behavior. In a Chinese traditional view, house is a symbol of wealth, and house may represent the repayment ability of borrowers. In this study, it is proven investors' herd behavior is more likely to occur in the listings of borrowers who own a property, while our study also proves it is irrational to pursue the "house-owner-borrowers."

Data Availability

The data used to support the findings of this study are available from the corresponding author upon request.

Conflicts of Interest

The authors declare no conflicts of interest.

Acknowledgments

This work was supported by the National Natural Science Foundation of China (Grant nos. 71790594, 71661137001, and 71532009).

References

[1] "The 44th China statistical report on internet development," 2019, http://www.cac.gov.cn/2019-08/30/c_1124938750.htm,%202019-08-30.

[2] S. Freedman and G. Z. Jin, "Do social networks solve information problems for peer-to-peer lending? evidence from prosper.com," *SSRN Electronic Journal*, 2008.

[3] A. V. Banerjee, "A simple model of herd behavior," *The Quarterly Journal of Economics*, vol. 107, no. 3, pp. 797–817, 1992.

[4] R. Shiller, "Conversation, information, and herd behavior," *American Economic Review*, vol. 85, pp. 181–185, 1995.

[5] A. P. Zemsky, "Multidimensional uncertainty and herd behavior in financial markets," *The American Economic Review*, vol. 88, no. 3, pp. 724–748, 1998.

[6] S. Bikhchandani and S. Sharma, "Herd behavior in financial markets," *IMF Staff Papers*, vol. 47, no. 3, 2001.

[7] J. C. Yang, Y. C. Ho, X. Yan, and Y. Tan, "Investor platform choice: herding, platform attributes, and regulations," *Journal of Management Information Systems*, vol. 35, pp. 86–116, 2018.

[8] Y. Zhao, W. Zhang, P. Wang, and D. Shen, "Borrower platform choice: the influencing factors on herding," *International Journal of Financial Engineering*, vol. 7, no. 1, Article ID 2050002, 2020.

[9] X. Xiong, C. Wang, and D. Shen, "Market participation willingness and investor's herding behavior: evidence from an emerging market," *Asia-Pacific Financial Markets*, vol. 27, 2020.

[10] A. Shleifer and L. H. Summers, "The noise trader approach to finance," *Journal of Economic Perspectives*, vol. 4, no. 2, pp. 19–33, 1990.

[11] G. Elison and D. Fudenberg, "Rules of thumb for social learning," *Journal of Political Economy*, vol. 101, 1993.

[12] K. A. Krumme and S. Herrero, "Lending behavior and community structure in an online peer-to-peer economic network," in *Proceedings of the 2009 International Conference on Computational Science and Engineering*, Vancouver, Canada, August 2009.

[13] M. Herzenstein, U. M. Dholakia, R. L. Andrews et al., "Strategic herding behavior in peer-to-peer loan auctions,"

Journal of Interactive Marketing, vol. 25, no. 1, pp. 27–36, 1990.

[14] E. Berkovich, "Search and herding effects in peer-to-peer lending: evidence from prosper.com," *Annals of Finance*, vol. 7, no. 3, pp. 389–405, 2011.

[15] E. Lee and B. Lee, "Herding behavior in online P2P lending: an empirical investigation," *Electronic Commerce Research and Applications*, vol. 11, no. 5, pp. 495–503, 2012.

[16] H. Yum, B. Lee, and M. Chae, "From the wisdom of crowds to my own judgment in microfinance through online peer-to-peer lending platforms," *Electronic Commerce Research and Applications*, vol. 11, no. 5, pp. 469–483, 2012.

[17] L. Liao, M. R. Li, Z. W. Wang et al., "Learning by observing: information discovery and herding behavior in P2P lending market," *Journal of Tsinghua University (Philosophy and Social Sciences)*, vol. 1, pp. 156–165, 2015.

[18] X. G. Li and Y. F. Liu, "Study on the formation mechanism for P2P herding effect in China and the countermeasures," *Cedit Reference*, vol. 33, no. 12, pp. 64–68, 2015.

[19] Y. L. Li, Y. Guo, and W. Zhang, "The analysis of impact factors on loan performance in Chinese P2P Microfinance market," *Journal of Finance Research*, vol. 7, pp. 126–138, 2013.

[20] Y. B. Lv, Y. W. Jiang, and X. Q. Zhang, "Research on overdue behavior and herd behavior of P2P platform online lending in China," *Statistic and Decision*, vol. 4, p. 162, 2016.

[21] J. Zhang and P. Liu, "Rational herding in microloan markets"" *Management Science*, vol. 58, no. 5, pp. 64–68, 2012.

[22] B. Luo and Z. Lin, "A decision tree model for herd behavior and empirical evidence from the online P2P lending market," *Information Systems and E-Business Management*, vol. 11, no. 1, pp. 141–160, 2013.

[23] D. Chen and Z. Lin, "Rational or irrational herding in online microloan markets: evidence from China," *Social Science Electronic Publishing*, 2014.

[24] J. H. Zeng and S. Yang, "Herding behavior of lenders in P2P lending markets and its rational test: evidence from PaiPaiDai market," *Modern Finance and Economics*, vol. 7, pp. 22–32, 2014.

Hindawi
Discrete Dynamics in Nature and Society
Volume 2021, Article ID 6681035, 14 pages
https://doi.org/10.1155/2021/6681035

Research Article

Pricing Corporate Bonds with Credit Risk, Liquidity Risk, and Their Correlation

Xinting Li,[1] **Baochen Yang**,[2] **Yunpeng Su**,[2] **and Yunbi An**[3]

[1]*College of International Relations, National University of Defense Technology, Nanjing 210000, China*
[2]*College of Management and Economics, Tianjin University, Tianjin 300072, China*
[3]*Odette School of Business, University of Windsor, Windsor N9B3P4, Canada*

Correspondence should be addressed to Baochen Yang; bchyang@tju.edu.cn

Received 7 December 2020; Revised 3 February 2021; Accepted 19 February 2021; Published 3 March 2021

Academic Editor: Xiao Li

This paper proposes a generalized bond pricing model, accounting for all the effects of credit risk, liquidity risk, and their correlation. We use an informed trading model to specify the bond liquidity payoff and analyze the sources of liquidity risk. We show that liquidity risk arises from reduced information accuracy and market risk tolerance, and it is market risk tolerance that links credit and liquidity. Then, we extend the traditional bond pricing model with only credit risk by incorporating liquidity risk into the framework in which the probabilities of the two risk events are estimated by a joint distribution. Using numerical examples, we analyze the role of the correlation between credit and liquidity in bond pricing, especially during a financial crisis. We document that the varying correlation between default and illiquidity explains the phenomenon of bond death spiral observed in a financial crisis. Finally, we take the US corporate bond market as an example to demonstrate our conclusions.

1. Introduction

Unlike government bonds, corporate bonds require risk compensation, which is referred to as yield spreads. The risk of corporate bonds is typically classified into two categories: credit risk and liquidity risk [1–5]. During the financial crisis of 2007–2008, these two risk premia increased alternately, leading to a substantial decline in bond prices, a phenomenon known as the bond death spiral. Empirical evidence shows that credit and liquidity risks interact with each other, and this interaction plays a crucial role in bond pricing. For example, some previous work documents that credit is correlated with liquidity spreads in the US bond market [6], which was particularly pronounced during the subprime crisis [7, 8]. As the correlation between the two risk factors in regression models renders the empirical results hard to interpret, researchers try to disentangle the two sources of risk in yield spreads to provide a robust analysis of yield spreads [9–12]. While this issue is empirically analyzed in the literature, there is a lack of theoretical analysis of the way in which the correlation arises and how it impacts yield spreads.

This paper proposes a generalized bond pricing model, accounting for all the effects of credit risk, liquidity risk, and their correlation. First, we incorporate liquidity risk into the traditional bond pricing model. The two important developments in the corporate bond literature are the structural-form [13] and reduced-form models [14]. The former provides a perfect explanation of corporate bond prices, while the latter is better able to evaluate the default probability and default loss using historical data. One of problems with these models is that most traditional models deal with credit risk only and ignore the effects of liquidity risk and its correlation with credit risk. Inspired by Jarrow et al. [15] who proposed a method for pricing callable bonds by considering credit risk and call risk within a unified framework, we consider both credit and liquidity risks as a factor that leads to the potential termination of obligations.

Similar to default, liquidating a bond can also be regarded as an event that terminates a loan contract from the bondholders' perspective. Therefore, we extend the traditional one-risk model to a two-risk model in which credit risk and liquidity risk are correlated.

Second, we explore the key factor that results in the correlation between the two risks. We note that liquidity risk encompasses multiple dimensions and is more complex than credit risk. Thus, we focus on liquidity risk to gauge how the correlation arises. While there is an extensive literature on liquidity risk, there is no unified aggregate proxy for liquidity [16–18]. One of the measures of bond liquidity is the marketability discount, which is the loss due to the quick sale of a bond. Market microstructure theory on marketability discount provides distinct views of liquidity. These models consider various factors such as information asymmetry, imperfect competition, and funding constraints to interpret the determination of the marketability discount [19–22]. Some studies incorporate these factors into traditional trading models and analyze their effects on asset trading, explaining changes in asset prices in different periods [23, 24]; others examine the role of these factors in asset pricing by calculating the deviation between the asset cash flows and trading price in a single-period model [21, 25–27]. Regardless of the approach used, these models all reach similar conclusions about the factors that impact the trading price. In particular, most of these articles show a strong linkage between information asymmetry and marketability discount.

Since liquidity loss arises from the trading process, in this paper, we use an informed trading model to specify a bond's marketability discount and analyze the sources of liquidity risk. We document that liquidity risk arises from reduced information accuracy and market risk tolerance. The reduction in market risk tolerance is due to the concerns about poor firm performance and worsening market conditions. Thus, market risk tolerance is related to the incidence of default, while information accuracy is irrelevant to default. In other words, changes in the correlation between credit and liquidity are driven by changes in market risk tolerance. Moreover, to calculate the probabilities of default and trade with a nonzero correlation, we adopt a Frank Copula function to describe the joint distribution of the two events.

Third, using numerical examples, we analyze the role of the correlation between credit and liquidity in bond pricing and explain the phenomenon of bond death spiral observed in a financial crisis. We find that a positive correlation between default and trade decreases yield spreads, while a negative one increases them. In addition, we analyze both credit-leading crisis and liquidity-leading crisis by dividing the crisis time interval into sufficiently short subintervals. We explore the effect of the varying correlation, which arises from decreasing market risk tolerance, on both credit and liquidity risk premia in each subinterval. We find that, during a financial crisis, a decrease in market risk tolerance changes the correlation from positive to negative, which leads to the risk contagion, ultimately resulting in the bond death spiral.

Fourth, we take the US corporate bond market as example to illustrate how the correlation between credit risk and liquidity risk influences bond prices under different market conditions. Using a Markov-switching model to describe the changes of the relationship between yield spreads and risk factors, we show that the correlation plays an important role in bond market during financial crisis. Moreover, the changes of correlation parameters during a crisis are consistent with what our bond pricing model predicts and provide evidence in support of the numerical analysis.

The remainder of the paper is structured as follows. Section 2 describes the model framework. Section 3 discusses the method of estimating parameters in our model. Section 4 uses numerical examples to show how the correlation influences bond prices, particularly the role of the correlation in bond pricing during the crisis time. Section 5 provides the empirical analysis of the US bond market. Section 6 concludes.

2. The Model Framework

There are two alternative approaches to modeling credit risk: the structural model [13] and the reduced model [28]. The traditional structural approach assumes a stochastic process for firm value to evaluate bonds, while the reduced approach assumes an exogenous process for a firm's default time and recovery rate. From a theoretical point of view, the structural model better explains the process for bond prices. However, the perfect information assumption in this model contradicts with the theoretical and empirical evidence on credit market equilibrium [29]. Since most information used in this model is not readily available, previous research finds that the structural model is not able to accurately explain real yield spreads [30–32]. In contrast, the reduced model is better able to evaluate the probability and loss of credit risk by using historical default and trade data instead of the companies' asset value information.

In this paper, we adopt the reduced modeling approach to analyze our research issues. However, the traditional reduced model deals with credit risk only. Jarrow et al. [15] propose a reduced-form approach for valuing callable corporate bonds by characterizing the call probability via an intensity process. Following this line of thought, we develop a model framework that accommodates both credit risk and liquidity risk, in which the two risks are characterized by two events, default and trade, meaning the end of a lending relationship.

Assume that the economic uncertainty is characterized by a filtered probability space $\{\Omega, F, P\}$satisfying the usual conditions, where Ω is the sample space, F is the set of events, and P is the statistical probability measure. We use $\{(Y, T), (Y_d, \tau_d), (Y_s, \tau_s)\}$ to denote the cash flows from a zero-coupon corporate bond under various scenarios. The first claim (Y, T) represents the obligation of the firm to pay Y dollars at maturity T. The second claim (Y_d, τ_d) represents the case of default, in which investors receive a residual value Y_d dollars at the default time τ_d. Y_d is just part of the bond's face value, and the ratio of Y_d to Y is referred to as the

recovery rate, denoted as y_d. The third claim (Y_s, τ_s) represents the case of trade, where investors sell the bond for Y_s dollars at time τ_s. The payoff of this trade is less than the present value of its future cash flow due to imperfect market conditions. In theory, the trade price is based on the bond cash flow, but is also determined by several other factors that are exogenous. We refer to $y_s = (Y_s/Y)$ as the payoff ratio. Both the default recovery rate and the liquidity payoff ratio depend on market conditions and can be stochastic.

Accordingly, without the cost of time, the payoff from a zero-coupon bond with a face value of \$1 and maturity date of T can be expressed as follows:

$$Z = y_d 1_{\{\tau_d < \tau_s, \tau_d < T\}} + y_s 1_{\{\tau_s < \tau_d, \tau_s < T\}} + 1_{\{T < \tau_d, T < \tau_s\}}, \quad (1)$$

where $1_{\{\cdot\}}$ is an indicator function. Let r_f be the instantaneous risk-free interest rate and r be risky interest rate. Assume that the process of the risk-free rate is independent of that of the risky rate. The value of the bond at time t is given as

$$\begin{aligned} V(t,T) &= E_t^Q \left\{ e^{-\int_t^T r(u) + r_f(u)\mathrm{d}u} \right\} \\ &= E_t^Q \left\{ e^{-\int_t^{T_0} r_f(u)\mathrm{d}u} \right\} E_t^Q \left\{ e^{-\int_t^T r(u)\mathrm{d}u} \right\} \\ &= E_t^Q \left\{ e^{-\int_t^{T_0} r_f(u)\mathrm{d}u} \right\} E_t^Q\{Z\}, \end{aligned} \quad (2)$$

where V is the value of the bond, Q is the equivalent (to P) probability measure such that all discounted bond prices are martingales with respect to the information set at time t, and E^Q is the expectation operator under probability measure Q. As we can see, the value of the bond consists of two parts, $E_t^Q\left\{e^{-\int_t^{T_0} r_f \mathrm{d}u}\right\}$ and $E_t^Q\{Z\}$. The former is the discounted value at the risk-free rate (which is not the focus of this paper), and the latter is the discounted value at the risky interest rate, and the primary source of yield spreads.

The default and trade probabilities are $P_d = P[\tau_d < T, \tau_d < \tau_s]$ and $P_s = P[\tau_s < T, \tau_s < \tau_d]$, respectively. Then, the expected payoff Z from the zero-coupon bond is

$$E_t^Q\{Z\} = y_d P_d + y_s P_s + 1P_m, \quad (3)$$

where P_m represents the probability of holding the bond until maturity. Apparently, $P_d + P_s + P_m = 1$.

Equation (3) represents a generalized model framework that accounts for the effects of the incidences of both default and trade. Importantly, in this model, default and trade are allowed to be correlated. To value a bond, we need to evaluate bondholders' losses arising from default or trade and the instantaneous probabilities of the two related events.

3. Estimating Liquidity Payoff and Probabilities of Default and Trade

3.1. Liquidity Payoff. Reduced pricing models use historical data to estimate the default loss. However, it is difficult to estimate the loss of trade using historical data, as liquidity risk is more complex than credit risk. Illiquidity can be defined as the value that bondholders must give up for bond liquidating. As discussed in Section 2, the liquidity payoff is the bond's cash flow minus its marketability discount. The payoff ratio can be expressed as

$$y_s = \gamma(1 - w), \quad (4)$$

where γ is the value of the bond with face value of \$1 considering credit risk only and w is the marketability discount. As the estimation of γ is well defined in previous bond pricing models [14, 33], y_s can be obtained if the expression of marketability discount w is known.

Equation (4) implies that liquidity risk arises from the trading process, and we can measure liquidity loss in terms of marketability discount. Note that information risk is identified as a crucial factor in the trading process [34–36]. In particular, previous studies show that information asymmetry is one of the most important factors affecting bond prices [37, 38]. Therefore, to examine the marketability discount, we consider a bond trading discount model with information asymmetry.

3.1.1. Marketability Discount. Following Lambert et al. [27], we assume that there are two types of investors in the bond market: a limited number of informed investors (such as institutional investors) and infinite uninformed investors (such as individual investors) who have no private information but can learn from market prices. The market is competitive, and all investors are risk averse and maximize their personal utilities.

At any time before maturity, let $\widetilde{Y}$ represent the present value of the bond's cash flow considering default risk and P represent its trading price. We first consider informed investors' behavior in the market. As the superior trader in the market, an informed trader owns private information about the bond value $Y_{\text{in}} = \widetilde{Y} + \varepsilon_{\text{in}}$, where ε_{in} is an error with a mean of 0 and variance of σ_{in}^2 (the precision is denoted by $\Pi_{i\varepsilon}$). Correspondingly, the precision of the informed investor's evaluation of the bond is $\Pi_{\text{in}} = \Pi_v + \Pi_{i\varepsilon}$. Thus, the expected bond value based on his private information is

$$E\left[\widetilde{Y} \middle| \Omega_{\text{in}}\right] = E[\widetilde{Y}] + \frac{\Pi_{i\varepsilon}}{\Pi_{\text{in}}}\left(Y_{\text{in}} - E[\widetilde{Y}]\right), \quad (5)$$

where Ω_{in} is the information set for the informed investor. Equation (5) indicates that the conditional expectation of bond value is composed of two parts: the expected bond value and the evaluation error.

We suppose the informed trader has constant absolute risk tolerance λ_{in}. Based on his belief as to how his demand affects the market, this investor chooses his demand for

bonds, D_{in}, to maximize his profits, S_{in}, which are given as follows:

$$S_{\text{in}} = \left\{ E\left[\widetilde{Y}|\Omega_{\text{in}}\right] - P - \frac{D_{\text{in}}}{2\lambda_{\text{in}}\Pi_{\text{in}}} \right\} D_{\text{in}}. \tag{6}$$

Taking the partial derivative of S_{in} with respect to D_{in} and setting it equal to 0 gives

$$D_{\text{in}} = \left(E\left[\widetilde{Y}|\Omega_{\text{in}}\right] - P\right)\Pi_{\text{in}}\lambda_{\text{in}}. \tag{7}$$

Similarly, for an uninformed trader, the value of the bond is $Y_{\text{un}} = \widetilde{Y} + \varepsilon_{\text{un}}$, where ε_{un} is an error with mean 0, variance σ^2_{un}, and precision $\Pi_{u\varepsilon}$. The uninformed trader's constant absolute risk tolerance is λ_{un} and her demand for bonds is D_{un}. Thus, her expected value and profit function are as follows, respectively:

$$E\left[\widetilde{Y}|\Omega_{\text{un}}\right] = E[\widetilde{Y}] + \frac{\Pi_{u\varepsilon}}{\Pi_{\text{un}}}\left(Y_{\text{un}} - E[\widetilde{Y}]\right), \tag{8}$$

$$S_{\text{un}} = \left\{ E\left[\widetilde{Y}|\Omega_{\text{un}}\right] - P - \frac{D_{\text{un}}}{2\lambda_{\text{un}}\Pi_{\text{un}}} \right\} D_{\text{un}}. \tag{9}$$

Taking the derivative of equation (9) with respect to D_{un} and setting it equal to 0 yields

$$D_{\text{un}} = \left(E\left[\widetilde{Y}|\Omega_{\text{un}}\right] - P\right)\Pi_{\text{un}}\lambda_{\text{un}}. \tag{10}$$

Let L be the supply in the bond market and N (M) represent the number of informed (uninformed) traders. The market clearing condition is as follows:

$$\text{ND}_{\text{in}} + \text{MD}_{\text{un}} = L. \tag{11}$$

As assumed, there are infinite uninformed investors in the market with limited wealth. They do not have any private information about the bond value, but they can analyze market prices to infer the private information owned by informed investors. For simplicity, we assume that M is large (i.e., $M \longrightarrow +\infty$) and λ_{un} is small (i.e., $\lambda_{\text{un}} \longrightarrow 0$), and the product of $M$and λ_{un} converges to a nonnegative constant ω, or $M\lambda_{\text{un}} \longrightarrow \omega$.

We can prove that the value the uninformed trader learns from market prices can be expressed as follows:

$$Y_{\text{learn}} = \widetilde{Y} + \varepsilon_{\text{in}} - \left(N\lambda_{\text{in}}\Pi_{i\varepsilon}\right)^{-1} L. \tag{12}$$

See the proof in Appendix A.

Similar to equation (8), we have the following:

$$E\left[\widetilde{Y}|\Omega_{\text{un}}\right] = E[\widetilde{Y}] + \frac{\Pi_{\text{learn}}}{\Pi_{\text{un}}}\left(Y_{\text{learn}} + E\left[Y_{\text{learn}}\right]\right), \tag{13}$$

where Π_{learn} is the precision of $\varepsilon_{\text{learn}}$ and $\Pi_{\text{un}} = \Pi_v + \Pi_\gamma$ is the precision of a uninformed investor's evaluation of the bond.

Thus, we can derive the marketability discount w, as follows:

$$w = E[\widetilde{Y}] - E[P] = \Pi^{-1}E(L)\lambda^{-1}, \tag{14}$$

where Π and λ are given as follows:

$$\Pi = \frac{N\lambda_{\text{in}}\Pi_{\text{in}} + M\lambda_{\text{un}}\Pi_{\text{un}}}{N\lambda_{\text{in}} + M\lambda_{\text{un}}}, \tag{15}$$

$$\lambda = N\lambda_{\text{in}} + M\lambda_{\text{un}}. \tag{16}$$

The proofs of equations (14) to (16) are provided in Appendix B. Equation (14) is the gap between the trading price of a bond and its future cash flow.

3.1.2. Decomposition of Marketability Discount. The trading discount model provides a method to measure the marketability discount, and equations (14) to (16) show that the marketability discount depends on a variety of variables, such as participants' information accuracy, risk tolerance, number of participants, and amount of supply. Now, we simplify these expressions and explore the economic implications of the model.

Based on equation (15), Π can be considered as the weighted average value of $\Pi_{i\varepsilon}$ and Π_{un}, where the weights are $N\lambda_{\text{in}}\left(N\lambda_{\text{in}} + M\lambda_{\text{un}}\right)^{-1}$ and $M\lambda_{\text{un}}\left(N\lambda_{\text{in}} + M\lambda_{\text{un}}\right)^{-1}$, respectively. $N\lambda_{\text{in}}$ ($M\lambda_{\text{un}}$) measures all informed (uninformed) traders' risk tolerance or wealth. Thus, Π measures the market average information accuracy level, and it does not change with wealth but can be affected by information transparency. Since $\lambda$is the sum of two risk tolerances of informed and uninformed investors as can be seen in equation (16), it measures total risk tolerance of all investors, which is referred to as the market risk tolerance. Unlike Π, λ can be affected by wealth.

The changes of these two factors, information accuracy Π or the market risk tolerance λ, are closely related to bond supply. Accordingly, in equation (14), L can be divided into two parts: L_Π and L_λ. L_Π is caused by information asymmetry, and L_λ is caused by reduced market risk tolerance.

Similarly, marketability discount is also influenced by market average information accuracy level and market risk tolerance, and thus, the marketability discount in equation (14) can be rewritten as follows:

$$w = \left(\Pi^{-1}E\left(L_\Pi\right)\right)\left(E\left(L_\lambda\right)\lambda^{-1}\right) = \Pi^*\lambda^*. \tag{17}$$

Equation (17) says that an increase in Π^* leads to an increase in liquidity risk. This is because a decrease in the average information accuracy of the market Π, which can be due to the inaccuracy of firms' information disclosure or the lack of investors' capability of gathering and processing information, will have a negative effect on trading, as shown in dramatic crashes in the US stock market, most notably the 1929 and 1987 crashes. In a market where uninformed investors are unable to distinguish hedging activity from information-based trades, large numbers of such investors may revise downward their expectations when there are, what appear to be, infinitesimal shifts in information or other small shocks that lead to lower prices [39]. Thus, equation (17) implies that the liquidity loss can be due to the reduction in information accuracy.

In addition, an increase in λ^* can also result in higher liquidity risk. This is because the total risk tolerance λ

declines as a result of the deterioration of a firm's own performance or poor macroeconomic conditions, which might lead to bond default. In the case of firms' poor performance, lack of confidence in the firms' capability of meeting their obligations makes investors more cautious when trading to avoid losses, reducing λ_x (x = in or un). In the case of poor economic conditions, traders may not have sufficient funds to absorb trading losses, leading to decreased risk tolerance, λ_x. The former fear of loss arises directly from the deteriorating financial health of firms, while the latter is a macroeconomic factor that indirectly increases traders' fear of default via the aggregate market liquidity. These two types of fear make investors more cautious when making trading decisions and more sensitive to default risk, leading to a lower value of λ^*. Thus, equation (17) implies that the liquidity loss can also be due to the reduced market risk tolerance.

Identifying the sources of liquidity risk has several implications. First, it provides an explanation of liquidity risk in bond pricing and a method to calculate liquidity payoff. Plugging the expression of marketability discount in equations (17) into (4) gives the payoff ratio as follows:

$$y_s = \gamma - \Pi^* \lambda^*. \tag{18}$$

Second, it provides a theoretical explanation about the correlation between credit and liquidity risks in bond markets. Previous studies [8, 9] show that liquidity risk is related to default risk, and their impacts on yield spreads are not independent of one another, but these studies are not able to explain the causes of the correlation. We find that bond liquidity risk arises from reduced information accuracy and market risk tolerance. The first factor reflects the opacity of information and investors' ability to capture the information, which are determined by exogenous factors such as market regulations and the overall quality of market investors. This factor is independent of the credit level of bonds. In contrast, reduced market risk tolerance arises from deterioration of the firm's performance and worsening economic conditions, both of which contribute significantly to corporate default and make investors more concerned about the loss of their investments. In conclusion, there are significant differences between these two factors. The former is independent of default risk, while the latter is related to default risk. Moreover, a decrease in market risk tolerance not only aggregates the marketability discount but also influences the correlation between credit and liquidity risks.

3.2. Probabilities of Default and Trade. The traditional reduced-form model provides a framework for us to price corporate bonds, whereas the trading discount model specifies liquidity loss as a trading process. Given our discussions in Section 3.1, we can obtain a generalized bond pricing model by combining the traditional and trading methods. Plugging equation (18) into (3), we obtain the expected payoff of a zero-coupon bond as follows:

$$E_t^Q\{Z\} = y_d P_d + (\gamma - \Pi^* \lambda^*) P_s + P_m. \tag{19}$$

In this section, we turn our attention to estimating the probabilities of default and trade. Following Jarrow et al. [15] who characterized both the call and default as a point process, we assume that both default and trade arrive with an intensity process, where their intensities are $h_d(t)$ and $h_s(t)$, respectively. For a sufficiently small number Δ, the intensity process can be expressed as

$$\begin{aligned} h_d(t)\Delta &= P\left(t < \tau_d < t + \Delta | \tau_d > t\right) = \frac{F_d'(t)}{1 - F_d(t)}, \\ h_s(t)\Delta &= P\left(t < \tau_s < t + \Delta | \tau_s > t\right) = \frac{F_s'(t)}{1 - F_s(t)}. \end{aligned} \tag{20}$$

Then, for $x \in [t, t + \Delta]$, the marginal distributions can be calculated as follows:

$$\begin{aligned} F_d(x) &= 1 - e^{-h_d(x-t)t}. \\ F_s(x) &= 1 - e^{-h_s(x-t)t}. \end{aligned} \tag{21}$$

Since the incidences of default and trade are not independent, we use a joint distribution function to describe the probabilities of the two events. To this end, we assume time τ_d and τ_s have a joint probability density function $f(\tau_d, \tau_s)$ and a joint probability distribution function $F(\tau_d, \tau_s)$. Therefore, in the interval $[t, t + \Delta]$, the probabilities of the two events, $P_d(\Delta)$and $P_s(\Delta)$, can be expressed as

$$P_d(\Delta) = \int_t^{t+\Delta} \left(\frac{\partial F}{\partial x}|_{y=+\infty} - \frac{\partial F}{\partial x}|_{y=x} \right) \mathrm{d}x, \tag{22a}$$

$$P_s(\Delta) = \int_t^{t+\Delta} \left(\frac{\partial F}{\partial y}|_{x=+\infty} - \frac{\partial F}{\partial y}|_{x=y} \right) \mathrm{d}y. \tag{22b}$$

Given that risk varies with macroeconomic and market conditions, we divide the interval $[0, T]$ into N subintervals $[t_i, t_{i+1}]$ ($i = 1, \ldots, N$), where N is big enough so that each subinterval is very short. In each subinterval, the probabilities can be written as $P_{d,i} = P[\tau_d \le t_{i+1}, \tau_d \le \tau_s | \Phi_i]$ and $P_{s,i} = P[\tau_s \le t_{i+1}, \tau_s \le \tau_d | \Phi_i]$, where Φ_i is the information set at time t_i in which $\tau_d > t_i$ and $\tau_s > t_i$.

Proposition 1. *The probabilities of the two events in* $[0, T]$ *are given by*

$$P_d = \sum_{i=1}^{n} P_{d,i} \prod_{j=1}^{i} \left(1 - P_{d,j} - P_{s,j}\right), \tag{23a}$$

$$P_s = \sum_{i=1}^{n} P_{s,i} \prod_{j=1}^{i} \left(1 - P_{d,j} - P_{s,j}\right). \tag{23b}$$

Proof. See Appendix C

By specifying the joint distribution function $F(x, y)$, the probabilities of the two events can be estimated using equations 23a and 23b. With the estimates of the losses of default and trade, we are able to price bonds using equation (19), which accounts for liquidity risk, credit risk, and their correlation. We use the Frank Copula function as the cumulative distribution function in our numerical analysis, which is as follows:

$$F(x, y) = C(u, v) = -\frac{1}{\alpha}\ln\left\{1 + \frac{\left(e^{-\alpha u} - 1\right)\left(e^{-\alpha v} - 1\right)}{e^{-\alpha} - 1}\right\}, \tag{24}$$

where $\alpha \neq 0$ and u and v represent the distribution functions of default and trade, respectively. The marginal distributions are given as follows:

$$F_x = \frac{h_d e^{-h_d x}\Psi_y\left(\Psi_x + 1\right)}{\Psi_y\Psi_x + \left(e^{-\alpha} - 1\right)},$$
$$F_y = \frac{h_s e^{-h_s x}\Psi_x\left(\Psi_y + 1\right)}{\Psi_y\Psi_x + \left(e^{-\alpha} - 1\right)}, \tag{25}$$

where

$$\Psi_x = \exp\left\{-\alpha\left(1 - e^{-h_d x}\right)\right\} - 1,$$
$$\Psi_y = \exp\left\{-\alpha\left(1 - e^{-h_s y}\right)\right\} - 1. \tag{26}$$

As noted, the impacts of reduced information accuracy and market risk tolerance on bond pricing differ from each other. Information accuracy influences $h_s(t)$ and y_s, while market risk tolerance impacts $h_s(t)$, y_s, and α. □

4. Numerical Analysis

The correlation between credit and liquidity risks has an effect on the estimated probabilities of default and trade. In this section, we analyze the influence of the correlation on bond pricing and investigate the role it plays in explaining bond death spiral in a financial crisis. For simplicity, we assume that all parameters in our model are constants in each subinterval $[t_i, t_{i+1}]$.

4.1. Correlation and Bond Pricing. The correlation between credit and liquidity risks varies over time and thus parameter α changes. In general, a slight decline in the credit level in a company makes investors more sensitive to bond prices and increases the turnover rates, resulting in a positive correlation parameter α. As $\alpha > 0$ means that an increase in credit risk reduces liquidity risk, a positive α represents a negative correlation between credit and liquidity. However, if the credit level drops drastically, investors' fear of default increases sharply, thereby decreasing the market risk tolerance substantially. Then, the demand for bonds in the market is reduced, leading to fewer transactions, and thus a negative α. $\alpha < 0$ means that an increase in credit risk increases liquidity risk and thus represents a positive correlation between credit and liquidity. As stated in Section 3, the correlation between credit risk and liquidity risk is influenced by the percentage of market risk tolerance λ^* in trading cost w. Then, $\alpha \propto (-\lambda^*/w)$. Here, we assume that α is linearly related to (λ^*/w), and $\alpha = 10 - 20(\lambda^*/w)$.

In this analysis, we consider various values of α to gauge the influence of the correlation on bond pricing. To this end, we consider bonds with a face value of 100 dollars and maturities ranging from 1 to 30 years. We use the average annualized yield spreads of these bonds as a measure of risk impact on bond prices. The model parameters are specified as follows: $h_d = 0.1$, $h_s = 0.2$, $y_d = 0.5$ $y_s = \gamma(1 - w)$, and $w = 0.3$, λ^* ranges from 0 to 0.3, and α ($\alpha = 10 - 20(\lambda^*/w)$) ranges from -10 to 10 ($\alpha = 0$ means no correlation). The results are plotted in Figure 1(a).

Figure 1(a) shows that the yield spreads of bonds with different maturities vary with the value of the correlation parameter α. As noted, a positive α implies active trading in the market, which means that it is easy for investors to trade bonds to reduce their holding risk, resulting in lower yield spreads. On the contrary, in the case of a negative α, it is difficult for investors to sell their bonds, as the probability of default is high. Thus, investors have to lower the prices to sell or continue to hold their bonds with high credit risk, which decreases the payoff of bonds directly or indirectly, leading to a higher yield spreads. Mathematically, a positive correlation parameter α reduces the probability of both default and trade, or $P_d = P[\tau_d < T, \tau_d < \tau_s]$ and $P_s = P[\tau_s < T, \tau_s < \tau_d]$. Conversely, a negative correlation parameter α can lead to a higher probability of both risk events, or $P_d + P_s$, for both short- and long-term bonds. Moreover, the changes in yield spreads become less pronounced when the absolute value of the correlation parameter, $|\alpha|$, is higher.

To further analyze the correlation effects, we consider the α effects of investment grade and speculative grade bonds. To illustrate, we use parameter values for investment grade bonds as follows: $h_d = 0.05$, $h_s = 0.4$, $y_d = 0.75$, $y_s = \gamma(1 - w)$, $w = 0.3$, λ^* ranges from 0 to 0.3, and $\alpha(\alpha = 10 - 20(\lambda^*/w))$ ranges from -10 to 10 ($\alpha = 0$ means no correlation). For speculative grade bonds, these values are $h_d = 0.35$, $h_s = 0.4$, $y_d = 0.35$, $y_s = \gamma(1 - w)$, $w = 0.3$, and α ranges from -10 to 10. We use $((r_\alpha - r_0)/r_0)$, where r_α is the average yield spread of bonds with different maturities when $\alpha \neq 0$ and r_0 is the yield spread when $\alpha = 0$, as a proxy for the correlation effect. Figure 1(b) plots the correlation effect as a function of α. The figure shows that speculative grade and short-term bonds are more sensitive to α, regardless of whether α is positive or negative.

4.2. Correlation and Yield Spreads during a Financial Crisis. A financial crisis can be driven by either a sharp drop in the credit level of bonds or the lack of liquidity as a result of poor macroeconomic conditions. Accordingly, there are two types of crisis: credit-leading crisis and liquidity-leading crisis. While the market reacts quickly to credit or liquidity shocks, it takes time for the market to fully absorb the information. In this section, we analyze various stages of the two types of crisis to show the role that correlation plays in

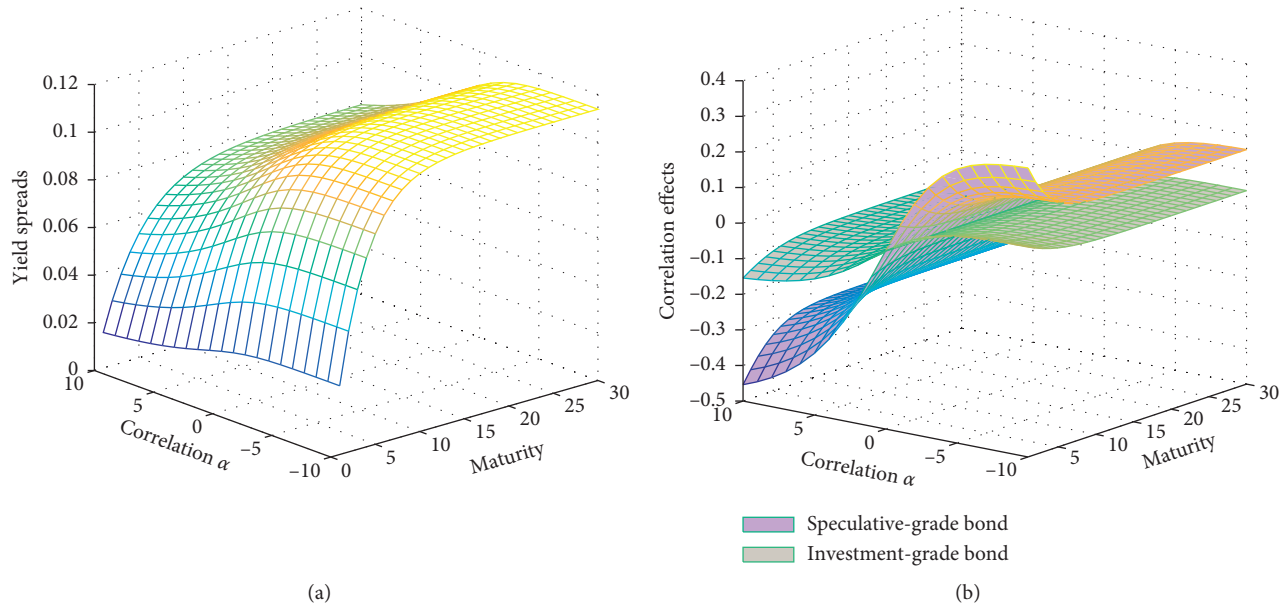

Figure 1: The influence of correlation parameter α on yield spreads.

explaining the changes in yield spreads and risk premia in different stages and interpret the way in which bond death spiral forms during a financial crisis.

4.2.1. Credit-Leading Crisis. Credit-leading crisis is caused by a sudden drop in the credit level of bonds, which may be due to significant news events or reported changes in fundamentals. This drop decreases investors' risk tolerance, leading to a substantial decrease in market risk tolerance. The sudden and disruptive re-pricing of Euro area sovereign credit risk in 2008–2012 is a vivid example. To avoid crisis, Euro area governments announced a set of rescue packages to increase confidence in their banking systems [39]. As noted in Section 4.1, in this case correlation parameter, α changes from positive to negative. On the contrary, as we see in Section 3, a decrease in market risk tolerance results in a lower liquidity payoff. Investors tend to sell their bonds as quickly as possible in the market to reduce their risk. To alleviate price shocks, in this case, investors tend to split a sell order into several trades rather than executing in a single trade [1]. For this reason, we assume that reduced market risk tolerance does not change the parameters of trade intensity. Additionally, due to the deterioration of market conditions, companies are prone to conceal information from investors, which reduces information accuracy.

In summary, credit crash influences the credit level, market risk tolerance, payoff of liquidity, and information accuracy, which in turn impact yield spreads. To illustrate, we consider these in four stages. The changes in model parameters in each stage are described as follows:

(1) In the first stage, credit risk rises. In other words, default payoff y_d declines and default intensity h_d rises. Thus, the value of the bond's cash flow decreases, and the marketability discount w increases slightly. Then, liquidity payoff y_s falls, given that y_s equals $\gamma(1-w)$.

(2) In the second stage, the market risk tolerance decrease significantly, namely, (λ^*/w) rises. As a result, the correlation parameter α changes from positive to negative.

(3) In the third stage, the payoff of liquidity drops. As part of liquidity, reduced market risk tolerance decreases the payoff of liquidity.

(4) Payoff of liquidity continues to decline due to worsening information transparency.

The changes in these parameters in these stages are plotted in Figure 2.

Figure 3 plots the average values of yield spreads as well as credit and liquidity premia for bonds with various maturities considered in different stages. In each period, yield spreads increase over time. From Figures 2 and 3, we see that increases in yield spreads are caused not only by increases in liquidity and credit risks but also by changes in the correlation parameter. In stage 2, while both default and trade parameters remain unchanged, the yield spreads increase significantly due to the sharp drop in market risk tolerance.

The credit and liquidity risk premia presented in Figure 3 also show an up-trend during all the periods. At the first two stages, credit risk plays a dominant role in the changes in yield spreads, as default parameters change substantially. During these two periods, liquidity risk moves up mildly. The increase in (λ^*/w) in stage 2 is the primary reason for the increase in liquidity risk in stage 3. A significant drop in trade payoff caused by transaction dilemma brings a notable increase in liquidity premium, which accounts for a large part of the yield spreads.

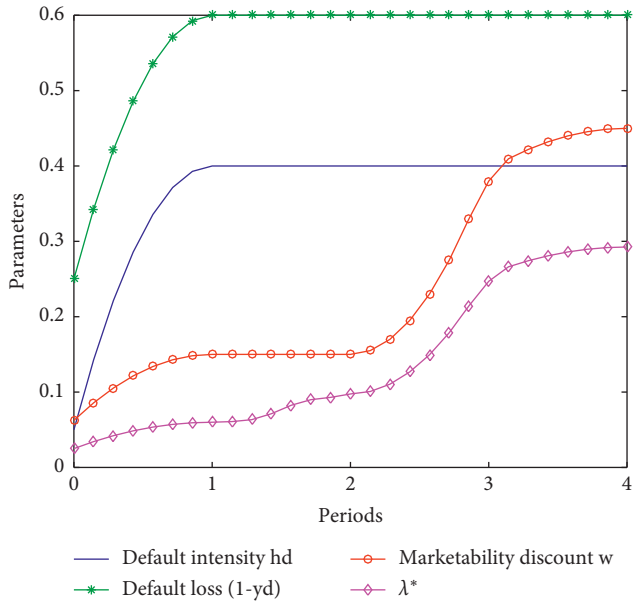

Figure 2: Parameter settings for credit-leading crisis.

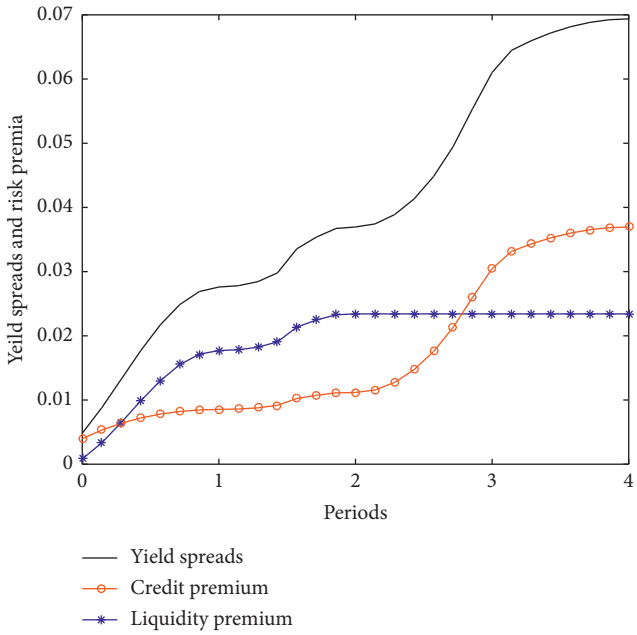

Figure 3: Yield spreads and risk premium in credit-leading crisis.

4.2.2. Liquidity-Leading Crisis. Liquidity-leading crisis is caused by a sudden drop in market liquidity. During such a crisis, investors become more sensitive to market risk, which triggers flight-to-liquidity. Wegener et al.'s [40] study points out that the global financial crisis caused a traditional liquidity crisis that also affected the German covered bond market. Wegener et al. [12] discuss the reason of the increase of sovereign credit risk in Europe and find that the financial crisis in the US is a trigger for the EMU debt crisis. The bursting US home price bubble lead to flight-to-quality effects to Germany and a loss of investors confidence in the fiscal situation of the peripheral countries. In other words, bond investors' risk tolerance declines, lowering market risk tolerance. Consequently, the correlation parameter changes from positive to negative, as noted in Section 4.1. The lack of capital not only results in flight-to-liquidity but also tightens corporations' capital constraints, which in turn increases the likelihood of default. Thus, credit risk increases correspondingly.

Similar to the credit-leading crisis analyzed in Section 4.2.1, liquidity-leading crisis also has effects on yield spreads through its impacts on the payoff of liquidity, correlation level, credit level, and degree of information accuracy. As the deterioration of information accuracy does not impact credit risk and the correlation between credit and liquidity, as shown in Section 4.2.1, we demonstrate the effects of liquidity crisis in only three stages:

(1) Liquidity risk rises substantially. Due to the increase of marketability discount w, liquidity payoff y_s drops quickly.

(2) The market risk tolerance drops, and (λ^*/w) grows up. Then, the correlation parameter α changes quickly from positive to negative.

(3) Credit level declines due to tightened capital constraints, as we can see that the default payoff declines and default intensity increases in this period.

In Section 4.1, we note that the correlation effect can be influenced by the credit level. To provide a full picture of the role of correlation in the liquidity-leading crisis, we consider both investment and speculative bonds. The parameters for these two types of bonds are as follows: $h_d = 0.05$, $h_s = 0.4$, $y_d = 0.75$, $y_s = 0.875$, and $\alpha = 2$ represent the initial state of an investment grade bond and $h_d = 0.35$, $h_s = 0.4$, $y_d = 0.35$, $y_s = 0.775$, and $\alpha = 2$ represent the initial state of a speculative grade bond. The corresponding parameters are presented separately in Figures 4(a) and 4(b).

Figures 5(a) and 5(b) plot the yield spreads and risk premia of these two types of bonds in three different periods. Similar to the conclusion in the analysis of crisis-leading risk, yield spreads rise over time in every step in a liquidity-leading crisis. However, for different bonds, the correlation plays a different role during the crisis. In particular, in the second period, yield spreads are relatively stable in Figure 5(a), but rise significantly in Figure 5(b). Thus, for speculative grade bonds, the effect of correlation is much stronger. The risk premia plotted in Figures 5(a) and 5(b) also corroborate this. For investment grade bonds, the credit risk premium changes mildly in the first two periods and then shoots up, while for speculative grade bonds, it begins to increase in period 2 and rises further thereafter.

The numerical results show that speculative grade bonds can be easily crashed by liquidity-leading crisis, and the crash is worse and earlier than investment grade bonds. This is consistent with the US market data in the financial crisis of 2008 [1].

Our analysis demonstrates two types of crisis in the bond market. As noted, default and liquidity risks are correlated, which widens risk spreads. High credit risk leads to deterioration of liquidity and vice versa. These two types of risk

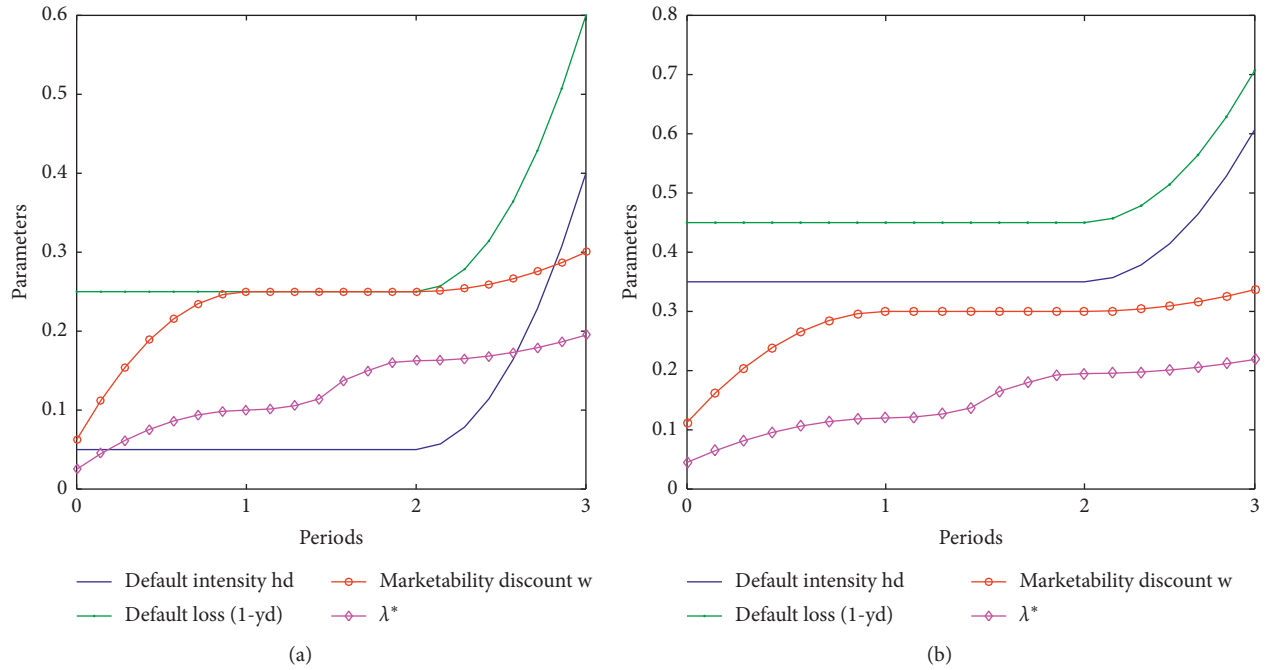

Figure 4: Parameter settings for liquidity-leading crisis (investment-grade/speculative-grade bond).

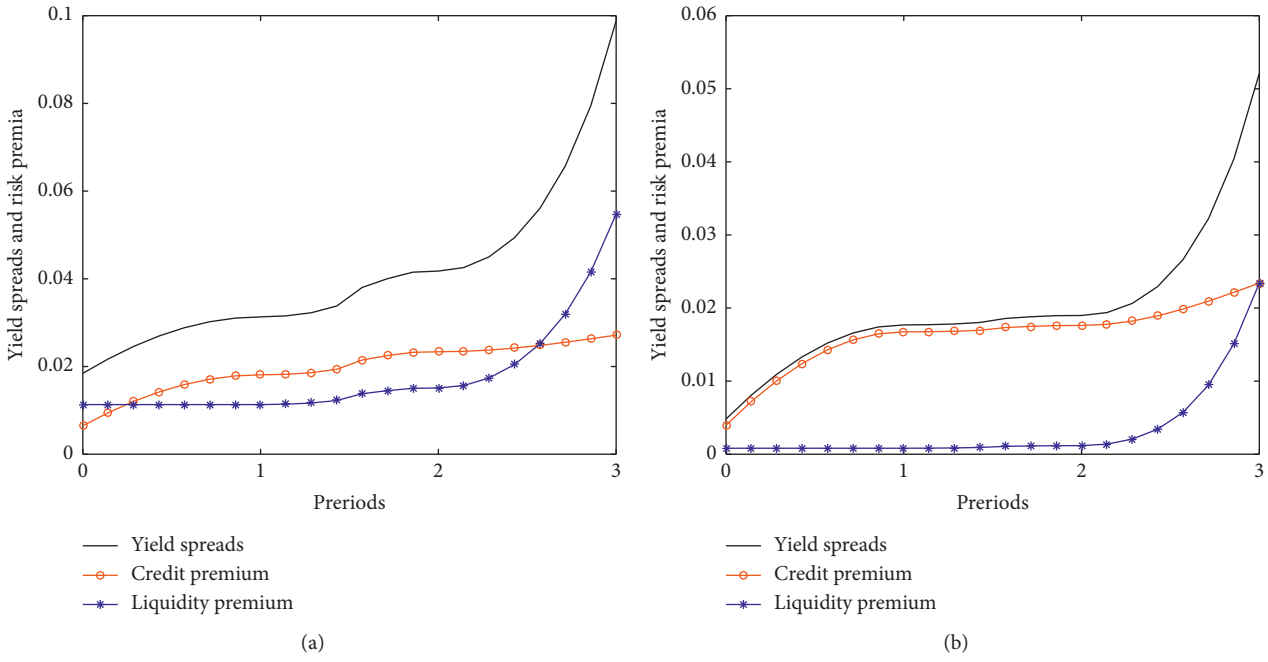

Figure 5: Yield spreads and risk premium in liquidity-leading crisis (investment-grade/speculative-grade bond).

in the bond market influence one another, forming a continuous cycle of risk. A decreasing credit level leads to reduced investors' risk tolerance, which leads to a greater and negative correlation parameter α and higher liquidity risk. The lack of liquidity further lowers investors' risk tolerance. As a result, credit and liquidity risks become more correlated, and credit risk increases further. This process continues, which can trigger a bond death spiral in the bond market. In such a death spiral, the reduction in information accuracy acts as a catalyst.

5. An Illustration with US Data

We take the US corporate bond market. We remove the following types of bonds from our sample: bonds that are not listed or traded in the US public market, bonds with a

Table 1: Estimated coefficients for the Markov-switching model.

	C	$\gamma \times$ SP	Expected duration	Transition probabilities	
				State1	State2
State1	2.008*** (0.00)	0.008*** (0.00)	131.92	0.99 (0.00)	0.06 (0.32)
State2	4.582*** (0.00)	0.011*** (0.00)	17.32	0.01 (0.32)	0.94 (0.00>)

Note. This table provides the estimated coefficients for the Markov-switching model: $ys_t = \alpha_i + \beta_i \gamma_t \times \mathrm{SP}_t + \varepsilon_{i,t}$, where $i = 1$ or 2 represents different states. We rely on the transaction records in Bloomberg for the sample period from January 2006 to December 2018. The liquidity risk is proxied by γ proposed by Bao etal. [41], based on the bond price trading deviation theory, to make a comparative study. The credit risk is proxied by the current S&P rating, and all ratings are assigned a number to facilitate the analysis; for example, 22 refers to a *D* rating, . . . and 1 refers to AAA. The first two columns show the values of α and β for the two regimes, where the second row of each regression result reports the *p*-values for the HAC statistics calculated by Newey–West standard errors. *** indicates the significance at the 1% level. The third column is the expected duration of each regime. The last two columns report the transition probabilities between different states and the corresponding *p*-values for HAC statistics calculated by Newey–West standard errors.

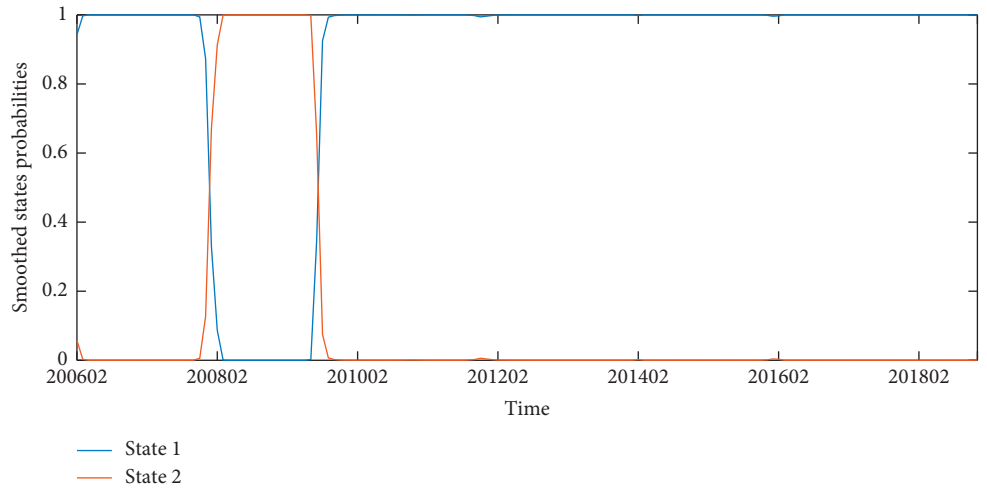

Figure 6: Smoothed states' probabilities.

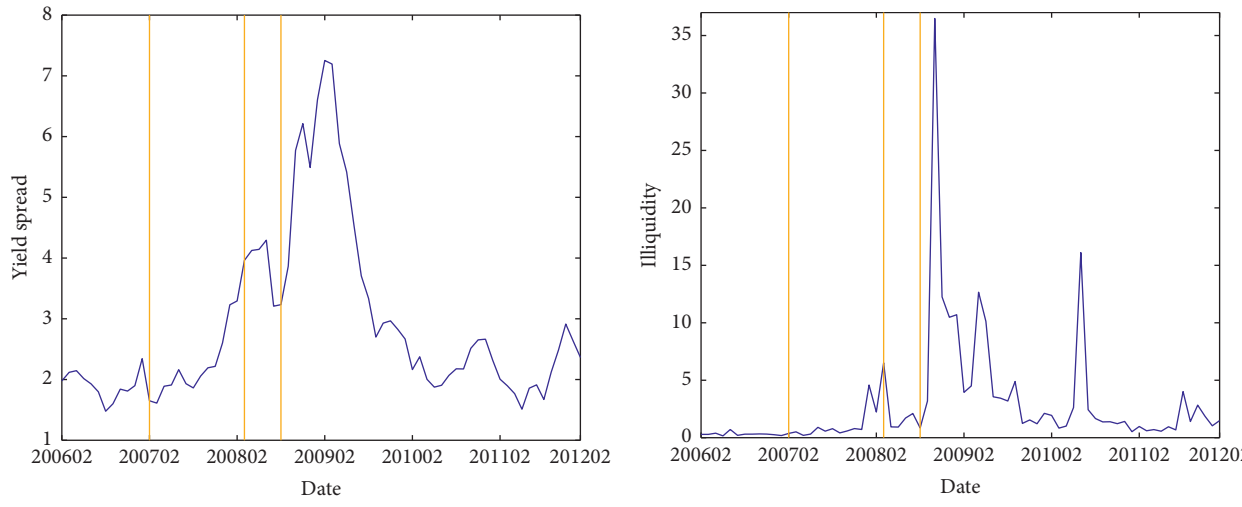

Figure 7: Continued.

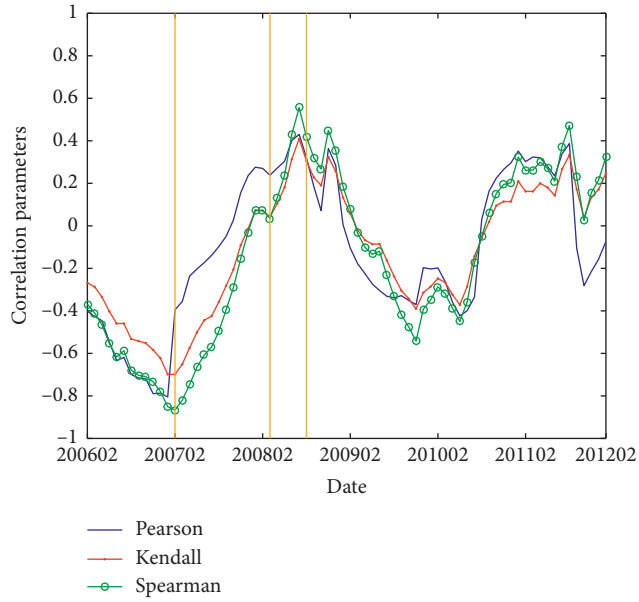

(c)

Figure 7: Yield spreads, liquidity risk, and the correlation parameters during financial crisis.

maturity of less than one year, convertible bonds, bonds that trade under $10 or above $1000, bonds with floating rate, bonds with a floating coupon rate, bonds with less than one year to maturity, bonds that nonzero-trading months are less than 20, government-related or financial institution-related bonds, and bonds without Standard and Poor's ratings. Our final sample includes 9972 corporate bonds. As an example to document how the correlation between credit and liquidity affects bond prices. We use the transaction records in Bloomberg for the sample period from January 2006 to December 2018.

We model the yield spread with a two-state Markov-switching regime to analyze the changes in yield spread during different time periods as follows:

$$ys_t = \alpha_i + \beta_i \gamma_t \times \mathrm{SP}_t + \varepsilon_{i,t}, \tag{27}$$

where $i = 1$ or 2 represent different regimes. The dependent variable ys_t is the corporate bond yield spread, and the independent variable $\mathrm{SP}_t \times \gamma_t$ is the product of credit risk and liquidity risk, which are measured by the S&P rating level and illiquidity proxy proposed by Bao etal. [41], respectively. Our ADF test on the two variables shows they are both stationary, and the ADF-statistics of ys_t and $\mathrm{SP}_t \times \gamma_t$ are -6.64 and -6.57, respectively.

Table 1 provides the results for equation (27). Our model distinguishes regimes which are highly persistent. The probability of remaining in the present state is 99% and 94%, respectively. The smoothed probabilities are given in Figure 6. For most of the time, the correlation between credit risk and liquidity risk affects the yield spread slightly and this state is more stable. However, at the end of 2007, the regime of the regression model changes, and the correlation plays a more important role in bond pricing, that is, the deterioration of market leads to changes in the premia of credit risk, liquidity risk, and their correlation.

The Markov-switching model confirms that the correlation between credit risk and liquidity risk can significantly influence the yield spread, especially during the financial crisis.

To analyze how the correlation changes during crisis, we plot three correlation parameters for different months in Figure 7. In early 2007, default risk in subprime mortgages increased dramatically, leading to the so-called subprime crisis. This crisis deteriorated the overall credit of the corporate bond market, which caused great losses in bond prices in Figure 7(a). Following the credit crisis, the liquidity premium increased slightly in 2007, as shown in Figure 7(b), similar to the analysis in Section 4.2.1. Meanwhile, the correlation in Figure 7(c) between credit risk and liquidity risk kept climbing during this period. The increased correlation eventually triggered a series of defaults in the market, including the bankruptcy of Lehman. Due to this high credit risk, the liquidity risk and yield spreads further increased. The combination of rising credit and liquidity risks constituted an ongoing spiral, in which market conditions constantly deteriorated, as shown in our analysis. During the bond death spiral, lower information accuracy also caused greater market volatility around the time of the Federal Reserve bailout of Bear Stearn, which had an impact on the liquidity risk and bond prices, but did not influence correlation parameters, as shown in Figure 7(c).

Note: Figure 7 plots the yield spreads, liquidity risk, and correlation parameters of the U.S. corporate bonds; the sample period is from February, 2006 to February, 2012. Figure (c) plots Pearson, Kendall, and Spearman correlation

parameters with 20-month rolling window. The three vertical lines represent the subprime crisis, downfall of Bear Stearns, and Lehman bankrupt.

6. Conclusion

In this paper, we propose a generalized bond pricing model that incorporates credit risk, liquidity risk, and their correlation. We analyze the way in which the correlation between the two risks arises and explore the role of the correlation in explaining bond pricing.

Using the trading model, we specify the liquidity payoff and show that liquidity risk arises from two sources: information accuracy and market risk tolerance. It is the market risk tolerance rather than information accuracy that links credit and liquidity. By adopting a joint probability distribution, Frank Copula function, we calculate the probabilities of default and trade. Using numerical examples, we show how the correlation determines yield spreads under various market conditions. We show that a credit-leading crisis and a liquidity-leading crisis interact with each other and can result in a drastic decline in bond prices. Our model provides an explanation for the bond death spiral observed in a financial crisis. Moreover, we analyze the influence of the correlation in the US corporate bond market in different periods, and the empirical results provide evidence in support of our numerical analysis.

Appendix

A

Proof. of equation (12).

Substituting equation (5) into $D_{\text{in}} = (E[\tilde{Y}|\Omega_{\text{in}}] - P)\Pi_{\text{in}}$ λ_{in} gives the following:

$$D_{\text{in}} = \lambda_{\text{in}}\Pi_{v}E[\tilde{Y}] + \lambda_{\text{in}}\Pi_{i\varepsilon}Y_{\text{in}} - \lambda_{\text{in}}\Pi_{\text{in}}P. \tag{A.1}$$

Equation (A.1) shows that D_{in} is a linear function of private information and price.

Substituting equations (A.1) and (10) into equation (11) yields

$$P = \Delta\left(N\lambda_{\text{in}}\Pi_{v} + N\lambda_{\text{in}}\Pi_{i\varepsilon}Y_{\text{in}} + \omega\Pi_{un}E\left[\tilde{Y}|\Omega_{\text{un}}\right] - L\right), \tag{A.2}$$

where $\Delta = (N\lambda_{\text{in}}\Pi_{\text{in}} + \omega\Pi_{\text{un}})^{-1}$. Equation (A.2) suggests that, for the uninformed trader, P is a linear function of the informed trader's information and the supply of bonds.

Solving for Y_{in} from equation (A.2), we obtain

$$Y_{\text{in}} = \left(N\Delta\lambda_{\text{in}}\Pi_{i\varepsilon}\right)^{-1}\left(P - \Delta\left(N\lambda_{\text{in}}\Pi_{v} + \omega\Pi_{\text{un}}E\left[\tilde{Y}|\Omega_{\text{un}}\right] - L\right)\right). \tag{A.3}$$

Because the market bond supply is not observable, to get the private information of the informed trader, the uninformed trader can infer the private information Y_{in} as follows:

$$Y_{\text{learn}} = \left(N\Delta\lambda_{\text{in}}\Pi_{i\varepsilon}\right)^{-1}\left(P - \Delta\left(N\lambda_{\text{in}}\Pi_{v} + \omega\Pi_{\text{un}}E\left[\tilde{Y}|\Omega_{\text{un}}\right]\right)\right). \tag{A.4}$$

Thus, there is a deviation between Y_{learn} and Y_{in}, and Y_{learn} can be rewritten as

$$Y_{\text{learn}} = Y_{\text{in}} - \left(N\Delta\lambda_{\text{in}}\Pi_{i\varepsilon}\right)^{-1}L. \tag{A.5}$$

□

B

Proof. of equations (14)–(16).

Based on equation (5), the expected value of cash flows for informed investors $E[\tilde{Y}|\Omega_{\text{in}}]$ is

$$E\left[E\left[\tilde{Y}|\Omega_{\text{in}}\right]\right] = E[\tilde{Y}] + \frac{\Pi_{i\varepsilon}}{\Pi_{\text{in}}}\left(E\left[Y_{\text{in}}\right] - E[\tilde{Y}\,]\right) = E[\tilde{Y}\,]. \tag{B.1}$$

Plugging $Y_{\text{in}} = \tilde{Y} + \varepsilon_{\text{in}}$ into equation (A.5), we obtain the cash flows for uninformed investors:

$$Y_{\text{learn}} = \tilde{Y} + \left(\varepsilon_{\text{in}} - \left(N\lambda_{\text{in}}\Pi_{i\varepsilon}\right)^{-1}L\right) = \tilde{Y} + \varepsilon_{\text{learn}}. \tag{B.2}$$

We denote the precision of $\varepsilon_{\text{learn}}$ as Π_{learn}; then, the expected value for uninformed investors is

$$E\left[\tilde{Y}|\Omega_{\text{un}}\right] = E[\tilde{Y}] + \frac{\Pi_{\text{learn}}}{\Pi_{\text{un}}}\left(Y_{\text{learn}} - E\left[Y_{\text{learn}}\right]\right). \tag{B.3}$$

The expected value of $E[\tilde{Y}|\Omega_{\text{un}}]$ is

$$E\left[E\left[\tilde{Y}|\Omega_{\text{un}}\right]\right] = E[\tilde{Y}] + \frac{\Pi_{\text{learn}}}{\Pi_{\text{un}}}\left(E\left[Y_{\text{learn}}\right] - E\left[Y_{\text{learn}}\right]\right) = E[\tilde{Y}]. \tag{B.4}$$

Substituting equations (7) and (10) into equation (11) gives

$$N\left(E\left[\tilde{Y}|\Omega_{\text{in}}\right] - P\right)\Pi_{\text{in}}\lambda_{\text{in}} + M\left(E\left[\tilde{Y}|\Omega_{\text{un}}\right] - P\right)\Pi_{\text{un}}\lambda_{\text{un}} = L. \tag{B.5}$$

Solving for P from equation (B.5) gives

$$P = \left(NE\left[\tilde{Y}|\Omega_{\text{in}}\right]\Pi_{\text{in}}\lambda_{\text{in}} + ME\left[\tilde{Y}|\Omega_{\text{un}}\right]\Pi_{\text{un}}\lambda_{\text{un}} - L\right)\left(N\Pi_{\text{in}}\lambda_{\text{in}} + M\Pi_{\text{un}}\lambda_{\text{un}}\right)^{-1}. \tag{B.6}$$

Given that $E[\tilde{Y}|\Omega_{\text{in}}] = E[\tilde{Y}]$ and $E[E[\tilde{Y}|\Omega_{\text{un}}]] = E[\tilde{Y}]$, the expected value of equation (B.6) is

$$E[P] = \left(NE[\tilde{Y}]\Pi_{\text{in}}\lambda_{\text{in}} + ME[\tilde{Y}]\Pi_{\text{un}}\lambda_{\text{un}} - E[L]\right)\left(N\Pi_{\text{in}}\lambda_{\text{in}} + M\Pi_{\text{un}}\lambda_{\text{un}}\right)^{-1}. \tag{B.7}$$

Rearranging equation (B.7) gives

$$E[\tilde{Y}] - E[P] = E[L]\left(N\Pi_{\text{in}}\lambda_{\text{in}} + M\Pi_{\text{un}}\lambda_{\text{un}}\right)^{-1}. \tag{B.8}$$

Namely,

$$E[\tilde{Y}] - E[P] = \left(\frac{N\lambda_{\text{in}}\Pi_{\text{in}} + M\lambda_{\text{un}}\Pi_{\text{un}}}{N\lambda_{\text{in}} + M\lambda_{\text{un}}}\right)^{-1} E[L] \left(N\lambda_{\text{in}} + M\lambda_{\text{un}}\right)^{-1}. \tag{B.9}$$

□

C

Proof. of Proposition 1.

$P_{d,i}$ and $P_{s,i}$ represent the probabilities of default and trade, respectively, in each subinterval $[t_i, t_{i+1}]$. As $P_{d,i} = P[\tau_d < \tau_s, \tau_d < t_{i+1} | \tau_s > t_i, \tau_d > t_i]$ and $P_{s,i} = P[\tau_s < \tau_d, \tau_s < t_{i+1} | \tau_s > t_i, \tau_d > t_i]$, following equations 22a and 22b, we obtain

$$P_{d,i} = \int_{t_i}^{t_{i+1}} \left(\frac{\partial F_i}{\partial x}|_{y=+\infty} - \frac{\partial F_i}{\partial x}|_{y=x}\right) \mathrm{d}x, \tag{C.1a}$$

$$P_{s,i} = \int_{t_i}^{t_{i+1}} \left(\frac{\partial F_i}{\partial y}|_{x=+\infty} - \frac{\partial F_i}{\partial y}|_{x=y}\right) \mathrm{d}y, \tag{C.1b}$$

where F_i is the joint distribution in subinterval $[t_i, t_{i+1}]$. Let $P_i = P_{d,i} + P_{s,i}$ represents the probability of any event occurring in subinterval $[t_i, t_{i+1}]$ and $p^k = P[\tau \le t_{k+1}]$ is the probability of any event occurring in the first k periods. Then, p^k can be written as

$$p^k = 1 - \prod_{i=i}^{k} (1 - P_i). \tag{C.3}$$

Using the formula of total probability, we get the probabilities of default and trade in interval $[0, T]$ as follows:

$$P_d = \sum_{i=1}^{n} P_{d,i}\left(1 - p^i\right), \tag{C.4a}$$

$$P_s = \sum_{i=1}^{n} P_{s,i}\left(1 - p^i\right). \tag{C.4b}$$

Plugging equation (C.3) into equations C.4a and C.4b, we obtain

$$P_d = \sum_{i=1}^{n} P_{d,i} \prod_{1}^{i} (1 - P_i), \tag{C.5a}$$

$$P_s = \sum_{i=1}^{n} P_{s,i} \prod_{1}^{i} (1 - P_i). \tag{C.5b}$$

□

Data Availability

The data used to support the findings of this study are available from Bloomberg Terminal at https://www.bloomberg.net/with the permission of Bloomberg. Restrictions apply to the availability of these data, which were used under license for this study.

Conflicts of Interest

The authors declare that they have no conflicts of interest.

Acknowledgments

This work was supported by the National Natural Science Foundation of China (Grant nos. 71471129 and 71501140) and Tianjin Philosophy and Social Science Planning Project (Grant no. TJGL19-018).

References

[1] J. Dick-Nielsen, P. Feldhütter, and D. Lando, "Corporate bond liquidity before and after the onset of the subprime crisis," *Journal of Financial Economics*, vol. 103, no. 3, pp. 471–492, 2012.

[2] J.-Z. Huang and M. Huang, "How much of the corporate-treasury yield spread is due to credit risk?" *Review of Asset Pricing Studies*, vol. 2, no. 2, pp. 153–202, 2012.

[3] V. V. Acharya, Y. Amihud, and S. T. Bharath, "Liquidity risk of corporate bond returns: conditional approach," *Journal of Financial Economics*, vol. 110, no. 2, pp. 358–386, 2013.

[4] L. Guo, "Determinants of credit spreads: the role of ambiguity and information uncertainty," *The North American Journal of Economics and Finance*, vol. 24, pp. 279–297, 2013.

[5] H. H. Huang, H.-Y. Huang, and J. J. Oxman, "Stock liquidity and corporate bond yield spreads: theory and evidence," *Journal of Financial Research*, vol. 38, no. 1, pp. 59–91, 2015.

[6] J. Ericsson and O. Renault, "Liquidity and credit risk," *The Journal of Finance*, vol. 61, no. 5, pp. 2219–2250, 2006.

[7] M. Kalimipalli and S. Nayak, "Idiosyncratic volatility vs. liquidity? Evidence from the US corporate bond market,"

Journal of Financial Intermediation, vol. 21, no. 2, pp. 217–242, 2012.

[8] M. Rossi, "Realized volatility, liquidity, and corporate yield spreads," *Quarterly Journal of Finance*, vol. 04, no. 01, Article ID 1450004, 2014.

[9] N. Friewald, R. Jankowitsch, and M. G. Subrahmanyam, "Illiquidity or credit deterioration: a study of liquidity in the US corporate bond market during financial crises," in *Managing and Measuring Risk: Emerging Global Standards and Regulations after the Financial Crisis*World Scientific, Singapore, 2013.

[10] J. Helwege, J.-Z. Huang, and Y. Wang, "Liquidity effects in corporate bond spreads," *Journal of Banking & Finance*, vol. 45, pp. 105–116, 2014.

[11] K. Schwarz, "Mind the gap: disentangling credit and liquidity in risk spreads," 2017.

[12] C. Wegener, T. Basse, P. Sibbertsen, and D. K. Nguyen, "Liquidity risk and the covered bond market in times of crisis: empirical evidence from Germany," *Annals of Operations Research*, vol. 282, no. 1-2, pp. 407–426, 2019.

[13] R. C. Merton, "On the pricing of corporate debt: the risk structure of interest rates," *The Journal of Finance*, vol. 29, no. 2, pp. 449–470, 1974.

[14] D. Duffie and K. J. Singleton, "Modeling term structures of defaultable bonds," *Review of Financial Studies*, vol. 12, no. 4, pp. 687–720, 1999.

[15] R. Jarrow, H. Li, S. Liu, and C. Wu, "Reduced-form valuation of callable corporate bonds: theory and evidence," *Journal of Financial Economics*, vol. 95, no. 2, pp. 227–248, 2010.

[16] Y. Amihud, "Illiquidity and stock returns: cross-section and time-series effects," *Journal of Financial Markets*, vol. 5, no. 1, pp. 31–56, 2002.

[17] L. Chen, D. A. Lesmond, and J. Wei, "Corporate yield spreads and bond liquidity," *The Journal of Finance*, vol. 62, no. 1, pp. 119–149, 2007.

[18] R. Schestag, P. Schuster, and M. Uhrig-Homburg, "Measuring liquidity in bond markets," *Review of Financial Studies*, vol. 29, no. 5, pp. 1170–1219, 2016.

[19] C. S. Armstrong, J. E. Core, D. J. Taylor, and R. E. Verrecchia, "When does information asymmetry affect the cost of capital?" *Journal of Accounting Research*, vol. 49, no. 1, pp. 1–40, 2011.

[20] D. Vayanos and J. Wang, "Market liquidity—theory and empirical evidence," in *Handbook of the Economics of Finance*Elsevier, Amsterdam, Netherlands, 2013.

[21] R. A. Lambert and R. E. Verrecchia, "Information, illiquidity, and cost of capital," *Contemporary Accounting Research*, vol. 32, no. 2, pp. 438–454, 2015.

[22] B. Daley and B. Green, "An information-based theory of time-varying liquidity," *The Journal of Finance*, vol. 71, no. 2, pp. 809–870, 2016.

[23] D. Vayanos and J. Wang, "Liquidity and asset returns under asymmetric information and imperfect competition," *Review of Financial Studies*, vol. 25, no. 5, pp. 1339–1365, 2011.

[24] Q. Chen, Z. Huang, and Y. Zhang, "The effects of public information with asymmetrically informed short-horizon investors," *Journal of Accounting Research*, vol. 52, no. 3, pp. 635–669, 2014.

[25] S. J. Grossman and J. E. Stiglitz, "On the impossibility of informationally efficient markets," *The American Economic Review*, vol. 70, no. 3, pp. 393–408, 1980.

[26] D. Easley and M. O'hara, "Information and the cost of capital," *The Journal of Finance*, vol. 59, no. 4, pp. 1553–1583, 2004.

[27] R. A. Lambert, C. Leuz, and R. E. Verrecchia, "Information asymmetry, information precision, and the cost of capital," *Review of Finance*, vol. 16, no. 1, pp. 1–29, 2011.

[28] R. A. Jarrow and S. M. Turnbull, "Pricing derivatives on financial securities subject to credit risk," *The Journal of Finance*, vol. 50, no. 1, pp. 53–85, 1995.

[29] R. A. Jarrow, "Credit market equilibrium theory and evidence: revisiting the structural versus reduced form credit risk model debate," *Finance Research Letters*, vol. 8, no. 1, pp. 2–7, 2011.

[30] R. Jarrow, "Default parameter estimation using market prices," *Financial Analysts Journal*, vol. 57, no. 5, pp. 75–92, 2001.

[31] Y. H. Eom, J. Helwege, and J.-Z. Huang, "Structural models of corporate bond pricing: an empirical analysis," *Review of Financial Studies*, vol. 17, no. 2, pp. 499–544, 2004.

[32] S. T. Bharath and T. Shumway, "Forecasting default with the Merton distance to default model," *Review of Financial Studies*, vol. 21, no. 3, pp. 1339–1369, 2008.

[33] D. B. Madan and H. Unal, "Pricing the risks of default," *Review of Derivatives Research*, vol. 2, no. 2-3, pp. 121–160, 1998.

[34] J. Ng, "The effect of information quality on liquidity risk," *Journal of Accounting and Economics*, vol. 52, no. 2-3, pp. 126–143, 2011.

[35] R. Sadka, "Liquidity risk and accounting information," *Journal of Accounting and Economics*, vol. 52, no. 2-3, pp. 144–152, 2011.

[36] C. A. Botosan and M. A. Plumlee, "Are information attributes priced?" *Journal of Business Finance & Accounting*, vol. 40, no. 9-10, pp. 1045–1067, 2013.

[37] T. T. Tang, "Information asymmetry and firms' credit market access: evidence from Moody's credit rating format refinement," *Journal of Financial Economics*, vol. 93, no. 2, pp. 325–351, 2009.

[38] C.-W. Lu, T.-K. Chen, and H.-H. Liao, "Information uncertainty, information asymmetry and corporate bond yield spreads," *Journal of Banking & Finance*, vol. 34, no. 9, pp. 2265–2279, 2010.

[39] P. C. B. Phillips and S. Shi, "Detecting financial collapse and ballooning sovereign risk," *Oxford Bulletin of Economics and Statistics*, vol. 81, no. 6, pp. 1336–1361, 2019.

[40] C. Wegener, R. Kruse, and T. Basse, "The walking debt crisis," *Journal of Economic Behavior & Organization*, vol. 157, pp. 382–402, 2019.

[41] J. Bao, J. Pan, and J. Wang, "The illiquidity of corporate bonds," *The Journal of Finance*, vol. 66, no. 3, pp. 911–946, 2011.

Hindawi
Discrete Dynamics in Nature and Society
Volume 2021, Article ID 6656176, 15 pages
https://doi.org/10.1155/2021/6656176

Research Article

Economic Policy Uncertainty Linkages among Asian Countries: Evidence from Threshold Cointegration Approach

Prince Mensah Osei,[1] **Reginald Djimatey**,[2] **and Anokye M. Adam**[3]

[1]*Faculty of IT & Business, Ghana Communication Technology University, Kumasi-Campus, Kumasi, Ghana*
[2]*Department of Entrepreneurship and Business Sciences, School of Management Sciences and Law, University of Energy and Natural Resources, Sunyani, Ghana*
[3]*Department of Finance, School of Business, University of Cape Coast, Cape Coast, Ghana*

Correspondence should be addressed to Anokye M. Adam; aadam@ucc.edu.gh

Received 6 October 2020; Revised 12 January 2021; Accepted 21 January 2021; Published 31 January 2021

Academic Editor: Dehua Shen

This paper employs the threshold cointegration methodology to assess the long- and short-run dynamics of asymmetric adjustment between economic policy uncertainty (EPU) of China-India, China-Japan, China-Korea, India-Japan, India-Korea, and Japan-Korea pairs using monthly EPU data ranging from January 1997 to April 2020. The relationship between the EPU pairs is examined in terms of Engle-Granger and threshold cointegrations. The findings provide evidence of long-run threshold cointegration and that the adjustments towards the long-run equilibrium position are asymmetric in the short run for the China-India and India-Japan EPU pairs in M-TAR specification with nonzero threshold values. Also, the results suggest a unidirectional causal relationship between China-India, China-Japan, and India-Korea EPU pairs in the long and short run using the spectral frequency domain causality approach. However, a bidirectional causal relationship between China-Korea, India-Japan, and Japan-Korea pairs exists in the long and short run. Therefore, the findings provide some clues to economic policymakers within the Asian subregion for possible policy uncertainty synergies and spillovers among the Asian countries.

1. Introduction

Weakening global economic growth in recent years has been attributed to heightened uncertainty in the economic policies of advanced economies. Global issues such as 1997-98 Asian financial crisis, September 11 terrorist attacks in the United States (US), Gulf War II, 2008 global financial crisis, European sovereign debt crisis, Brexit referendum, and Covid-19 pandemic are perceived to have raised economic policy uncertainty (EPU) with consequential effects on private domestic demand in many economies. Usually, the rise in uncertainty after such events may lead to a gradual widespread of "wait" and "see" attitude, resulting in postponed spending projects until anticipation for economic activity to become more obvious [1, 2]. Although EPU linkages are considered at the cross-country level, the impact of such uncertainty on economic activity and the behaviour of economic agents at the household and firm levels cannot be underestimated [3–6]. The key question that has lingered in the minds of international macroeconomists and policymakers is the extent to which EPU shocks emanating from one country affect the economic policy uncertainty as well as the business cycles in another country. Specifically, small open economies with free capital mobility, sizeable openness, and a large financial sector are greatly influenced by the international transmission of EPU shocks.

Emerging market economies have experienced large swings in business cycles, financial market returns, and macroeconomic fundamentals due to EPU shock transmission from advanced and developed economies. For example, EPU spillovers from the United States (US) and the European Union (EU) would have crucial global consequences because of their relatively large size, strong trade, and financial linkages with other economies. Aside looking

at EPU impact from the global perspective, regional and subregional EPU linkage is eminent due to regional and subregional economic integration. Economies within the same subregion with considerable large financial sectors are likely to experience increased EPU codependency, especially during postmajor economic, financial, and political shocks.

The Asian economies have emerged as force in the global economic architecture in production, trade, and financial sector. For example, the Asian financial sector which is highly susceptible to shock from uncertainty represents 37% of the total world banking and insurance market capitalisation [7–9]. Again, the Asian economy over the last decade has increased its share of global Gross Domestic Product (GDP) from 24% to 31%, and with a deepened regional integration, the possibility of policy uncertainty shocks to transmit from one Asian country to another would be apparent. This regional integration that underpins the economic policy linkages of the Asian economies is evident in the revival of China's relationships with India, Japan, and South Korea, as well as the reboot of China, Japan, and the Republic of Korea trilateral summit. The possible regional integration of the Asian economy and its contagion effects prevailed during the 1997/98 Asian financial crisis that started in Thailand and spread across the subregion. Therefore, examining the comovement of EPU among the Asian countries is of great importance because of its impact on array of economic activities such as stock markets, housing price, commodity prices, and many more [10–22].

In this paper, we investigate the EPU linkages among four Asian countries, comprising China, Japan, South Korea, and India using threshold cointegration techniques to determine the long- and short-run asymmetric adjustments and comovement of EPUs between these countries. Our choice of threshold cointegration method over the traditional linear cointegration method is based on its ability to detect the presence of a long-run relationship between time series variables and to unearth asymmetries in adjustment towards fundamental values with respect to positive and negative shocks. Thus, the power of linear cointegration test is lower in an asymmetric adjustment process [23]. Moreover, because the nexus of time series variables is higher in harsh periods than in tranquil periods, it makes it important to use threshold cointegration to be able to detect the presence of long-run equilibrium relationship with asymmetric adjustments towards the fundamental values between EPUs. Enders and Siklos [24] threshold cointegration method is employed to study the asymmetric long-run relationship between EPU of the four Asian countries because the impact of economic issues such as EPU is mostly nonstationary and nonlinear.

In addition, we focus our study on Asian countries, precisely China, Japan, South Korea, and India because of their economic size and power within the Asian subregion, and the EPU shock of one of these countries can easily influence the EPU and other macroeconomic factors of the other. Moreover, the widespread 1997/98 Asian financial crises across other Asian countries give a clear indication of how contagious policy inconsistency in one of these countries could be, which is motivating enough for our study to focus on Asian countries. Focusing on Asia as an emerging economy brings about interesting dynamics to the study of EPU linkages among countries because of the central role the Asian economy plays in global production networks [25–28] and the evidence of most of the Asian emerging economies catching up financially with the matured economies [29, 30]. Although any of the Asian countries could have been selected for this study but due to limitation of data on EPU of most of the developing countries, only these four Asian countries have complete data over the whole sample period.

Studies that focus on EPU regarding the Asian economy investigate the impact of EPU spillovers of advanced economies on the Asian financial markets, most especially the stock markets [31–33]. None of the previous studies explicitly focused on investigating EPU shock transmission among the Asian countries that showed widespread contagion of the 1997/98 Asian financial crisis. The study that is close to ours is Balcilar et al.'s study [34], they investigated the impact of EPU shock transmission of US and EU on local EPU and other macroeconomic factors of the Asian economy using quantile vector autoregression (QVAR) but did not examine EPU linkages among the Asian countries. To the best of our knowledge, this is the first study to investigate the transmission of EPU shocks from one Asian country to another using a threshold cointegration approach. The findings of the study reveal a long-run relationship between the EPU pairs of the countries and the adjustment of positive deviations in the short run was more rapid in general than negative deviations, implying that EPU of one country responds quickly when another country's EPU increases. Additionally, the Granger causality tests in the frequency domain suggest both unidirectional and bidirectional causalities of the EPU pairs in the long and short run.

Therefore, using the threshold cointegration would uncover the upward and downward adjustments of the short-run deviation of one country's EPU shock transmission to other country's EPU in the long-run. Knowing the extent to which local EPUs of Asian countries link together would help policymakers of the Asian economies to be on their guard and watch economic policies of not only the advanced economies but countries within their subregion so that they can mitigate any possible adverse effects these uncertainties may bring to bear on their economies. The results from the empirical analysis showed long-run threshold cointegration with asymmetry in the short run, in particular for China-India and India-Japan. Again, a unidirectional causal relationship between China-India, China-Japan, and India-Korea EPU pairs in the long and short run using the spectral frequency domain causality approach were observed. Finally, long- and short-run bidirectional causal relationship between China-Korea, India-Japan, and Japan-Korea pairs were found. These findings present important policy implication for dealing with uncertainty spillover in the region. The rest of the study is organised as follows. Section 2 reviews the relevant literature while Section 3 outlines the methodology and description of the data. Section 4 presents the empirical results, and the conclusion of the study is provided in Section 5.

2. Literature Review

EPUs over the period have surged at the bane of the global financial crisis (GFC) and the Eurozone's serial crises as well as partisan policy disputes in the US. As suggested by the Federal Open Market Committee [35], the uncertainty about US and European fiscal, regulatory and monetary policies contributed to a steep economic decline in 2008/09 and slow recovery afterwards. According to Klößner and Sekkel [36], the uncertainty spillover that increases notably around turbulent times accounts for more than 25% of the dynamics of the policy uncertainty index. These policy uncertainties have a significant impact on financial markets and a growing interest in the literature relating to the link between EPU and international financial markets, most especially the stock markets, which have led several researchers to focus on this area. Thus, studies by Brogaard and Detzel [37], Arouri et al. [38], Bahmani-Oskooee and Saha [12], Adam [39], Asafo-Adjei et al. [40], and Chiang [41] have demonstrated that heightened uncertainty hurts stock returns. Moreover, Pastor and Veronesi [42], Liu and Zhang [43], Tsai [44], and Jurado et al. [19] with different research orientations focus on the impact of uncertainty on stock market volatility and find that the inclusion of EPU can enhance the predictability of stock returns. This assertion confirms Hansen et al.'s [45] finding, which indicates that an upward shift in stock volatility is due to heightened policy uncertainty.

Specifically, Pastor and Veronesi [46] showed that higher policy uncertainty is associated with lower stock prices, higher volatility, and higher correlations among stock returns. Using Granger causality tests, Sum [47] investigated the effect of US EPU on five ASEAN countries comprising of Indonesia, Malaysia, Philippines, Singapore, and Thailand and found that US EPU harms stock market returns of related countries. Chuliá et al. [48] examined the impact of US policy and US equity market uncertainties on domestic and other stock market returns. Their findings provide evidence that an uncertainty shock lessons stock market returns both in developed and developing countries in uncertain times. In addition, Trung [49] tests the impact of U.S. uncertainty on emerging economies and finds that an upward shift in U.S. policy uncertainty inhibits international capital inflows and investment activity, which causes stock prices to fall in emerging economies. Bhattarai et al. [50] investigated the spillover indices of US uncertainty shock on fifteen emerging market economies (EMEs) by utilizing the panel vector autoregressive (VAR) method. They found evidence that the US uncertainty has harmful effects on EME stock prices, exchange rates, country spreads, and capital inflows into them. Akadiri et al. [51] found evidence of causality between international tourism arrivals (ITAs) and EPU of three regions of America, Europe, and Asia-Pacific using annual frequency panel data that consist of 12 countries in a multivariate Granger causality model setting. Their results revealed two-way causality relationship between ITAs and EPU in France, Ireland, and United States and one-way causality relationship from ITAs to EPU in Brazil, Canada, China, and Germany, while between ITAs and EPU in Chile, Japan, South Korea, Russia, and Sweden, there were no causality relationships. To establish the nexus between EPU and carbon dioxide (CO_2) emissions, Adams et al. [52] used the World Uncertainty Index to analyse the long-run relationship of EPU, energy consumption, and CO_2 emissions for countries including Brazil, China, India, Israel, Russia, Saudi Arabia, South Africa, Turkey, Ukraine, and Venezuela over the period 1996 to 2017. Their results based on the panel pooled mean group-autoregressive distributed lag model showed a significant association between EPU and CO_2 emissions in the long run. The causality analysis conducted also revealed bidirectional relationship between EPU and CO_2 emissions.

Beside numerous studies that focus on EPU, stock price movements, and other macroeconomic variables, other studies focus on cross-country effects of uncertainty. For example, Klößner and Sekkel [36] used the policy uncertainty index to examine cross-country EPU effects of six developed countries and found evidence of a significant spillover effect of policy uncertainty from the US and the United Kingdom (UK) to other countries which are the recipients of policy uncertainty shock during and after the crises period. Luk et al. [53] studied EPU spillovers of US, Europe, Mainland China, and Japan in small open economies, using Hong Kong as a case study. They constructed EPU for Hong Kong from 1998 to 2016 and found large spillovers of uncertainty from major economies to Hong Kong. Cekin et al. [54] investigated the dependence structure of EPU in four Latin American economies (Brazil, Chile, Colombia, and Mexico) and by employing vine copula modelling with various forms of tail dependence, they found significant dependencies in economic uncertainty among the Latin American economies. By adopting QVAR model approach, Balcilar et al. [34] extended their examination of external EPU spillovers of US and EU to the local EPU of five Asian economies (China, Hong Kong, Japan, South Korea, and India). They found that global economic policy uncertainties makeall Asian countries' domestic EPU fragile, except China and Hong Kong. Bai et al. [55] investigated the economic risk contagion among major economies including the US, UK, Germany, France, Japan, and China using an innovative spillover analysis method in time and frequency domains. The empirical results showed that in time-domain framework, the economic uncertainty of the six largest economies are strongly connectedwith the US happens as both major risk spillover contributors and receiver in the frequency domain, especially, at the short-term frequency. Their results also revealed that the static net EPU spillover effects indicate on average that the US is the key transmitter, while the UK and China are the major spillover receivers.

Even though there are vast number of studies on EPU shock spillover linkages between developed and developing economies and its impact on the financial markets, none of the studies enumerated examines EPU linkages among the Asian countries, having in mind the widespread contagion of the 1997/98 Asian financial crisis across the Asian subregion. Also, our adoption of the threshold cointegration method of Enders and Siklos [24] differentiates our study from the existing studies in terms of methodology as none of the studies to the best of our knowledge has used the approach

employed in our study to investigate EPU shock transmission across developed and emerging economies in general and among the Asian economies in particular.

3. Methodology and Data Description

3.1. Threshold Cointegration and Error Correction Model. To investigate the dynamic adjustment properties from EPU of one country to the other, the threshold cointegration test technique introduced by Enders and Siklos [24] is followed to identify the existence of an asymmetric long-run relationship between the EPUs of four Asian countries. To start with, Engle and Granger [56] long-run cointegration test is used to establish the stability, linearity, and long-run relationship between the EPU pairs of countries. The test is performed under the assumption that the linearity in the adjustment to the long-run equilibrium, as well as an increase or decrease in the deviation from the long-run equilibrium relationship, is symmetric. The long-run relationship between the EPU pairs of the four countries is estimated as follows:

$$\mathrm{EPU}_{j,t} = \alpha_0 + \alpha_1 \mathrm{EPU}_{i,t} + \mu_t, \tag{1}$$

where $\mathrm{EPU}_{j,t}$ and $\mathrm{EPU}_{i,t}$, respectively, represent EPU of country j and i at time t and μ_t is the normally distributed residual or error term with zero expected mean and constant variance.

To cater for the presence of nonlinearity in the variables and the adjustment process, the linear cointegration technique cannot detect as such. Therefore, for this reason, we apply Enders and Siklos [24] threshold cointegration where the long-run cointegration is linear but the adjustment to long-run equilibrium level is nonlinear. Therefore, we employ the threshold autoregressive (TAR) and momentum threshold autoregressive (M-TAR) models of Enders and Siklos [24] threshold cointegration to estimate the long-run cointegration and nonlinear adjustments to the long-run equilibrium level. The TAR model is specified as follows:

$$\Delta\mu_t = I_t \rho_1 \mu_{t-1} + (1 - I_t)\rho_2 \mu_{t-1} + \sum_i^k \gamma_i \Delta\mu_{t-i} + \varepsilon_t, \tag{2}$$

where μ_t is the residual in equation (1) substituted into equation (2) and ε_t is a zero-mean, constant variance, independent identically distributed (iid) random variable. I_t denotes the Heaviside indicator function specified as

$$\mathrm{TAR}: I_t = \begin{cases} 1, & \text{if } \mu_{t-1} \geq \tau, \\ 0, & \text{if } \mu_{t-1} < \tau, \end{cases} \tag{3}$$

where τ is the threshold value that is endogenously suggested by Chan [57]. The M-TAR model is also specified by replacing the indicator variable I_t and the level of previous period's residual μ_{t-1} in equation (2), respectively, by M_t and the change in the level of previous period's residual $\Delta\mu_{t-1}$ with the Heaviside indicator function stated as follows:

$$\mathrm{M-TAR}: M_t = \begin{cases} 1, & \text{if } \Delta\mu_{t-1} \geq \tau, \\ 0, & \text{if } \Delta\mu_{t-1} < \tau. \end{cases} \tag{4}$$

If μ_{t-1} and $\Delta\mu_{t-1}$ are above the threshold value τ, then the adjustment coefficient is $\rho_1\mu_{t-1}$, while on the other hand, the adjustment coefficient becomes $\rho_2\mu_{t-1}$, if μ_{t-1} and $\Delta\mu_{t-1}$ are below the threshold value τ. The threshold procedure involves three stages. The first stage is to estimate the TAR and M-TAR models for the cointegration procedure. At this stage, the null hypothesis of no cointegration (H_0: $\rho_1 = \rho_2 = 0$) is tested by comparing the critical values of the F-statistics with their corresponding actual values Φ in accordance with Enders and Siklos [24]. If the null hypothesis of no cointegration is rejected, the long-run cointegration between the EPU of country j and the EPU of country i exists and this takes us to the second stage of the threshold cointegration procedure. In the second stage, the symmetry of the null hypothesis (H_0: $\rho_1 = \rho_2$) is estimated. If we reject the null hypothesis of symmetry, thus $|\rho_1| \neq |\rho_2|$, there exists nonlinear threshold cointegration between the EPU of country j and the EPU of country i. We proceed to stage three where we estimate the threshold vector error correction model (TVECM) to adjust the short-run deviation from the long-run equilibrium. TAR specification of TVECM expression for EPU of country j and country i is stated as follows:

$$\Delta\mathrm{EPU}_{j,t} = \alpha_{j,0} + I_t \rho_{1,j} \mu_{t-1} + (1 - I_t)\rho_{2,j}\mu_{t-1} + \sum_k^n \beta_{j,k} \Delta\mathrm{EPU}_{i,t-k} + \sum_k^n + \varepsilon_{j,t}, \tag{5}$$

$$\Delta\mathrm{EPU}_{i,t} = \alpha_{i,0} + I_t \rho_{1,i} \mu_{t-1} + (1 - I_t)\rho_{2,i}\mu_{t-1} + \sum_k^n \alpha_{i,k} \Delta\mathrm{EPU}_{i,t-k} + \sum_k^n \beta_{i,k} \Delta\mathrm{EPU}_{j,t-k} + \varepsilon_{i,t}, \tag{6}$$

where ρ_1 and ρ_2, respectively, denote the speed of adjustment parameters for positive (above) and negative (below) deviations for one country's EPU from its long-run equilibrium, $\alpha_{j,0}$ and $\alpha_{i,0}$ are the constant terms, and $\Delta\mathrm{EPU}_{j,t-k}$ and $\Delta\mathrm{EPU}_{i,t-k}$ are the adjustments of EPU for country j and country i. respectively. $\alpha_{j,t}$, $\alpha_{i,t}$, $\beta_{j,t}$, and $\beta_{i,t}$ are the coefficients that quantify the short-term relationship among the EPU of country j, its lag, and the EPU of country i while $\varepsilon_{j,t}$

and $\varepsilon_{i,j}$ represent white noise disturbance terms. For M-TAR specification of TVECM expression, we replace I_t in equations (5) and (6) by M_t as defined by equation (4).

Because the parameters of the vector autoregression (VAR) model comprise of complex nonlinear functions, it complicates the statistical inference for the feedback measures over time [58, 59]. For this reason, we follow a Granger causality test in the frequency domain introduced by Breitung and Candelon [60] which is more useful if the causal links between variables change according to frequency such as the short and long run. We, therefore, adopt the spectral frequency domain approach to investigate the causal relationship between two time series variables based on bivariate spectral density matrix of VAR among different frequencies. According to Breitung and Candelon [60], the null hypothesis $(H_0)M_{y\longrightarrow x}(\omega) = 0$ corresponds to H_0: $R(\omega)\beta = 0$, where β is the vector of the coefficients on a given EPU index and

$$R(w) = \begin{pmatrix} \cos(\omega) & \cos(2\omega) & \dots & \cos(p\omega) \\ \sin(\omega) & \sin(2\omega) & \dots & \sin(p\omega) \end{pmatrix}. \tag{7}$$

The F-statistics in equation (7) are distributed as $F(2, T-2p)$ for $\omega \in (0, \pi)$, where T is the number of observations that measure the VAR model of order p. Performing the frequency domain analysis would allow us to observe nonlinear and causality cycles for high or low frequencies, and by presenting the relationship between the EPUs of the countries in a VAR system, a bidirectional relationship between the EPU_j of country j and EPU_i of country i in the short- and long-run is expressed as follows:

$$\text{EPU}_j = \lambda_1 \text{EPU}_{j,t-1} + \cdots + \lambda_p \text{EPU}_{j,t-p} + \theta_1 \text{EPU}_{i,t-1} + \cdots + \theta_p \text{EPU}_{i,t-p} + \varepsilon_{j,t}, \tag{8}$$

$$\text{EPU}_i = \lambda_1 \text{EPU}_{i,t-1} + \cdots + \lambda_p \text{EPU}_{i,t-p} + \theta_1 \text{EPU}_{j,t-1} + \cdots + \theta_p \text{EPU}_{j,t-p} + \varepsilon_{i,t}. \tag{9}$$

3.2. Data Description. The monthly EPU index data complied on four major Asian countries including China, India, Japan, and South Korea by Baker et al. [61] is used for the study. The index is based on the news coverage frequency of policy-related economic issues which serves as a proxy for policy-related economic uncertainty. There are many uncertainty measures for developed economies but less is said about emerging and developing economies as available EPU indices for developing countries are scanty in time scope. The EPU index that provides a scaled measure of the appearance of uncertainty in news surrounding economic issues is sourced from http://www.policyuncertainty.com. The data range from January 1997 to April 2020 during which the world experienced different categories of regional and global financial crises, such as the 1997-1998 Asian financial crisis, 2007–2009 global financial crises, 2010 European debt crisis, and 2015 stock market crash in China.

Figure 1 presents the time series plots of EPU of China, India, Japan, and South Korea. As shown in Figure 1, major regional and global events such as the 1997-98 Asian financial crises, 9/11 terrorist attacks in 2001, 2007-08 global financial crises, 2010 European debt crises, and Chinese stock market crash in 2015 broadly reflect spikes in the comovement of EPUs among China, India, Japan, and South Korea. We observe that the comovement of countries' EPUs during periods of such crises intensifies, confirming the fact that economic policymakers and the public including both local and foreign investors, are usually uncertain about the consequences of policy directions of a country in the periods of economic crisis.

Table 1 reports the main descriptive statistics of the variables over the period January 1997 to April 2020. On average, China has the highest EPU index among the EPU of the other countries, with India recording the lowest EPU index. The EPU of China exhibits higher variability than the other EPUs as shown by its minimum, maximum, and the standard deviation statistics, while Japan has lowest fluctuations in its EPU index as shown by its low standard deviation over the entire sample period. Overall, the EPU index of all countries are not normally distributed according to their skewness, kurtosis, Jarque–Bera test, and Shapiro test which indicate the presence of fat tails and confirms the stylized fact about the distribution of time series data being asymmetric.

Preliminary investigation of the comovement between the EPU pairs is carried out by assessing the unconditional correlation between the pairs and the results are presented in Table 2. The results show that the correlation coefficients of all the pairs are positive, indicating that the EPUs move in the same directional in pairs. The results also reveal a strong correlation between the Korea-China pair and Japan-India pair while a weak correlation can be observed between India-China pair.

4. Results and Discussion

4.1. Unit Root Test. We start our analysis by performing unit root tests to check whether the series are stationary or not using an autoregressive model. The augmented Dickey–Fuller (ADF) test, Phillips–Perron unit root test and Kwiatkowski, Phillips, Schmidt, and Shin (KPSS) test [62–64] are applied to test for the stationarity of the time series data used in our study as per the following equation:

$$\Delta x_t = (\varnothing - 1)x_{t-1} + \sum_{i=1}^{k-1} \lambda_i \Delta x_{t-i} + \mu_t + \nu_t, \tag{10}$$

where x_t is the series at time t, $\mu_t = \mu_0 + \mu_1 t$ is the deterministic term (μ_0 is the constant term and $\mu_1 t$ is the deterministic trend), and ν_t is a white noise process.

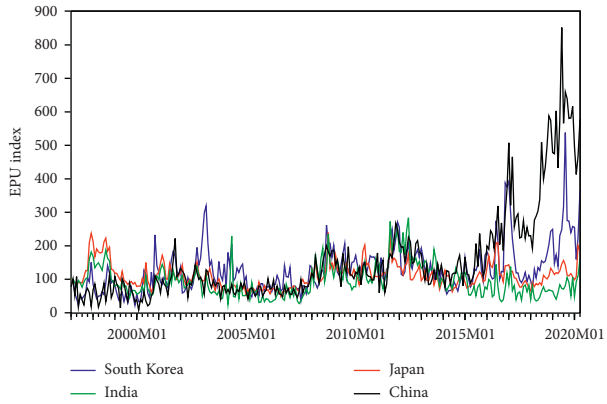

Figure 1: The relationship between the EPU indices

Table 1: Descriptive statistics.

	EPU_China	EPU_India	EPU_Japan	EPU_Korea
Mean	154.9016	94.7735	110.1837	128.7583
Min.	8.3459	24.9398	48.8858	22.4275
Max.	852.0525	283.6891	239.0284	538.1768
Std. Dev.	138.6951	46.954	36.4347	70.4422
Skewness	2.1668	1.2326	1.1455	1.7319
Kurtosis	4.7689	1.8143	1.4204	5.0573
Jarque–Bera	493.03*	111.54*	86.495*	446.74*
Shapiro	0.7389*	0.9122*	0.9210*	0.8779*

Note: *denotes the rejection of null hypothesis at 5% significance level.

Table 2: Unconditional linear correlation.

	EPU_C	EPU_I	EPU_J	EPU_K
EPU_C	1			
EPU_I	0.0004	1		
EPU_J	0.2171	0.6212	1	
EPU_K	0.6594	0.2587	0.3509	1

The results of the unit root tests of all series are shown in Table 3. In Table 3, the null hypothesis of all series at the level having unit roots cannot be rejected based on McKinnon [65] critical values at 5% level of significance using the ADF test, but after taking the first difference of the series, the ADF unit root test shows that all series are stationary at 5% level of significance, indicating that the series are integrated of order 1, $I(1)$. In addition to the ADF test, the Perron unit root test rejects the existence of unit root for all series at level, except Chinese EPU (EPU_C), which cannot be rejected at level, but after taking the first difference, the null hypothesis is rejected at 5% significance level, implying stationarity of EPU_C at first difference.

Moreover, the results of KPSS test show the rejection of the null hypothesis of stationarity of all series at level at 5% significant level. However, at first difference of all series, the stationarity hypotheses cannot be rejected at 5% level of significance. This indicates the presence of unit roots in the series at level but are however stationary after taking the first difference. It is key to note that all the variables have unit root problems in the presence of structural breaks. The structural break occurs around in 1997 mostly for EPU of India, Japan and South Korea, which brings to light the commencement of the Asian financial crisis. Moreover, a substantial break in China's EPU occurs around February 2018 where the Sino-US trade conflict intensified. In all, the ADF test and KPSS test confirm the presence of unit root in all series at level but the series are stationary after taking the first difference while the Phillip–Perron unit root test results indicate stationarity of series at level, except EPU_C that is stationary after taking first difference. Because the Phillip–Perron unit root test suffers from serious size distortions in the pure autoregressive case even in moderately large samples [66], we conclude based on the results of the ADF.

4.2. Testing for Nonlinear Characteristics of the Variables. To be able to proceed with the nonlinear cointegration analysis, we employ the nonlinear unit root test proposed by Kapetanios et al. [67], which has been considered as a nonlinear version of the ADF test. The purpose of Kapetanios, Snell, and Shin (KSS) test is to outline a testing procedure to specify the presence of nonstationary against a nonlinear exponential smoothing transition autoregressive (ESTAR) process which is globally stationary. The KSS is given by the following ESTAR specification:

$$\Delta y_t = \varphi y_{t-1}\left[1 - e^{-\theta\left(y_{t-1}-c\right)^2}\right] + \varepsilon_t, \tag{11}$$

where y_t is the time series of interest, φ is the unknown parameter, and ε_t is an iid error with mean zero and constant variance. The exponential transition function $[1 - e^{-\theta(y_{t-1}-c)^2}]$ is adopted in the test to present the nonlinear adjustment. When $c = 0$ is assumed, then equation (11) becomes

$$\Delta y_t = \varphi y_{t-1}\left[1 - e^{-\theta\left(y_{t-1}\right)^2}\right] + \varepsilon_t. \tag{12}$$

The null hypothesis of unit root, H_0: $\theta = 0$, is tested against the nonlinear ESTAR process, $H_1 > 0$, in equation (12). Because according to Kapetanios et al. [67] the null hypothesis cannot be directly tested, a reparameterization of equation (12) is suggested by computing a first-order Taylor series approximation to obtain auxiliary regression equation given by

$$\Delta y_t = \gamma y_{t-1}^3 + \varepsilon_t. \tag{13}$$

The case where the errors in equation (13) are serially correlated, it is extended with p augmentations to correct for serially correlated errors to become

$$\Delta y_t = \gamma y_{t-1}^3 + \sum_{j=1}^{p} p_j \Delta y_{t-j} + \varepsilon_t. \tag{14}$$

The null hypothesis of nonstationarity to be tested with either equation (13) or (14) is H_0: $\gamma = 0$ against the alternative H_1: $\gamma < 0$. The t-test statistics is given by $t = (\widehat{\gamma}/se(\widehat{\gamma}))$, where $\widehat{\gamma}$ is the ordinary least square (OLS) estimate of γ and $se(\widehat{\gamma})$ is the standard error of $\widehat{\gamma}$. The critical values of the t statistics of the KSS unit root test are given for

Table 3: Unit root test results for all series.

ADF unit root test								Phillip–Perron unit root test						KPSS unit root test					
Level	Lag	Break date	Statistics	First difference	Lag	Break date	Statistics	Level	Lag	Statistics	First difference	Lag	Statistics	Level	Lag	Statistics	First difference	Lag	Statistics
EPU_C	4	201802	−4.0197	EPU_C	4	2019M06	−19.8666*	EPU_C	3	−3.7357	EPU_C	3	−27.7487*	EPU_C	1	1.5498*	EPU_C	1	0.0159
EPU_I	3	199704	−4.9129	EPU_I	2	2004M05	−19.5823*	EPU_I	5	−6.4978*	EPU_I			EPU_I	2	0.549*	EPU_I	3	0.022
EPU_J	5	199706	−3.2941	EPU_J	2	1997M12	−14.4354*	EPU_J	4	−5.5395*	EPU_J			EPU_J	1	0.5333*	EPU_J	1	0.0131
EPU_K	8	201904	−3.3005	EPU_K	5	1997M05	−20.2156*	EPU_K	2	−5.7414*	EPU_K			EPU_K	1	0.1909*	EPU_K	2	0.0146

Note: *denotes the rejection of the null hypothesis at 5% significance level. Lag lengths are chosen according to AIC. Critical values are from McKinnon [65] and KPSS unit root tests that all the series under consideration are stationary after taking first difference indicating that all are $I(1)$ (integrated of order one).

three cases referred to the model with the raw data, the demeaned data, and the detrended data at 1%, 5%, and 10% levels. In the case of our study, we present the KSS test results using critical values for the model with the raw data.

Table 4 presents the results of KSS unit root test. The null hypothesis of linear stationary cannot be rejected for China's EPU at 5% significant level indicating that China's EPU does not exhibit nonlinear characteristics. However, the null hypothesis of linear stationary is rejected for India's EPU, Japan's EPU, and Korea's EPU, which imply they are nonlinear stationary. Because three out of the four EPU indices exhibit nonlinear behaviour, it is therefore worth employing nonlinear models to investigate the nonlinear relationships between the EPU pairs.

4.3. Engle-Granger Cointegration. We apply the Engle-Granger cointegration test procedure as the first step to our cointegration analysis based on the estimation of equation (1) to ascertain the presence of long-run relationship between the EPU pairs of countries. Table 5 presents the models' residuals for all EPU pairs and the test results show that the null hypothesis of no cointegration is rejected at 5% level. This means that each EPU is cointegrated with one another, confirming the long-run relationship between all the EPU pairs of the countries. According to the long-run regression results in Table 5, a change in one country's EPU would influence the movement in other country's EPU in the same direction.

4.4. Enders-Siklos Cointegration Test Results. We employ Enders and Siklos [24] test to investigate the nonlinear threshold cointegration and the results are displayed in Tables 6 and 7. Both Tables 6 and 7 show the threshold effects and focus on convergence, threshold cointegration, and adjustment in the long-run equilibrium following a deviation in EPUs in the model expressed as the linear combinations of the pair of EPU variables. In both tables, the first column shows the various cointegration model specifications and the second and the third columns show the values of the adjustment parameters ρ_1 and ρ_2, while the fourth and the fifth columns, respectively, show the F statistic for the null hypothesis of no cointegration and the test results for the symmetric adjustment. Specifically, Table 6 exhibits the TAR parameter estimates by assuming a threshold value for each model to be zero which is deterministic in nature. The point estimates in the TAR model show the convergence of long-run equilibrium and that the speed of convergence for positive divergence is almost the same as the speed of convergence of negative divergence from the long-run equilibrium of all the paired EPU models, although the larger of the t statistics is the positive adjustment parameter ρ_1 which is greater than the 5% critical value, except the EPUs of India-Japan model where the larger of the t statistics is the negative adjustment parameter ρ_2. For all the models, the F-joint statistics (thus hypothesis that $\rho_1 = \rho_2 = 0$) are greater than the 5% critical value, implying that the null hypothesis of no cointegration is rejected at 5% significance level. This suggests long-run relationship between the EPU pairs of countries. On the other hand, F-equal statistics (thus hypothesis that $\rho_1 = \rho_2$) that test the null hypothesis of symmetric adjustment is lower than the 5% critical value for all the models, indicating that the null hypothesis of symmetric adjustment cannot be rejected. This implies the speed of adjustment from positive deviation is not significantly different from the speed of adjustment from negative deviation, signifying the rate at which one country's EPU responds to rise or fall in another country's EPU which is almost the same according to the TAR model.

Table 4: KSS unit root test results.

	EPU_C	EPU_I	EPU_J	EPU_K
Test statistics	−2.3455	−4.509*	−4.2881*	−5.6913*

Note: *represents significance at 5% level corresponding to −2.94 critical value.

Because the threshold value is not always zero, we follow the approach of Chan [57] to search for approximate threshold values to estimate consistent M-TAR models of all the EPU pairs. The threshold values with a minimum value of Akaike Information Criteria (AIC) obtained are 34.814 for China-India EPU pair, −31.058 for China-Japan EPU pair, 57.357 for China-Korea EPU pair, 7.932 for India-Japan EPU pair, 25.746 for India-Korea EPU pair, and 2.575 for Japan-Korea EPU pair. Table 7 shows a similar analysis as in Table 6 using the M-TAR specification to check for asymmetric movement in one country's EPU in relation to changes in another country's EPU. Similarly, the larger of the t statistics is the positive adjustment parameter ρ_1 which is greater than 5% critical value, implying the test statistics are significant at 5% level except for the EPUs of China-Korea model where the larger of the t statistics is the negative adjustment parameter ρ_2. The M-TAR model estimates suggest convergence in the long-run equilibrium and the speed of convergence for positive deviation is faster than the speed of convergence for negative deviation for China-India and India-Japan models, indicating an asymmetric adjustment in EPU pairs between these countries. The null hypothesis of no cointegration is rejected in all models as the value of F-joint statistics is greater than 5% critical value. This indicates that all models show a long-run equilibrium relationship between the EPU pairs of countries. To detect the possibility of asymmetric adjustment, the null hypothesis of symmetric adjustment cannot be rejected for most of the models, except for China-India and India-Japan combinations, where the F-equal statistics are greater than 5% critical value, indicating that the speed of adjustment of positive and negative deviations from long-run equilibrium is different. Thus, China's EPU reverts quickly to the equilibrium path whenever the EPU of India rises more than a fall and vice versa. Likewise, a rise in Japan's EPU leads to India's EPU reverting quickly to the equilibrium path more than a fall in Japan's EPU and it is also true for the converse.

4.5. The Error Correction Model Estimation Results in M-TAR Specification. To finally analyse the asymmetric cointegration adjustment, we estimate the M-TAR error correction

Table 5: Engle-Granger cointegration results.

	EPU_C/EPU_I	EPU_C/EPU_J	EPU_C/EPU_K	EPU_I/EPU_J	EPU_I/EPU_K	EPU_J/EPU_K
Test statistics	−9.0694*	−8.7004*	−16.3803*	−18.9545*	−16.6225*	−17.7117*

Note: *represents 5% significance level with a corresponding critical value equal to −1.95 level. Each column represents EPU pair combination of the models' residuals.

Table 6: Enders-Siklos cointegration test results according to the TAR model.

Model	ρ_1	ρ_2	$\rho_1 = \rho_2 = 0$	$\rho_1 = \rho_2$	Conclusion
EPU_C/EPU_I	−0.228* (−4.267)	0.202* (−2.782)	12.21* (0.000)	0.091 (0.764)	Cointegration exist/symmetric adjustment
EPU_C/EPU_J	−0.249* (−4.954)	−0.153* (−2.209)	14.223* (0.000)	1.315 (0.253)	Cointegration exist/symmetric adjustment
EPU_C/EPU_K	−0.432* (−6.481)	0.350* (−4.138)	27.252* (0.000)	0.651 (0.420)	Cointegration exist/symmetric adjustment
EPU_I/EPU_J	0.229* (−3.870)	−0.304* (−4.278)	15.224* (0.000)	0.723 (0.396)	Cointegration exist/symmetric adjustment
EPU_I/EPU_K	−0.214* (−4.091)	−0.206* (−2.751)	11.546* (0.000)	0.007 (0.933)	Cointegration exist/symmetric adjustment
EPU_J/EPU_K	−0.231* (−4.511)	−0.172* (−2.383)	12.419* (0.000)	0.461 (0.498)	Cointegration exist/symmetric adjustment

Note: *represents significance at 5% level. Numbers in parenthesis and square brackets are t-values and p values, respectively.

Table 7: Enders-Siklos cointegration test results according to the M-TAR model.

Model	ρ_1	ρ_2	$\rho_1 = \rho_2 = 0$	$\rho_1 = \rho_2$	Conclusion
EPU_C/EPU_I	−0.365* (−4.601)	−0.163* (−3.184)	14.812* (0.000)	4.871* (0.028)	Cointegration exist/asymmetric adjustment
EPU_C/EPU_J	−0.223* (−4.081)	−0.508* (−3.279)	13.520* (0.000)	0.034 (0.853)	Cointegration exist/symmetric adjustment
EPU_C/EPU_K	−0.368* (−3.371)	−0.410* (−6.868)	26.940* (0.000)	0.13 (0.719)	Cointegration exist/symmetric adjustment
EPU_I/EPU_J	−0.375* (−5.645)	−0.160* (−2.384)	17.766* (0.000)	5.686* (0.018)	Cointegration exist/asymmetric adjustment
EPU_I/EPU_K	−0.304* (−4.116)	−0.165* (−3.141)	12.699* (0.000)	2.515 (0.114)	Cointegration exist/symmetric adjustment
EPU_J/EPU_K	−0.265* (−4.604)	−0.151* (−2.447)	13.207* (0.000)	1.91 (0.168)	Cointegration exist/symmetric adjustment

Note: *represents significance at 5% level. Numbers in parentheses and square brackets are t-values and p values, respectively.

model (M-TVECM) specified in the modified equations (5) and (6) to establish the short-run relationships between the EPUs of the countries. Though only China-India and India-Japan EPU models produced asymmetry in the adjustment mechanism as shown in Table 7, the adjustment parameters ρ_1 and ρ_2 which represent the coefficients of the long-run relationship between the EPU pairs for the remaining models showed the significance of both positive and negative adjustments at 5% level, and since $|\rho_1| \neq |\rho_2|$, we estimate the M-TVECM for all the EPU pairs and the results are presented in Table 8. In Table 8, we have 12 M-TVECM estimated and each model comprises of each country's EPU as a dependent variable yielding three models each with the corresponding independent variables. The results suggest that the speed of adjustment of positive deviation is quicker than the negative one for most models except for three models where Korea is the dependent variable with the adjustment of negative deviations being more rapid than the positive ones. Because the coefficients of the error correction term which represent the coefficients of the long-run relationship are significant, we conclude that long-run relationship exists between the EPU pairs. Specifically, for the models where China's EPU is the dependent variable, the adjustment of the positive deviation of India's EPU is significant at 10% level, showing a positive relationship between India's EPU and China's EPU in the short run while the adjustment of the positive deviation of Korea's EPU is significant at 1% level and the joint coefficient of Korea's EPU positively impacts China's EPU in the short run. The adjustment of both positive and negative deviations of Japan's EPU is not significant at 5% level, indicating the failure of China's EPU to respond to the deviation of Japan's EPU in the short run. These results imply that upward movements in the EPU of India and Korea will cause upward movement in China's EPU as well.

In addition, models where India's EPU acts as the dependent variable, the adjustment of the positive deviation of China's EPU is although significant at 5% level and India's EPU rarely reacts to the deviation of China's EPU in the short run but instead converges to the equilibrium value in the long run. The adjustment of the positive deviation of Japan's EPU is significant at 1% level and Japan's EPU influences India's EPU positively in the short run. In the same breath, India's EPU responds to a positive deviation of Korea's EPU in the short run, as the adjustment of the positive deviation of Korea's EPU is significant at 1% level, indicating a positive relationship between Korea's EPU and India's EPU in the short run. These results imply that the increase in Japan's EPU and Korea's EPU caused an increase in India's EPU. Furthermore, having Japan's EPU as the dependent variable in the model, the adjustment of positive deviation of China's EPU is significant at 5% level but Japan's EPU rarely responses to short-run movements in China's EPU, instead it returns to the equilibrium path in the long run. Similarly, the fluctuations in India's EPU neither influences Japan's EPU in the short run nor the adjustment in either direction of the deviation of India's EPU is significant at 5% level, implying that the movement in India's

Table 8: The M-TVECM coefficient estimates.

Dep var		EPU_C			EPU_I			EPU_J			EPU_K	
Ind var	EPU_I	EPU_J	EPU_K	EPU_C	EPU_J	EPU_K	EPU_C	EPU_I	EPU_K	EPU_C	EPU_I	EPU_J
ΔEPU_C1	−0.702***	−0.559***	−0.676***							−0.210*		
	(−5.190)	(−4.543)	(0.5.636)							(−1.710)		
ΔEPU_C2	−0.630***	−0.548***	−0.596***									
	(−5.085)	(−4.345)	(−4.612)									
ΔEPU_I1	0.671***			0.338***	−0.484***	−0.466***						
	(3.586)			(−2.633)	(−3.541)	(−3.439)						
ΔEPU_I2				−0.416***	−0.420***	−0.432***						
				(−3.114)	(−3.063)	(−3.359)						
ΔEPU_J1					0.257*							0.428**
					(1.670)							(−2.048)
ΔEPU_J3							−0.317**	−0.383***	−0.0.320**			−0.490**
							(−2.382)	(−2.619)	(−2.455)			(−2.212)
ΔEPU_J4		−0.349*										
		(−1.755)										
ΔEPU_K1			0.304***			0.142**					−0.300**	
			(2.768)			(2.219)					(−2.082)	
ΔEPU_K2			0.421***									−0.203*
			(3.440)									(−1.750)
ΔEPU_K3									−0.091*		−0.318***	
									(−1.766)		(−2.670)	
ρ_1	0.097*	0.006	−0.176***	−0.233**	−0.260***	−0.161*	−0.150**	−0.155	−0.256***	−0.201	−0.023	−0.164**
	(1.837)	(0.163)	(−2.668)	(−2.239)	(−2.735)	(−1.661)	(−2.434)	(−1.628)	(−3.294)	(−1.110)	(−0.220)	(−1.996)
ρ_2	−0.050	−0.044	0.105***	−0.087	−0.038	−0.094	0.198	−0.117	0.012	−0.402***	−0.211***	−0.235***
	(−0.1.452)	(−0.935)	(2.606)	(−1.551)	(−0.461)	(−1.610)	(1.047)	(−1.355)	(0.161)	(−4.661)	(−2.810)	(−2.651)

Note: ***, **, and *represent 1%, 5%, and 10% levels, respectively. Numbers in parentheses represent t-values. "Dep var" denotes dependent variables and "Ind var" denotes independent variables. Each column under a dependent variable represents a model comprising of the dependent variable and an independent variable.

EPU does not impact the movement in Japan's EPU in the short run. In addition, the adjustment of the positive deviation of Korea's EPU is significant at 1% level, showing a negative relationship between Korea's EPU and Japan's EPU in the short run, implying that a rise in Korea's EPU leads to a fall in Japan's EPU.

Moreover, having Korea's EPU as the dependent variable in the model, we observe that the adjustment of the negative deviations of China's EPU and India's EPU and that of Japan's are significant at 1% level and these variables have a negative relationship with Korea's EPU in the short run except India's EPU, implying that upward movements in EPUs of China and Japan result in downward movement in Korea's EPU. Therefore, the abovementioned findings suggest both unidirectional and bidirectional movements between the EPUs of the countries in the short run either in the same or opposite direction to the bidirectional movements. In summary, movements in India's EPU affect China's EPU in the short run but not in the reverse case; while there is no significant short-run relationship between China's and Japan's EPUs, Japan influences China's EPU in the long run and this is consistent with Bai et al. [53] who found China to be the principal receiver of EPU spillover. For the case of China-Korea and India-Korea EPU pairs, there is a bidirectional movement between the pairs but in the opposite direction. Thus, while upward movement in Korea's EPU results in the upward movements in China's and India's EPUs, upward movements in both China's and India's EPUs result in downward movement in Korea's EPU and this relationship suggests a diversification potential for investors. Also, an upward movement in Japan's EPU causes India's EPU to move in the same direction in the short run but the movement in India's EPU in either direction does not impact movement in Japan's EPU in the short run. We can again infer from the M-TVECM that movements in EPUs of Japan and Korea impact the movement in the other in the opposite direction, indicating a significant negative relationship between these two variables in the short run. Thus, a rise in Japan's EPU results in a decline in Korea's EPU while an increase in Korea's EPU also results in a decline in Japan's EPU which again provides diversification opportunities for investors.

4.6. Estimating Causality among the EPUs in the Frequency Domain. As a final step in our analysis, we explore the existence of spectral causality among the EPU indices of the countries over the short and long run by estimating equations (7), (8), and (9). The test statistics for all frequencies in the interval $(0, \pi)$ are computed at 5% significance level and the frequencies correspond to a wavelength of $(2\pi/\omega) \sim 2$ years. The 5% critical value for the F-statistics with 2 and $(T - 2p)$ degrees of freedom corresponding to 2 and 272 degrees of freedom where the value of T is 280 observations and p is 4 (VAR order) is computed. Figure 2 shows the Granger causality between the EPUs of China and India in the frequency domain and at the 5% significance level.The null hypothesis that China's EPU does not Granger cause India's EPU cannot be rejected, implying that China's EPU does not significantly influence India's EPU in short and long run. On the other hand, India's EPU does cause China's EPU at frequencies corresponding to 5 to 6 months in the long run and 2 to 3 months in the short run. This shows a unidirectional causality between China's and India's EPU in the short and long run which indicates that the movement in India's EPU affects China's EPU through the short and long run.

Figure 3 shows the causality of China's EPU and Japan's EPU in the short and long run. The figure reveals China's EPU does not Granger cause Japan's EPU either in the short or long run at 5% significance level. This implies that the movement in China's EPU does not influence Japan's EPU in the short and long run. Japan's EPU Granger causes China's EPU at frequencies corresponding to 3 to 4 months in the long run, indicating unidirectional causality. This finding indicates that movement in Japan's EPU affects the movement in China's EPU in the long run. Figure 4 shows the frequency domain causality of China's EPU and Korea's EPU in the short and long run. Korea's EPU Granger causes China's EPU at 5% significant level at frequencies corresponding to 3 to 4 months in the long run, while China's EPU Granger causes Korea's EPU at frequencies corresponding 2 to 6 months in the short through to the long run. This is an indication of bicausality which implies that EPUs of both China and Korea influence each other in the long run.

Figure 5 displays the Granger causality of Japan's EPU and India's EPU in the frequency domain. The figure reveals the rejection of the null hypothesis that EPU of Japan does not Granger cause the EPU of India at all frequencies significant at 5% level which is rejected, indicating the movement in EPU of Japan affects movement in India's EPU in the long and short run. In the reverse case, India's EPU Granger causes Japan's EPU at significant frequencies corresponding to 2 to 3 months in the short run. The result shows bidirectional causality between the EPUs of Japan and India implying that movement in one EPU influences the other in the short and long run. Figure 6 depicts the frequency domain Granger causality of Korea's EPU and India's EPU at frequencies significant at 5% level. The null hypothesis that India's EPU does not Granger cause Korea's EPU cannot be rejected at all frequencies at 5% significance level, indicating that movement in India's EPU does not significantly influence the movement in Korea's EPU while Korea's EPU Granger causes India's EPU at frequencies corresponding to 2 to 3 months in the long run, implying the influence of Korea's EPU on the movement in India's EPU.

Finally, Figure 7 shows the Granger causality of Korea's EPU and Japan's EPU in the frequency domain. The EPU of Korea Granger causes the EPU of Japan at significant

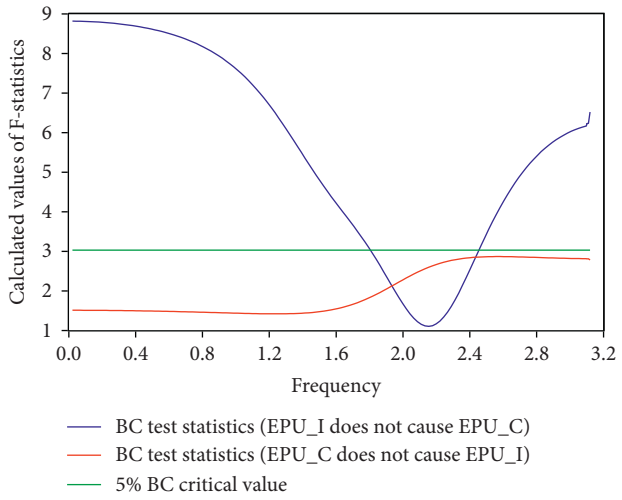

Figure 2: The frequency domain causality between China's and India's EPU indices. The part of the lines mentioned above the critical value-line indicates rejection of the null hypothesis of no Granger causality.

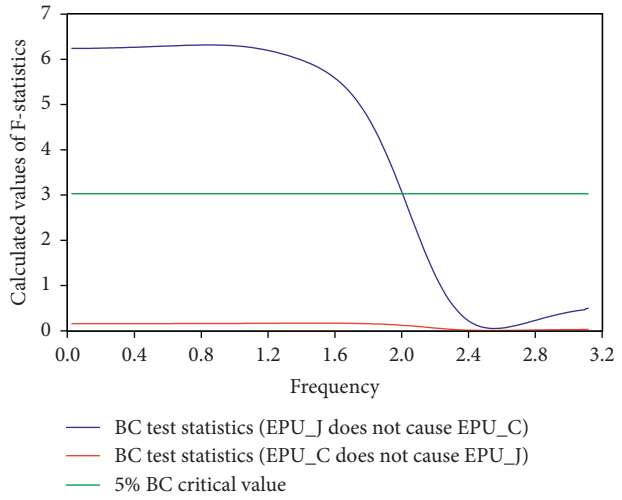

Figure 3: The frequency domain causality between China's and Japan's EPU indices. The part of the lines above the critical value-line indicates rejection of the null hypothesis of no Granger causality.

frequencies at 5% level corresponding to 2 to 3 months in the short run, implying that movement in Korea's EPU influences Japan's EPU in the short run. For the converse, Japan's EPU Granger causes Korea's EPU at frequencies corresponding to 3 to 5 months in the long run and 2 to 3 months in the short run. This implies a bidirectional causality between Korea's EPU and Japan's EPU in the long and short run. Thus, movements in both EPUs impact the other. The causal relationship between the EPU pairs of the countries is evidenced by the integration of the Asian economy through the formation of greater trade and investment linkages underpinned by East Asia's supply chain and production fragmentation and served as an engine of global trade and economic growth [66].

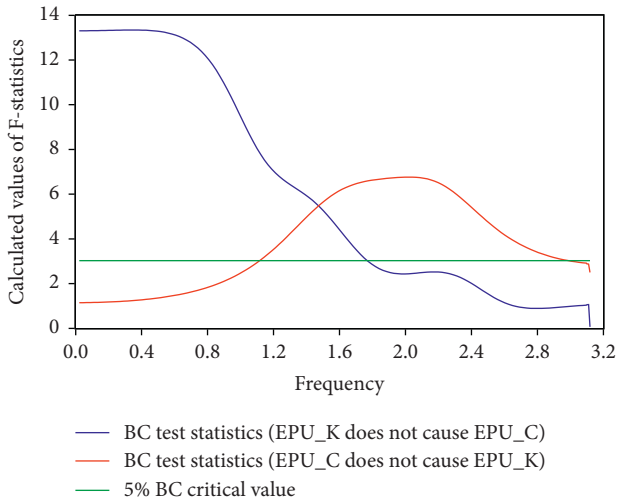

Figure 4: The frequency domain causality between China's and Korea's EPU indices. The part of the lines above the critical value-line indicates rejection of the null hypothesis of no Granger causality.

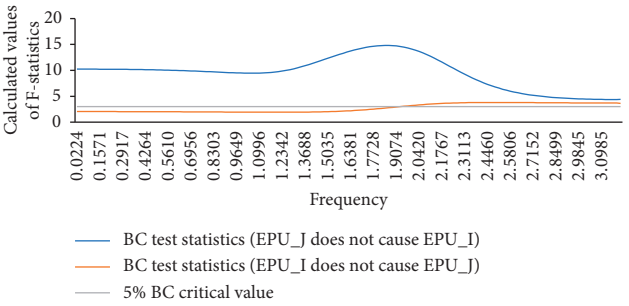

Figure 5: The frequency domain causality between Japan's and India's EPU indices. The part of the lines above the critical value-line indicates rejection of the null hypothesis of no Granger causality.

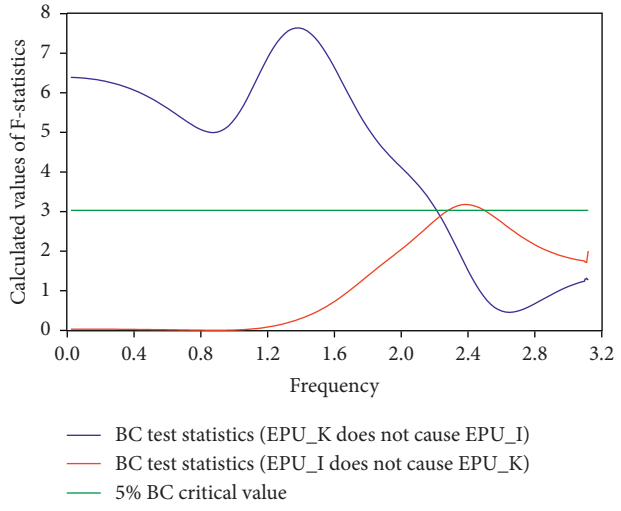

Figure 6: The frequency domain causality between Korea's and India's EPU indices. The part of the lines above the critical value-line indicates rejection of the null hypothesis of no Granger causality.

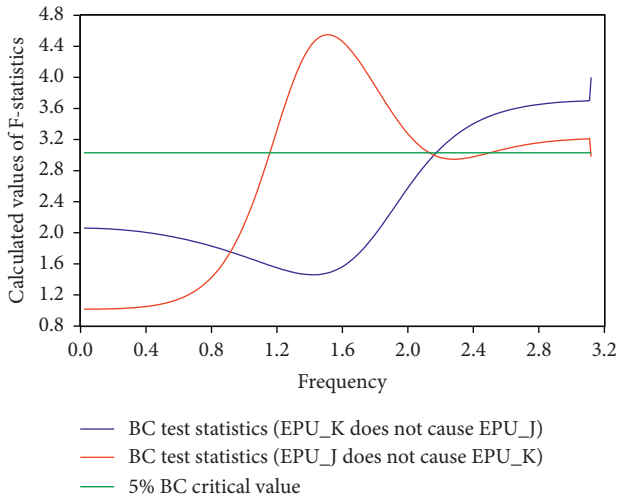

Figure 7: The frequency domain causality between Korea's and Japan's EPU indices. The part of the lines above the critical value-line indicates rejection of the null hypothesis of no Granger causality.

5. Conclusion

We have investigated the linkages between EPU pairs of four Asian countries from January 1997 to April 2020 by examining the cointegration, asymmetric cointegration, and causal relationship in the frequency domain between the EPU pairs of China, India, Japan, and South Korea, allowing for asymmetric adjustments towards long-run equilibrium. The Engle-Granger cointegration test reveals the existence of long-run relationships between the EPU pairs. Because the Engle-Granger cointegration lacks a threshold adjustment in the long-run, we employed the TAR and M-TAR models, following Enders and Siklos [24], to determine the asymmetric response of each EPU in the combination of China-India, China-Japan, China-Korea, India-Japan, India-Korea, and Japan-Korea EPU models. The TAR and M-TAR models support the threshold adjustment between the EPU pairs, which further discloses asymmetries in the EPU model adjustment process. Though the null hypothesis of no cointegration was rejected for both TAR and M-TAR models, the null hypothesis of symmetric adjustment was not rejected for all models with TAR specification with zero threshold value. However, for the M-TAR model with nonzero threshold values, the symmetric adjustment null hypothesis was rejected for China-India and India-Japan EPU pairs, indicating asymmetry in the adjustment of positive and negative divergence from the long-run equilibrium. We, therefore, estimated the M-TVECM using the M-TAR specification. The findings show that the EPUs influence each other in the short run and the threshold error term shows the speed of adjustment for positive deviation which is faster than the negative deviations for all models, except the case where Korea's EPU is the dependent variable where the speed of adjustment for negative deviations is more rapid than the adjustment of positive deviations. In all, apart from the Korea's EPU that responds quickly to the decline in other EPUs in the short run, the remaining EPUs respond quickly to a rise in value of the other EPU indices.

In addition, the bivariate analysis to establish long- and short-run relationship between the EPU pairs of the countries in the frequency domain reveals both unidirectional and bidirectional Granger causality between the EPU pairs. The findings suggest a unidirectional causality between China-India, China-Japan, and India-Korea EPU pairs where India and Japan Granger cause China's EPU in the long and short run while Korea's EPU Granger causes India's EPU in the long run, indicating that both India and Japan influence movement in China's EPU and Korea's EPU which, on one hand, influence the movement in India's EPU. However, the bidirectional causality between China-Korea pair in the long and short run exists. The findings also reveal bidirectional causality between India-Japan and Japan-Korea EPU pairs in the long and short run showing that each EPU influences movement in the other EPU in the pair in either long run or short run or both.

The linkages and comovements between the EPU pairs of countries established in our study provide policy implications to the policymakers and local and international investors of these countries, as well as the countries within the Asian subregion. Heightened economic policy inconsistency spawns fear in investors, leading to "wait" and "see" attitudes which can "impede business prospects and households' consumption and this can threaten all facets of the economy including weakened stock market performance, increased unemployment rate, volatile financial market, rising inflation, etc. Therefore, economic policymakers should be aware of the potential EPU linkages among countries so that prudent measures could be put in place to instill confidence of a growing economy in the investment community.

Data Availability

The economic policy uncertainty data were supplied by https://www.policyuncertainty.com/about.html and economic policy uncertainty is under license and so cannot be made freely available.

Conflicts of Interest

The authors declare that they have no conflicts of interest.

References

[1] N. Bloom, "The impact of uncertainty shocks," *Econometrica*, vol. 77, no. 3, pp. 623–685, 2009.

[2] G. Caggiano, E. Castelnuovo, and G. Nodari, *Uncertainty and Monetary Policy in Good and Bad Times*, Melbourne Institute, Melbourne, Australia, 2017.

[3] B. S. Bernanke, "Irreversibility, uncertainty, and cyclical investment," *The Quarterly Journal of Economics*, vol. 98, no. 1, pp. 85–106, 1983.

[4] C. D. Carroll, "Buffer-stock saving and the life cycle/permanent income Hypothesis," *The Quarterly Journal of Economics*, vol. 112, no. 1, pp. 1–55, 1997.

[5] N. Bloom, S. Bond, and J. V. Reenen, *The Dynamics of Investment under Uncertainty*, IFS Working Papers from Institute for Fiscal Studies, London, UK, 2001.

[6] R. Bansal and A. Yaron, "Risks for the long run: a potential resolution of asset pricing Puzzles," *The Journal of Finance*, vol. 59, no. 4, pp. 1481–1509, 2004.

[7] S. Gilchrist, J. W. Sim, and E. Zakrajšek, *Uncertainty, Financial Frictions, and Investment Dynamics*, National Bureau of Economic Research, Cambridge, MA, USA, 2014.

[8] D. Caldara, C. Fuentes-Albero, S. Gilchrist, and E. Zakrajšek, "The macroeconomic impact of financial and uncertainty shocks," *European Economic Review*, vol. 88, pp. 185–207, 2016.

[9] A. Sheng, C. S. Ng, and C. Edelmann, *ASIA FINANCE 2020 Framing a New Asian Financial Architecture*, Oliver Wyman, Fung Global Institute, Hong Kong, China, 2020.

[10] C. Christou, J. Cunado, R. Gupta, and C. Hassapis, "Economic policy uncertainty and stock market returns in Pacific-Rim countries: evidence based on a Bayesian panel VAR model," *Journal of Multinational Financial Management*, vol. 40, pp. 92–102, 2017.

[11] F. Balli, G. S. Uddin, H. Mudassar, and S.-M. Yoon, "Cross-country determinants of economic policy uncertainty spillovers," *Economics Letters*, vol. 156, pp. 179–183, 2017.

[12] M. Bahmani-Oskooee and S. Saha, "On the effects of policy uncertainty on stock prices: anasymmetric analysis," *Quantitative Finance and Economics*, vol. 3, no. 2, pp. 412–424, 2019a.

[13] T. C. Chiang, "Economic policy uncertainty, risk and stock returns: evidence from G7 stock markets," *Finance Research Letters*, vol. 29, pp. 41–49, 2019.

[14] E.-C. Chung and D. R. Haurin, "Housing choices and uncertainty: the impact of stochastic events," *Journal of Urban Economics*, vol. 52, no. 2, pp. 193–216, 2002.

[15] H. Yu, "Government policies and housing price instability," *Public Policy Review*, vol. 22, no. 2, pp. 74–115, 2008.

[16] D. Su, X. Li, O.-R. Lobonţ, and Y. Zhao, "Economic policy uncertainty and housing returns in Germany: evidence from a bootstrap rolling window," *Zbornik Radova Ekonomskog Fakulteta U Rijeci: Časopis Za Ekonomsku Teoriju I Praksu/ Proceedings of Rijeka Faculty of Economics: Journal of Economics and Business*, vol. 34, no. 1, pp. 43–61, 2016.

[17] J.-H. Jeon, "The impact of asian economic policy uncertainty: evidence from Korean housing market," *The Journal of Asian Finance, Economics and Business*, vol. 5, no. 2, pp. 43–51, 2018.

[18] L. Karnizova and J. Li, "Economic policy uncertainty, financial markets and probability of US recessions," *Economics Letters*, vol. 125, no. 2, pp. 261–265, 2014.

[19] K. Jurado, S. C. Ludvigson, and S. Ng, "Measuring uncertainty," *American Economic Review*, vol. 105, no. 3, pp. 1177–1216, 2015.

[20] H. Mumtaz and K. Theodoridis, "Common and country specific economic uncertainty," *Journal of International Economics*, vol. 105, pp. 205–216, 2017.

[21] I. O. Olanipekun, H. Güngör, and G. Olasehinde-Williams, "Unraveling the causal relationship between economic policy uncertainty and exchange market pressure in BRIC countries: evidence from bootstrap panel Granger causality," *SAGE Open*, vol. 9, no. 2, 2 pages, 2019.

[22] P. Alessandri and H. Mumtaz, "Financial regimes and uncertainty shocks," *Journal of Monetary Economics*, vol. 101, pp. 31–46, 2019.

[23] N. S. Balke and T. B. Fomby, "Threshold cointegration," *International Economic Review*, vol. 38, pp. 627–645, 1997.

[24] W. Enders and P. L. Siklos, "Cointegration and threshold adjustment," *Journal of Business & Economic Statistics*, vol. 19, no. 2, pp. 166–176, 2001.

[25] T. Ito and P.-L. Vézina, "Production fragmentation, upstreamness, and value added: evidence from Factory Asia 1990-2005," *Journal of the Japanese and International Economies*, vol. 42, pp. 1–9, 2016.

[26] M. Helble and B.-L. Ngiang, "From global factory to global mall? East Asia's changing trade composition and orientation," *Japan and the World Economy*, vol. 39, pp. 37–47, 2016.

[27] J. Aizenman and S.-I. Fukuda, "The pacific rim and the global economy: future financial and macro challenges," *Journal of International Money and Finance*, vol. 74, pp. 229–231, 2017.

[28] B. Shepherd, "Mega-regional trade agreements and Asia: an application of structural gravity to goods, services, and value chains," *Journal of the Japanese and International Economies*, vol. 51, pp. 32–42, 2018.

[29] S.-I. Fukuda, "Finance in asia rising: growth and resilience in an uncertain global economy," 2013.

[30] H. Ito and M. Kawai, "Trade invoicing in major currencies in the 1970s-1990s: lessons for renminbi internationalization," *Journal of the Japanese and International Economies*, vol. 42, pp. 123–145, 2016.

[31] Y. Wanhai, Y. Guo, H. Zhu, and Y. Tang, "Oil price shocks, economic policy uncertainty and industry stock returns in China: asymmetric effects with quantile regression," *Energy Economics*, vol. 68, pp. 1–18, 2017.

[32] R. Li, S. Li, D. Yuan, and K. Yu, "Does economic policy uncertainty in the U.S. influence stock markets in China and India? Time-frequency evidence," *Applied Economics*, vol. 52, no. 39, p. 4300, 2020.

[33] T. C. Chiang, "Economic policy uncertainty and stock returns: evidence from the Japanese market," *Quantitative Finance and Economics*, vol. 4, no. 3, pp. 430–458, 2020.

[34] M. Balcilar, Z. A. Ozdemir, H. Ozdemir, and M. Wohar, "Transmission of US and EU economic policy uncertainty shock to Asian economies in bad and good times," *Discussion Paper Series, IZA Instittute of Labor Economics*, vol. 18, 2020.

[35] http://www.federalreserve.gov/monetarypolicy/ fomcminutes20091216.htmFederal Open Market Committee, "Minutes of the December 2009 Meeting," 2009, HYPERLINK http://www.federalreserve.gov/monetarypolicy/ fomcminutes20091216.htm.

[36] S. Klößner and R. Sekkel, "International spillovers of policy uncertainty," *Economics Letters*, vol. 124, no. 3, pp. 508–512, 2014.

[37] J. Brogaard and A. Detzel, "The asset-pricing implications of Government economic policy uncertainty," *Management Science*, vol. 61, no. 1, pp. 3–18, 2015.

[38] M. Arouri, C. Estay, C. Rault, and D. Roubaud, "Economic policy uncertainty and stock markets:long run evidence from the us," *Finance Research Letters*, vol. 18, pp. 136–141, 2016.

[39] A. M. Adam, "Susceptibility of stock market returns to international economic policy: evidence from effective transfer entropy of Africa with the implication for open innovation," *Journal of Open Innovation: Technology, Market, and Complexity*, vol. 6, no. 3, p. 71, 2020.

[40] E. Asafo-Adjei, D. Agyapong, S. K. Agyei, S. Frimpong, R. Djimatey, and A. M. Adam, "Economic policy uncertainty and stock returns of Africa: a wavelet coherence analysis," *Discrete Dynamics in Nature and Society*, vol. 2020, Article ID 8846507, 2020.

[41] T. C. Chiang, "Financial risk, uncertainty and expected returns: evidence from Chinese equity markets," *China Finance Review International*, vol. 9, no. 4, pp. 425–454, 2019.
[42] Ľ. Pástor and P. Veronesi, "Political uncertainty and risk premia," *Journal of Financial Economics*, vol. 110, no. 3, pp. 520–545, 2013.
[43] L. Liu and T. Zhang, "Economic policy uncertainty and stock market volatility," *Finance Research Letters*, vol. 15, pp. 99–105, 2015.
[44] I.-C. Tsai, "The source of global stock market risk: a viewpoint of economic policy Uncertainty," *Economic Modelling*, vol. 60, pp. 122–131, 2017.
[45] L. P. Hansen, T. J. Sargent, and T. D. Tallarini, "Robust permanent income and pricing," *Review of Economic Studies*, vol. 66, no. 4, pp. 873–907, 1999, https://econpapers.repec.org/article/ouprestudhttps://econpapers.repec.org/article/ouprestud/.
[46] L. Pástor and P. Veronesi, "Uncertainty about government policy and stock prices," *The Journal of Finance*, vol. 67, no. 4, pp. 1219–1264, 2012.
[47] V. Sum, "The ASEAN stock market performance and economic policy uncertainty in the United States," *Economic Papers: A Journal of Applied Economics and Policy*, vol. 32, no. 4, pp. 512–521, 2013.
[48] H. Chuliá, R. Gupta, J. M. Uribe, and M. E. Wohar, "Impact of US uncertainties on emerging and mature markets: evidence from a quantile-vector autoregressive approach," *Journal of International Financial Markets, Institutions and Money*, vol. 48, pp. 178–191, 2017.
[49] N. B. Trung, "The spillover effect of the US uncertainty on emerging economies: a Panel VAR Approach," *Applied Economics Letters*, vol. 26, no. 3, pp. 210–216, 2019.
[50] S. Bhattarai, A. Chatterjee, and W. Y. Park, "Global spillover indices of US uncertainty," *Journal of Monetary Economics*, vol. 19, 2019.
[51] S. S. Akadiri, A. A. Alola, and G. Uzuner, "Economic policy uncertainty and tourism: evidence from the heterogeneous panel," *Current Issues in Tourism*, vol. 23, no. 20, p. 2507, 2019.
[52] S. Adams, F. Adedoyin, E. Olaniran, and F. V. Bekun, "Energy consumption, economic policy uncertainty and carbon emissions; causality evidence from resource rich economies," *Economic Analysis and Policy*, vol. 68, pp. 179–190, 2020.
[53] P. Luk, M. Cheng, P. Ng, and K. Wong, "Economic policy uncertainty spillovers in small open economies: the case of Hong Kong," *Pacific Economic Review*, vol. 25, no. 1, 2018.
[54] S. E. Cekin, A. K. Pradhan, A. K. Tiwari, and R. Gupta, "Measuring co-dependencies of economic policy uncertainty in Latin American countries using vine copulas," *The Quarterly Review of Economics and Finance*, vol. 14, 2019.
[55] L. Bai, X. Zhang, Y. Liu, and Q. Wang, "Economic risk contagion among major economies: new evidence from EPU spillover analysis in time and frequency domains," *Physica A: Statistical Mechanics and its Applications*, vol. 535, 2019 https://ideas.repec.org/s/eee/phsmap.html.
[56] R. F. Engle and C. W. J. Granger, "Co-integration and error correction: representation, estimation, and testing," *Econometrica*, vol. 55, no. 2, pp. 251–276, 1987.
[57] K. S. Chan, "Consistency and limiting distribution of the least squares estimator of a threshold autoregressive model," *The Annals of Statistics*, vol. 21, no. 1, pp. 520–533, 1993.
[58] J. Geweke, "Measurement of linear dependence and feedback between multiple time Series," *Journal of the American Statistical Association*, vol. 77, no. 378, pp. 304–313, 1982.
[59] Y. Hosoya, "The decomposition and measurement of the interdependency between second-order stationary processes," *Probability Theory and Related Fields*, vol. 88, no. 4, pp. 429–444, 1991.
[60] J. Breitung and B. Candelon, "Testing for short- and long-run causality: a frequency-domain approach," *Journal of Econometrics*, vol. 132, no. 2, pp. 363–378, 2006.
[61] S. R. Baker, N. Bloom, and S. J. Davis, "Measuring economic policy uncertainty ∗ ," *The Quarterly Journal of Economics*, vol. 131, no. 4, pp. 1593–1636, 2016.
[62] D. A. Dickey and W. A. Fuller, "Likelihood ratio statistics for autoregressive time series with a unit root," *Econometrica*, vol. 49, no. 4, pp. 1057–1072, 1981.
[63] P. C. B. Phillips and P. Perron, "Testing for a unit root in time series regression," *Biometrika*, vol. 75, no. 2, pp. 335–346, 1988.
[64] D. Kwiatowski, P. C. B. Peter, P. Schmidt, and Y. Shin, "Testing the null hypothesis of stationarity against the alternative of a unit root: how sure are we that economic time series have a unit root?," *Journal of Econometrics*, vol. 54, pp. 159–178, 1992.
[65] J. G. McKinnon, "Numerical distribution functions for unit root and cointegration tests," *Journal of Applied Econometrics*, vol. 11, no. 6, pp. 601–618, 1996.
[66] G. W. Schwert, "Tests for unit roots: a Monte Carlo investigation," *Journal of Business and Economic Statistics*, vol. 7, pp. 147–159, 1989.
[67] G. Kapetanios, A. Snell, and Y. Shin, "Testing for unit root in the nonlinear STAR framework," *Journal of Econometrics*, vol. 112, pp. 359–379, 2003.

Hindawi
Discrete Dynamics in Nature and Society
Volume 2021, Article ID 6668912, 9 pages
https://doi.org/10.1155/2021/6668912

Research Article

Dynamic Cross-Correlations Analysis on Economic Policy Uncertainty and US Dollar Exchange Rate: AMF-DCCA Perspective

Ruwei Zhao[1] **and Yian Cui**[2]

[1]*School of Business, Jiangnan University, Wuxi, Jiangsu 214122, China*
[2]*Research Institute, Shenzhen Stock Exchange, Shenzhen 518038, China*

Correspondence should be addressed to Yian Cui; yacui@szse.cn

Received 11 October 2020; Revised 7 December 2020; Accepted 9 January 2021; Published 30 January 2021

Academic Editor: Giancarlo Consolo

In this paper, we employ the multifractal detrended cross-correlation analysis (MF-DCCA) as the measurement instrument for the dynamic cross-correlation inspection between US economic policy uncertainty (EPU) index and US dollar exchange rate return (Ret). By calculating the cross-correlation statistics, we find mild acceptance of cross-correlation between EPU and Ret qualitatively. With further application of MF-DCCA methodology, we find strong power law cross-correlation existence within all scaling orders. Also, apparent persistence of cross-correlation has been discovered with significant Hurst exponents of all orders. Besides, we find that long-term cross-correlation demonstrates more persistence and higher degree of multifractality than those in the short term. Finally, we utilize the rolling window and binominal measurement analysis as revisits of the model. The results are consistent with model statements.

1. Introduction

It is well documented that macro factors demonstrate powerful influence in pricing financial assets, such as stocks and bonds [1–3]. However, few studies concentrate on the exchange market. Also, to have a better observation of economic policy fluctuation in a quantitative way, Baker et al. [4] develop the novel economic policy uncertainty index with the retrieval of mainstream newspapers, which is widely employed in the financial academic field [5–22]. With this view, we connect the prevailing economic policy uncertainty index with US dollar, the world's largest trading currency, to check if US macro policy adjustment would shed light on the fluctuation of US dollar exchange rate. Due to the introduction of Fractal Market Hypothesis (FMH) suggested by Mandelbrot and Van Ness [23], many researchers are inclined to employ fractal analysis methodology, such as multifractal detrended cross-correlation analysis (MF-DCCA), as the statistical instrument for the fractal characteristics discovery between nonstationary financial time series [24–32]. Zhang et al. [25] carried out a study regarding the correlation between media news and stock market index return with MF-DCCA approach. They found quantitative evidence for the cross-correlation multifractality existence between media news and SSE 50 index return. They further conducted the rolling window analysis, and the results show that scaling exponents are all above critical values, showing strong evidence of multifractality persistence between media news and index return. Zhou et al. [28] took an information content investigation of financial derivatives in China market. With MF-DCCA approach, they found that put-call ratio demonstrates antipersistent cross-correlation with 50 ETF return. Meanwhile, for the option-to-stock volume ratio, no significant cross-correlation was detected.

In this study, we employ the economic policy uncertainty index, constructed through semantic analysis techniques with hundreds of mainstream newspapers, as the representative of national economic policy fluctuation. Many prior studies have confirmed the applicability

of the economic policy uncertainty index and MF-DCCA approach [5–22, 24–32]. With this view, we utilize the MF-DCCA as a vehicle to check the existence of multifractal cross-correlation between US economic policy uncertainty index and US dollar exchange rate index return. We calculate the fluctuation function and find widespread power law cross-correlation existence. Moreover, the cross-correlations between series demonstrate strong persistence with significant exponents of all scaling orders. In addition, we calculate the time turning point and break the whole-time length into short-term and long-term periods. We find that long-term cross-correlation performs much better in persistence and multifractality compared with those in the short term. In the end, we revisit the MF-DCCA model with the rolling window and binominal measurement analysis. The results confirm series multifractality with the qualified exponents and close distances between arithmetic average and cross-correlation exponents.

Our study contributes to the existing literature from three perspectives. First, we utilize the novel US economic policy uncertainty index as the measurement for the US economic policy fluctuation and concatenate it with the US dollar exchange rate index with MF-DCCA methodology. Particularly, we find strong power law cross-correlation existence between US economic policy fluctuation and US dollar exchange rate return within all scaling orders. Also, the cross-correlations demonstrate reliable persistence with significant exponents. With this view, our empirical findings were consistent with the financial studies associated with MF-DCCA [24–32]. Second, our study originates from the exchange market perspective, providing deeper insight into the evolution dynamics of the US dollar exchange rate. Third, as the world's largest trading currency, our findings would provide valuable suggestions for investor's risk management in the US dollar exchange market by hedging with economic fluctuation.

The rest of this paper is organized as follows: Section 2 describes the data. Section 3 illustrates the multifractal cross-correlation methodology. Section 4 demonstrates the empirical results. Section 5 concludes the paper.

2. Literature Review

In this study, we investigate whether multifractal cross-correlation between economic policy uncertainty and US dollar index exists with the application of multifractal detrended cross-correlation analysis (MF-DCCA). With this view, we develop the review from the impact of economic policy uncertainty on asset pricing and the application of MF-DCCA in financial time series perspectives.

2.1. Economic Policy Uncertainty. Many studies have revealed that macro factors, such as changes in economic policies, present significant power in pricing financial assets. Bhamra et al. [3] and Chen [2] provided theoretical models embedded with economic uncertainty to answer the credit spread puzzles. However, to have a general measurement of economic policy uncertainty in a quantitative way, Baker et al. [4] constructed a novel index of economic policy uncertainty based on the analysis of newspaper coverage frequency, which is widely employed by financial researchers. Lee et al. [5] connected the China economic policy uncertainty index with US household portfolio changes. They found that US household would decrease stock holdings with increasing China economic policy uncertainty, especially for the states with more exports to China. Attig et al. [6] studied the relation between economic policy uncertainty index and company dividend payout policy internationally. The empirical findings suggest that corporate executives prefer to distribute more dividends to shareholders in the higher EPU times. Yang et al. [14] investigated whether economic policy uncertainty index holds prediction for the excess return. They found that the greater dispersion of economic policy uncertainty index would result in a higher rate of excess return in China's stock market. Hsieh and Nguyen [11] carried out a study on economic policy uncertainty index and illiquidity return premium. They found that the premium between illiquidity and liquidity portfolios would be larger when the economic policy uncertainty index begins to have an upward trend.

2.2. Multifractal Detrended Cross-Correlation Analysis. Extensive studies contribute to methodology development of nonstationary time series analysis. Kantelhardt et al. [33] proposed multifractal detrended fluctuation analysis (MF-DFA) for the examination of nonstationary time series, extending prior detrended fluctuation analysis (DFA) proposed by Peng et al. [34, 35]. Podobnik and Stanley [36] put forward detrended cross-correlation analysis (DCCA) enabling cross-correlation investigation between two nonstationary time series. However, detrended cross-correlation analysis is from the single fractal perspective, resulting in potential information loss of the time series. To have deeper insight into two nonstationary time series, Zhou [37] advanced the prevailing multifractal detrended cross-correlation analysis (MF-DCCA) by combining MF-DFA with DCCA. Ruan et al. [24] studied the multifractal characters among China's agricultural futures returns. They found credible multifractality existences among soybean, soymeal, and soyoil futures returns. Cai et al. [29] studied the cross-correlations between crude oil price and implied volatility indices. They found that the cross-correlation multifractalities are ubiquitous between series. Alaoui et al. [30] studied the cross-correlation between Bitcoin price and volume. With the application of MF-DCCA, they found adequate evidence supporting the cross-correlation multifractality between Bitcoin price and volume. Wang et al. [31] examined the cross-correlation between crude oil and agriculture futures under the shock of COVID-19. They found that the persistence between series is greatly enhanced after the involvement of COVID-19 and the cross-correlation between crude oil and sugar future presents strongest multifractality.

3. Data Description

We obtain the daily data of US EPU index by downloading it directly from the website (http://www.policyuncertainty.com/us_monthly.html). US daily EPU index is based on the article archives from Access World News NewsBank service. The Access World News NewsBank database contains over 1000 newspapers from widely known to small local newspapers across US. The measure for this index is the number of articles that contain at least one term from each of 3 sets of terms. The first set is economic or economy. The second is uncertain or uncertainty. The third set is legislation or deficit or regulation or congress or federal reserve or white house. We derive US dollar index as proxy for US foreign exchange market from Yahoo Finance. The sample periods of US daily EPU index and US dollar index are from 1 January 1985 to 8 October 2020.

In addition, we employ two log values as proxies for the cross-correlation inspection between EPU and US dollar index. The calculation processes are as follows:

$$Ret_t = \ln\left(\frac{p_t}{p_{t-1}}\right), \quad EPU_t = \ln(epu_t), \tag{1}$$

where P_t is the closing price of US dollar exchange rate at day t and EPU_t is the daily value of EPU index. Table 1 reports the descriptive statistics of EPU index and US dollar exchange rate return. As we can see in Table 1, the means of Ret and EPU (0.00 and 4.39) are smaller than the medians (0.00 and 4.40), showing a left-skew character, which is consistent with negative numbers of skewness (−0.08 and −0.13). For the kurtosis, the two series demonstrate sharp peak characteristics with values greater than 3 (5.22 and 3.39). In addition, we calculate the Jarque-Bera coefficients within each series to check the normality existence. We can find that both series present strong rejections of the normal distributions with coefficients significant at 1% levels (1878.42*** and 83.08***). Also, the standard deviation of EPU (0.68) is much larger than that of Ret (0.01), indicating a higher level of volatility.

Table 1: Descriptive statistics of Ret and EPU.

Variable	Ret	EPU
Mean	0.00	4.39
Median	0.00	4.40
Standard deviation	0.01	0.68
Max	0.03	6.69
Min	−0.04	1.20
Skewness	−0.08	−0.13
Kurtosis	5.22	3.39
Jarque-Bera	1878.42***	83.08***
N	9129	9129

The Ret and EPU terms are short for the daily US dollar exchange rate return and the US economic policy uncertainty index. N refers to the number of observations. ***Statistical significance at 1% level.

4. Methodology

In this section, we employ the prevailing MF-DCCA approach to check whether multifractality exists between the US dollar exchange rate and US economic policy uncertainty. We first utilize the methodology proposed by Podobnik and Stanley [36] to have a qualitative cross-correlation examination between series. Second, we apply the MF-DCCA approach to check if the correlations hold multifractality with the changes of scaling parameters.

4.1. Cross-Correlation Test. Before the MF-DCCA inspection, we employ a cross-correlation statistics proposed by Podobnik and Stanley [36] to have a qualitative cross-correlation check between US dollar exchange rate return and US economic policy uncertainty index. The cross-correlation statistics is constructed through two steps. Firstly, we need to have a cross-correlation indicator. The indicator C_i is created as follows:

$$C_i = \frac{\sum_{k=i+1}^{N} x_k y_{k-i}}{\sqrt{\sum_{k=1}^{N} x_k^2 \sum_{k=1}^{N} y_k^2}}, \tag{2}$$

where $\{x_k\}$ and $\{y_k\}$ are the two time series with equal lengths of N.

Secondly, we calculate the cross-correlation statistics with the involvement of prior indicator C_i. The statistics construction process is as shown in the following equation:

$$Q_{cc}(m) = N^2 \sum_{i=1}^{m} \frac{C_i^2}{N-i}, \tag{3}$$

where C_i is the cross-correlation indicator, N is the number of observations, and m works as the degree of freedom. The cross-correlation statistics $Q_{cc}(m)$ follow the $\chi^2(m)$ distribution with m degrees of freedom. The null hypothesis of the cross-correlation test proposed by Podobnik and Stanley [36] states that the cross-correlation indicator C_i demonstrates no significant difference from zero. With this view, we compare the cross-correlation statistics $Q_{cc}(m)$ and chi-square critical value $\chi^2(m)$ with m degrees of freedom to see whether the value of the cross-correlation statistics $Q_{cc}(m)$ is greater than that of the chi-square critical value $\chi^2(m)$. If so, the null hypothesis would be rejected and a reliable cross-correlation between two time series can be confirmed in a statistical way.

4.2. MF-DCCA. Zhou [37] proposed the multifractal cross-correlation analysis (MF-DCCA) for the cross-correlation inspection between time series, which is widely employed in the academic field. With this view, we employ the prevailing MF-DCCA methodology as a vehicle to check if the multifractal cross-correlation exists between the return of US dollar exchange rate and US economic policy uncertainty index. The MF-DCCA approach is derived from the detrended fluctuation analysis. The five detailed construction steps are as follows.

Step 1. We have two equal-length time series $\{x_k\}$ and $\{y_k\}$ as the indicators of the US dollar exchange rate return and US economic policy uncertainty index, where k is from 1 to N. N denotes the number of the total observations. Afterwards, two other detrended profiles $X(i)$ and $Y(i)$ are created by original time series $\{x_k\}$ and $\{y_k\}$, where i is from 1 to N, respectively. The detailed calculation process is as follows:

$$X(i) = \sum_{k=1}^{i} (x_k - \overline{x}),$$
$$Y(i) = \sum_{k=1}^{i} (y_k - \overline{y}), \tag{4}$$

where $\overline{x}$ and $\overline{y}$ are arithmetic average values of the time series $\{x_k\}$ and $\{y_k\}$. With this view, it is easy to find that $X(N) = Y(N) = 0$.

Step 2. We further divide two detrended profiles $X(i)$ and $Y(i)$ into N_s nonoverlapping segments. Each segment is a separate time series with s observations. The calculation process of length interval N_s is as follows:

$$N_s = int\left(\frac{N}{s}\right), \tag{5}$$

where N refers to the number of total observations. "int" is the symbol of integer function, which accounts for the collection of the maximum integer toward the real number. In addition, the total number N sometimes cannot be divided completely by scale s without any remainder. This would generate a short part segment ignorance at the end of each profile. To maximize the value of the entire series, we regenerate N_s segments from the end to the top of the profile. As a result, each profile holds two N_s segments after this procedure.

Step 3. To acquire the local trend of each of the two N_s segments, we perform a polynomial fitness check with each segment. As a result, the variance of each segment ν is constructed as follows:

If $\nu = 1, 2, 3, \ldots, N_s$, the variance of segment ν, $F^2(\nu, s)$, is as follows:

$$F^2(\nu, s) = \frac{1}{s} \sum_{i=1}^{s} |X((\nu - 1)s + i) - p_\nu^n(i)| \cdot |Y((\nu - 1)s + i) - p_\nu^n(i)|. \tag{6}$$

If $\nu = N_s + 1, N_s + 2, N_s + 3, \ldots, 2N_s$, the variance of segment ν, $F^2(\nu, s)$, is as follows:

$$F^2(\nu, s) = \frac{1}{s} \sum_{i=1}^{s} |X(N - (\nu - N_s)s + i) - p_\nu^n(i)| \cdot |Y(N - (\nu - N_s)s + i) - p_\nu^n(i)|, \tag{7}$$

where $p_\nu^n(i)$ is the n-th-order polynomial fitness check of segment ν.

Step 4. We take the arithmetic average of all the detrended segment variances, which generates the q-th order of the fluctuation function. The fluctuation functions are constructed by the values of q. The equations are as follows.

If $q \neq 0$,

$$F_q(s) = \left[\frac{1}{2N_s} \sum_{\upsilon=1}^{2N_s} \left[F^2(\upsilon, s)\right]^{q/2}\right]^{1/q}. \tag{8}$$

If $q = 0$,

$$F_0(s) = \exp\left[\frac{1}{4N_s} \sum_{\upsilon=1}^{2N_s} \ln\left[F^2(\nu, s)\right]\right]. \tag{9}$$

Generally speaking, the fluctuation function $F_q(s)$ is determined by the time length s under a certain value of q. In addition, the fluctuation function equals the traditional detrended cross-correlation analysis process when the value of q is 2. With this view, we repeat the procedures from Step 2 to Step 4 with various selections of s, which is an essential part of the multifractal analysis and, finally, leads to our last procedure, Step 5.

Step 5. Due to the multilength value selection of s, the fluctuation function $F_q(s)$ with different scaling orders q can be observed by checking the gradient of the log–log plots of $F_q(s)$ versus s. If the time series $X(i)$ and $Y(i)$ present a cross-correlation with multifractal property, the fluctuation function $F_q(s)$ would demonstrate a power law relationship with a large enough time length s between the two time series:

$$F_q(s) \sim s^{H_{XY}(q)}, \tag{10}$$

where $H_{XY}(q)$ is on behalf of the gradient of the log-log plots of $F_q(s)$ with the variation in the values of q. $H_{XY}(q)$ is estimated by the ordinary least-squares process.

With this view, we find that the slopes of the functions $F_q(s)$ and $H_{XY}(q)$ varied upon the value changes of scaling order q. Also, when $q = 2$, $H_{XY}(q)$ works as the standard Hurst exponent. If the scaling exponent, $H_{XY}(2)$, is larger than 0.5, we believe that a persistent cross-correlation exists. However, if the scaling exponent of $H_{XY}(2)$ is less than 0.5, we believe that persistent cross-correlation between the time series $X(i)$ and $Y(i)$ does not exist. If the scaling exponent $H_{XY}(2)$ is equal to 0.5, the cross-correlation between the time series $X(i)$ and $Y(i)$ shows no significance. With widespread application of the Hurst exponent, $H_{XY}(2)$ has been commonly viewed as the generalized Hurst exponent. Thus, if the scaling exponent $H_{XY}(q)$ is equal to a constant by any given value of scaling order q, the time series cross-correlation is believed to hold the monofractal characteristic. In contrast, if $H_{XY}(q)$ monotonously decreases with the increasing value of q, the time series are determined to be cross-correlated with multifractal property. Additionally, we can derive from equations (4) and (6) that when q is greater than zero, the segment ν, which is on behalf of the large fluctuation of $F^2(\nu, s)$, plays a vital role in valuing fluctuation function $F_q(s)$. With this view, the scaling exponent $H_{XY}(q)$ could be employed as a proxy for the illustration of the large fluctuation scaling character. Conversely, if q is less than zero, the scaling exponent $H_{XY}(q)$ would be responsible for the small fluctuation scaling character.

5. Empirical Results

5.1. Cross-Correlation Test. To have a qualitative view of the cross-correlation between the US dollar exchange rate and US economic policy uncertainty index, we follow the work of Podobnik and Stanley [36] by calculating cross-correlation indicator, C_i, and statistics, $Q_{cc}(m)$. Figure 1 demonstrates the cross-correlation statistic $Q_{cc}(m)$ and chi-square critical value $\chi^2(m)$ at 5% significant level with degrees of freedom from 1 to $N-1$. The black and green lines are responsible for the critical value of $\chi^2(m)$ and statistic $Q_{cc}(m)$, respectively. We can find that partial $Q_{cc}(m)$ statistics are equal to the critical values; thus, the null hypothesis of no cross-correlations cannot be fully accepted, which would result in a cross-correlation between US dollar exchange rate and US economic policy uncertainty index.

5.2. Multifractal Detrended Cross-Correlation Analysis. Section 5.1 provides qualitative evidence that US dollar exchange rate return and US economic policy uncertainty index would have cross-correlation with significant statistics. To have a more solid cross-correlation inspection in a quantitative way, we utilize the prevailing multifractal detrended cross-correlation analysis as the vehicle, which is extensively employed in the time series studies. We calculate the fluctuation function $F_{xyq}(S))$ with growing scaling order

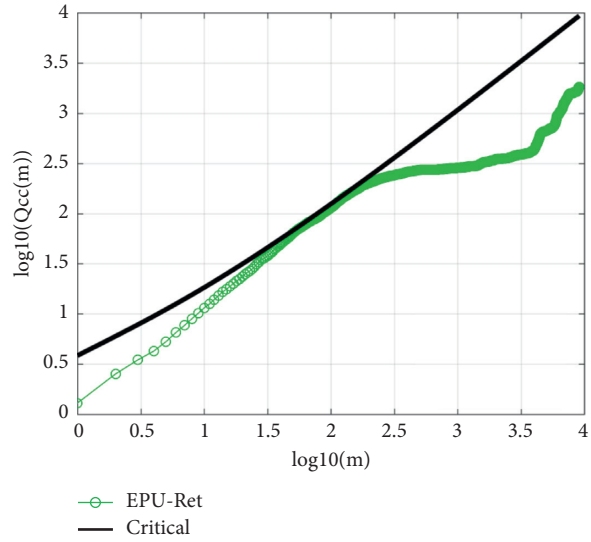

FIGURE 1: Log-log plot of cross-correlation statistic $Q_{cc}(m)$ for EPU and Ret.

q from −10 to 10 by one step length. Figure 2 plots the log-log trend of $F_{xyq}(S))$ varying upon the time length s between US dollar exchange rate return and US economic policy uncertainty index (Ret and EPU). The lines increasing from bottom to the top are on behalf of corresponding scale orders from −10 to 10. It is easy to find that $F_{xyq}(S))$ demonstrates apparent rising trend with the gradual increase of s with all scale orders, showing a power law correlation existence within the two time series.

As one of the essential inspection procedures for US dollar exchange rate return and US economic policy uncertainty index cross-correlation check, we calculate the Hurst exponent conditional on scaling order. Figure 3 shows the Hurst exponent evolution pattern upon variation of order q. We can find that the Hurst exponent values of US economic policy uncertainty index and US dollar exchange rate return (EPU-Ret) demonstrate downward pattern with increasing scale order. However, all values are greater than 0.5, indicating cross-correlation persistence between US economic policy uncertainty index and US dollar exchange rate return (EPU-Ret).

In order to have a deep insight of Hurst exponent evolution conditional on the time length s, we follow the methodology proposed by Podobnik et al. [38]. Podobnik et al. [38] divided the whole-time length into two parts, the short-term length and long-term length with a cutoff point at S^*, which indicates a fundamental change in Hurst exponent linear tendency. If the time length S is greater than that of S^*, we attribute it as long-term length and vice versa. As shown in Figure 2, $\log_{10}(S^*)$ is equal to 2.2 (S^* equals 158), marked by the vertical dashed line. Figure 4 presents the short-term and long-term Hurst exponent evolutions. We can find that the long-term Hurst exponents for EPU-Ret are all larger than those in the short term, indicating a more persistent cross-correlation compared with that in the short term. Also, we can find that both long-term and short-term Hurst exponents decline as scaling order q increases.

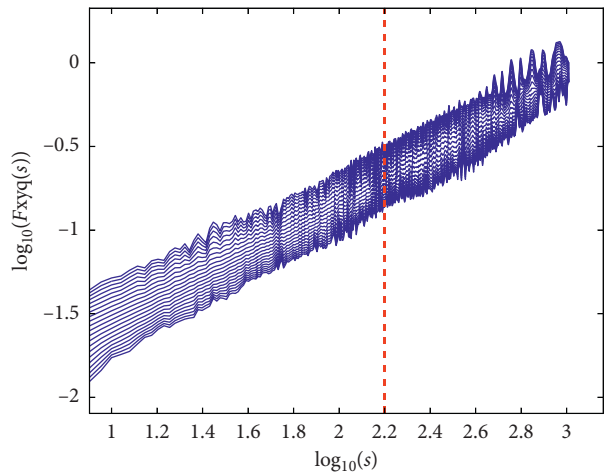

Figure 2: Log-log plot of F_{xyq} (S) versus s for EPU and Ret.

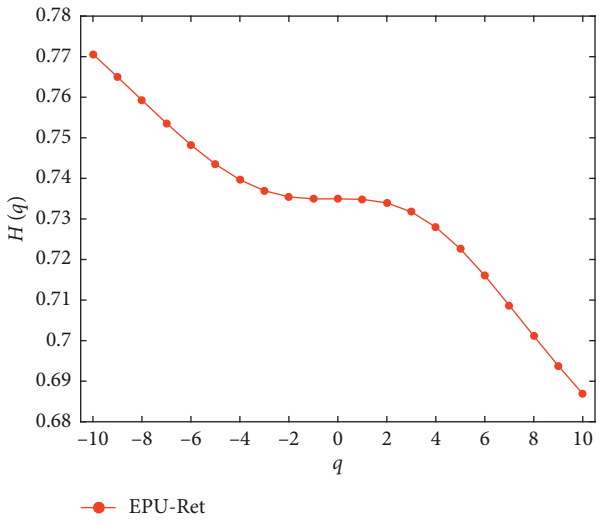

Figure 3: Hurst exponent H (q) versus q for the EPU-Ret.

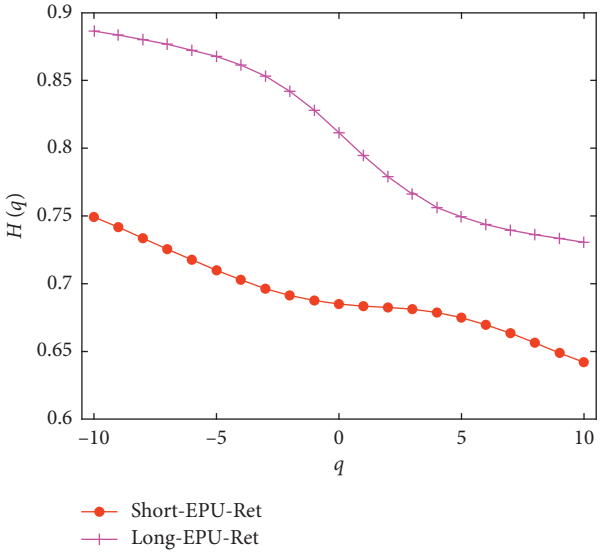

Figure 4: Short-term and long-term Hurst exponent H (q) versus q for the EPU-Ret.

With this view, the large fluctuation holds less cross-correlation than the small one. In addition, we introduce ΔH_q, the difference between max and min H_q, proposed by Yuan et al. [39], as the measurement instrument of multifractality degree. A smaller value of ΔH_q refers to a lower degree of multifractality. ΔH_q is constructed as follows:

$$\Delta H_q = \max\left(H_q\right) - \min\left(H_q\right). \tag{11}$$

As reported in the last row of Table 2, we can find that long-term ΔH_q (0.1559) is larger than that in the short term (0.1071), indicating a more stable cross-correlation within series.

5.3. Rolling Window Analysis. In this section, we perform the MF-DCCA with rolling window approach to check the cross-correlation dynamic character between US dollar exchange rate return and US economic policy uncertainty index. Due to sample size expansion, we take a four times multiplier of the rolling window setting of Zhang et al. [40] with 2000 trading days as window length and 32, 64, 128, 256, 512, and 1024 as scale s. Also, to have a more general view of trend evolution, we follow the work of Zhang et al. [41] with q as 2, 6, and 10. Figure 5 presents the Hurst exponent evolution following rolling window methodology. It is easy to find that the exponent line never moves down 0.5, showing reliable cross-correlation persistence between EPU and Ret. In addition, we perform two other robustness tests with window sizes of 1500 and 2500 as shown in Figures 6 and 7, respectively. It is easy to find that all the lines are above 0.5, which are consistent with findings in Figure 5.

5.4. A Binomial Measure from P-Model. Podobnik and Stanley [36] proposed that when scale order q equals 2, the Hurst exponent within two autoregressive fractional integrated series of same random noise would roughly bear an equivalence to the mean value of the corresponding individual Hurst exponents. Also, Zhou [37] found that if multifractality can be discovered through an iterative way,

Table 2: Short-term and long-term Hurst exponent $H(q)$ versus q.

q	EPU-Ret $S^* = 158$	
	$S < S^*$	$S > S^*$
−10	0.7491	0.8863
−9	0.7415	0.8833
−8	0.7335	0.8801
−7	0.7255	0.8765
−6	0.7174	0.8725
−5	0.7097	0.8676
−4	0.7026	0.8613
−3	0.6963	0.8530
−2	0.6912	0.8420
−1	0.6874	0.8279
0	0.6848	0.8115
1	0.6833	0.7945
2	0.6822	0.7789
3	0.6809	0.7661
4	0.6787	0.7563
5	0.6749	0.7490
6	0.6697	0.7436
7	0.6633	0.7394
8	0.6562	0.7360
9	0.6490	0.7331
10	0.6419	0.7305
ΔH_q	0.1071	0.1559

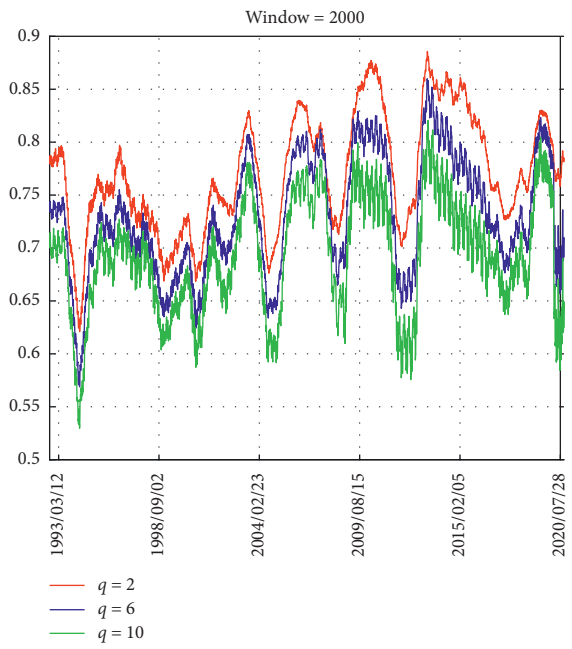

Figure 5: Dynamic Hurst exponents evolution for EPU-Ret ($q = 2$, 6, and 10, and window = 2000).

the following equation for two binomial measure series would exist:

$$H_{xy}(q) = \frac{H_{xx}(q) + H_{yy}(q)}{2}. \quad (12)$$

Figure 8 plots the Hurst exponents evolution with three time series. We can find that the exponents of $H_{xx}(q)$ and

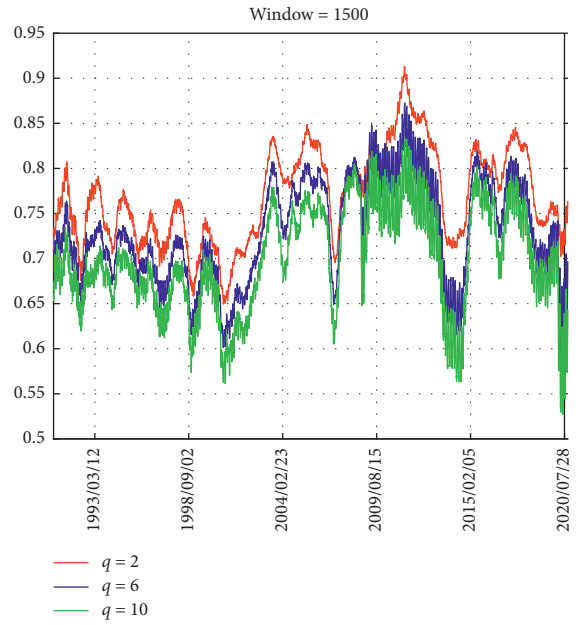

Figure 6: Dynamic Hurst exponents evolution for EPU-Ret ($q = 2$, 6, and 10, and window = 1500).

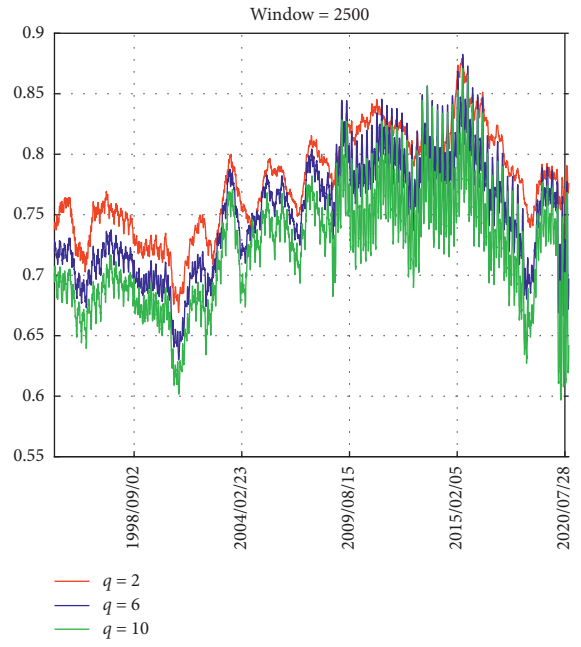

Figure 7: Dynamic Hurst exponents evolution for EPU-Ret ($q = 2$, 6, and 10, and window = 2500).

$H_{yy}(q)$ demonstrate downward patterns with reduced values as q increases, indicating multifractality existence of EPU and Ret series. Also, the arithmetic average of $H_{xx}(q)$ and $H_{yy}(q)$ presents larger value than that of $H_{xy}(q)$ as q below 0 and vice versa for q greater than 0. In addition, the differences between the arithmetic average and $H_{xy}(q)$ are small and almost symmetrically distributed. Taking this view into consideration, we believe that the differences can be offset and $H_{xy}(q)$ and $(H_{xx}(q) + H_{yy}(q))/2$ are roughly equal within the whole scaling orders.

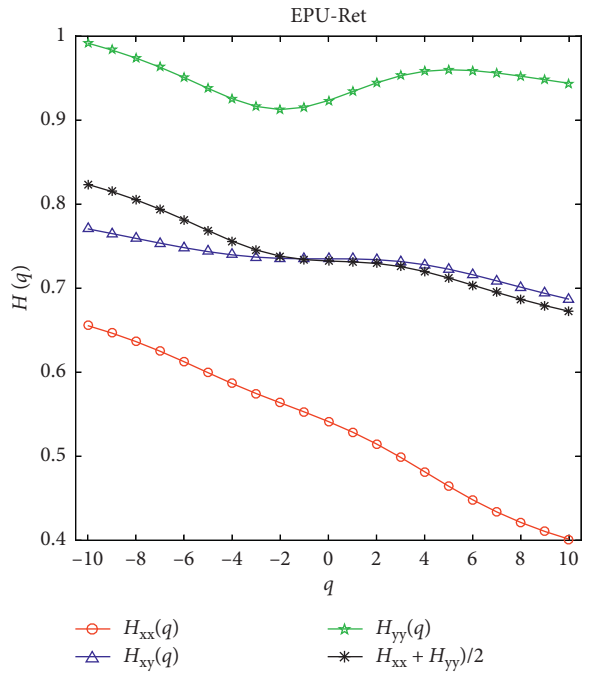

FIGURE 8: Hurst exponents $H(q)$ versus q for EPU-EPU, EPU-Ret, and Ret-Ret.

6. Conclusions

Multifractal detrended cross-correlation analysis has been confirmed as a trustworthy instrument for the detection of cross-correlation multifractality properties between series by many studies in the financial field. With this view, we utilize the fashionable logarithmic US economic policy uncertainty index as the proxy of the US economic policy uncertainty and concatenate it with the matching US dollar exchange rate return. We calculate the cross-correlation statistics and find weak evidence in the existence of cross-correlation between US dollar exchange rate return and US economic policy uncertainty index in the qualitative view. To have more quantitative insight of the multifractal cross-correlation character within series, we employ the MF-DCCA methodology. We find that US dollar exchange rate return and US economic policy uncertainty index present power law cross-correlations with all the scaling orders, confirming the multifractality property between series. Besides, we find that the Hurst exponents between US dollar exchange rate return and US economic policy uncertainty index are all above the critical values with all scaling orders, confirming reliable cross-correlation persistence. Also, the long-term cross-correlation demonstrates more persistence and higher degree of multifractality with larger exponents. Finally, we perform additional rolling window and binomial measure checks. We find that both results are consistent with the model statements.

Data Availability

The EPU and US dollar index data used to support the findings of this study are included within the article.

Disclosure

The views expressed in this paper are those of the authors and do not necessarily represent the views of the Shenzhen Stock Exchange.

Conflicts of Interest

The authors declare that they have no conflicts of interest.

Acknowledgments

This work was supported by the National Natural Science Foundation of China (71901107, 72001149, and 71790594) and the Fundamental Research Funds for the Central Universities (2019JDZD16).

References

[1] R. Bansal and A. Yaron, "Risks for the long run: a potential resolution of asset pricing puzzles," *The Journal of Finance*, vol. 59, no. 4, pp. 1481–1509, 2004.

[2] H. Chen, "Macroeconomic conditions and the puzzles of credit spreads and capital structure," *The Journal of Finance*, vol. 65, no. 6, pp. 2171–2212, 2010.

[3] H. S. Bhamra, L.-A. Kuehn, and I. A. Strebulaev, "The levered equity risk premium and credit spreads: a unified framework," *Review of Financial Studies*, vol. 23, no. 2, pp. 645–703, 2010.

[4] S. R. Baker, N. Bloom, and S. J. Davis, "Measuring economic policy uncertainty*," *The Quarterly Journal of Economics*, vol. 131, no. 4, pp. 1593–1636, 2016.

[5] K. Lee, Y. Jeon, and C. Jo, "Chinese economic policy uncertainty and U.S. households' portfolio decisions," *Pacific-Basin Finance Journal*, vol. 64, Article ID 101452, 2020.

[6] N. Attig, S. El Ghoul, O. Guedhami, and X. Zheng, "Dividends and economic policy uncertainty: international evidence," *Journal of Corporate Finance*, vol. 66, p. 101785, 2020.

[7] F. Li, T. Liang, and H. Zhang, "Does economic policy uncertainty affect cross-border M&As? —— a data analysis based on Chinese multinational enterprises," *International Review of Financial Analysis*, vol. 73, p. 101631, 2020.

[8] G. Zhang, J. Han, Z. Pan, and H. Huang, "Economic policy uncertainty and capital structure choice: evidence from China," *Economic Systems*, vol. 39, no. 3, pp. 439–457, 2015.

[9] E. Demir and O. Ersan, "Economic policy uncertainty and cash holdings: evidence from BRIC countries," *Emerging Markets Review*, vol. 33, pp. 189–200, 2017.

[10] Y. Zhu, Y. Sun, and X. Xiang, "Economic policy uncertainty and enterprise value: evidence from Chinese listed enterprises," *Economic Systems*, vol. 39, p. 100831, 2020.

[11] H.-C. Hsieh and V. Q. T. Nguyen, "Economic policy uncertainty and illiquidity return premium," *The North American Journal of Economics and Finance*, p. 101291, 2020.

[12] R. D'Mello and F. Toscano, "Economic policy uncertainty and short-term financing: the case of trade credit," *Journal of Corporate Finance*, vol. 64, p. 101686, 2020.

[13] S. Barraza and A. Civelli, "Economic policy uncertainty and the supply of business loans," *Journal of Banking & Finance*, vol. 121, p. 105983, 2020.

[14] J. Yang, C. Yang, and X. Hu, "Economic policy uncertainty dispersion and excess returns: evidence from China," *Finance Research Letters*, p. 101714, 2020.

[15] X. Wang, W. Xu, and Z. Zhong, "Economic policy uncertainty, CDS spreads, and CDS liquidity provision," *Journal of Futures Markets*, vol. 39, pp. 461–480, 2019.

[16] G. Çolak, A. Gungoraydinoglu, and Ö. Öztekin, "Global leverage adjustments, uncertainty, and country institutional strength," *Journal of Financial Intermediation*, vol. 35, pp. 41–56, 2018.

[17] X. Li, "The impact of economic policy uncertainty on insider trades: a cross-country analysis," *Journal of Business Research*, vol. 119, pp. 41–57, 2020.

[18] X.-M. Li, "New evidence on economic policy uncertainty and equity premium," *Pacific-Basin Finance Journal*, vol. 46, pp. 41–56, 2017.

[19] B. Lin and R. Bai, "Oil prices and economic policy uncertainty: evidence from global, oil importers, and exporters' perspective," *Research in International Business and Finance*, vol. 56, p. 101357, 2021.

[20] C. H. J. Cheng, C.-W. Chiu, W. B. Hankins, and A.-L. Stone, "Partisan conflict, policy uncertainty and aggregate corporate cash holdings," *Journal of Macroeconomics*, vol. 58, pp. 78–90, 2018.

[21] H. Gulen and M. Ion, "Policy uncertainty and corporate investment," *The Review of Financial Studies*, vol. 29, pp. 523–564, 2016.

[22] P. Wang, X. Li, D. Shen, and W. Zhang, "How does economic policy uncertainty affect the bitcoin market?" *Research in International Business and Finance*, vol. 53, p. 101234, 2020.

[23] B. B. Mandelbrot and J. W. Van Ness, "Fractional brownian motions, fractional noises and applications," *SIAM Review*, vol. 10, no. 4, pp. 422–437, 1968.

[24] Q. Ruan, H. Cui, and L. Fan, "China's soybean crush spread: nonlinear analysis based on MF-DCCA," *Physica A: Statistical Mechanics and Its Applications*, vol. 554, p. 123899, 2020.

[25] Z. Zhang, Y. Zhang, D. Shen, and W. Zhang, "The dynamic cross-correlations between mass media news, new media news, and stock returns," *Complexity*, vol. 2018, Article ID 7619494, 11 pages, 2018.

[26] X. Xiong, K. Xu, and D. Shen, "Dynamic cross-correlations between investors' attention and CSI300 index futures," *Fluctuation and Noise Letters*, vol. 18, no. 4, p. 1950022, 2019.

[27] S. Li, X. Lu, and X. Liu, "Dynamic relationship between Chinese RMB exchange rate index and market anxiety: a new perspective based on MF-DCCA," *Physica A: Statistical Mechanics and Its Applications*, vol. 541, p. 123405, 2020.

[28] Y. Zhou, B. Lu, D. Lv, and Q. Ruan, "The informativeness of options-trading activities: non-linear analysis based on MF-DCCA and Granger test," *Physica A: Statistical Mechanics and Its Applications*, vol. 534, p. 122269, 2019.

[29] Y. Cai, X. Lu, Y. Ren, and L. Qu, "Exploring the dynamic relationship between crude oil price and implied volatility indices: a MF-DCCA approach," *Physica A: Statistical Mechanics and Its Applications*, vol. 536, p. 120973, 2019.

[30] M. E. Alaoui, E. Bouri, and D. Roubaud, "Bitcoin price–volume: a multifractal cross-correlation approach," *Finance Research Letters*, vol. 31, 2018.

[31] J. Wang, W. Shao, and J. Kim, "Analysis of the impact of COVID-19 on the correlations between crude oil and agricultural futures," *Chaos, Solitons & Fractals*, vol. 136, p. 109896, 2020.

[32] W. Zhang, P. Wang, X. Li, and D. Shen, "Multifractal detrended cross-correlation analysis of the return-volume relationship of bitcoin market," *Complexity*, vol. 2018, pp. 8691420–20, 2018.

[33] J. W. Kantelhardt, S. A. Zschiegner, E. Koscielny-Bunde, S. Havlin, A. Bunde, and H. E. Stanley, "Multifractal detrended fluctuation analysis of nonstationary time series," *Physica A: Statistical Mechanics and Its Applications*, vol. 316, no. 1-4, pp. 87–114, 2002.

[34] C.-K. Peng, S. V. Buldyrev, A. L. Goldberger et al., "Long-range correlations in nucleotide sequences," *Nature*, vol. 356, no. 6365, pp. 168–170, 1992.

[35] C.-K. Peng, S. V. Buldyrev, S. Havlin, M. Simons, H. E. Stanley, and A. L. Goldberger, "Mosaic organization of DNA nucleotides," *Physical Review E*, vol. 49, no. 2, pp. 1685–1689, 1994.

[36] B. Podobnik and H. E. Stanley, "Detrended cross-correlation analysis: a new method for analyzing two nonstationary time series," *Physical Review Letters*, vol. 100, Article ID 084102, 2008.

[37] W.-X. Zhou, "Multifractal detrended cross-correlation analysis for two nonstationary signals," *Physical Review E*, vol. 77, Article ID 066211, 2008.

[38] B. Podobnik, I. Grosse, D. Horvatić, S. Ilic, P. C. Ivanov, and H. E. Stanley, "Quantifying cross-correlations using local and global detrending approaches," *The European Physical Journal B*, vol. 71, no. 2, p. 243, 2009.

[39] Y. Yuan, X.-t. Zhuang, and X. Jin, "Measuring multifractality of stock price fluctuation using multifractal detrended fluctuation analysis," *Physica A: Statistical Mechanics and Its Applications*, vol. 388, no. 11, pp. 2189–2197, 2009.

[40] W. Zhang, P. Wang, X. Li, and D. Shen, "Quantifying the cross-correlations between online searches and Bitcoin market," *Physica A: Statistical Mechanics and Its Applications*, vol. 509, pp. 657–672, 2018.

[41] W. Zhang, Y. Li, Z. Zhang, and D. Shen, "The dynamic cross-correlations between foreign news, local news and stock returns," *Physica A: Statistical Mechanics and Its Applications*, vol. 509, pp. 861–872, 2018.

Hindawi
Discrete Dynamics in Nature and Society
Volume 2021, Article ID 6674379, 11 pages
https://doi.org/10.1155/2021/6674379

Research Article

Dynamic Cross-Correlation between Online Sentiment and Stock Market Performance: A Global View

Kewei Xu,[1] **Yuanyuan Pang**,[1] **and Jiatong Han**[2]

[1]*College of Management and Economics, Tianjin University, Tianjin 300072, China*
[2]*School of Finance, Tianjin University of Finance and Economics, Tianjin 300072, China*

Correspondence should be addressed to Yuanyuan Pang; tju_pyy2015@163.com

Received 5 November 2020; Revised 10 December 2020; Accepted 15 January 2021; Published 27 January 2021

Academic Editor: Luca Pancionie

This paper focuses on investigating the dynamic cross-correlation relationship between online sentiment and returns of major global stock markets based on the MF-DCCA method. We use Daily Happiness (DHS), an index derived from Twitter posts through textual analysis as a proxy of online sentiment. By dividing the global financial markets into developed and developing ones, we are able to test the heterogeneous relationship between stock market performance and sentiment at different economic developing level. Empirical results show that there exists a power-law cross-correlation relationship between financial market and online sentiment in some developed countries and all developing countries, and the relationship is more stable in the developing countries. Moreover, we apply rolling window analysis to capture the dynamic evolution characteristics and find the relationship has a strong consistency over time. Our work provides a much more delicate perspective to test the relationship between online sentiment and financial markets performance and enriches the existing literature.

1. Introduction

Investor behavior in financial market cannot be fully explained by classical financial theory under the hypothesis of completely rational person. The behavioral financial theory takes human behavioral bias including limited investor attention [1–3] and emotional behavior into consideration, guiding researchers to examine the relationship between sentiment and financial market performance. Various proxies have been come up with the aim of capturing sentiment precisely, including closed-end fund discount [4, 5], indices extracted from financial and market indicators [6], and indices generated by textual analysis through either financial newspapers [7] or social media [8, 9]. Compared with others, the sentiment indicator, based on social media information, is exogenous to financial markets and can be acquired at high frequencies, making it practical in sentiment study.

The interaction between media sentiment and stock market activity began to draw widespread attention since Tetlock [7] found that the emotional orientation of Wall Street Journal content has the function of predicting board movements of stock market, and high media pessimism reveals a downward price pressure on stock market. Alanyali [8] did a similar research based on Financial Times press issues. With the rapid development of modern technology, social media contains not only newspapers but also Internet social platforms, making capturing social media sentiment through Internet search engine data possible. Various proxies have been employed to represent online sentiment, and these sentiment proxies can be based on Facebook posts [9, 10], Google search [11, 12], or Baidu search index [13, 14]. In particular, Bollen et al. [15] analyze the text content of daily Twitter and found that the sentiment index derived from Twitter is correlated with Dow Jones Industrial Average over time. Another widely used sentiment indicator based on Twitter posts is Daily Happiness Index (DHS), an index extracted from 10% of all tweets using textual analysis. DHS is derived from the worldwide social media Twitter with millions of thousands of users, and the massive users around the world ensure the rationality of using DHS to measure online sentiment. Compared with the sentiment index extracted from financial market, DHS provides a

broader horizon of sentiment. In fact, a strand of recent papers have documented a link between sentiment proxies strictly exogenous to financial markets and stock returns, including the loss of sports games [16], morning sunshine [17], TV program [18], and even sunspots and the stars [19]. Meanwhile, DHS is strictly exogenous to the financial market and avoids the endogenous problems that may arise later. The existing literature using DHS as a sentiment proxy mainly focuses either on the linear relationship between sentiment and stock market performance [20–22] or on the lead-lag Granger causality relationship in developed financial markets [23]. These research methods have shortcomings in capturing the microdynamic changes and nonlinear relationship between sentiment and stock market performance. A more simulation model is urgently needed to generate more pervasive and accurate profile of sentiment.

Deepening of globalization not only enables people from different countries to share messages via the same social media, but also makes financial markets worldwide connect with each other [24–27] more intensely. Thus, it is of great importance to characterize the correlation between online sentiment and financial market performance in a worldwide perspective and further study the heterogeneity of the relationship between sentiment and different markets. In this paper, we investigate the cross-correlation between online sentiment and returns of major global financial markets. Specifically, we choose Daily Happiness (DHS) as the exogenous proxy for online sentiment and characterize the nonlinear relationship between sentiment and stock market returns dynamically through MF-DCCA, which has been proved to be practical in simulating multifractal features of financial market.

Our research may contribute to the existing literature in two ways: On one hand, we characterize the dynamic relationship between online sentiment and stock market return using MF-DCCA, and the cross-correlation between the two is distinguished in different wavebands. Thus, a much more delicate perspective has been found to test the relationship between sentiment and financial markets. On the other hand, previous researches mainly use DHS as a sentiment proxy of either the US market [7] or other individual market [9,10]. In this paper, we divide the global stock market into subsamples according to the economic development level and compare the similarities and differences of the cross-correlation relationship between online sentiment and stock market performance.

The rest of the paper is organized as follows. Section 2 introduces the model and methodology, Section 3 describes the data in this study, Section 4 presents the empirical results, and Section 5 concludes the paper.

2. Methodology

We mainly follow the rationale of Zhou [27], using MF-DCCA (multifractal detrended cross-correlation analysis) model to assume the dynamic relationship between online sentiment and stock market. MF-DCCA model is a Frontier approach to measure nonlinear and unstable correlations. This research branch is originated from [28], in which DEA model is proposed and gradually became the most widely used nonlinear analyzed method. Subsequent studies continue to optimize DEA model [29–31]. Podobnik and Stanley [32] creatively apply DEA to the long-range cross-correlation analysis of two nonstationary series and construct a new method named DCCA. On this basis, Zhou [27] added multifractal function method into DCCA and proposed MF-DCCA. MF-DCCA has advantages in fitting nonlinearity and multifractals in the cross-correlation between time series in the financial market and has been widely used [32–38].

For any two equal-time series of length N $\{x_i\}$, $\{y_i\}$, $i = 1, 2, \ldots, N$, there are five main steps to construct MF-DCCA algorithm.

Step 1. Construct two accumulated differential sequences as profiles:

$$\begin{aligned} X_t &= \sum_{k=1}^{t} (x_k - \overline{x}), \\ Y_t &= \sum_{k=1}^{t} (y_k - \overline{y}), \quad t = 1, 2, \ldots, N, \\ \overline{x} &= \frac{1}{N} \sum_{k=1}^{N} x_k, \\ \overline{y} &= \frac{1}{N} \sum_{k=1}^{N} y_k, \end{aligned} \tag{1}$$

where $\overline{x}$ and $\overline{y}$ are the mean values of the time series, respectively.

Step 2. Divide X_t and Y_t into $N_s = \mathrm{int}(N/s)$ nonoverlapping segments of equal lengths s. Notably, N is often difficult to maintain as an integer multiple of s, which will cause the part of the end of the sequence that is less than s to be discarded by calculating $\mathrm{int}(N/s)$. To solve this, we perform the same segmentation process from the end forward again and finally get $2N_s$ nonoverlapping parts containing all the information in the original time series.

Step 3. For each segment, evaluate the local trend with least squares fit, and then calculate the difference between the original time series and the fitting polynomial to get the detrended covariance.

For segment $\lambda = 1, 2, \ldots, N_s$,

$$F^2(s, \lambda) = \frac{1}{s} \sum_{k=1}^{s} \left| X_{(\lambda-1)s+k}(k) - \widetilde{X_\lambda}(k) \right| \left| Y_{(\lambda-1)s+k}(k) - \widetilde{Y_\lambda}(k) \right|. \tag{2}$$

For the flashback segment $\lambda = N_s + 1, N_s + 2, \ldots, 2N_s$,

$$F^2(s, \lambda) = \frac{1}{s} \sum_{k=1}^{s} \left| X_{N-(\lambda-N)s+k}(k) - \widetilde{X_\lambda}(k) \right| \left| Y_{N-(\lambda-N)s+k}(k) - \widetilde{Y_\lambda}(k) \right|. \tag{3}$$

Step 4. Take the average value of all the detrended covariances to obtain the q-order fluctuation function. For any $q \neq 0$,

$$F_q(s) = \left\{ \frac{1}{2N_s} \sum_{\lambda=1}^{2N_s} \left[F^2(s,\lambda) \right]^{q/2} \right\}^{1/q}. \quad (4)$$

For any $q = 0$,

$$F_q(s) = \exp\left\{ \frac{1}{4N_s} \sum_{\lambda=1}^{2N_s} \left[F^2(s,\lambda) \right] \right\}. \quad (5)$$

It is worth noting that MF-DCCA degenerates to the conventional DCCA method when $q = 2$.

Step 5. Draw a log-log graph with $F_q(s)$ set as the y axis and s as the x axis, and observe the trends at different scales. Specifically, there exists a power-law cross-correlation relationship of the following form if the two series have long-range cross-correlation:

$$F_q(s) \backsim s^{H_{xy}(q)}, \quad (6)$$

where the scaling exponent $H_{xy}(q)$ for each q can be obtained by observing the slope of the log–log plots of $F_q(s)$ versus s through ordinary least squares.

$H_{xy}(q) < 0.5$ reveals that the two series fluctuate towards the opposite direction. On the contrary, when $H_{xy}(q) > 0.5$, there is a positive cross-correlation between the two sequences; that is, when one sequence fluctuates in the positive direction, the other will also fluctuate in the same direction. No significant cross-correlation relationship exists if $H_{xy}(q) = 0.5$. If $q = 2$, MF-DCCA collapses to DCCA, and the exponent $H_{xy}(q)$ is equivalent to the generalized Hurst exponent.

3. Data

We use the Daily Happiness Index (DHS) extracted from Twitter as a proxy for online sentiment in accordance with previous literature [20–23]. DHS is compiled by Hedonometer using Amazon's Mechanical Turk service and natural language text analysis algorithm (For more details on DHS, see http://hedonometer.org/index.html). DHS conveys 10% of all daily Twitter information (Nearly 50 million text messages). Massive real social data ensure the authority of DHS in measuring the online sentiment. We obtain DHS index from September 10th, 2008, to August 31st, 2019.

We use market size and trading volume as the basis for selecting representative financial markets in this study. Our empirical sample includes the world's top 20 stock market daily data indices, covering Asian, European, and American main stock exchanges. Among these 20 indices, S & P500, NASDAQ, and Dow Jones Industrial Average and other four indices are all from USA. We choose the two highest-ranked indices, S & P 500 and NASDAQ as representatives in order to solve multicollinearity between indices. Meanwhile, we drop Shanghai Composite Index from our sample because Twitter is prohibited in Chinese Mainland, and DHS cannot reflect the online sentiment of local Chinese mainland effectively. Our final sample is, thus, containing 11 stock market indices of 10 countries in total (All stock market data used in this paper are from YAHOO! Finance: http://finance.yahoo.com). The developed markets include the United States (S & P500 and NASDAQ), the United Kingdom (FTSE), Germany (DAX), France (FCHI), Japan (Nikkei), and South Korea (KOSPI), and the developing countries include Brazil (BVSP), Mexico (MXX), India (BSE), and Indonesia (JKSE), respectively. The time interval is from September 10th, 2008, to August 31st, 2019, and non-synchronized time period data is excluded in each group to ensure comparability. Table 1 presents daily summary statistics of return (%) of each financial market indices in our final sample, whereas Figure 1 depicts the trend for DHS.

This table shows the descriptive statistics for our sentiment indicator-DHS and 11 major global market index returns, including the United States (S & P500 and NASDAQ), the United Kingdom (FTSE), Germany (DAX), France (FCHI), Japan (Nikkei), and South Korea (KOSPI), and the developing countries include Brazil (BVSP), Mexico (MXX), India (BSE), and Indonesia (JKSE), respectively. Mean represents the mean value of each variable, while Std. stands for standard deviation. We also report the quartile of each variable. Figures are expressed in percentage.

4. Empirical Results

4.1. Cross-Correlation Test. It is necessary to verify whether there is a cross-correlation between online sentiment and stock market returns before using MF-DCCA for dynamic cross-correlation analysis. Following previous studies [29, 30, 34, 35], we employ Q_{cc} statistic test to quantitatively measure the cross-correlations between online sentiment and stock market returns. The cross-correlation statistic Q_{cc} between the time series $\{x_i\}$ and $\{y_i\}$ is defined as

$$Q_{cc}(m) = N^2 \sum_{i=1}^{m} \frac{c_i^2}{N-i}, \quad (7)$$

where their cross-correlation function is shown as follows:

$$c_i = \frac{\sum_{k=i+1}^{N} \text{return}_k \text{dhs}_{k-i}}{\sqrt{\sum_{k=1}^{N} \text{return}_k^2 \sum_{k=1}^{N} \text{dhs}_k^2}}. \quad (8)$$

According to Podobnik and Stanley [29], the cross-correlation statistic $Q_{cc}(m)$ is approximately $\chi^2(m)$ distributed with m degrees of freedom. The null hypothesis of χ^2 test is that there is no cross-correlation between the two series. In other words, if the statistic $Q_{cc}(m)$ is larger than the critical value of Chi-Square test, the null hypothesis is rejected, indicating that two series are cross-correlated.

Figure 2 shows the cross-correlation test result between stock market returns and online sentiment measured by DHS in developed countries, while Figure 3 exhibits the test results in the developing ones. The horizontal axis indicates the degrees of freedom m after the natural logarithm, and the vertical axis is the statistic $Q_{cc}(m)$. Full line marked with circles is the cross-correlation statistics of online sentiment

Table 1: Descriptive statistics: DHS and return (%) of financial market indices.

	Obs.	Mean	Std.	Min	25%	Median	75%	Max
DHS	4002	6.021	0.046	5.774	5.987	6.020	6.053	6.357
S & P500	2758	0.040	1.242	−9.035	−0.374	0.065	0.551	11.580
NASDAQ	2758	0.056	1.341	−9.142	−0.455	0.096	0.681	11.806
FTSE	2663	0.017	0.904	−4.838	−0.434	0.024	0.515	3.840
DAX	2640	0.033	1.406	−7.073	−0.565	0.069	0.675	11.402
FCHI	2787	0.020	1.421	−9.037	−0.618	0.037	0.686	11.176
Nikkei	2644	0.031	1.548	−11.406	−0.659	0.068	0.811	14.150
KOSPI	2648	0.022	1.182	−10.571	−0.460	0.040	0.586	11.946
BVSP	2640	0.037	1.707	−11.393	−0.846	0.030	0.904	14.656
MXX	2726	0.025	1.162	−7.008	−0.510	0.036	0.573	11.005
BSE	2734	0.039	1.278	−10.956	−0.556	0.055	0.635	17.339
JKSE	2736	0.060	1.248	−10.690	−0.478	0.100	0.640	7.640

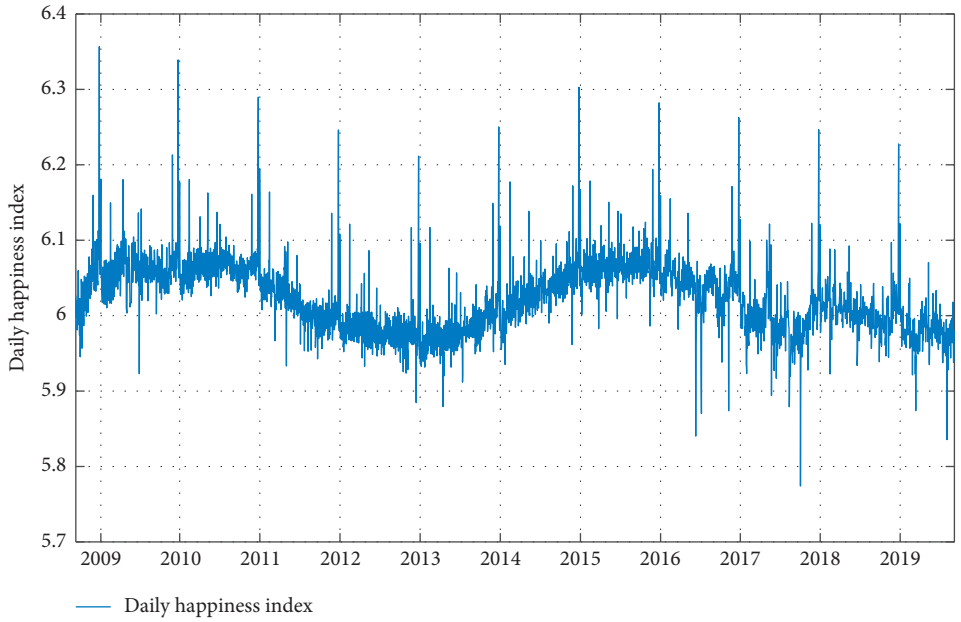

Figure 1: Evolution of daily happiness index during 2008–2019.

and the corresponding financial market. Full line representing the critical value of the $\chi^2(m)$ distribution $Q_{cc}(m)$ with m degrees of freedom at the 5% significance level is shown as comparison. We set freedom m ranging from 1 to 1500.

The results in Figure 2 show that, in the United States, Japan, and Germany, the cross-correlation statistics $Q_{cc}(m)$ of these four financial markets are all lager than the critical value regardless of degrees of freedom, suggesting a significant cross-correlation between online sentiment and financial market return in these countries. As to the other two developed countries, South Korea and UK, the cross-correlation statistics $Q_{cc}(m)$ are quite close to or even lower than the critical value of $\chi^2(m)$ distribution at 5% significant level under large degrees of freedom. The empirical results show that, in the developed countries, the relationship between online sentiment and stock market return is heterogeneous. When it comes to the developing countries, we can see that, in Figure 3, the cross-correlation statistics $Q_{cc}(m)$ are all higher than the critical value. To sum up, the cross-correlation between online sentiment and financial market return is stronger in the developing countries compared with that in the developed ones. The empirical results provide a complementary to Zhang et al. [21] by analyzing the different dynamic correlations between financial markets and sentiment in developing and developed countries, respectively. In addition, compared with Da et al. [11, 12], we are concerned about the cross-correlation rather than linear relationship between online sentiment and stock market performance.

4.2. MF-DCCA. In the $Q_{cc}(m)$ test of cross-correlation, South Korea, UK, and France cannot reject the null hypothesis; that is, there is insufficient evidence to prove that there is a significant cross-correlation between financial market return and the online sentiment measured by DHS index. The other seven countries reject the null hypothesis, confirming a significant cross-correlation between financial

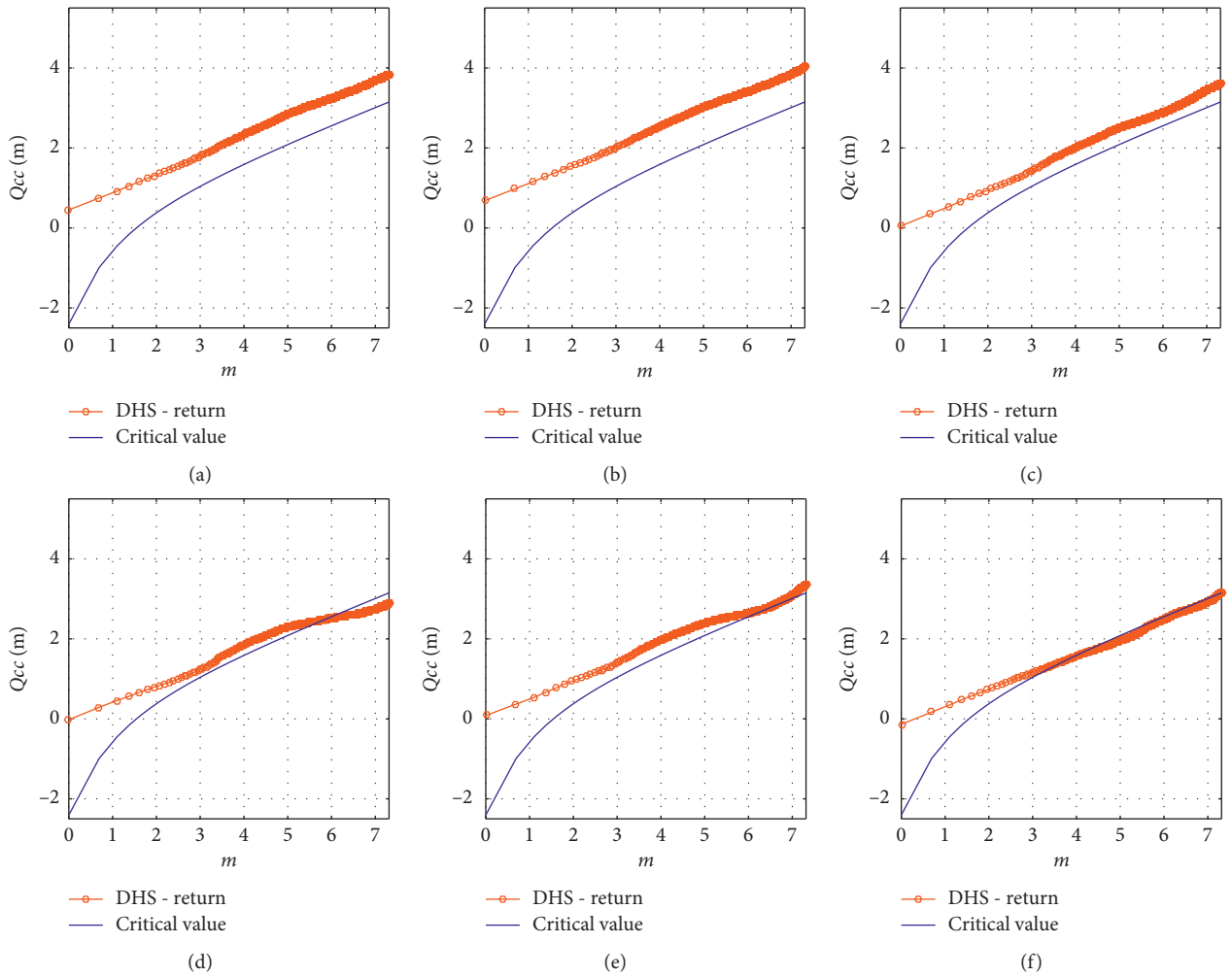

FIGURE 2: The cross-correlation statistics between online sentiment (DHS) and stock market return in developed countries: (a) US: SP500, (b) US: Nasdaq, (c) Japan: Nikkei, (d) Korea: KOSPI, (e) Germany: DAX, and (f) UK: FTSE.

market return and online sentiment. The cross-correlation test based on the statistics $Q_{cc}(m)$ gives a clue for the presence of cross-correlation qualitatively. In this part, we try to test the cross-correlations quantitatively by estimating the cross-correlation exponent using MF-DCCA method.

In this paper, the range of the slitting length s is set to $10 < s < (N/4)$ (N is the length of the financial market return sequence in each group), and the fluctuation function order q is set to be ranging from −10 to 10. The corresponding online sentiment sequence belongs to the small-band sequence when $q < 0$; otherwise, it belongs to the large-band sequence. Figure 4 shows the log–log plots of $\log(F_q(s))$ versus $\log(s)$ as $q = -10, -9, \ldots, 9, 10$ for the fluctuation function of financial markets and investor sentiment in both developed countries(left side) and developing ones (right side). It can be seen that all curves belonging to 8 financial markets overall present an obvious linear trend despite the fluctuation with the changes of different interval length s. The empirical results demonstrate that there is a significant power-law cross-correlation between financial markets and online sentiment.

In Figure 4, the fluctuation function of financial market returns and online sentiment in various countries shows a relatively stable trend before $\log(s^*)$, and after that, the trend changed significantly. s^* is the "crossover" defined by Podobnik et al. [32]. We use the crossover to divide the cross-correlation between two sequences into short-term relationships (when $s < s^*$) and long-term relationships (when $s > s^*$). Specifically, in the developed countries, the "crossover" of the cross-correlation relationship between the market return of S & P500 (USA), NASDAQ (USA), Nikkei225 (Japan), and DAX (German) and online sentiment occurs at about 245 days, 255 days, 95 days, and 102 days, respectively. Among the developing countries, the "crossover" of the cross-correlation between the return of the BVSP (Brazil), JKSE (Indonesia), MXX (Mexico), BSE (India), and online sentiment is at about 79 days, 96 days, 61 days, and 161 days, respectively.

We further construct the scaling exponent $H_{xy}(q)$ of the fluctuation function between the return of each financial market and online sentiment under different time length s and different order q, so as to explore the heterogeneity of markets in different countries. Table 2 shows the average value of scaling cross-correlation exponents $H_{xy}(q)$ in the developed countries and developing countries under

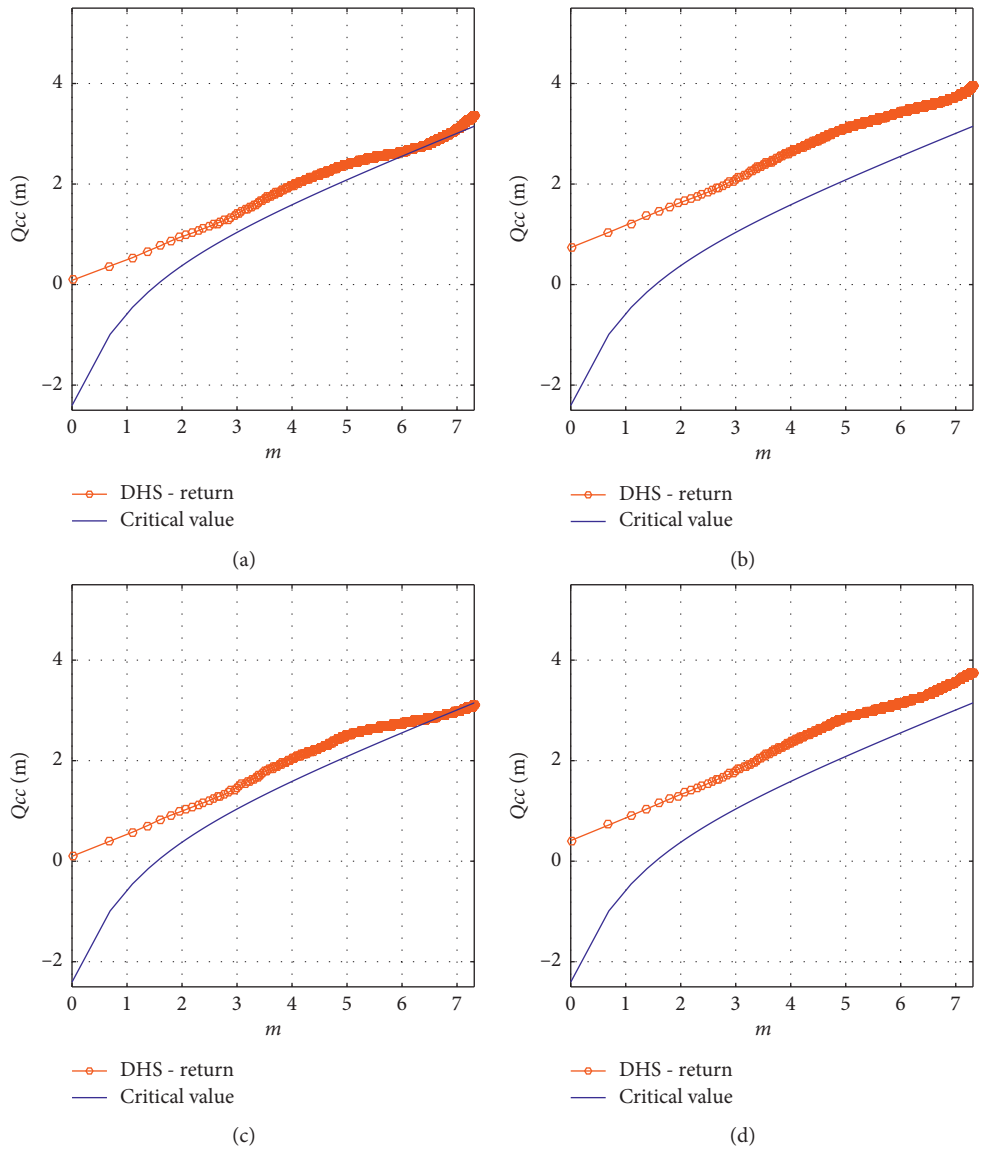

FIGURE 3: The cross-correlation statistics between online sentiment (DHS) and stock market return in developing countries: (a) Brazil: BVSP, (b) Indonesia: JKSE, (c) Mexico: MXX, and (d) India: BSE.

different order q for long term $(S > S^*)$ and short term $(S < S^*)$. As is shown, when $q = 2$, $H_{xy}(2)$ are all greater than 0.5 in different countries, proving a strong positive cross-correlation between financial market return and online sentiment. In other words, financial market returns tend to change in the same direction as online sentiment measured by DHS does. However, it is also noteworthy that, in our sample, the fluctuation scaling exponent $H_{xy}(q)$ in the developed countries is smaller than that in the developing countries. In addition, in the developed countries, $H_{xy}(q)$ is close to 0.5 $(H_{xy}(2) = 0.5564)$ in the short term (when $s < s^*$), which means that the degree of synergy between the financial markets and online sentiment is low.

To further study the multifractal nature of the cross-correlation coefficient between financial market and online sentiment, we calculate the degree of multifractal ΔH_q under different wavebands:

$$\Delta H_q = \max\left(H_q\right) - \min\left(H_q\right). \tag{9}$$

The greater the ΔH_q is, the greater the degree of multifractal is. The last three rows of Table 2 show the crossover between the two under different order q. Overall, the fractal degree of the cross-correlation between financial market and online sentiment in the developing countries is significantly greater than that in the developed countries. The empirical results show that the relationship between financial market return and online sentiment is more stable in the developed countries, whereas they have weaker cross-correlation relationship compared with the developing countries. It is easy to conclude that although the cross-correlation between the return of financial markets and online sentiment in developing countries is stronger, the volatility is also greater, and the relationship is more unstable.

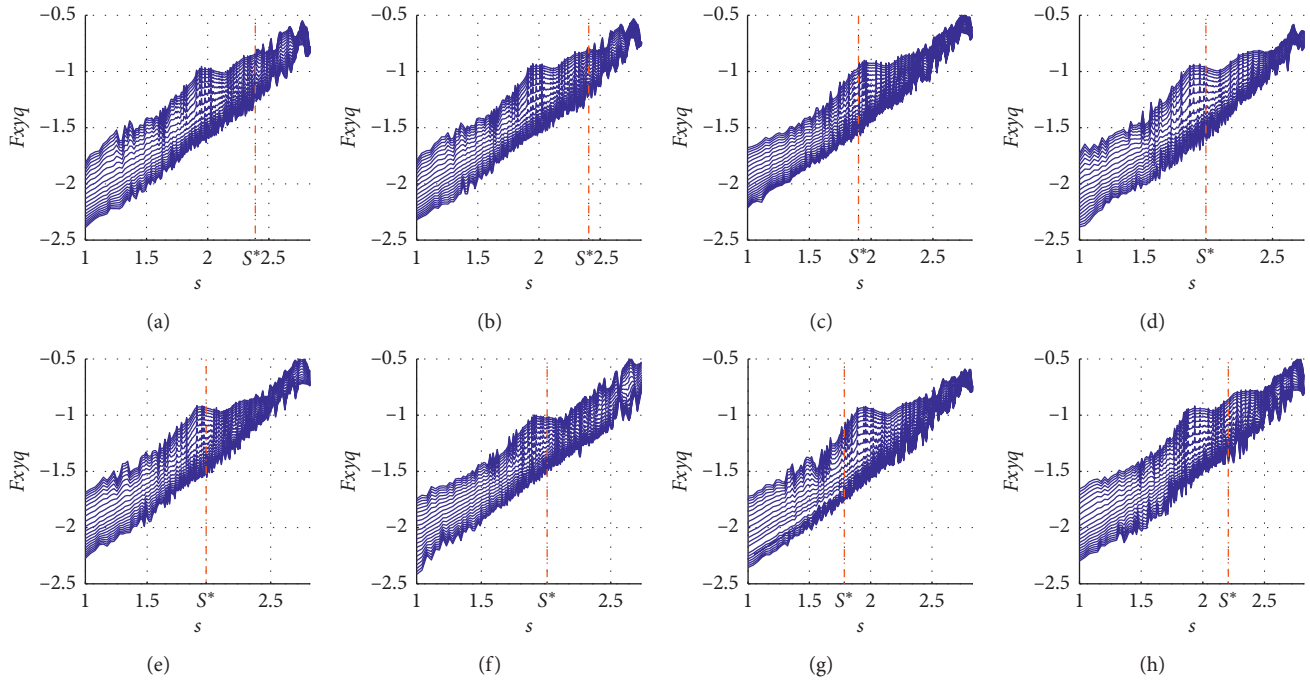

Figure 4: Log-log plots of $\log(F_q(s))$ versus $\log(s)$ for the developed (developing) financial markets return and online sentiment: (a) US: SP500, (b) US: Nasdaq, (c) Brazil: BVSP, (d) Indonesia: JKSE, (e) Japan: Nikkei, (f) Germany: DAX, (g) Mexico: MXX, and (h) India: BSE.

Table 2: Average value of scaling cross-correlation exponents $H_{xy}(q)$ for the stock market returns and online sentiment in developed and developing countries.

Q	Developed countries		Developing countries	
	$S < S^*$	$S > S^*$	$S < S^*$	$S > S^*$
−10	0.6630	0.8555	0.8045	1.0520
−9	0.6562	0.8520	0.7976	1.0478
−8	0.6487	0.8482	0.7899	1.0432
−7	0.6405	0.8441	0.7814	1.0383
−6	0.6317	0.8396	0.7723	1.0329
−5	0.6222	0.8346	0.7626	1.0270
−4	0.6121	0.8289	0.7526	1.0202
−3	0.6014	0.8218	0.7424	1.0119
−2	0.5900	0.8125	0.7320	1.0012
−1	0.5782	0.7997	0.7220	0.9864
0	0.5668	0.7816	0.7141	0.9656
1	0.5583	0.7569	0.7130	0.9356
2	0.5564	0.7249	0.7270	0.8932
3	0.5628	0.6873	0.7588	0.8384
4	0.5738	0.6485	0.7962	0.7788
5	0.5838	0.6124	0.8261	0.7235
6	0.5901	0.5814	0.8453	0.6767
7	0.5931	0.5557	0.8564	0.6388
8	0.5937	0.5349	0.8622	0.6083
9	0.5928	0.5179	0.8648	0.5839
10	0.5912	0.5040	0.8657	0.5640
ΔH $(q < 0)$	0.0848	0.0559	0.0825	0.0656
ΔH $(q > 0)$	0.0354	0.2528	0.1526	0.3716
ΔH (all)	0.1066	0.3515	0.1526	0.4880

Considering different wavebands ($q < 0$ or $q > 0$), the degree of fractal in the small waveband ($q < 0$) of financial markets and online sentiment in developing countries is significantly smaller than that in the large waveband ($q > 0$). This supplement shows that, in the developing countries, the cross-correlation between financial markets and online sentiment is more stable in small wave band.

This finding is consistent with most studies except Zhang et al. [40], whose work proves that, in the long run, the relationship between internet activity and Chinese market volatility is more accurate. This may partially be due to the difference between China and our sample countries in financial market composition as well as internet development level.

4.3. Rolling Windows Discussion. Grech and Mazur [39] argued that the exponent at a given time depends on the time-window length. To rule out the impact of time-window length, we redo the empirical test using MF-DCCA based on rolling windows. MF-DCCA based on rolling window is practical in capturing the dynamic evolution characteristics of the cross-correlation relationship between the financial market of various countries and the online sentiment measured by DHS. Following Wang et al. (2010), we set one year (about 250 trading days) as the time interval and 1 trading day as the step size of the rolling window. Figures 5 and 6 are the results of cross-correlation relationship between financial market return and online sentiment through rolling window test.

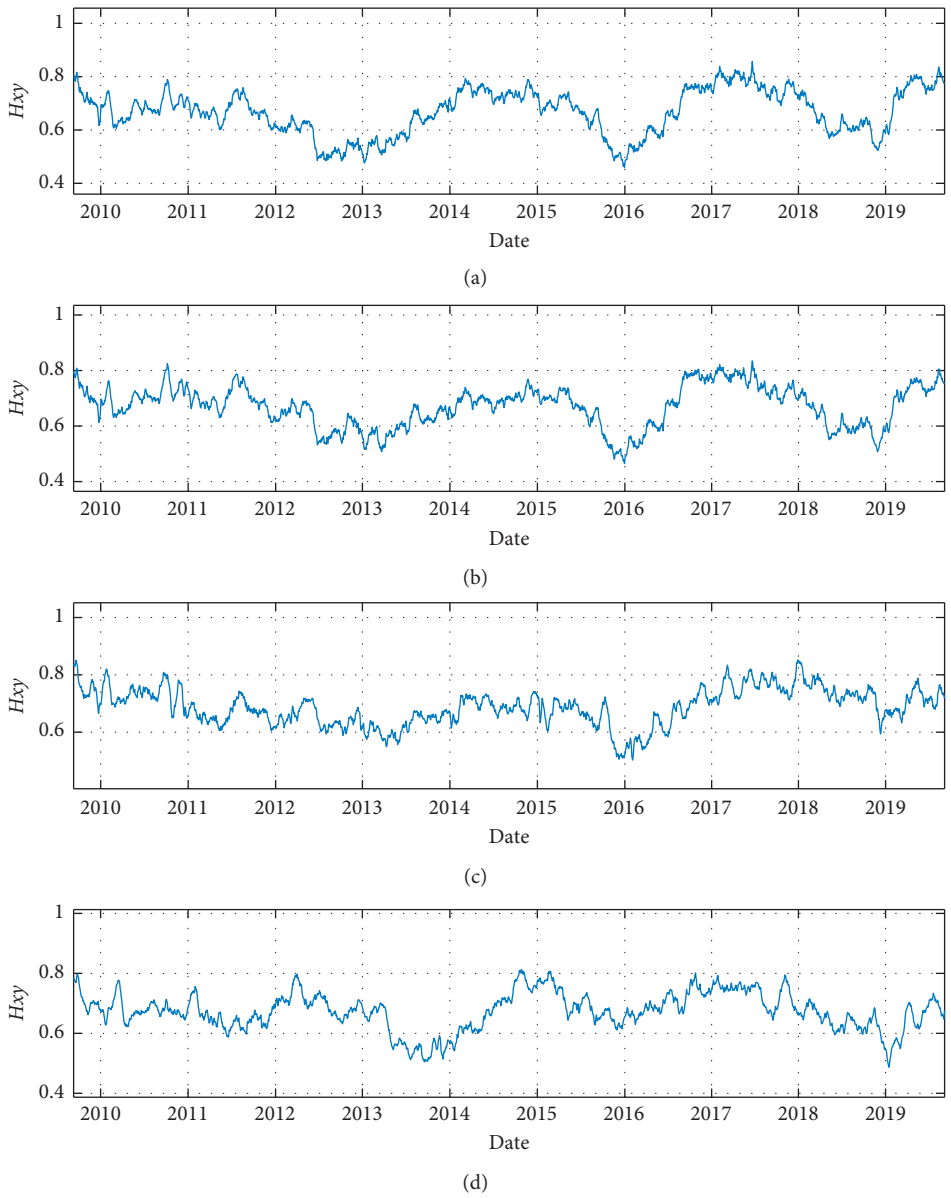

Figure 5: The dynamic evolution of the cross-correlation between financial market return and online sentiment in developed countries ($q = 2$): (a) US: SP500, (b) US: Nasdaq, (c) Japan: Nikkei, and (d) Germany: DAX.

It can be seen from the figures that the cross-correlation relationship between financial market returns and online sentiment shows strong consistency over time, and this finding applies to all countries. Moreover, the cross-correlation relationship has declined rapidly with the short sharp drop of the global financial market at the end of 2015. The scaling exponent $H_{xy}(2)$ of some countries even fell below the critical value, which indicates that the cross-correlation relationship between financial market return and online sentiment can be affected by macroeconomic environment and even changed from positive to negative.

Table 3 shows the statistical characteristics of the dynamic cross-correlation between financial market returns and online sentiment in various countries. Overall, the averages of scaling exponent index $H_{xy}(2)$ are all greater than 0.5 regardless of the nationality, giving a clue that the financial markets and online sentiment generally show a positive cross-correlation worldwide. Besides, the standard deviation of the $H_{xy}(2)$ of the developing markets is generally larger than that of the developed country markets; this implies that financial markets in the developing countries tend to fluctuate more and more easily be affected by online sentiment, and this situation has improved in the developed countries. Zhang et al. [20] focus on testing whether there exists the linear or nonlinear Granger causality between sentiment and major financial markets returns, and they find out a strong relationship in the USA, but in the Middle East and North Africa, there only exists one direction Granger

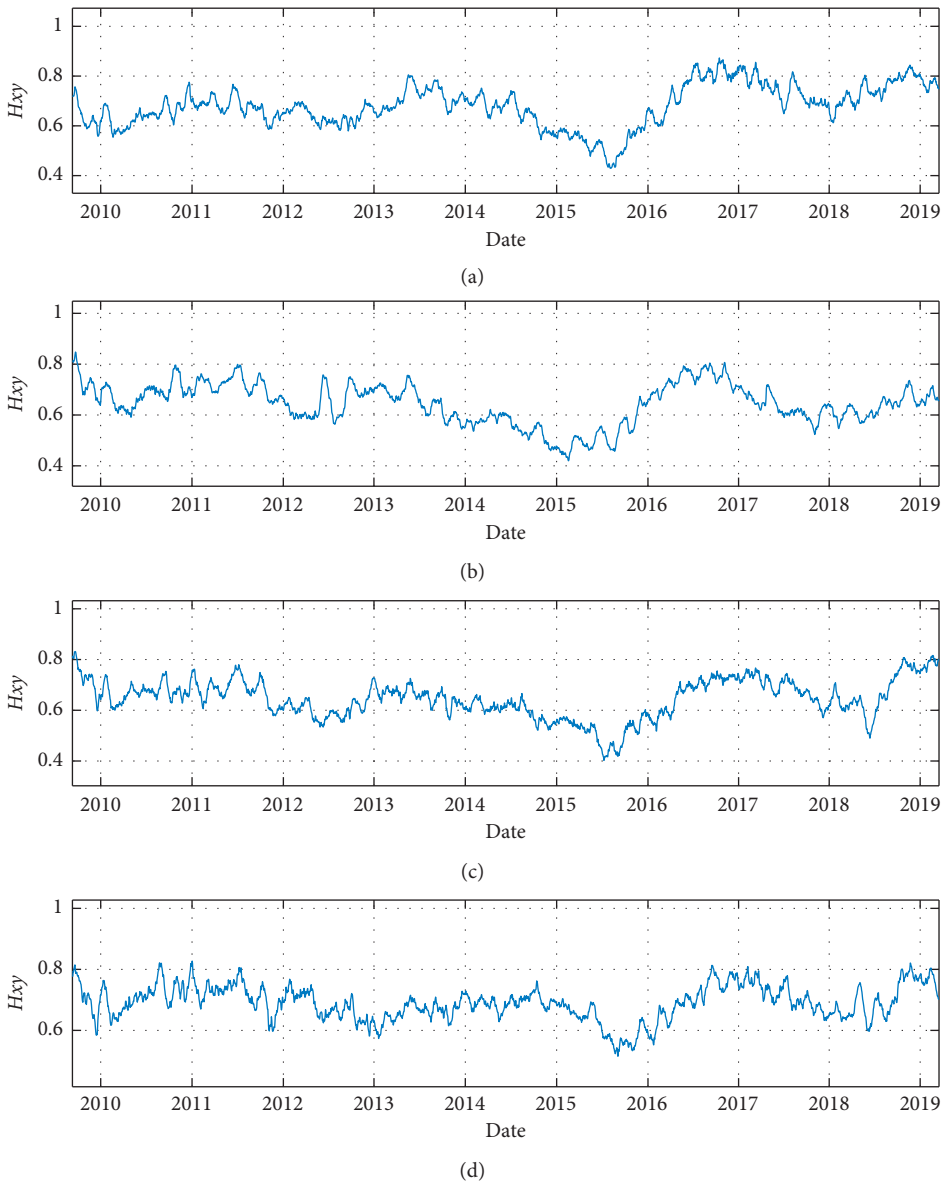

Figure 6: The dynamic evolution of the cross-correlation between financial market return and online sentiment in developing countries ($q = 2$): (a) Brazil: BRL, (b) Indonesia: Jakarta, (c) Mexico: MXX, (d) India: BSE.

Table 3: Statistical characteristics of dynamic cross-correlation between financial markets return and online sentiment.

	Mean	Std	Min	Max
S & P500	0.6684	0.0848	0.4595	0.8569
NASDAQ	0.6705	0.0746	0.4648	0.8347
Nikkei	0.6878	0.0638	0.5027	0.8514
DAX	0.6739	0.0627	0.4869	0.8128
BVSP	0.6798	0.0834	0.4291	0.8728
JKSE	0.6448	0.0813	0.4197	0.8478
MXX	0.6450	0.0763	0.4023	0.8317
BSE	0.6685	0.0650	0.5011	0.8104

causality pattern from DHS to market returns. Different from theirs, we find evidence that the developing countries tend to be fluctuated more intensely by online sentiment; this may be because we focus on dynamic correlations, while Zhang et al. [23] were concerned with causality relationship between sentiment and financial market performance.

5. Conclusion

In this paper, we investigate the cross-correlation between financial market return and online sentiment based on MF-DCCA method. We choose representative financial markets covering developed and developing countries in different regions and calculate the market index returns, and Daily Happiness Index (DHS) is applied as a proxy variable for online sentiment.

We firstly find that there is no generic cross-correlation between financial market returns and online sentiment in the developed countries; specifically, we do not find a cross-correlation relationship between financial market return and online sentiment in South Korea and UK. Yet, our research shows that there exists a power-law cross-correlation relationship between financial market and online sentiment in some developed countries and all developing countries represented by Brazil and India in our sample, and the cross-correlation relationship is stronger than that in the developed ones.

We further set the different time interval lengths and retest the cross-correlation relationship and find that whether in the long-term or short term, there is a significant positive cross-correlation between the financial market returns and online sentiment; that is, the financial market returns tend to change in the same direction as online sentiment does measured by the Daily Happiness Index (DHS). It is worth noting that the cross-correlation between financial market return in the developed countries and online sentiment is weak in the short term. Moreover, we study the cross-correlation under different fractal degrees ranging from −10 to 10. The empirical results show that cross-correlation between financial markets and online sentiment in the developed countries is more stable.

Finally, we perform rolling window analysis to capture the dynamic evolution characteristics of cross-correlation relationship. We find that the cross-correlation relationship between financial market and online sentiment has a strong consistency over time, but the cross-correlation relationship between financial markets and online sentiment in the developing countries fluctuates more drastically.

Our findings confirm the dependency between online sentiment and global financial markets, and we also suggest the heterogeneous relationship between sentiment and market performance in different economies. As is shown, the emerging financial markets in the developing countries fluctuate drastically and show a certain degree of instability compared with the developed ones. The underlying mechanism on explaining this may be attributed to the degree of market maturity, regulatory effectiveness, and financial literacy of market participants. This needs an interdisciplinary analysis from a more holistic perspective. We leave these questions for future research.

Data Availability

More details on DHS can be obtained from http://hedonometer.org/index.html. All stock market data used in this paper are from YAHOO!Finance (http://finance.yahoo.com).

Conflicts of Interest

The authors declare no conflicts of interest.

Acknowledgments

This work was supported by the National Natural Science Foundation of China (71532009 and 71901160).

References

[1] Y. Hu, X. Li, J. W. Goodell, and D. Shen, "Investor attention shocks and stock co-movement: substitution or reinforcement?" *International Review of Financial Analysis*, vol. 73, Article ID 101617, 2020.

[2] Y. Hu, X. Li, and D. Shen, "Attention allocation and international stock return comovement: evidence from the Bitcoin market," *Research in International Business and Finance*, vol. 54, Article ID 101286, 2020.

[3] X. Li, D. Shen, and W. Zhang, "Do Chinese internet stock message boards convey firm-specific information?" *Pacific-Basin Finance Journal*, vol. 49, pp. 1–14, 2018.

[4] M. E. Zweig, "An investor expectations stock price predictive model using closed-end fund premiums," *The Journal of Finance*, vol. 28, no. 1, pp. 67–78, 2012.

[5] C. M. C. Lee, A. Shleifer, and R. H. Thaler, "Investor sentiment and the closed-end fund puzzle," *The Journal of Finance*, vol. 46, no. 1, pp. 75–109, 1991.

[6] J. A. Wurgler and M. P. Baker, "Investor sentiment and the cross-section of stock returns," *Economic Management Journal*, vol. 61, no. 4, pp. 1645–1680, 2006.

[7] P. C. Tetlock, "Giving content to investor sentiment: the role of media in the stock market," *Journal of Finance*, vol. 62, no. 3, pp. 1139–1168, 2007.

[8] M. Alanyali, H. S. Moat, and T. Preis, "Quantifying the relationship between financial news and the stock market," *Scientific Reports*, vol. 3, p. 3578, 2013.

[9] M. Karabulut, "Fuzzy unordered rule induction algorithm in text categorization on top of geometric particle swarm optimization term selection," *Knowledge Based Systems*, vol. 54, pp. 288–297, 2013.

[10] A. Siganos, E. Vagenas-Nanos, and P. Verwijmeren, "Facebook's daily sentiment and international stock markets," *Journal of Economic Behavior & Organization*, vol. 107, pp. 730–743, 2014.

[11] D. A. Zhi, J. Engelberg, and P. Gao, "In search of attention," *Journal of Finance*, vol. 66, no. 5, pp. 1461–1499, 2011.

[12] Z. Da, J. Engelberg, and P. Gao, "The sum of all fears investor sentiment and asset prices," *Review of Financial Studies*, vol. 28, no. 1, pp. 1–32, 2015.

[13] W. Zhang, D. Shen, Y. Zhang, and X. Xiong, "Open source information, investor attention, and asset pricing," *Economic Modelling*, vol. 33, pp. 613–619, 2013.

[14] D. Shen, W. Zhang, X. Xiong, X. Li, and Y. J. Zhang, "Trading and non-trading period Internet information flow and

intraday return volatility," *Physica A: Statistical Mechanics and its Applications*, vol. 451, pp. 519–524, 2016.

[15] J. Bollen, H. Mao, and X. J. Zeng, "Twitter mood predicts the stock market," *Journal of Computational Science*, vol. 2, no. 1, pp. 1–8, 2010.

[16] A. Edmans, D. Garca, and Y. Norli, "Sport sentiment and stock returns," *The Journal of Finance*, vol. 62, no. 4, pp. 1967–1998, 2007.

[17] D. Hirshleifer and T. Shumway, "Good day sunshine: stock returns and the weather," *Journal of Finance*, vol. 58, no. 3, pp. 1009–1032, 2003.

[18] G. M. Lepori, "Investor mood and demand for stocks: evidence from popular tv series finales," *Journal of Economic Psychology*, vol. 48, pp. 33–47, 2015.

[19] R. Novy-Marx, "Predicting anomaly performance with politics, the weather, global warming, sunspots, and the stars," *Journal of Financial Economics*, vol. 112, no. 2, pp. 137–146, 2014.

[20] X. Li, D. Shen, M. Xue, and W. Zhang, "Daily happiness and stock returns: the case of Chinese company listed in the United States," *Economic Modelling*, vol. 64, pp. 496–501, 2017.

[21] W. Zhang, X. Li, D. Shen, and A. Teglio, "Daily happiness and stock returns: some international evidence," *Physica A Statal Mechanics & Its Applications*, vol. 460, pp. 201–209, 2016.

[22] D. Shen, L. Liu, and Y. Zhang, "Quantifying the cross-sectional relationship between online sentiment and the skewness of stock returns," *Physica A: Statistical Mechanics and its Applications*, vol. 490, no. Supplement C, pp. 928–934, 2018.

[23] W. Zhang, P. Wang, X. Li, and D. Shen, "Twitter's daily happiness sentiment and international stock returns: evidence from linear and nonlinear causality tests," *Journal of Behavioral and Experimental Finance*, vol. 18, p. 53, 2018.

[24] S. Kalemli-Özcan, A. Chanda, L. Alfaro, and S. Sayek, "Does foreign direct investment promote growth? exploring the role of financial markets on linkages," *Journal of Development Economics*, vol. 91, no. 2, pp. 242–256, 2007.

[25] Y. Hong, Y. Liu, and S. Wang, "Granger causality in risk and detection of extreme risk spillover between financial markets," *Journal of Econometrics*, vol. 150, no. 2, pp. 271–287, 2009.

[26] A. B. Rejeb and M. Arfaoui, "Financial market interdependencies: a quantile regression analysis of volatility spillover," *Research in International Business and Finance*, vol. 36, pp. 140–157, 2016.

[27] W. X. Zhou, "Multifractal detrended cross-correlation analysis for two nonstationary signals," *Physical Review E Statal Nonlinear & Soft Matter Physics*, vol. 77, no. 6, Article ID 066211, 2008.

[28] C. K. Peng, S. V. Buldyrev, S. Havlin, M. Simons, and A. L. Goldberger, "Mosaic organization of dna nucleotides," *Physical Review. E, Statistical Physics, Plasmas, Fluids, and Related interdisciplinary Topics*, vol. 49, no. 2, pp. 1685–1689, 1994.

[29] E. Alessio, A. Carbone, G. Castelli, and V. Frappietro, "Second-order moving average and scaling of stochastic time series," *The European Physical Journal B-Condensed Matter and Complex Systems*, vol. 27, no. 2, pp. 197–200, 2002.

[30] J. W. Kantelhardt, S. A. Zschiegner, E. Koscielny-Bunde, A. Bunde, and H. E. Stanley, "Multifractal detrended fluctuation analysis of nonstationary time series," *Physica A Statal Mechanics & its Applications*, vol. 316, no. 1–4, pp. 87–114, 2002.

[31] G. F. Gu and W. X. Zhou, "Detrending moving average algorithm for multifractals," *Physical Review E*, vol. 82, no. 1, Article ID 011136, 2010.

[32] B. Podobnik and H. E. Stanley, "Detrended cross-correlation analysis: a new method for analyzing two non-stationary time series," *Physical Review Letters*, vol. 100, no. 8, Article ID 084102, 2008.

[33] J. Li, X. Lu, and Y. Zhou, "Cross-correlations between crude oil and exchange markets for selected oil rich economies," *Physica A: Statistical Mechanics and its Applications*, vol. 453, pp. 131–143, 2016.

[34] G. Cao, L. Xu, and J. Cao, "Multifractal detrended cross -correlations between the Chinese exchange market and stock market," *Physica A Statal Mechanics & its Applications*, vol. 391, no. 20, 2012.

[35] W. Shi, P. Shang, J. Wang, and A. Lin, "Multiscale multifractal detrended cross-correlation analysis of financial time series," *Physica A Statistical Mechanics & its Applications*, vol. 403, pp. 35–44, 2014.

[36] X. Lu, X. Sun, and J. Ge, "Dynamic relationship between Japanese yen exchange rates and market anxiety: a new perspective based on mf-dcca," *Physica A: Statal Mechanics and its Applications*, vol. 474, pp. 144–161, 2017.

[37] Y. Wang and L. Liu, "Is wti crude oil market becoming weakly efficient over time?: new evidence from multiscale analysis based on detrended fluctuation analysis," *Energy Economics*, vol. 32, no. 5, pp. 987–992, 2010.

[38] Z. Li and X. Lu, "Cross-correlations between agricultural commodity futures markets in the US and China," *Physica A Statistical Mechanics & its Applications*, vol. 391, no. 15, pp. 3930–3941, 2012.

[39] W. Zhang, K. Yan, and D. Shen, "Can the Baidu Index predict realized volatility in the Chinese stock market?" *Financial Innovation*, vol. 7, no. 7, 2021.

[40] D. Grech and Z. Mazur, "Can one make any crash prediction in finance using the local hurst exponent idea?" *Physica A Statistical Mechanics & its Applications*, vol. 336, no. 1-2, pp. 133–145, 2004.

Hindawi
Discrete Dynamics in Nature and Society
Volume 2020, Article ID 6640180, 12 pages
https://doi.org/10.1155/2020/6640180

Research Article

Forecasting Oil Price by Hierarchical Shrinkage in Dynamic Parameter Models

Yuntong Liu,[1] **Yu Wei**,[1] **Yi Liu**,[2] **and Wenjuan Li**[3]

[1]*School of Finance, Yunnan University of Finance and Economics, Kunming, China*
[2]*Faculty of Transportation Engineering, Kunming University of Science and Technology, Kunming, China*
[3]*School of Statistics & Mathematics, Yunnan University of Finance and Economics, Kunming, China*

Correspondence should be addressed to Yu Wei; weiyusy@126.com

Received 8 October 2020; Revised 14 November 2020; Accepted 20 November 2020; Published 3 December 2020

Academic Editor: Dehua Shen

The aim of this paper is to forecast monthly crude oil price with a hierarchical shrinkage approach, which utilizes not only LASSO for predictor selection, but a hierarchical Bayesian method to determine whether constant coefficient (CC) or time-varying parameter (TVP) predictive regression should be employed in each out-of-sample forecasting step. This newly developed method has the advantages of both model shrinkage and automatic switch between CC and TVP forecasting models; thus, this may produce more accurate predictions of crude oil prices. The empirical results show that this hierarchical shrinkage model can outperform many commonly used forecasting benchmark methods, such as AR, unobserved components stochastic volatility (UCSV), and multivariate regression models in forecasting crude oil price on various forecasting horizons.

1. Introduction

Crude oil price is one of the key indicators of the global macroeconomy and financial markets [1–6]. However, the oil price prediction is a complex process since various factors affect oil pricing [2] and the influence degree of these factors on oil price varies over time [7–11]. So, finding a proper oil price forecasting method, which is not merely able to select the important predictors but also reflect the dynamics of predictors impact, is of interest for a wide range of applications [12–19].

A vast of literatures [2, 4, 5, 11, 13, 18, 20–25] indicate that except for previous oil prices, other parameters such as basic oil supply, demand and oil stock effects, financial market forces, market sentiment and uncertainty, macroeconomy, and geopolitical influences are also main influencing factors. If adding all these explanatory variables into the multivariate regression or autoregression (AR) class framework, it may lead to overfitting and misspecification problems and thereby constrain the forecast accuracy [7, 26, 27]. Additionally, time-varying effect of these parameters should be also considered in oil price forecasting, but drawing the time-varying effect into regression models would make the overfitting problem worse [7, 11, 28].

In this study, we introduce a prevailing Bayesian approach which not only overcomes overparametrization and misspecification problems in oil price prediction, but also discusses the time-varying properties of explanatory parameters in both short and long oil price forecasting horizons. This study mainly makes three contributions to the literature on oil price forecasting as follows.

First, we can estimate a large number of explanatory parameters with limited observations. Usually, low-frequency dataset is easier to access and process than high-frequency dataset; putting more informative explanatory variables into the model can help macroeconomists, politicians, and other market participants get more comprehensive information on the crude oil price. Further, we implement least absolute shrinkage and selection operator (LASSO) shrinkage method to handle all the considered endogenous and exogenous explanatory factors and select the most powerful influential factors automatically. Although previous studies [6, 29–33] simulate that LASSO-based approaches show better out-of-sample forecasts and

surpass both AR class models and time-varying parameter models, it is unclear whether LASSO operator is also outperforming other commonly used benchmark models in oil price forecasting. Examining the LASSO operator effectiveness may help oil market decision-makers identify significant influential indicators efficiently and seize investment opportunities.

Besides, for better explaining the oil price, we introduce more comprehensive exogenous (see Table 1) and endogenous variables (e.g., observations from previous time steps) as regression predictors. On the one hand, bringing previous oil prices into the regression enables comparison with autoregression models (AR) and time-varying vector autoregression (TVP-VAR) models, which are commonly used and proved models in energy price prediction that can generate accurate forecasts [18, 34–37]. On the other hand, we introduce a more comprehensive exogenous factors framework, which avoids model misspecification. Most of the oil price forecasting studies [3, 16, 34, 38–40] only focus on several key oil price predictors and ignore the rest due to the limited variables processing capacity; this leads to error of misspecification, while using the LASSO operator in this study can shrink the coefficient on unimportant explanatory variables to zero and include all the exogenous variables within the model without having to worry about multi-indicators' processing capacity.

Second, it has been well documented that the predictive ability of the forecast parameters on crude oil prices varies over time [7–11, 18, 41]. This motivates us to study the time-varying properties of the regression coefficients. Shrinkage model in time-varying parameters is described by [28] and is considered an effective forecasting method [32]. Accordingly, we apply LASSO for the time-varying regression model in the oil market and evaluate oil price forecasting performance. This Bayesian-based estimation method can predict both long-term and short-term forecast horizons via monthly information. With hierarchical shrinkage in oil price predictors, we can select the most relevant predictors and pick out time-varying parameters automatically. It is worth noting that few works investigate parameters dynamic properties incorporating a large set of predictors in a single model. Our study provides empirical evidence regarding the most powerful contributor in forecasting oil prices and judges its dynamic properties simultaneously.

Third, we extend our ideas for using the mean of the log predictive likelihood (MLPL) to check the entire of predictive distribution robustness, which fill gaps of the commonly used forecasting performance measurement—the mean of the squared forecast errors (MSFE) and the mean of the absolute value of the forecast errors (MAFE) [19, 23, 27, 28]—which can only judge the point forecasts. We also examine the forecasting performance by changing regressors, dependence variables, and rolling window estimation regimes for robustness check. Our out-of-sample evidence indicates that LASSO hierarchical shrinkage models outperform other competing models in most cases; LASSO can select informational variables automatically and efficiently.

The remainder of this paper is organized as follows: Section 2 presents the econometric approach and comparison models. Section 3 introduces our data. Section 4 provides the out-of-sample empirical results and discussion. In Section 5, we present the robustness checks, and Section 6 concludes.

2. Empirical Models and Computation Processes

2.1. Empirical Models. Crude oil has both commodity and financial properties. As aforementioned, apart from the previous oil prices, we still have hundreds of influencing exogenous variables and seasonal adjustment should also be taken into account. In this case, the suitable full model for forecasting crude oil price is given by

$$\mathrm{Oil}_{t+h} = c + \sum_{k=1}^{k} \beta_k x_{kt} + \sum_{r=0}^{p-1} \alpha_r \mathrm{Oil}_{t-r} + \sum_{j=1}^{11} \gamma_j \mathrm{dum}_j + \varepsilon_{t+h}, \tag{1}$$

where Oil_{t+h} is the future crude oil price we want to forecast at h-periods ahead, c is the intercept, and $\varepsilon_t \sim N(0, \sigma_t^2)$ is the error term. $\sum_{k=1}^{k} \beta_k x_{kt}$ represents the sum of exogenous variables part, k is the number of explanatory variables, and β_k is the kth regression parameter. $\sum_{i=0}^{p} \alpha_r \mathrm{Oil}_{t-r}$ includes the sum of p lags of oil price;α_r is the rth lag coefficient. $\sum_{j=1}^{11} \gamma_j \mathrm{dum}_j$ is the sum of 11 monthly dummies which is added for seasonal adjusting. γ_j is the jth dummy variable coefficient. In total, the number of potential independent variables should be $m = 1 + k + p + 11$.

Each part of the model (intercept$\sum_{j=1}^{11} \gamma_j \mathrm{dum}_j$, $\sum_{r=0}^{p-1} \alpha_r \mathrm{Oil}_{t-r}$, or $\sum_{k=1}^{k} \beta_k x_{kt}$) can be excluded from the model. Briefly, the computation steps can analyze models by adding different terms into the model, then judging the time-varying properties, and selectively do LASSO shrinkage for the variable parameters in both constant variance (homoskedasticity of σ_t) and stochastic variance (heteroskedasticity of σ_t) regimes. So, the model structure is diversifying to the following three restrictive forms:

(1) AR(p) model

$$\mathrm{Oil}_{t+h} = c + \sum_{r=0}^{p-1} \alpha_r \mathrm{Oil}_{t-r} + \sum_{j=1}^{11} \gamma_j \mathrm{dum}_j + \varepsilon_{t+h}. \tag{2}$$

The model specifies that the future crude oil price depends linearly on its past values.

(2) Multivariate regression model

$$\mathrm{Oil}_{t+h} = c + \sum_{k=1}^{k} \beta_k x_{kt} + \sum_{j=1}^{11} \gamma_j \mathrm{dum}_j + \varepsilon_{t+h}. \tag{3}$$

The model considers the effect of several key exogenous variables but excludes endogenous variables' influence on the oil price.

Table 1: Variable definitions.

Category	Label	Definition	Unit	Data source
Crude oil price	WTI	WTI spot price	Dollars per barrel	Energy Information Administration (EIA)
	Brent	Europe Brent spot price		
Crude oil supply	OS_World	Crude oil production, world	Thousand barrels per day	
Crude oil demand	OD_cons	Total petroleum consumption		
Crude oil stocks	OD_stocks	Total petroleum stocks	Million barrels	
Gold price	P_gold	Gold fixing price	US dollars per troy ounce	
Exchange rate	US_ex	Trade weighted US dollar index: broad, goods, index	Percentage	Federal Reserve Bank of St. Louis
Stock market price index	S&P500	S&P500 index		
Natural gas price	P_gas	Henry Hub Natural Gas Spot Price	Dollars per million btu	Energy Information Administration (EIA)
Market sentiment	VIX	VIX index	Percentage	Federal Reserve Bank of St. Louis
Macroeconomy affecting factors	IP_total	Industrial production: total index		
	Kilian	Kilian index		Kilian's website
Political change	EPU	Global policy uncertainty	Percentage	Economic policy uncertainty website
	Google	Google trend index	Percentage of popularity	Google trends

All the variables are calculated by the first log difference in order to make them stationary, except for the Kilian index, which is naturally stationary series. Neither measures of these variables are seasonally adjusted.

(3) The unobserved components stochastic volatility (UCSV) model

$$\text{Oil}_{t+h} = c + \sum_{j=1}^{11} \gamma_j \text{dum}_j + \varepsilon_{t+h}, \tag{4}$$

which assumes that the future oil price consists of components with a direct interpretation that cannot be observed.

These three models are commonly used and proved that they can generate relatively accurate linear regression prediction [18, 34–37, 42–45]. Same as the full model (equation (1)), these three restricted model versions can also do hierarchical parameter shrinkage and decide which variable parameter varies with time. In Section 4.2, we compare the full model and the three restricted models in prediction performance with the same prior choices and basic model structures. The specific econometric method computation processes are as follows.

2.2. Judging Time-Varying Properties and Forecasting Power of Predictors. To briefly describe the computation processes, the full variable model (equation (1)) can be simplified as

$$\begin{aligned} \text{Oil}_{t+h} &= \beta_t^* z_t + \varepsilon_{t+h}, \\ \beta_t^* &= \beta_{t-1}^* + \nu_t, \end{aligned} \tag{5}$$

where the variable of interest, Oil_{t+h}, can be defined as $\text{Oil}_{t+h} = \log(p_{t+h}) - \log(p_t)$. The variable matrix $z_t = [1, x_1, \ldots, x_k, \Delta\log(p_t), \ldots, \Delta\log(p_{t-p+1}), \text{dum}_1, \ldots, \text{dum}_{11}]$, and the corresponding coefficients matrix of z_t is $\beta_t^* = [c, \beta_1, \ldots, \beta_{k+p+11}]'$.

In equation (5), we assume $\varepsilon_t \sim N(0, \sigma_t^2)$ and $\nu_t \sim N(0, \Omega)$. σ_t^2 can be stochastic or constant volatility. The errors are assumed to be independent of each other and independent at all leads and lags. Ω is of dimension $m \times m$, which can be large relative to the number of observations. To keep the model relatively brief, we assume Ω is a diagonal matrix, $\Omega = \text{diag}(\omega_1^2, \ldots, \omega_m^2)$.$\Omega$ introduces shrinkage in the time variation then switches the constant coefficients to time-varying coefficients. If ω_i is zero, the ith ($i = 1, \ldots, m$) coefficient is constant over time, and larger values of ω_i mean more time variation. In order to elicit ω_i, Belmonte et al. [28] separate the model into two parts, one part is constant (represented by βz_t) and the other part is time-varying (represented by $\beta_t z_t$). Equation (5) will change to

$$\begin{aligned} Oil_{t+h} &= \beta z_t + \beta_t z_t + \varepsilon_{t+h}, \\ \beta_t &= \beta_{t-1} + \nu_{t+h}, \\ \beta_0 &= 0, \end{aligned} \tag{6}$$

where $\beta = \beta_0^*$ and $\beta_t = \beta_0^* - \beta$. Then, let $\widetilde{\beta}_{t,t} = \beta_{i,t}/\omega_i$ and transform equation (6) to

$$\begin{aligned} \text{Oil}_{t+h} &= \sum_{i=1}^{r} \beta_i z_{i,t} + \sum_{i=1}^{r} \omega_i \widetilde{\beta}_{i,t} z_{i,t} + \varepsilon_{t+h}, \\ \widetilde{\beta}_{i,t} &= \widetilde{\beta}_{i,t-1} + \nu_{i,t}, \\ \widetilde{\beta}_{i,0} &= 0, \end{aligned} \tag{7}$$

where $\nu_{i,t} \sim N(0,1)$ for $i = 1, \ldots, r$.

Through implementing LASSO in terms of equation (7), we can judge the time-varying properties and forecasting power of predictors. Four possible computation cases are discussed as follows:

(1) ω_i shrank to 0, but β_i is not shrunk to 0; then, the ith variable parameter is constant over time

(2) Both ω_i and β_i shrank to 0; then, the ith variable is irrelevant for forecasting the oil price

(3) ω_i is not shrunk to 0, but β_i shrank to 0; then, the ith variable parameter has small time-varying characteristics (since $\widetilde{\beta}_{i,0} = 0$, the coefficient will volatile around a value of zero)

(4) Both ω_i and β_i are not shrunk to 0; then, the ith variable is relevant for forecasting the oil price and the time-varying coefficient is unrestricted around zero

2.3. Hierarchical Parameter Shrinkage. The parameters of interest are $\beta = (\beta_1, \ldots, \beta_m)'$, $\widetilde{\beta}_t = (\widetilde{\beta}_{1,t}, \ldots, \widetilde{\beta}_{m,t})'$, and $\omega = (\omega_1, \ldots, \omega_m)'$; we can use the Bayesian LASSO shrinkage priors to estimate these parameters. According to the study of [28], the LASSO shrinkage can be obtained by starting from normal hierarchical priors for β and ω.

Hierarchy shrinkage 1: for the constant coefficients, the priori for β_i $(i = 1, \ldots, m)$ is independent with $\beta_i|\tau_i^2 \sim N(0, \tau_i^2)$ and exponential mixing density $\tau_i^2|\lambda \sim \exp(\lambda^2/2)$. λ is the shrinkage parameter for constant coefficients and we assume $\lambda^2 \sim \text{Gamma}(a_1, a_2)$. So, the first hierarchy is conditional on λ to estimate τ_i^2 then obtain β_i.

Hierarchy shrinkage 2: from equation (4), we can infer that the time-varying parameters $\widetilde{\beta}_t$(for $t = 1, \ldots, T$) prior is of the form $\widetilde{\beta}_t|\widetilde{\beta}_{t-1} \sim N(\widetilde{\beta}_{t-1}, I_r)$, where $\widetilde{\beta}_0 = 0$. The hierarchical priori of ω_i, conditionally independent with $\omega_i|\xi_i^2 \sim N(0, \xi_i^2)$, is also with exponential mixing density $\xi_i^2|\kappa \sim \exp(\kappa^2/2)$. The shrinkage parameter κ lies at the bottom of the hierarchy and we assume $\kappa^2 \sim \text{Gamma}(b_1, b_2)$. The second hierarchy is conditional on κ; we can in turn to derive ξ_i^2 and ω_i, at last, judge whether $\widetilde{\beta}$ is time-varying or not.

For the two hierarchy shrinkage processes mentioned above, we set the prior hyperparameters $a_1 = a_2 = b_1 = b_2 = 0.001$, which implies proper but very noninformative priors. For constant coefficients model, which removes the TVP part of the model, we set $b_1 = 100000$ to make ωi shrink very close to zero and its prior variance is 0.1.

To complete these two hierarchical shrinkage computations, [28] provides Markov Chain Monte Carlo (MCMC) algorithm blocks and precise steps to draw the parameter posteriors. After using a nonparametric kernel smoothing algorithm on the parameter posteriors, we can obtain an approximation of the oil price predictive density.

As LASSO shrinkage can be applied to both constant coefficients and time-varying coefficients, the full model and restricted models can derive several versions for the following:

(1) LASSO on constant coefficients and time-varying parameters: both constant and time-varying part use LASSO priors and do hierarchical shrinkage.

(2) LASSO only on constant coefficients: this model omits the time-varying part ($\sum_{i=1}^{r} \omega_i \widetilde{\beta}_{i,t} z_{i,t}$ in equation (7)) LASSO priors and uses a relatively noninformative and nonhierarchical normal prior for ω_i.

(3) LASSO only on time-varying parameters: this model omits the constant part ($\sum_{i=1}^{r} \beta_i z_{i,t}$) LASSO priors and uses a relatively noninformative and nonhierarchical normal prior for β_i.

(4) TVP regression model: this model is traditional time-varying multivariate parameter model which does not hierarchical shrinkage for parameters. Use noninformative LASSO priors for both ω_i and β.

(5) Constant coefficients model: this model removes the time-varying part ($\sum_{i=1}^{r} \omega_i \widetilde{\beta}_{i,t} z_{i,t}$) by setting prior hyperparameters $b_1 = 100000, b_2 = 0.001$, which implies an extremely tight prior on ω_i with prior concentrated very close to 0.

2.4. Evaluation Criteria. The results of predictive density or forecasting points from the previous steps are useful to quantitatively compare the out-of-sample predictive performance among different models. Following the convention in the literature on prediction measurement, we use point forecasting loss functions of MAFE and MSFE to demonstrate the ranking of model forecasts [17, 23, 29, 31]. Further, since researchers and policymakers focus more on total distribution forecast uncertainty than just a point forecast, we also adopt the mean of the log predictive likelihood (MLPL) to evaluate the entire predictive distributions. The specific formulations of these three measuring statistics are listed below:

$$\text{MAFE} = \frac{1}{T-h-t_0+1} \sum_{t=t_0}^{T-h} |\text{Oil}_{t+h} - \text{Oil}_{t+h}^0|,$$

$$\text{MSFE} = \frac{1}{T-h-t_0+1} \sum_{t=t_0}^{T-h} \left(\text{Oil}_{t+h} - \text{Oil}_{t+h}^0\right)^2,$$

$$\text{MLPL} = \frac{1}{T-h-t_0+1} \sum_{t=t_0}^{T-h} \log\left[p\left(\text{Oil}_{t+h} = \text{Oil}_{t+h}^0 | \text{Data}_t\right)\right]. \tag{8}$$

Respectively, T is the end date, t_0 is the start date, h is prediction length, Oil_{t+h} is the predictive median of oil price, and Oil_{t+h}^0 is the corresponding real value. Smaller MAFE and MSFE and larger MLPL indicate stronger forecasting ability.

3. Data

This paper uses two prevailing proxies in crude oil pricing: the monthly spot price of Brent crude oil as dependent variable and West Texas Intermediate (WTI) oil futures for robustness check. Both datasets span from January 2004 to December 2018 yielding $t = 180$ observations; the out-of-sample evaluation period consists of the last 110 observations.

On the foundation of previous studies [3, 16, 34, 38–40], we select a relatively comprehensive predictors framework to forecast crude oil price and use available real-time data. The exogenous variable dataset consists of crude oil fundamentals (include crude oil supply, demand, and stocks),

capital market prices (gold price, exchange rate, and stock market price index), substitute product price (natural gas price), market sentiment index (volatility index), macroeconomic influencing factors (industrial production and Kilian indexes), and political change (global policy uncertainty and Google trend). This variable set not only captures the information in both the supply and demand of crude oil but also includes activities related to the financial market and macroeconomy. Accordingly, they are widely used variables for crude oil price forecasting.

The ADF and PP test in Table 2 indicate that no variables have unit roots after first-order logarithmic difference, which means all the series are stationary time series, so we can use these series for further econometric modeling. The two dependent variables—WTI and Brent—are left-skewed, leptokurtic, and nonnormal distribution. Within 20 lags, the Q-statistics of both WTI index and Brent spot price series show significant autocorrelation, which suggest that past oil prices have influences on the current oil price, so it is reasonable to include AR terms in the model.

To examine whether the current oil price is affected by the past oil prices, we further include the logged first difference of 12 lags of the Brent crude oil price index in the model. In addition, an intercept and 11 monthly dummies (omitting the January dummy) are designed to distinguish monthly or seasonal effects on the crude oil prices.

All the explanatory variables are standardized to have mean zero and variance one. The model can flexibly include an intercept, different numbers of lags, 11 monthly dummies, and 12 predictors listed above. In addition, it can forecast oil prices a month ahead (short term) and a year ahead (long term).

In summary, the full variable model includes 36 coefficients to estimate with fewer than 15 years of data, which is a relatively short dataset. Omitting 12 predictors and 11 dummies, the model leads to AR models or TVP-AR models. If the lags are further excluded, it leads to TVP models or multivariate regression models. If only 11 dummies are left in the model, model form changes to UCSV model. In total, for each sample size rolling window estimation, we compute 20 different versions of full models and 100 competing models to check the models' robustness.

4. Empirical Results

4.1. Time-Varying and Shrinkage Parameters Results. This section focuses on time-varying and shrinkage coefficients represented by ω_i^2 and $\tau_i^2.\omega_i$ close to zero means the ith ($i = 1, \ldots, m$) coefficient is constant over time; larger values of ω_i allow for more time variation. While the smaller value of τ^2 ensures a higher degree of shrinkage, larger τ^2 indicates the prior is more dispersed and shrinkage is less. In order to better explain the time-varying and shrinkage properties, we post the full model (LASSO shrinkage on both constant coefficients and time-varying parameters) results for Brent oil as an instant.

These results show moderate shrinkage in most coefficients, but the shrinkage degree varies. Table 3 shows that in one-month ahead ($h = 1$) forecasting, ω_i^2 for crude oil consumption, gold price, and industrial production index tend to shrink more than the coefficients on other variables, which indicate that the influence on crude oil price from these three variables is relatively time-invariant. In contrast, in short-term forecasting, the impacts of crude oil production on oil prices vary over time. The τ_i^2 of gas price, industrial production index, and the Kilian index shrink most among all exogenous variables; this signifies that the role of substitute product of oil, production level, and macroeconomic factors will not exert a significant effect on crude oil price in the short term. Instead, the three representative market uncertainty variables—VIX, EPU, and Google trend—show low-level shrinkage, so the policy uncertainty, market sentiment, and topic heat have a greater effect on the oil prices in the short term.

In the long-run ($h = 12$) forecasting, crude oil stocks, SP500, and the Kilian index show larger ω_i^2 than other variables, which means larger time variation in these coefficients. Moreover, the Kilian index presents the largest τ^2, which indicates that Kilian's index is a powerful predictor for oil price long-term forecasting. In the contrary, trade-weighted US dollar index, gas price, and production level are relatively unimportant factors.

Table 4 exhibits that the half-year ago oil prices have big impact on current oil price in the short-run forecasting; the influences from the end and beginning of the quarter are moderate. Table 5 depicts that the crude oil prices bear little relationship to the cycle of the seasons, because all the monthly dummies shrink more than the most of the other predictors and lags.

4.2. Forecasting Results Evaluation. In the tables, all the results are presented relative to the corresponding full model (LASSO on both constant coefficients and TVPs); smaller MAFE or MSFE, or larger MLPL than full model statistics indicate that the restricted model is forecasting better than the benchmark model.

The upper metrics of Table 6 results indicate that in one-month ahead forecasting, there is evidence that LASSO on constant coefficients outperforms other restricted models in both stochastic and constant volatility, which meet the short-term forecasting expectation that the majority coefficients do not change over time. Table 3 results are consistent with Table 6 and proved our opinion again.

In terms of the latter forecast metrics—the annual forecasting horizon—coefficients tend to show more time variation, so the full model has the best performance.

It is worth noting that the TVP regression models and constant coefficients models produce the worst forecasts in both cases according to MLPL. The results verified again that the new Bayesian hierarchical LASSO outperforms the traditional counterparts and enhances the prediction accuracy. Additionally, the bad performance of LASSO only on time-varying parameters indicates that the inclusion of time-variant parameters in the model is necessary for the oil prices forecasting.

To sum up, all results exhibit the advantages of the Bayesian hierarchical shrinkage. Firstly, putting a LASSO prior allows

Table 2: Descriptive statistics.

	WTI	BRENT	OD_CONS	OD_STOCKS	OS_WORLD	P_GOLD	US_EX
Mean	0.0009	0.0015	−0.0001	0.0003	0.0004	0.0028	0.0003
Median	0.0058	0.0069	−−0.0008	0.0005	0.0005	0.0027	0.0002
Maximum	0.0929	0.0851	0.0242	0.0090	0.0094	0.0537	0.0440
Minimum	−0.1442	−0.1351	−0.0264	−0.0086	−0.0064	−0.0904	−0.0178
Std. dev.	0.0389	0.0395	0.0107	0.0033	0.0029	0.0222	0.0070
Skewness	−0.8849***	−0.9662***	−0.0293	−2.2210	−0.0453	−0.4846***	1.4488***
Kurtosis (excess)	1.7698***	1.5476***	−0.5727	−0.0127	−0.1753	1.4502***	8.2127***
Jarque–Bera	46.7237***	45.7129***	2.4715	1.4584	0.2903	22.6911***	565.6776***
Q(20)	45.1300***	40.8931***	282.3031***	108.7411***	43.0371***	27.1741	26.0612
PP test	−9.4826***	−9.7966***	−20.9879***	−14.3289***	−13.5263***	−15.2111***	12.0550***
ADF	−6.6839***	−9.7414***	−3.2129**	−3.7359***	−7.0902***	−15.1254***	−11.9771***
	SP500	P_GAS	VIX	IP_TOTAL	EPU	KILIAN	Google
Mean	0.0019	−0.0010	0.0010	0.0004	0.0035	13.7941	0.0046
Median	0.0045	−0.0034	−0.0072	−0.0005	0.0041	2.1302	0.0000
Maximum	0.0444	0.1649	0.3703	0.0162	0.2831	187.8978	0.3358
Minimum	−0.0806	−0.1766	−0.2111	−0.0222	−0.2448	−163.4310	−0.2320
Std. dev.	0.0172	0.0549	0.0887	0.0072	0.0835	79.2186	0.1000
Skewness	−1.0534***	0.1095	0.6745***	0.1728	0.3511*	0.3115*	0.8297***
Kurtosis (excess)	3.1059***	1.1509***	1.5779***	0.0032	1.2777***	−0.7538**	1.0399***
Jarque–Bera	105.0568***	10.2378***	32.1443***	0.8914	15.8510***	7.1318***	28.6037***
Q(20)	40.0941***	24.4420	33.8112**	219.2882***	33.3670**	1659.5120***	18.3661
PP test	−11.2842***	−13.9759***	−16.6098***	−20.3007***	−15.4433***	−2.1650**	−14.1582***
ADF	−5.3398***	−13.8972***	−7.2381***	−3.9125***	−10.8053***	−2.6820***	−14.0785**

Symbols *, **, and *** denote rejections of the null hypothesis at the 10%, 5%, and 1% significance levels, respectively. The Jarque–Bera statistic is used to test the null hypothesis of the normal distribution. $Q(20)$ is the Ljung-Box Q statistics with lag order of 20. ADF refers to the statistics from the augmented Dickey–Fuller unit root tests. The entire sample period is from January 2004 to December 2018.

Table 3: Posterior means and standard deviation of ω_i^2 and τ^2 for exogenous predictors.

Predictor	$h=1$		$h=12$	
	ω_i^2	τ^2	ω_i^2	τ^2
INTERCEPT	1.691$E-03$	1.721$E-02$	**5.852** $E-$**02**	4.832$E-03$
	4.552$E-03$	3.507$E-02$	1.455$E-02$	7.005$E-03$
OD_CONS	1.223$E-03$	1.668$E-02$	2.247$E-04$	5.939$E-03$
	2.203$E-03$	3.193$E-02$	3.202$E-04$	8.661$E-03$
OD_STOCKS	1.558$E-03$	2.320$E-02$	1.132$E-03$	5.094$E-03$
	2.308$E-03$	4.347$E-02$	2.140$E-03$	8.442$E-03$
OS_PROD	**4.510** $E-$**03**	2.039$E-02$	3.591$E-04$	4.553$E-03$
	6.680$E-03$	3.548$E-02$	7.997$E-04$	6.569$E-03$
GOLD	6.845$E-03$	1.688$E-02$	3.195$E-04$	4.943$E-03$
	1.034$E-02$	3.506$E-02$	4.571$E-04$	7.695$E-03$
US_EX	1.507$E-03$	1.884$E-02$	6.058$E-04$	4.508$E-03$
	2.977$E-03$	3.919$E-02$	1.079$E-03$	8.013$E-03$
SP500	1.162$E-03$	2.338$E-02$	1.441$E-03$	5.481$E-03$
	2.443$E-03$	5.809$E-02$	1.869$E-03$	8.684$E-03$
GAS	9.481$E-04$	1.380$E-02$	6.770$E-04$	4.342$E-03$
	1.799$E-03$	2.929$E-02$	1.408$E-03$	8.098$E-03$
VIX	2.877$E-03$	**2.454** $E-$**02**	4.482$E-04$	**9.406** $E-$**03**
	5.570$E-03$	5.135$E-02$	5.983$E-04$	1.401$E-02$
IP	8.177$E-04$	1.453$E-02$	4.197$E-04$	4.817$E-03$
	1.542$E-03$	2.883$E-02$	8.323$E-04$	7.580$E-03$
EPU	2.595$E-03$	2.019$E-02$	3.585$E-04$	**6.666** $E-$**03**
	6.928$E-03$	3.991$E-02$	1.467$E-03$	8.442$E-03$
KILIAN	2.884$E-03$	1.426$E-02$	**1.337** $E-$**03**	**1.239** $E-$**02**
	7.256$E-03$	3.152$E-02$	1.705$E-03$	1.370$E-02$
Google	3.367$E-03$	**2.978** $E-$**02**	9.316$E-04$	7.450$E-03$
	6.438$E-03$	5.414$E-02$	9.836$E-04$	9.335$E-03$

Note. The bold text noted indicates relatively larger value among all ω_i^2 and τ^2, while the underlined text represents values relatively smaller ones.

Table 4: Posterior means and standard deviation of ω_i^2 and τ^2 for lags.

Lags	$h=1$		$h=12$	
	ω_i^2	τ^2	ω_i^2	τ^2
1	**4.292 $E-03$**	2.350$E-02$	4.613$E-04$	5.335$E-03$
	8.873$E-03$	4.947$E-02$	1.124$E-03$	7.308$E-03$
2	1.407$E-03$	1.517$E-02$	7.182$E-04$	4.762$E-03$
	4.063$E-03$	2.832$E-02$	9.439$E-04$	6.510$E-03$
3	1.484$E-03$	1.716$E-02$	6.976$E-04$	8.312$E-03$
	3.116$E-03$	3.761$E-02$	1.287$E-03$	1.249$E-02$
4	1.040$E-03$	1.587$E-02$	4.530$E-04$	4.833$E-03$
	2.353$E-03$	3.271$E-02$	9.666$E-04$	7.340$E-03$
5	1.268$E-03$	1.499$E-02$	9.913$E-04$	4.767$E-03$
	3.672$E-03$	3.030$E-02$	1.152$E-03$	7.669$E-03$
6	9.445$E-04$	1.849$E-02$	7.573$E-04$	4.690$E-03$
	1.875$E-03$	3.977$E-02$	1.374$E-03$	7.282$E-03$
7	1.563$E-03$	**2.183 $E-02$**	3.827$E-04$	4.349$E-03$
	3.164$E-03$	4.417$E-02$	6.040$E-04$	6.625$E-03$
8	1.746$E-03$	2.010$E-02$	6.014$E-04$	5.303$E-03$
	3.673$E-03$	3.964$E-02$	1.525$E-03$	8.904$E-03$
9	1.387$E-03$	1.336$E-02$	3.603$E-04$	4.652$E-03$
	2.672$E-03$	2.807$E-02$	6.767$E-04$	6.961$E-03$
10	1.591$E-03$	1.191$E-02$	8.393$E-04$	**5.798$E-03$**
	2.848$E-03$	2.392$E-02$	1.430$E-03$	1.116$E-02$
11	4.017$E-03$	1.635$E-02$	5.315$E-04$	5.441$E-03$
	7.294$E-03$	3.271$E-02$	1.024$E-03$	7.460$E-03$
12	1.307$E-03$	1.288$E-02$	**1.031 $E-03$**	5.542$E-03$
	2.731$E-03$	2.699$E-02$	1.667$E-03$	7.646$E-03$

Note. The bold text noted indicates relatively larger value among all ω_i^2 and τ^2, while the underlined text represents values relatively smaller ones.

Table 5: Posterior means and standard deviation of ω_i^2 and τ^2 for monthly dummies.

Dummies	$h=1$		$h=12$	
	ω_i^2	τ^2	ω_i^2	τ^2
1	**1.137 $E-02$**	**3.553 $E-02$**	1.498$E-03$	5.688$E-03$
	2.505$E-02$	7.022$E-02$	2.571$E-03$	1.037$E-02$
2	1.972$E-03$	1.617$E-02$	1.490$E-03$	6.749$E-03$
	6.910$E-03$	3.400$E-02$	3.898$E-03$	1.077$E-02$
3	1.996$E-03$	1.851$E-02$	6.993$E-04$	5.422$E-03$
	5.533$E-03$	4.477$E-02$	1.383$E-03$	8.975$E-03$
4	1.788$E-03$	1.732$E-02$	8.008$E-04$	5.116$E-03$
	5.006$E-03$	3.710$E-02$	1.551$E-03$	7.011$E-03$
5	1.322$E-03$	1.895$E-02$	1.404$E-03$	5.145$E-03$
	3.293E-03	4.164$E-02$	2.564$E-03$	7.389$E-03$
6	7.115$E-03$	1.769$E-02$	1.425$E-03$	**6.803$E-03$**
	1.534$E-02$	3.484$E-02$	2.453$E-03$	9.165$E-03$
7	2.157$E-03$	1.658$E-02$	7.892$E-04$	5.889$E-03$
	5.331$E-03$	3.614$E-02$	1.423$E-03$	9.500$E-03$
8	1.415$E-03$	1.627$E-02$	**3.182$E-03$**	5.242$E-03$
	3.236$E-03$	3.636$E-02$	7.964$E-03$	8.526$E-03$
9	3.228$E-03$	1.909$E-02$	1.314$E-03$	6.328$E-03$
	8.431$E-03$	3.732$E-02$	3.359$E-03$	9.615$E-03$
10	2.274$E-03$	1.932$E-02$	6.981$E-04$	5.538$E-03$
	5.342$E-03$	4.034$E-02$	1.450$E-03$	8.144$E-03$
11	4.155$E-03$	1.898$E-02$	1.020$E-03$	5.402$E-03$
	9.748$E-03$	5.034$E-02$	1.884$E-03$	7.023$E-03$

Note. The bold text noted indicates relatively larger value among all ω_i^2 and τ^2, while the underlined text represents values relatively smaller ones.

the data to decide whether the coefficients are time-varying and by how much they vary and restricts the TVP regression models coefficients wandering too widely which can obtain a better forecast performance. Secondly, in allusion of the misspecification problem, LASSO priors can automatically discover the lack of time variation in coefficients and shrinking the coefficients of unnecessary variables to zero, which improve the prediction accuracy and solve misspecification efficiently. Thirdly, hierarchical shrinkage in time-varying series facilitates researchers' start with a very flexible model with a relatively short dataset; the model results allow researchers and practitioners identify the most powerful predictors more efficiently then make the right investment decisions.

To investigate whether forecast performance varies over time, we present Figure 1, which uses the model with LASSO prior to both constant coefficients and time-varying parameters (TVPs) with forecasting horizon $h=1$ (similar patterns are found with the other computation results).

From (a) and (b) in Figure 1, it can be seen that the constant and stochastic volatility versions of the model forecast roughly as well as each other; however, many conflicts occur during the time of the shale oil revolution in 2014. MAFE, MSFE, and MLPL will have a similar pattern for most of the time, but inconsistent during periods of oil price intense volatility. What is happening is that the heteroskedastic version includes too much increase in volatility which began with the shale oil revolution since MLPL measures the whole distribution prediction performance. This has little impact on the point forecasts MAFE and MSFE which do not differ by much between the constant and stochastic versions of the model.

5. Robustness Checks

5.1. Robustness to Different Models' Specification. Firstly, we conduct the robustness check by changing the variable set; the out-of-sample performance of AR, multivariate, and UCSV models are shown in the following tables.

Tables 7–9 indicate that, like the full model, smaller MAFE and MSFE and larger MLPL are also observed in LASSO on constant coefficients and LASSO on both constant and TVPs in AR, multivariate, and UCSV models. These results suggest that hierarchical shrinkage method can also outperform other competing models even with changes in the model structures.

5.2. Robustness Check by Alternative Estimation Window. In this section, we change the estimation window from the recursive rolling window to the rolling window; the results are shown in Table 10. LASSO on constant coefficients and TVPs and LASSO only on constant results are qualitatively similar in both rolling window and recursive rolling window.

Further, we change three in-sample window sizes suggested by [6, 46, 47] to check the robustness of hierarchical shrinkage models. In 40%, 50%, and 60% different out-of-sample evaluation periods, the results show that models with LASSO shrinkage exhibit lower MAFE and MSFE and higher

Table 6: Measures of forecast performance for log return of Brent with the full models.

	Constant variance			Stochastic variance		
	MAFE	MSFE	MLPL	MAFE	MSFE	MLPL
Model (h = 1)						
LASSO on constant and TVPs	0.072	0.009	2.886	0.088	0.013	2.126
LASSO only on constant coeff.	0.061	0.007	3.377	0.075	0.010	2.896
LASSO only on TVPs	0.112	0.021	1.970	0.107	0.018	1.696
TVP regression model	0.100	0.016	2.222	0.114	0.019	1.589
Constant coeff. model	0.100	0.016	2.189	0.106	0.017	1.658
Model (h = 12)						
LASSO on constant and TVPs	0.373	0.223	0.545	0.407	0.265	0.414
LASSO only on constant coeff.	0.389	0.224	0.468	0.463	0.340	0.325
LASSO only on TVPs	0.678	0.809	0.308	0.710	0.842	0.232
TVP regression model	0.648	0.707	0.295	0.709	0.833	0.226
Constant coeff. model	0.658	0.717	0.289	0.689	0.809	0.227

Note. The value noted in bold and underlined text indicates a model performing the best out of all models, while the bold and italic text represents a model performing the worst. MSFE, MAFE, and MLPL refer to the mean squared forecast error, mean absolute forecast error, and mean log predictive likelihood, respectively.

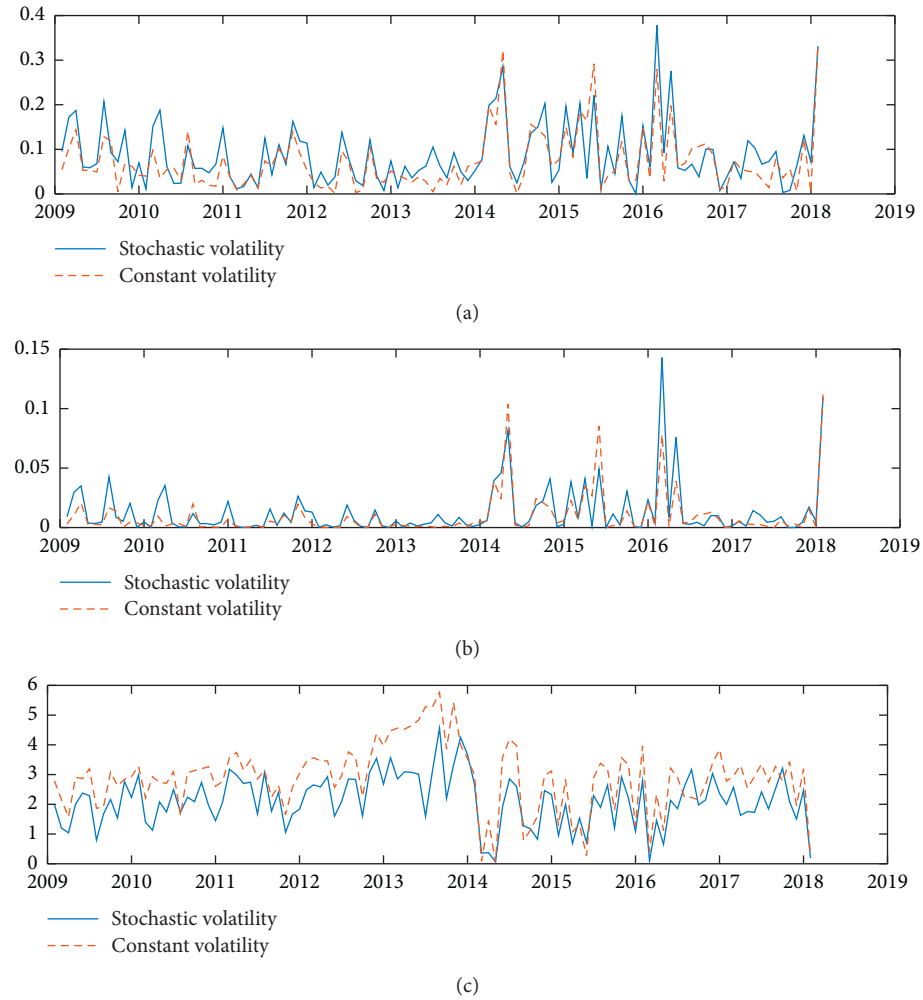

Figure 1: Forecasting performance measurement of models with LASSO prior on constant and time-varying coefficients, $h = 1$. (a) is the absolute forecast errors, (b) is the forecast errors squared, and (c) is the log predictive likelihood.

MLPL in most cases, suggesting the out-of-sample results of the hierarchical shrinkage are robust to different computation algorithms and sample sizes.

5.3. Robustness to Alternative Dependent Variable. Table 11 reports the main out-of-sample forecasting results of another prevailing proxy of crude oil prices, WTI. The

Table 7: Measures of forecast performance for log return of Brent with autoregression (AR) models.

	Constant variance			Stochastic variance		
	MAFE	MSFE	MLPL	MAFE	MSFE	MLPL
Model (h = 1)						
LASSO on constant and TVPs	0.067	0.008	2.825	0.089	0.014	1.969
LASSO only on constant coeff.	0.061	0.007	3.209	0.079	0.010	2.722
LASSO only on TVPs	0.098	0.015	1.989	0.104	0.016	1.822
TVP regression model	0.090	0.013	2.299	0.100	0.015	1.960
Constant coeff. model	0.091	0.013	2.275	0.097	0.014	1.996
Model (h = 12)						
LASSO on constant and TVPs	0.293	0.163	0.673	0.480	0.385	0.359
LASSO only on constant coeff.	0.337	0.207	0.502	0.462	0.321	0.313
LASSO only on TVPs	0.549	0.485	0.358	0.637	0.684	0.299
TVP regression model	0.557	0.523	0.337	0.586	0.533	0.281
Constant coeff. model	0.557	0.520	0.337	0.576	0.506	0.275

Note. The value noted in bold and underlined text indicates a model performing the best out of all models, while the bold and italic text represents a model performing the worst. MSFE, MAFE, and MLPL refer to the mean squared forecast error, mean absolute forecast error, and mean log predictive likelihood, respectively.

Table 8: Measures of forecast performance for log return of Brent with multivariate models.

	Constant variance			Stochastic variance		
	MAFE	MSFE	MLPL	MAFE	MSFE	MLPL
Model (h = 1)						
LASSO on constant and TVPs	0.061	0.007	3.350	0.077	0.011	2.696
LASSO only on constant coeff.	0.059	0.006	3.556	0.071	0.008	3.203
LASSO only on TVPs	0.069	0.009	3.022	0.081	0.011	2.383
TVP regression model	0.072	0.008	3.037	0.077	0.010	2.953
Constant coeff. model	0.072	0.008	3.029	0.076	0.010	2.874
Model (h = 12)						
LASSO on constant and TVPs	0.320	0.168	0.663	0.386	0.236	0.470
LASSO only on constant coeff.	0.328	0.165	0.538	0.303	0.153	0.546
LASSO only on TVPs	0.363	0.213	0.566	0.395	0.244	0.452
TVP regression model	0.376	0.221	0.480	0.314	0.175	0.482
Constant coeff. model	0.376	0.223	0.479	0.343	0.197	0.439

Note. The value noted in bold and underlined text indicates a model performing the best out of all models, while the bold and italic text represents a model performing the worst. MSFE, MAFE, and MLPL refer to the mean squared forecast error, mean absolute forecast error, and mean log predictive likelihood, respectively.

Table 9: Measures of forecast performance for log return of Brent ($h = 1$) with UCSV models.

	Constant variance			Stochastic variance		
	MAFE	MSFE	MLPL	MAFE	MSFE	MLPL
Model (h = 1)						
LASSO on constant and TVPs	0.064	0.007	3.111	0.076	0.010	2.969
LASSO only on constant coeff.	0.060	0.007	3.229	0.066	0.007	3.474
LASSO only on TVPs	0.069	0.009	2.879	0.075	0.010	2.750
TVP regression model	0.070	0.008	2.898	0.069	0.008	3.071
Constant coeff. model	0.070	0.008	2.909	0.068	0.008	3.148
Model (h = 12)						
LASSO on constant and TVPs	0.280	0.137	0.807	0.283	0.138	0.629
LASSO only on constant coeff.	0.297	0.157	0.530	0.269	0.117	0.774
LASSO only on TVPs	0.281	0.137	0.778	0.275	0.135	0.768
TVP regression model	0.298	0.160	0.511	0.276	0.121	0.706
Constant coeff. model	0.301	0.160	0.517	0.283	0.124	0.799

Note. The value noted in bold and underlined text indicates a model performing the best out of all models, while the bold and italic text represents a model performing the worst. MSFE, MAFE, and MLPL refer to the mean squared forecast error, mean absolute forecast error, and mean log predictive likelihood, respectively.

Table 10: Measures of forecast performance for log return of Brent with recursive rolling window results.

	Constant variance			Stochastic variance		
	MAFE	MSFE	MLPL	MAFE	MSFE	MLPL
Model (h = 1)						
LASSO on constant and TVPs	0.066	0.008	3.273	0.083	0.012	2.438
LASSO only on constant coeff.	**0.061**	**0.007**	**3.460**	0.076	0.010	2.955
LASSO only on TVPs	**0.078**	**0.010**	**2.750**	0.088	0.013	2.423
TVP regression model	0.074	0.009	3.003	0.079	0.010	2.625
Constant coeff. model	0.074	0.009	2.991	0.077	0.010	2.696
Model (h = 12)						
LASSO on constant and TVPs	0.315	0.170	**0.712**	0.391	0.260	0.463
LASSO only on constant coeff.	**0.306**	**0.166**	0.592	0.328	0.206	0.702
LASSO only on TVPs	0.363	0.228	0.597	0.439	0.318	0.406
TVP regression model	0.411	0.270	0.481	0.392	0.253	0.486
Constant coeff. model	**0.412**	**0.274**	**0.480**	0.370	0.223	0.479

Note. The value noted in bold and underlined text indicates a model performing the best out of all models, while the bold and italic text represents a model performing the worst. MSFE, MAFE, and MLPL refer to the mean squared forecast error, mean absolute forecast error, and mean log predictive likelihood, respectively.

Table 11: Measures of forecast performance for log return of Brent with WTI forecasting.

	Constant variance			Stochastic variance		
	MAFE	MSFE	MLPL	MAFE	MSFE	MLPL
Model (h = 1)						
LASSO on constant and TVPs	0.075	0.009	2.629	0.093	0.014	1.883
LASSO only on constant coeff.	0.063	0.007	3.131	0.080	0.011	2.476
LASSO only on TVPs	0.137	0.029	1.626	0.129	0.029	1.390
TVP regression model	0.115	0.022	1.891	0.111	0.021	1.413
Constant coeff. model	0.114	0.022	1.912	0.112	0.021	1.432
Model (h = 12)						
LASSO on constant and TVPs	0.333	0.202	0.612	0.388	0.265	0.422
LASSO only on constant coeff.	0.340	0.192	0.529	0.482	0.427	0.419
LASSO only on TVPs	0.642	0.732	0.308	0.696	0.859	0.218
TVP regression model	0.630	0.766	0.291	0.651	0.812	0.208
Constant coeff. model	0.629	0.771	0.293	0.673	0.856	0.204

Note. The value noted in bold and underlined text indicates a model performing the best out of all models, while the bold and italic text represents a model performing the worst. MSFE, MAFE, and MLPL refer to the mean squared forecast error, mean absolute forecast error, and mean log predictive likelihood, respectively.

results are quite close to Brent oil, which provides further support for the superiority of the hierarchical shrinkage method in alternative proxy of crude oil price forecasting.

6. Conclusions

In this paper, we predict the crude oil price based on the Bayesian hierarchical shrinkage method with a relatively short dataset and comprehensive variables framework. This method avoids overfitting and misspecification problems faced by linear regression prediction and improves the oil price forecasting accuracy. It also takes parameters dynamic properties into account. So, practitioners or policymakers can easily identify the most powerful indicators and do appropriate strategies during different periods.

The point and distribution forecasting performance statistics suggest that the hierarchical shrinkage models exhibit significantly better out-of-sample forecasting performance than other competing models in both homoskedasticity and heteroskedasticity versions. Our results are robust to a wide range of model settings, including various model structures, different out-of-sample sizes, alternative estimation rolling windows, and crude oil proxies. Therefore, our study provides evidence regarding which indicators are informative and powerful to improve forecasting accuracy in the oil market.

Data Availability

The Brent and WTI crude oil price data are openly available on the website of EIA at https://www.eia.gov/dnav/pet/pet_pri_spt_s1_d.htm.

Conflicts of Interest

The authors declare that they have no conflicts of interest regarding the publication of this paper.

References

[1] L. Kilian, A. Rebucci, and N. Spatafora, "Oil shocks and external balances," *Journal of International Economics*, vol. 77, no. 2, pp. 181–194, 2009.

[2] K. Lang and B. R. Auer, "The economic and financial properties of crude oil: a review," *The North American Journal of Economics and Finance*, vol. 52, 2019.

[3] J. Li, S. Zhu, and Q. Wu, "Monthly crude oil spot price forecasting using variational mode decomposition," *Energy Economics*, vol. 83, pp. 240–253, 2019.

[4] R. A. Ratti and J. L. Vespignani, "Oil prices and global factor macroeconomic variables," *Energy Economics*, vol. 59, pp. 198–212, 2016.

[5] P. Zagaglia, "Macroeconomic factors and oil futures prices: a data-rich model," *Energy Economics*, vol. 32, no. 2, pp. 409–417, 2010.

[6] Y. Zhang, F. Ma, and Y. Wang, "Forecasting crude oil prices with a large set of predictors: can lasso select powerful predictors?" *Journal of Empirical Finance*, vol. 54, pp. 97–117, 2019.

[7] Y. Wang, L. Liu, and C. Wu, "Forecasting the real prices of crude oil using forecast combinations over time-varying parameter models," *Energy Economics*, vol. 66, pp. 337–348, 2017.

[8] M. Balcilar and Z. A. Ozdemir, "The nexus between the oil price and its volatility risk in a stochastic volatility in the mean model with time-varying parameters," *Resources Policy*, vol. 61, pp. 572–584, 2019.

[9] S. A. Ozdemir, I. John, K. Ivanovski, and R. Smyth, "Dynamics of oil price, precious metal prices and the exchange rate in the long-run," *Energy Economics*, vol. 84, p. 104508, 2019.

[10] M. Guidolin, E. Hansen, and M. Pedio, "Cross-asset contagion in the financial crisis: a bayesian time-varying parameter approach," *Journal of Financial Markets*, vol. 45, pp. 83–114, 2019.

[11] R. Kruse and C. Wegener, "Time-varying persistence in real oil prices and its determinant," *Energy Economics*, vol. 85, Article ID 104328, 2019.

[12] R. Alquist, L. Kilian, and J. Robert, "Forecasting the price of oil," *Handbook of Economic Forecasting*, vol. 427-507, 2013.

[13] J. Chai, J.-E. Guo, L. Meng, and S.-Y. Wang, "Exploring the core factors and its dynamic effects on oil price: an application on path analysis and bvar-tvp model," *Energy Policy*, vol. 39, no. 12, pp. 8022–8036, 2011.

[14] L. Lei, Y. Shang, Y. Chen, and Y. Wei, "Does the financial crisis change the economic risk perception of crude oil traders? A midas quantile regression approach," *Finance Research Letters*, vol. 30, pp. 341–351, 2019.

[15] R. Ma, C. Zhou, H. Cai, and C. Deng, "The forecasting power of epu for crude oil return volatility," *Energy Reports*, vol. 5, pp. 866–873, 2019.

[16] J. Wang, G. Athanasopoulos, R. J. Hyndman, and S. Wang, "Crude oil price forecasting based on internet concern using an extreme learning machine," *International Journal of Forecasting*, vol. 34, no. 4, pp. 665–677, 2018.

[17] J. Wang, X. Li, T. Hong, and S. Wang, "A semi-heterogeneous approach to combining crude oil price forecasts," *Information Sciences*, vol. 460-461, pp. 279–292, 2018.

[18] F. Wen, M. Zhang, M. Deng, Y. Zhao, and J. Ouyang, "Exploring the dynamic effects of financial factors on oil prices based on a tvp-var model," *Physica A: Statistical Mechanics and Its Applications*, vol. 532, p. 121881, 2019.

[19] Y. Zhang, F. Ma, and Y. Wei, "Out-of-Sample prediction of the oil futures market volatility: a comparison of new and traditional combination approaches," *Energy Economics*, vol. 81, pp. 1109–1120, 2019.

[20] A. Jadidzadeh and A. Serletis, "The global crude oil market and biofuel agricultural commodity prices," *The Journal of Economic Asymmetries*, vol. 18, Article ID e00094, 2018.

[21] M. S. Kim, "Impacts of supply and demand factors on declining oil prices," *Energy*, vol. 155, pp. 1059–1065, 2018.

[22] W. Thorbecke, "Oil prices and the U.S. Economy: evidence from the stock market," *Journal of Macroeconomics*, vol. 61, p. 103137, 2019.

[23] Y. Wei, J. Liu, X. Lai, and Y. Hu, "Which determinant is the most informative in forecasting crude oil market volatility: fundamental, speculation, or uncertainty?" *Energy Economics*, vol. 68, pp. 141–150, 2017.

[24] Y. Wei, S. Qin, X. Li, S. Zhu, and G. Wei, "Oil price fluctuation, stock market and macroeconomic fundamentals: evidence from China before and after the financial crisis," *Finance Research Letters*, vol. 30, pp. 23–29, 2019.

[25] Q. Wang, Y.-H. Chiu, and C.-R. Chiu, "Driving factors behind carbon dioxide emissions in China: a modified production-theoretical decomposition analysis," *Energy Economics*, vol. 51, pp. 252–260, 2015.

[26] J. H. Stock and M. W. Watson, "Generalized shrinkage methods for forecasting using many predictors," 2011, http://www.princeton.edu/%7Emwatson_generalized_shrinkage_February_2011.pdf%200–62.

[27] Y. Yi, F. Ma, Y. Zhang, and D. Huang, "Forecasting the prices of crude oil using the predictor, economic and combined constraints," *Economic Modelling*, vol. 75, pp. 237–245, 2018.

[28] M. A. G. Belmonte, G. Koop, and D. Korobilis, "Hierarchical shrinkage in timevarying parameter models," *Journal of Forecasting*, vol. 94, pp. 80–94, 2011.

[29] Y. Zhang, Y. Wei, Y. Zhang, and D. Jin, "Forecasting oil price volatility: forecast combination versus shrinkage method," *Energy Economics*, vol. 80, pp. 423–433, 2019.

[30] H. Miao, S. Ramchander, T. Wang, and D. Yang, "Influential factors in crude oil price forecasting," *Energy Economics*, vol. 68, pp. 77–88, 2017.

[31] J. Li and W. Chen, "Forecasting macroeconomic time series: lasso-based approaches and their forecast combinations with dynamic factor models," *International Journal of Forecasting*, vol. 30, no. 4, pp. 996–1015, 2014.

[32] G. Kapetanios and F. Zikes, "Time-varying lasso," *Economics Letters*, vol. 169, pp. 1–6, 2018.

[33] T. Park and G. Casella, "The bayesian lasso," *Journal of the American Statistical Association*, vol. 103, no. 482, pp. 681–686, 2012.

[34] J. Chai, L.-M. Xing, X.-Y. Zhou, Z. G. au, and J.-X. Li, "Forecasting the WTI crude oil price by a hybrid-refined method," *Energy Economics*, vol. 71, pp. 114–127, 2018.

[35] Q. Zhang, S. Li, and R. Li, "China's dependency on foreign oil will exceed 80% by 2030: developing a novel nmgm-arima to forecast China's foreign oil dependence from two dimensions," *Energy*, vol. 163, pp. 151–167, 2018.

[36] M. Matyjaszek, P. Riesgo Fernández, A. Krzemień, K. Wodarski, and G. Fidalgo Valverde, "Forecasting coking coal prices by means of arima models and neural networks, considering the transgenic time series theory," *Resources Policy*, vol. 61, pp. 283–292, 2019.

[37] E. A. Fidalgo Valverde, A. N. Çatık, and M. Balcılar, "The impact of oil prices on the stock returns in Turkey: a Tvp-var approach," *Physica A: Statistical Mechanics and Its Applications*, vol. 535, p. 122392, 2019.

[38] T. Yao and Y.-J. Zhang, "Forecasting crude oil prices with the Google index," *Energy Procedia*, vol. 105, pp. 3772–3776, 2017.

[39] S. Bekiros, R. Gupta, and A. Paccagnini, "Oil price forecastability and economic uncertainty," *Economics Letters*, vol. 132, pp. 125–128, 2015.

[40] A. Lanza, M. Manera, and M. Giovannini, "Modeling and forecasting cointegrated relationships among heavy oil and product prices," *Energy Economics*, vol. 27, no. 6, pp. 831–848, 2005.

[41] V. K. Singh, P. Kumar, and S. Nishant, "Feedback spillover dynamics of crude oil and global assets indicators: a system-wide network perspective," *Energy Economics*, vol. 80, pp. 321–335, 2019.

[42] Z. Mandalinci, "Forecasting inflation in emerging markets: an evaluation of alternative models," *International Journal of Forecasting*, vol. 33, p. 22, 2017.

[43] Bo Zhang, J. C. C. Chan, and J. L. Cross, "Stochastic volatility models with arma innovations: an application to G7 inflation forecasts," *International Journal of Forecasting*, vol. 36, no. 4, 2020.

[44] J. C. C. Chan, "Moving average stochastic volatility models with application to inflation forecast," *Journal of Econometrics*, vol. 176, p. 10, 2013.

[45] G. V. Moura and E. Douglas Turatti, "Efficient estimation of conditionally linear and Gaussian state space models," *Economics Letters*, vol. 124, p. 5, 2014.

[46] B. Rossi and A. Inoue, "Out-of-Sample forecast tests robust to the choice of window size," *Journal of Business & Economic Statistics*, vol. 30, pp. 432–453, 2011.

[47] A. Inoue, L. Jin, and B. Rossi, "Rolling window selection for out-of-Sample forecasting with time-varying parameters," *Journal of Econometrics*, vol. 196, no. 1, pp. 55–67, 2017.

Hindawi
Discrete Dynamics in Nature and Society
Volume 2020, Article ID 8865489, 15 pages
https://doi.org/10.1155/2020/8865489

Research Article

Detecting Falsified Financial Statements Using a Hybrid SM-UTADIS Approach : Empirical Analysis of Listed Traditional Chinese Medicine Companies in China

Ruicheng Yang and Qi Jiang

School of Finance, Inner Mongolia University of Finance and Economics, Hohhot 010070, China

Correspondence should be addressed to Ruicheng Yang; yang-ruicheng@163.com

Received 8 August 2020; Revised 10 October 2020; Accepted 27 October 2020; Published 21 November 2020

Academic Editor: Dehua Shen

By combining the similarity matching (SM) method with the utilities additives discriminates (UTADIS) method, we propose a hybrid SM-UTADIS approach to detect falsified financial statements (FFS) of listed companies. To evaluate the performance of this hybrid approach, we conduct experiments using the annual financial ratios of listed traditional Chinese medicine (TCM) companies in China. There are three stages in the detection procedure. First, we use the cosine similarity matching method to select matched companies for each considered company, derive the deviation data of each considered company as a sample dataset to capture the intrinsic law of the financial data, and further divide these into training and testing datasets for the next two stages. Second, we put the training dataset into the UTADIS to train the SM-UTADIS model. Finally, we use the trained SM-UTADIS model to classify the testing dataset and evaluate the performance of the proposed method. Furthermore, we use other approaches, such as single UTADIS and logistic and SM-logistic regression models, to detect FFS. By comparing these results to those of the hybrid SM-UTADIS approach, we find that the proposed hybrid approach greatly improves the accuracy of FFS detection.

1. Introduction

Falsified financial statements (FFS) are deliberate misstatements of material facts by management in a company's accounts with the aim of deceiving investors and creditors. FFS primarily consist of overstating profit, sales, or assets or understating liabilities, expenses, or losses [1,2]. Such illegitimate behaviours have a severe effect on the global economy because they significantly undermine the confidence of investors and creditors. Falsified financial statements have become a serious problem worldwide, especially in some fast-growing countries like China, where FFS often cause investor failure, such as huge losses.

With the current upsurge in FFS, there is an increasing demand for greater transparency and consistency and for more information to be incorporated in financial statements. Detecting FFS has attracted considerable attention from investors, creditors, regulators, academic researchers, etc. FFS detection has always been an important but complex task for accounting professionals, and this problem has been difficult for traditional internal audits to solve effectively. In fact, detecting FFS is a classification problem because we can classify FFS as a group and non-FFS as another group. Hence, there are many studies in the literature regarding FFS detection which introduce advanced techniques or construct formal models, such as statistical models, data mining techniques, and multicriteria decision models. The classic statistical models mainly include logistic regression models, discriminant analysis, and probit models. Among these models, logistic regression is the most widely used approach to detect FFS, and it was developed by statistician Cox [3]. Beasley [4] applies logistic regression to analyze 75 fraud and 75 nonfraud firms and derives that nonfraud firms have boards with significantly higher percentages of outside members than fraud firms. Ines et al. [5] explore fraud in financial statements using logistic regression and find that

performance pressure on managers is a factor leading to fraud in the financial statements. Hansen et al. [6] introduce a powerful generalized qualitative-response model, EGB2, to predict management fraud based on data developed by an international public accounting company; therefore, the EGB2 model mainly consists of Probit and logistic techniques. The results indicate a good predictive ability for both symmetric and asymmetric cost assumptions. In addition, Persons [7] uses logistic regression to predict fraudulent financial reporting. Spathis [8] uses logistic regression analysis estimated using financial ratios from companies to determine which ratios are related to FFS. Chen et al. [9] screen important variables using stepwise regression, and then they match logistic regression, support vector machine, and decision trees to construct classification models for comparison. Ye et al. [10] adopt a random forest approach to detect FFS by learning imbalanced data.

With the development of artificial intelligence, neural networks are developed rapidly and used in economic prediction problems. For example, Zhang et al. [11] use Long Short-Term Memory (LSTM) networks to predict stock price movement. The results show that the LSTM model outperforms other models with the best prediction accuracy. Also, neural networks have a better performance in FFS detection. Green and Choi [12] develop a neural network fraud classification model using endogenous financial data. A classification model from the learned behaviour pattern was applied to a test sample. During the preliminary stage of an audit, a financial statement classified as fraudulent signals an auditor to increase substantive testing. By combining feature selection and machine learning classification, Yao et al. [13] propose an optimized financial fraud detection model. Jan [14] finds that variables screened with an artificial neural network (ANN) and processed by CART yield the best classification results in the detection of financial statements fraud. Fanning and Cogger [15] use ANN to develop a model for detecting management fraud. Using publicly available predictors of fraudulent financial statements, they develop a model using eight variables with a high probability for detection. Pazarskis et al. [16] apply 30 financial ratios and several statistical tests to create a model that uses ratios as predictors in the analysis of financial statements for fraud. Temponeras et al. [17] present a new predictive model for fraud detection using a deep dense artificial neural network. Kirkos et al. [18] explore the effectiveness of data mining classification techniques in detecting companies that issue FFS. To identify factors associated with FFS, they investigate the performances of decision trees, neural networks, and Bayesian belief networks in the identification of fraud financial statements. Gupta and Gill [19] implement three data mining methodologies, a decision tree, naïve Bayesian classifier, and genetic programming, to detect FFS. The three data mining methods for the detection of financial statement fraud were compared on the basis of two important evaluation criteria: sensitivity and specificity.

Different from natural world data, financial statement data are often irregular and it is hard to capture their intrinsic law. To date, the statistical models and data mining techniques have not derived ideal results. Hence, many researchers borrowed multiple-criteria decision-making models to identify FFS. Multiple-criteria decision-making (MCDM) or multiple-criteria decision analysis (MCDA) is a subdiscipline of operations research that explicitly evaluates multiple conflicting criteria in decision-making (both in daily life and in settings such as business, government, and medicine); Zionts [20] popularized the acronym. The approach was first summarized comprehensively in a book by Roy Bernard [21]. The significant approach in MCDA is utilities additives (UTA) method, which is based on preference disaggregation that aims at the estimation of an additive utility function through the analysis of global judgments (ranking or grouping of alternatives) of decision-makers. Lagrèze and Siskos [22] assess the additive utility functions that aggregate multiple criteria in a composite criterion, using linear programming to estimate the parameters of the utility function. Siskos et al. [23] analyze the UTA method and its variants to summarize the progress made in this field. The UTA method is a well-known preference disaggregation method applied in many sorting problems. Furthermore, Corrente et al. [24] integrate the multiple-criteria hierarchy process and UTA method for dealing with MCDA in case of a hierarchical structure of the family of evaluation criteria. Mousseau et al. [25] consider the inverse multiple-criteria sorting problem (IMCSP) with UTA and other sorting methods for determining which actions to implement to provide guarantees on object classification. Mota [26] uses the approach to support project managers to focus on the main tasks of a project network.

Zopounidis and Doumpos [27] propose the UTADIS method based on the preference disaggregation approach and estimate a set of additive utility functions and utility profiles using linear programming techniques to minimize misclassification errors in sorting problems. They present the application of the UTADIS method in two real-world classification problems concerning the field of financial distress. Kosmidou et al. [28] use UTADIS to investigate the performance of small and large UK banks over multiple criteria, such as asset quality, capital adequacy, liquidity, and efficiency/profitability. The results determine the key factors that classify a bank as small or large and provide us with responsible banking decision-makers for future readjustments. Mehregan et al. [29] use the UTADIS method to classify securities and to form a profitable investment portfolio. Doumpos et al. [30] propose a robust multicriteria approach that can be used to provide early warning signals for possible future capital shortfalls that banks may face. These research results show that the proposed MCDA approach provides models with strong discriminative power. Recently, Spathis et al. [31] apply UTADIS classification method to detect factors associated with FFS; a jackknife procedure approach is used for model validation and comparison with multivariate statistical techniques, namely, discriminant and logistic analysis. The results indicate that the UTADIS methodology achieves relatively good results in detecting FFS.

Based on this, we borrow the UTADIS idea to detect the FFS of companies. The sample data are chosen from the

financial ratios of listed traditional Chinese medicine (TCM) companies in China, which is a historical and prosperous industry. The reasons why we choose this industry as our research sample are the following: (1) There is a necessary sample size of FFS for our research in this sector. (2) There are few mixed businesses in TCM industry, and the main business of this sector is relatively concentrated. This will ensure that the selected samples have the homogeneous feature in their main business. Accordingly, this also can reduce the interference of unrelated noises.

As we know, in the real world, the data of each financial ratio may change drastically over time. For example, the outbreak of an epidemic will raise the income of almost all of the companies in the TCM sector, whereas an increase in material costs will result in a decline in that sector. Accordingly, related financial ratios will change sharply, inducing FFS misjudgments. However, we observe that the operating performance of a company is usually similar to other companies in the same sector; therefore, such companies should have similar changes in their financial ratios. In view of this, we introduce the cosine similarity algorithm to help us select companies most similar to the matched companies and use their financial data to compute the deviation of the considered company. Then, the deviation data are used for UTADIS classification (more details in Section 2). The merit of the financial deviation data is that they reflect the intrinsic law of a considered company, making it easier to detect FFS with UTADIS. This is the main contribution of this paper, that is, based on the UTADIS method, we combine the similarity algorithm with UTADIS and formulate an integrated method, SM-UTADIS, for detecting FFS.

The remainder of this paper is organized as follows. In Section 2, we describe the proposed SM-UTADIS methodology, including the similarity computation, UTADIS method, and classification procedure. Section 3 provides the results obtained using the SM-UTADIS classification method and reports the comparisons with the single UTADIS and logistic regression approaches. Concluding remarks and opportunities for future research are presented in Section 4.

2. Model Description

For convenience, we first introduce the following notations that are used throughout the paper:

(1) Considered company A_c ($c = 1, 2, \ldots, C$): the c-th considered company whose annual financial data we classify into FFS and non-FFS groups.

(2) Candidate matching company $\#m$ ($m = 1, 2, \ldots, L$): the m-th candidate matching company.

(3) Matched company $\#M_q$ ($q = 1, 2, 3, \ldots, Q$): the q-th matched company with $Q \le L$; these matched companies are selected from the above candidate matching companies.

(4) Variables or financial ratios R_i^l ($i = 1, 2, \ldots, J$; $l = 1, 2, \ldots, C$ or L) represent the i-th variable or financial ratio of company $\#l$. In this paper, we choose the same financial ratios for all companies (including considered and candidate matching companies), and each different right superscript represents a different company. In total, there are J financial ratios for each company.

We propose a hybrid classification model that combines the SM and UTADIS methods, as illustrated in Figure 1. As shown in Figure 1, the procedure has three stages. In the SM stage, the cosine similarity matching algorithm is applied to select matched companies for each considered company. Using the initial financial data, we compute the deviation data of each considered company and gather all of the deviation financial data into the research sample. We further divide the research sample into training and testing datasets for the next two stages. In the second stage, we put the training dataset into the UTADIS to train the model. In the last stage, we put the testing data into the well-trained UTADIS model to predict the testing data and evaluate the classification performance of the proposed method.

In the detection procedure, the key algorithms are the cosine SM method in Stage 1 and UTADIS in Stages 2 and 3. Thus, we provide more explicit descriptions of the algorithms in the two following subsections.

2.1. Similarity Matching Method. The operating performance of a company is usually similar to other companies in the same industry. Therefore, there should be similar changes in the financial ratios of these companies. In view of this, for each considered company, we use the cosine similarity matching algorithm to select the most similar matched companies and to obtain the deviation data of each considered company. Without loss of generality, the algorithm for considered company A_c is as follows:

Step 1—Computation of cosine similarity: Cosine similarity is a measure of the similarity between two vectors of an inner product space that measures the cosine of the angle between them [32]. Here, we give the cosine similarity between considered company A_c and the candidate matching company $\#m$ ($m = 1, 2, \ldots, L$) as follows:

$$\begin{aligned} S_m^c &= \cos\left(\theta_m^c\right) \\ &= \frac{\vec{R^c} \cdot \vec{R^m}}{\left\|\vec{R^c}\right\|\left\|\vec{R^m}\right\|} \\ &= \frac{\sum_{j=1}^{J} R_j^c \times R_j^m}{\sqrt{\sum_{j=1}^{J}\left(R_j^c\right)^2}\sqrt{\sum_{j=1}^{J}\left(R_j^m\right)^2}}, \quad (m = 1, 2, \ldots, L), \end{aligned} \tag{1}$$

where S_m^c represents the similarity between considered company A_c and candidate matching company $\#m$ ($m = 1, 2, \ldots, L$), $\vec{R^c} = (R_1^c, R_2^c, \ldots, R_J^c)$ represents the financial ratio vector of considered company A_c, and

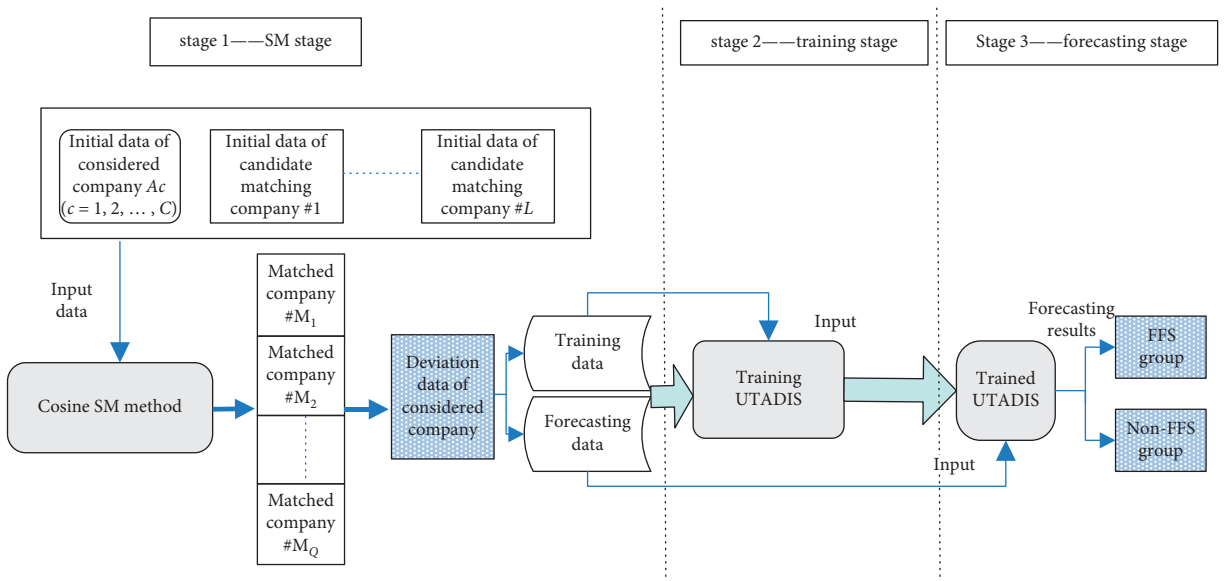

Figure 1: The procedure of FFS detection with the SM-UTADIS method.

$\overrightarrow{R^m} = (R_1^m, R_2^m, \ldots, R_J^m)$ represents the financial ratio vector of candidate matching company #m.

Step 2—Selection of matched companies: Now we rank the matched companies $\{S_m^c, m = 1, 2, \ldots, L\}$ in descending order with $\widehat{S}_1^c \geq \widehat{S}_2^c \geq \cdots \geq \widehat{S}_L^c$ and choose the first several companies as the matched companies. For example, if we choose P $(P \leq L)$ matched companies, we only choose companies with $\widehat{S}_1^c, \widehat{S}_2^c, \ldots, \widehat{S}_P^c$, and denote the P companies as the matched companies for considered company A_c.

Step 3—Computation of data deviation: Denote $\widehat{R}_j^p$ as the j-th financial ratio of the p-th $(p = 1, 2, \ldots, P)$ matched company, and using the corresponding financial data of the matched companies, we derive the deviation data of the j-th financial ratio for considered company A_c as follows:

$$\overline{R_j^c} = \frac{\left| R_j^c - (1/P) \sum_{p=1}^{P} \widehat{R}_j^p \right|}{(1/P) \sum_{p=1}^{P} \widehat{R}_j^p}. \tag{2}$$

Thus, we derive the deviation sample data for inputting into the UTADIS.

2.2. UTADIS Method. Following Zopounidis and Doumpos [27] and Spathis et al. [31], we give a brief description of the UTADIS method as follows.

Let $A = (a_1, a_2, \ldots, a_n)$ be a set of n annual financial datasets described along a set of m attributes or evaluation criteria $x_1, x_2, \ldots, x_J$; here, the attributes correspond to financial ratios. The goal is to classify the n annual financial datasets into q ordered classes $C_1, C_2, \ldots, C_q$, which are defined as $C_1 \succ C_2 \succ \cdots \succ C_q$ (C_1 is preferred to C_2, C_2 is preferred to C_3, and so on).

For each evaluation criterion x_j $(j = 1, 2, \ldots, J)$, the interval $X_j = [x_j^{\min}, x_j^{\max}]$ of its values is defined; here $x_j^{\min}$ and $x_j^{\max}$ represent the minimal and maximal values, respectively, of criterion X_j for all of the alternatives belonging to A. The internal X_j can be divided into a_{j-1} equal intervals $[x_j^i, x_j^{i+1}]$, $i = 1, 2, \ldots, a_{j-1}$, $x_j^1 = x_j^{\min}$, $x_j^{a_j} = x_j^{\max}$. a_j depends on the number of estimate points of the marginal utility u_j. Every break point x_j^i can be determined using the following formula:

$$x_j^i = x_j^{\min} + \frac{i-1}{a_j - 1}\left(x_j^{\max} - x_j^{\min}\right). \tag{3}$$

Our aim is to estimate the marginal utilities at each of these breakpoints. Suppose that the evaluation of each alternative a on the criterion x_j is $x_j(a) \in [x_j^i, x_j^{i+1}]$, and the marginal utility of each alternative $a \in A$ and $u_j[x_j(a)]$ can be roughly estimated through the linear interpolation:

$$u_j\left[x_j(a)\right] = u_j\left(x_j^i\right) + \frac{x_j(a) - x_j^i}{x_j^{i+1} - x_j^i}\left(u_j\left(x_j^{i+1}\right) - u_j\left(x_j^i\right)\right). \tag{4}$$

To achieve monotonicity of the criteria, the following conditions and the monotonicity constraints must be satisfied:

$$\left.\begin{aligned} & u_j\left(x_j^{i+1}\right) - u_j\left(x_j^i\right) \geq 0, \quad \forall j, \\ & \omega_{ji} = u_j\left(x_j^{i+1}\right) - u_j\left(x_j^i\right) \geq 0, \quad \forall i, j \\ & u_j\left(x_j^{\min}\right) = 0 \\ & u_j\left(x_j^i\right) = \sum_{k=1}^{i-1} \omega_{jk} \end{aligned}\right\}. \tag{5}$$

Using these transformations, (4) can be rewritten as

$$u_j\left[x_j(a)\right] = \sum_{k=1}^{i-1} \omega_{ji} + \frac{x_j(a) - x_j^i}{x_j^{i+1} - x_j^i}\omega_{ji}. \tag{6}$$

The total utility $U(a)$ of each alternative $a \in A$ can be expressed as

$$U(a) = \sum_{j=1}^{m} u_j\left(x_j(a)\right) \in [0,1]. \tag{7}$$

Estimations of the total utility model (marginal utilities of all breakpoints $x_j^i (i = 1, 2, \ldots, a_{j-1})$) and utility thresholds are accomplished through the solution of the following linear program:

$$\begin{aligned} \min F = & \sum_{a \in C_1} \sigma^+(a) + \cdots + \sum_{a \in C_k} \left[\sigma^+(a) + \sigma^-(a)\right] \\ & + \cdots + \sum_{a \in C_q} \sigma^-(a), \end{aligned} \tag{8}$$

subject to

$$\begin{aligned} & \sum_{j=1}^{m} u_j\left[x_j(a)\right] - t_1 + \sigma^+(a) \geq 0, \quad \forall a \in C_1, \\ & \left.\begin{aligned} & \sum_{j=1}^{m} u_j\left[x_j(a)\right] - t_{k-1} - \sigma^-(a) \leq -\delta \\ & \sum_{j=1}^{m} u_j\left[x_j(a)\right] - t_k + \sigma^+(a) \geq 0 \end{aligned}\right\}, \quad \forall a \in C_k, \\ & \sum_{j=1}^{m} u_j\left[x_j(a) - t_{q-1} - \sigma^-(a)\right] \leq -\delta, \quad \forall a \in C_q, \\ & \sum_{j=1}^{m} \sum_{i=1}^{a_{j-1}} \omega_{ji} = 1, \\ & t_{k-1} - t_k \geq \delta, \quad k = 2, 3, \ldots, q-1, \\ & \omega_{ji} \geq 0, \sigma^+(a) \geq 0, \sigma^-(a) \geq 0. \end{aligned} \tag{9}$$

Here, $\sigma^+(a)$ and $\sigma^-(a)$ are the two possible errors (misclassification errors) relative to the global utility $U(a)$; an overestimation error $\sigma^+(a)$ represents cases in which an alternative, according to its utility, is classified in a lower class than the class to which it belongs (e.g., an alternative is classified in class C_2 while belonging to class C_1), whereas an underestimation error $\sigma^-(a)$ represents cases in which an alternative, according to its utility, is classified in a higher class than the class to which it belongs. The threshold t_k is used to denote the strict preference relation between the utility thresholds that distinguish the classes; δ>0 is used to denote the strict preference relation between the utility thresholds that distinguish the classes.

By comparing each utility with the corresponding utility thresholds $t_k (t_1 > t_2 > \cdots > t_{q-1})$, we derive a decision rule for each alternative a to distinguish each class from the others:

$$\begin{aligned} & U(a) \geq t_1 \Longrightarrow a \in C_1, \\ & t_2 \leq U(a) < t_1 \Longrightarrow a \in C_2, \\ & \qquad \cdots \\ & t_k \leq U(a) < t_{k-1} \Longrightarrow a \in C_k, \\ & \qquad \cdots \\ & U(a) < t_{q-1} \Longrightarrow a \in C_q. \end{aligned} \tag{10}$$

Next, we examine the detection of FFS. In this study, only two classes of annual financial samples are considered, that is, non-FFS (group C_1) and FFS (group C_2), and the rule for the classification of a sample as FFS or non-FFS is as follows:

$$\begin{aligned} & U(a) \geq t \Longrightarrow a \in C_1, \\ & U(a) < t \Longrightarrow a \in C_2, \end{aligned} \tag{11}$$

where t is the corresponding utility threshold.

Based on the above classification rule, we classify the data into two classes: non-FFS and FFS. Here, the FFS class is the fraudulent financial data.

3. Experiment Results and Discussion

In this section, using the real financial data of the TCM sector in China, we evaluate the performance of the proposed SM-UTADIS approach. The computation results of this section are obtained using Matlab software.

3.1. Selection of Fraud Companies and Nonfraud Companies Experiment Results and Discussion. Currently, there are about 150 companies listed in the TCM sector in China, but most are involved in mixed business areas, and the main profit of some is not earned through traditional Chinese medicine. Such companies must be discarded; otherwise, they will obscure the evolving law of financial ratios as it relates to companies whose business is purely related to TCM. In addition, we must choose companies with financial ratios that include falsified data, but too much non-FFS data will dilute and hinder the identification process. Hence, only 24 TCM companies are used in our research. Among these 24 companies, three considered companies are regarded as fraud companies as they were accused of fraud in some years by the China Securities Regulatory Commission (CSRC). The other 21, as the candidate matching companies, are non-FFS, which are free of fraud. Of course, there is at least one annual financial data point in the fraudulent statements. For simplicity, we label the three considered companies as A1, A2, and A3, and the other 21 non-FFS candidate matching companies are labelled #1, #2, . . ., #21.

Next, we use the annual financial data of the three considered companies to evaluate the classification performance of the proposed SM-UTADIS method. The annual financial data cover the period from 2001 to 2016, and the data are collected from the Wind website (http://www.wind.com.cn/). If a company's financial statement in a specific year is identified as fraudulent by the CSRC, it is classified as a fraudulent observation. In contrast, financial statements that are free from falsified allegations are classified as nonfraudulent observations.

For each falsified company, we first identify the earliest year in which financial statement fraud was committed. Each period covers the years before and after the year of the event. Thus, seven consecutive annual financial statements are used in most cases except for some class in which consecutive annual financial statements are accused of fraud or the related data are not published. We get 36 firm-year

observations (i.e., annual financial statements) of the three considered companies as our research sample, out of which 24 are nonfraudulent (Class C_1) and 12 are fraudulent (Class C_2). Next, we divide these 36 annual observations into two groups: a training dataset and a testing dataset. To get better training and testing effects, the proportion of training and testing data is set to 1 : 1, respectively. Moreover, to maintain the rationality and validity of the division, we try to distribute the data of each company into the training and testing datasets as equally as possible. Therefore, the 6 falsified and 12 nonfalsified annual observations are treated as the training dataset, and the rest are treated as the testing dataset.

3.2. Choice of Financial Ratios. Based on Green and Choi [12], Mironiuc et al. [33], and Shin-Ying Huang et al. [34], 12 explanatory variables or financial ratios are selected as the sample variables; the definitions and measurements of these financial ratios (financial ratios that describe both the structure of the company assets and the level of the recorded performance care) are summarized in Table 1.

3.3. Similarity Computation and Matched Company Selection of Financial Ratios. For classification purposes, we match each falsified considered company with nonfalsified candidate matching companies in the same sector using cosine similarity analysis. In fact, we only need to compute the similarity of nonfraudulent years between the considered company and its candidate matching companies from the training dataset. If fraudulent data were included in the similarity computation, it would decrease identification efficiency because it would distort characteristics that are similar in the real world. Hence, for each considered company A_i $(i = 1, 2, 3)$, we select its nonfalsified annual financial data from the training dataset and the corresponding data of non-FFS candidate matching companies #1–#21 in the same years, and, using (1), we can compute the similarity between considered company (CM) A_c and its non-FFS candidate matching companies (CMC) #1–#21. The results of the similarity analysis are given in the following table.

Choosing the similarity threshold is the key issue for improving classification accuracy in the following training and forecasting stages. If the threshold value is too big, the number of matched companies will be small. However, if the threshold value is too small, the number of matching companies will become lagger. In fact, the threshold value will directly affect the selection of matched companies, and this will further affect the accuracy of the training and testing results. We hope to choose a suitable threshold that will allow for ideal training and testing accuracy. Through many trials, the 0.70 threshold value provides the best performance. After many trials and adjustments, we select our matched companies, and the similarity values are greater than 0.70. In Table 2, the first three maximal values are highlighted in grey for each considered company. There are two matched companies, #3 and #14, for considered company A_1, three matched companies, #1, #9, and #20, for considered company A_2, and one matched company, #18, for considered company A_3. Based on the initial financial data of each considered company and its matched companies, by (2), we can easily get the deviation data of all considered companies and further divide the data into a training dataset and a testing dataset. This concludes the data preparation for the next two stages.

3.4. Results and Discussion. Applying the proposed SM-UTADIS method to the training dataset, we get the marginal utility of each financial ratio as shown in Figure 2. The classification results and the utility threshold t are shown in Table 3.

In Figure 2, we see that the most significant ratios for discrimination in the training dataset are R_9, R_{10}, and R_{12}; their weights are 27.4971%, 23.7773%, and 12.8746%, respectively. The next is R_1 with a weight of 7.3757%. The other ratios show no significant differences in their contribution to FFS detection. Table 3 shows that the threshold t is 0.349489. Using classification rules (10), Table 3 shows that there are no misclassifications.

Furthermore, the prediction ability of the trained model developed by the UTADIS method is also tested using the testing dataset. Using the trained model, we derive classification results for the testing dataset. The results are presented in Table 4. To make it clear, the misclassifications are highlighted in grey. There are two misclassifications in the testing dataset; we summarize the type I error, type II error, and overall error in Table 5. Here, a type I error corresponds to an overestimation error $\sigma^-(a)$, meaning that an FFS observation is classified as non-FFS, whereas a type II error corresponds to an underestimation error $\sigma^+(a)$, meaning that a non-FFS observation is classified as FFS. According to the results in Table 5, the overall error rate is 11.1111%, and type I and type II errors are 16.6667% and 8.3333%, respectively.

3.5. Comparison with Single UTADIS Results and Discussion. To evaluate the performance of the proposed SM-UTADIS approach, we compare its classification results with those of single UTADIS using the same initial data of considered company A_c $(c = 1, 2, 3)$. Figure 3 illustrates the marginal utility of each financial ratio. Similar to the SM-UTADIS analysis, Figure 3 shows that the most significant ratios for discrimination in the training dataset are also R_9 and R_{10}, and their weights change to 24.3604% and 19.2855%, respectively. The other ratios show no significant differences in their contribution to FFS detection. Table 6 shows that there is no identification error in the training process. Using the trained model, we predict the testing dataset, and the classification results are shown in Table 7. Table 7 shows that there are 13 misclassification errors. The type I, type II, and overall errors are summarized in Table 8. Compared with Table 5, the classification results using the proposed SM-UTADIS are far superior to the results with single UTADIS.

3.6. Comparison of Logistic and SM-Logistic Models. Logistic regression is another popular method for FFS detection; it is widely used in many research areas, such as finance and social sciences. To test the performance of our

Table 1: Definition and measurement of financial ratios.

Notation	Definition of ratio	Measurement
R_1	Return on equity (ROE)	Net income/Average equity
R_2	Earnings before interest and taxes to return on assets (EBIT ROA)	Earnings before interest and taxes/Average total assets
R_3	Return on assets	[Net income + interest * (1 − tax rate)]/Total assets
R_4	Net profit to total operating income	Net profit/Total operating income
R_5	Operating profit to total operating income	Operating profit/Total operating income
R_6	Operating profit ratio	(Sales − Operating Costs − Operating expenses)/Sales
R_7	Current ratio	Current assets/Current liabilities
R_8	Quick ratio	(Current assets − Inventory − Prepaid expenses)/Current liabilities
R_9	Growth rate of net profit	(Net profit/Net profit in prior annual term) − 1
R_{10}	Growth rate of net assets	(Current net assets/Net assets in prior annual term) − 1
R_{11}	Total assets turnover ratio	Revenue/Average total assets
R_{12}	Ratio of liabilities to assets	Total debts/Total assets

Table 2: Similarity between considered company A_i ($i = 1, 2, 3$) and non-FFS candidate matching companies #1–#21.

CM	CMC	Similarity value
A_1	#1	−0.00493
	#2	−0.24823
	#3	0.927066
	#4	0.219229
	#5	−0.15931
	#6	0.128307
	#7	0.30172
	#8	0.352593
	#9	0.103669
	#10	−0.04005
	#11	−0.09919
	#12	−0.89803
	#13	0.325353
	#14	0.786474
	#15	0.474157
	#16	0.402147
	#17	0.022846
	#18	0.398805
	#19	0.034669
	#20	−0.023900
	#21	0.205393
A_2	#1	0.719112
	#2	0.235432
	#3	−0.099010
	#4	0.559809
	#5	0.129897
	#6	0.435574
	#7	0.632609
	#8	0.251317
	#9	0.705876
	#10	0.647896
	#11	0.537107
	#12	0.167555
	#13	0.378416
	#14	0.109826
	#15	0.052887
	#16	0.055193
	#17	0.670442
	#18	−0.195400
	#19	0.586637
	#20	0.781885
	#21	0.550248
A_3	#1	−0.06277
	#2	0.101022
	#3	0.301448
	#4	−0.07407
	#5	−0.002910
	#6	−0.733340
	#7	−0.101370
	#8	0.031707
	#9	−0.022590
	#10	−0.073700
	#11	−0.489810
	#12	−0.297000
	#13	−0.808090
	#14	0.147712
	#15	−0.043480
	#16	−0.019510
	#17	0.074003
	#18	0.891208
	#19	−0.354680
	#20	−0.036140
	#21	−0.012560

proposed SM-UTADIS method, we use logistic regression and SM-logistic regression (a combination of SM and logistic regression) to classify the same training and testing datasets and further compare the classification results with those of SM-UTADIS. The results of logistic and SM-logistic regression are presented in Tables 9 and 10, respectively. Comparing Table 9 with Table 10, we see fewer classification errors with the SM-logistic regression method than with single logistic regression; this implies that the SM technique improves the classification accuracy rate. However, the classification result of the SM-logistic regression method is not better than that of the SM-UTADIS method. Tables 5 and 10 show that the type I, type II, and overall errors with SM-logistic regression are far higher than those with SM-UTADIS (see Table 5). Therefore, by comparing the classification results of three approaches, we find that the superiority of the SM-UTADIS method over logistic regression and single regression is clear, whether classifying the training dataset or the testing dataset.

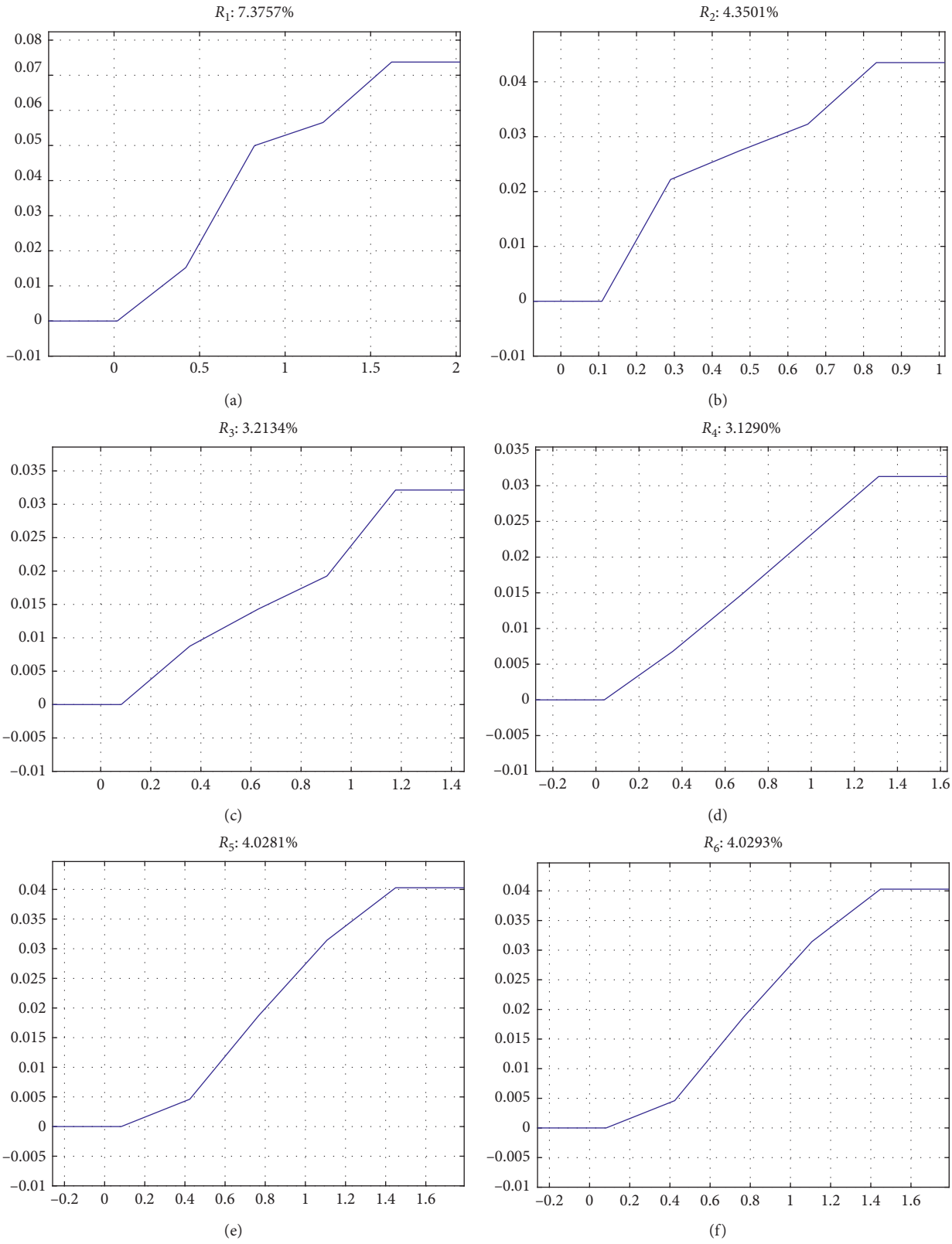

Figure 2: Continued.

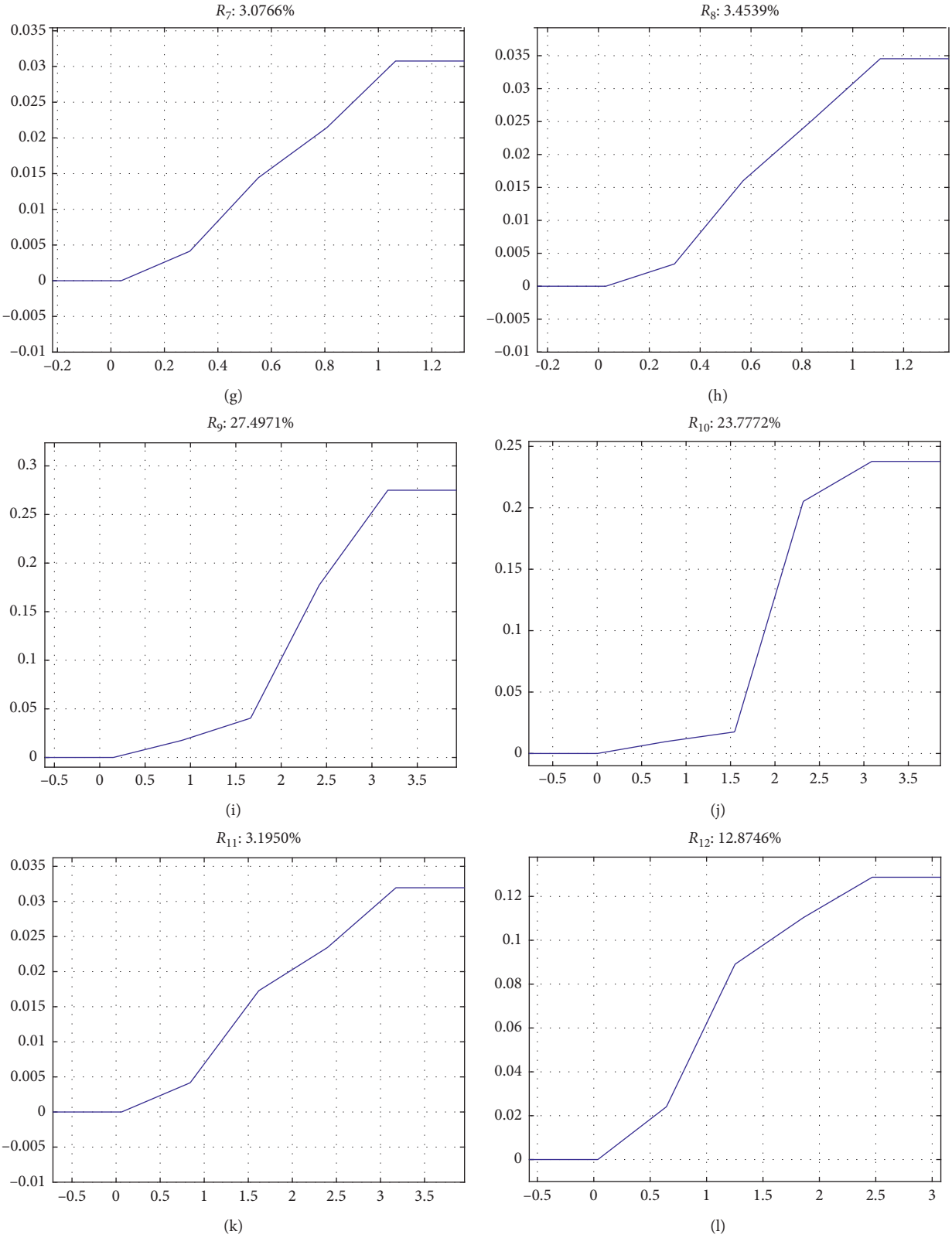

Figure 2: Marginal utility of each financial ratio with the SM-UTADIS method (training dataset).

Table 3: Classification results with the SM-UTADIS method (training dataset).

Considered company	Year	Actual class	Utility value	Estimated class
A_1	2001	C_1	0.419078	C_1
	2003	C_1	0.349516	C_1
	2009	C_1	0.358020	C_1
	2011	C_1	0.381929	C_1
A_2	2003	C_1	0.387177	C_1
	2005	C_1	0.358557	C_1
	2008	C_1	0.375054	C_1
	2013	C_1	0.413359	C_1
A_3	2003	C_1	0.350032	C_1
	2005	C_1	0.350784	C_1
	2010	C_1	0.354496	C_1
	2012	C_1	0.396284	C_1
Utility threshold t			0.349489	
A_1	2005	C_2	0.341412	C_2
	2007	C_2	0.328442	C_2
A_2	2004	C_2	0.323764	C_2
	2011	C_2	0.339731	C_2
A_3	2006	C_2	0.349420	C_2
	2008	C_2	0.346697	C_2

Table 4: Forecasting results with the trained SM-UTADIS model (testing dataset).

Considered company	Year	Actual class	Utility value	Estimated class
A_1	2002	C_1	0.349590	C_1
	2004	C_1	0.349710	C_1
	2010	C_1	0.358811	C_1
	2012	C_1	0.386387	C_1
A_2	2005	C_1	0.350307	C_1
	2006	C_1	0.380931	C_1
	2008	C_1	0.357234	C_1
	2014	C_1	0.312229	C_2
A_3	2004	C_1	0.352612	C_1
	2009	C_1	0.350430	C_1
	2011	C_1	0.351601	C_1
	2014	C_1	0.365781	C_1
Utility threshold t			0.349489	
A_1	2006	C_2	0.316715	C_2
	2008	C_2	0.353189	C_1
A_2	2010	C_2	0.325583	C_2
	2012	C_2	0.339748	C_2
A_3	2007	C_2	0.345021	C_2
	2013	C_2	0.050622	C_2

Table 5: Error summary with the SM-UTADIS method.

	Actual class	Total amounts	Number of errors identified	Type I errors	Type II errors	Overall errors
Training dataset	C_1	12	0	0	0	0
	C_2	6	0			
Testing dataset	C_1	12	1	16.6667%	8.3333%	11.1111%
	C_2	6	1			

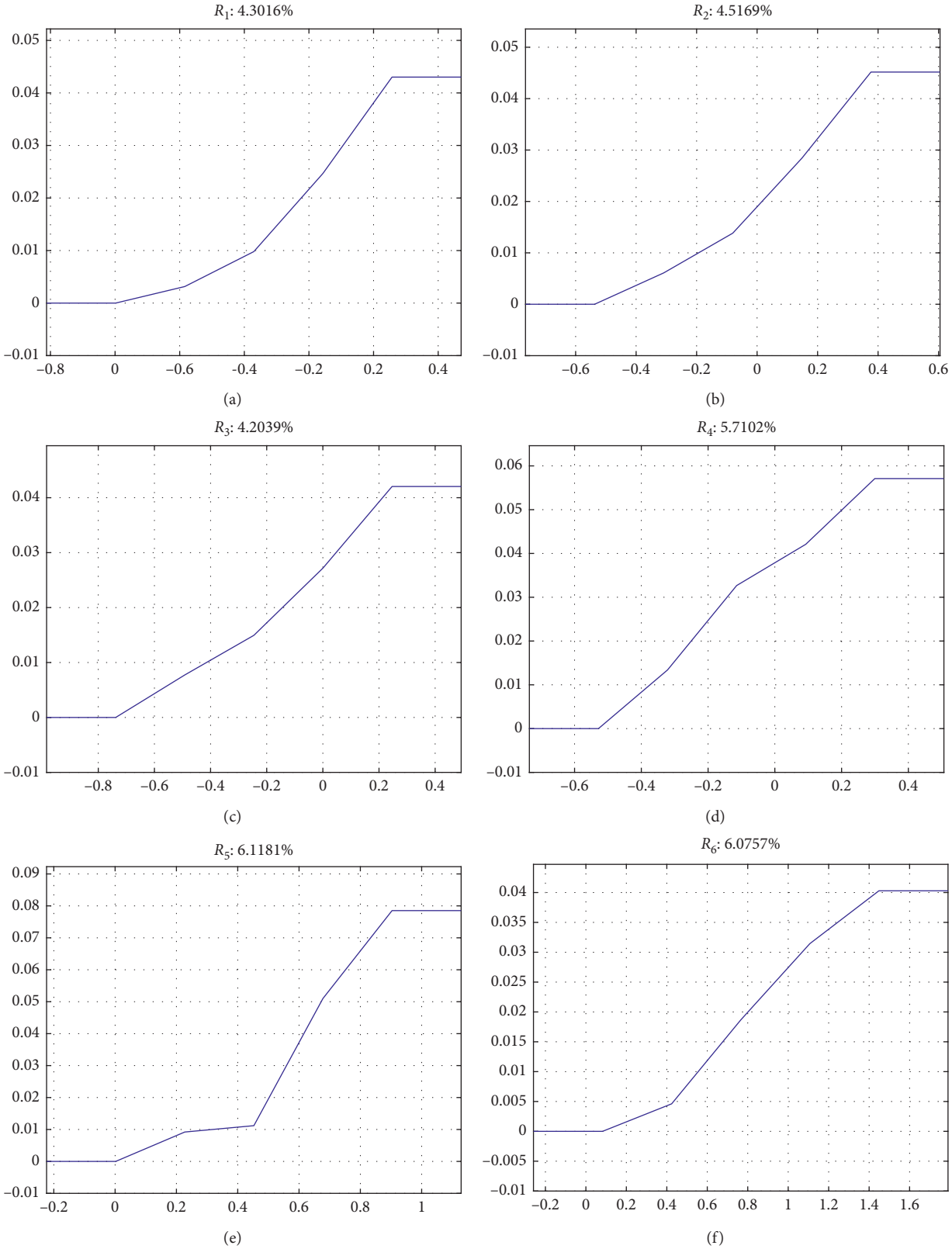

Figure 3: Continued.

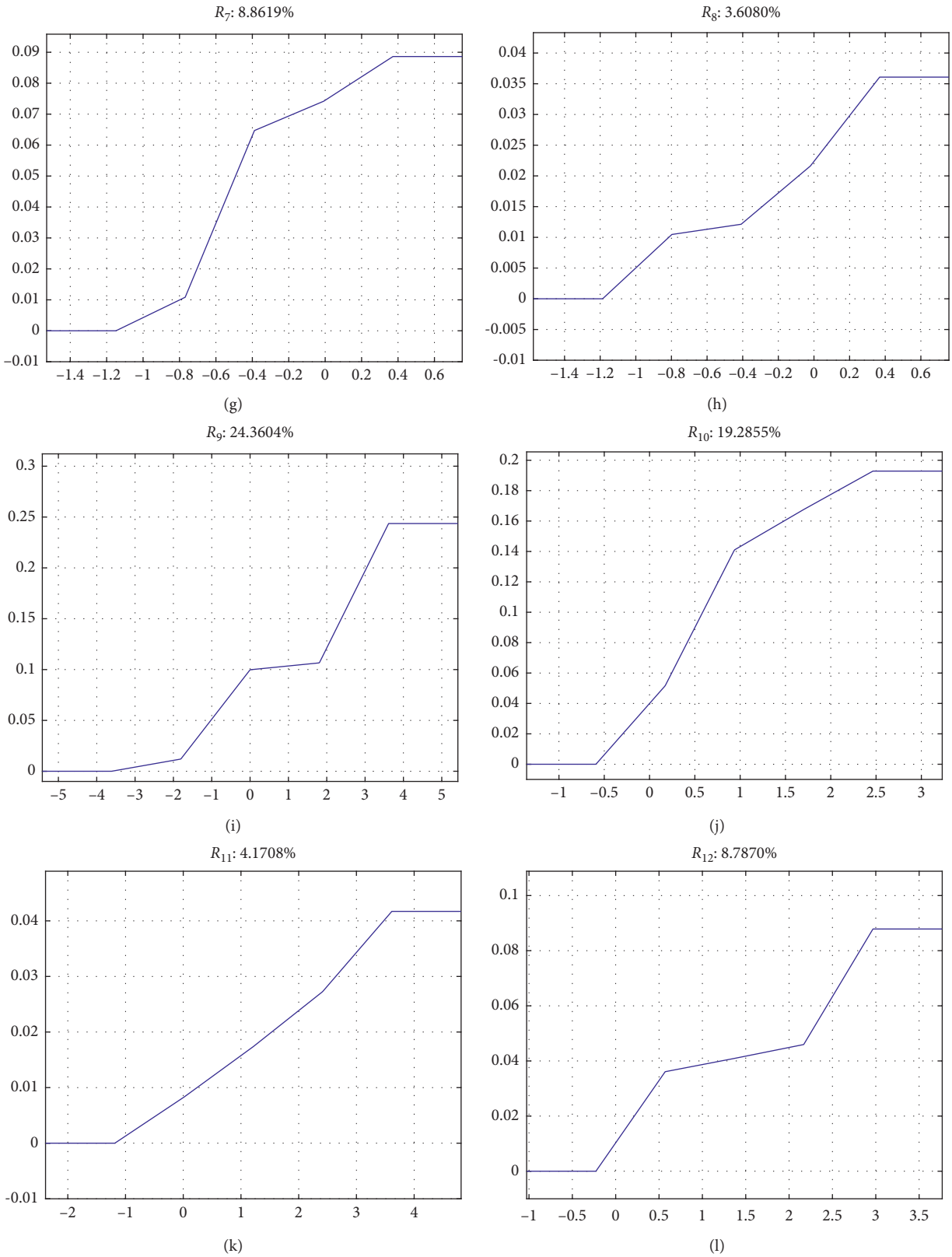

Figure 3: Marginal utility of each financial ratio using single UTADIS (training dataset).

Table 6: Classification results using the single UTADIS method (training dataset).

Considered company	Year	Actual class	Utility value	Estimated class
A_1	2001	C_1	0.337953	C_1
	2003	C_1	0.360633	C_1
	2009	C_1	0.422805	C_1
	2011	C_1	0.459080	C_1
A_2	2003	C_1	0.442766	C_1
	2005	C_1	0.360602	C_1
	2008	C_1	0.334531	C_1
	2013	C_1	0.369313	C_1
A_3	2003	C_1	0.392187	C_1
	2005	C_1	0.460778	C_1
	2010	C_1	0.319150	C_1
	2012	C_1	0.347777	C_1
Utility threshold t			0.319139	
A_1	2005	C_2	0.304669	C_2
	2007	C_2	0.283387	C_2
A_2	2004	C_2	0.290913	C_2
	2011	C_2	0.261104	C_2
A_3	2006	C_2	0.303683	C_1
	2008	C_2	0.316627	C_2

Table 7: Forecasting results using the trained single UTADIS model (training dataset).

Considered company	Year	Actual class	Utility value	Estimated class
A_1	2002	C_1	0.429631	C_1
	2004	C_1	0.474130	C_1
	2010	C_1	0.441629	C_1
	2012	C_1	0.437099	C_1
A_2	2005	C_1	0.303503	C_2
	2006	C_1	0.352361	C_1
	2008	C_1	0.382830	C_1
	2014	C_1	0.269696	C_2
A_3	2004	C_1	0.444084	C_1
	2009	C_1	0.280839	C_2
	2011	C_1	0.347777	C_1
	2014	C_1	0.469747	C_1
Utility threshold t			0.319139	
A_1	2006	C_2	0.285334	C_2
	2008	C_2	0.431728	C_1
A_2	2010	C_2	0.293083	C_2
	2012	C_2	0.363316	C_1
A_3	2007	C_2	0.363351	C_1
	2013	C_2	0.428283	C_1

Table 8: Error summary using single UTADIS method.

	Actual class	Total amounts	Number of errors identified	Type I errors	Type II errors	Overall errors
Training dataset	C_1	12	0	0	0	0
	C_2	6	0			
Testing dataset	C_1	12	3	66.67%	25%	38.8889%
	C_2	6	4			

Table 9: Error summary with single logistic regression method.

Data	Actual class	Total amount	Number of errors identified	Type I errors (%)	Type II errors (%)	Overall errors (%)
Training dataset	C_1	12	1	50	8.3333	22.2222
	C_2	6	3			
Testing dataset	C_1	12	2	83.3333	16.6667	38.8889
	C_2	6	5			

Table 10: Error summary with SM-logistic regression method.

Data	Actual class	Total amount	Number of errors identified	Type I errors	Type II errors (%)	Overall errors (%)
Training dataset	C_1	12	1	0	8.3333	5.5556
	C_2	6	0			
Testing dataset	C_1	12	3	33.3333%	25.0000	27.7778
	C_2	6	2			

4. Conclusions

Combining the SM method with UTADIS, a hybrid SM-UTADIS approach is proposed to detect falsified financial statements by classifying financial ratio data into FFS and non-FFS groups. To evaluate the performance of this hybrid method, we conduct experiments using the annual financial ratios of listed companies in the TCM sector in China. Compared with UTADIS and logistic and SM-logistic regression models, the results show that the hybrid SM method can improve the clustering accuracy, and the SM-UTADIS method has the highest prediction accuracy.

The main contributions of this paper are summarized as follows:

(1) From the candidate matching companies, the cosine similarity algorithm is introduced to select out the matched companies, similar to the considered companies. Based on this, we use the financial data of matched companies to compute the deviation of the considered company by SM method. The financial deviation data obtained by SM method can reflect the intrinsic law of a considered company more clearly and make it easier to detect FFS with UTADIS.

(2) We formulate a hybrid SM-UTADIS method by combining the cosine SM algorithm with UTADIS method for detecting FFS.

(3) We give an empirical analysis by taking the traditional Chinese medicine industry as our research sample and prove the outperformance of the proposed hybrid method.

The proposed hybrid method can also be used for FFS detection in other industries. Here, the traditional Chinese medicine industry is just chosen as an example to test our hybrid method in this paper. Note that the industry of research samples had better have the homogeneous feature in their main business. The usefulness of this study first comes from the possibility of applying current working methods in financial fraud detecting and the improvement of classification methods. The development direction of future research is to expand the sample of the analyzed companies, focus on specific activity objects, determine the characteristics of each department, and improve the proposed model according to the specific economic environment of each company, so as to provide the best possible guarantee for the existence of fraud.

The importance of this topic and its results stems from the promotion of the method to identify financial fraud, which may contribute to the successful prevention and detection of these catastrophic actions.

Data Availability

The data used to support the findings of this study can be accessed from the following online address: http://www.wind.com.cn/.

Conflicts of Interest

The authors declare no conflicts of interest.

Acknowledgments

This study was partially supported by the National Natural Science Foundation of China (Grant no. 71761029), Natural Science Foundation of Inner Mongolia Autonomous Region (Grant no. 2017MS717), and the Program for Innovative Research Team in Universities of Inner Mongolia Autonomous Region (Grant no. NMGIT1405).

References

[1] G. Apparao, A. Singh, G. S. Rao, B. L. Bhavani, K. Eswar, and D. Rajani, "Financial statement fraud detection by data mining," *International Journal of Advanced Networking and Applications*, vol. 1, no. 3, pp. 159–163, 2009.

[2] M. Omidi, Q. Min, V. Moradinaftchali, and M. Piri, "The efficacy of predictive methods in financial statement fraud," *The Scientific World Journal*, vol. 2014, Article ID 968712, 9 pages, 2014.

[3] D. R. Cox, "The regression analysis of binary sequences," *Journal of the Royal Statistical Society*, vol. 21, no. 1, p. 238, 1958.

[4] M. S. Beasley, "An empirical analysis of the relation between the board of director composition and financial statements," *Accounting Review*, vol. 71, no. 4, pp. 443–465, 1996.

[5] A. Ines, A. Ben, and J. Anis, "Detection of fraud in financial statements: French companies as a case study," *International Journal of Academic Research in Business and Social Sciences*, vol. 3, no. 5, pp. 2222–6990, 2013.

[6] J. V. Hansen, J. B. Mcdonald, W. F. Messier, and T. B. Bell, "A generalized qualitative-response model and the analysis of management fraud," *Management Science*, vol. 42, no. 7, pp. 1022–1032, 1996.

[7] O. S. Persons, "Using financial statement data to identify factors associated with fraudulent financial reporting," *Journal of Applied Business Research*, vol. 11, no. 3, pp. 38–46, 1995.

[8] C. T. Spathis, "Detecting false financial statements using published data: some evidence from Greece," *Managerial Auditing Journal*, vol. 17, no. 4, pp. 179–191, 2002.

[9] S.-D. Chen, Y.-J. J. Goo, and Z.-D. Shen, "A hybrid approach of stepwise regression, logistic regression, support vector machine, and decision tree for forecasting fraudulent financial statements," *The Scientific World Journal*, vol. 2014, Article ID 968712, 9 pages, 2014.

[10] H. Ye, L. Xiang, and Y. Gan, "Detecting financial statement fraud using random forest with SMOTE," *Materials Science and Engineering*, vol. 612, no. 5, 2019.

[11] Y. Zhang, G. Chu, and D. Shen, "The role of investor attention in predicting stock prices: the Long short-term memory networks perspective," *Finance Research Letters*, Article ID 101484, 2020.

[12] B. P. Green and J. H. Choi, "Assessing the risk of management fraud through neural-network technology," *Auditing: A Journal of Practice and Theory*, vol. 16, no. 1, pp. 14–28, 1997.

[13] J. Yao, J. Zhang, and L. Wang, "A financial statement fraud detection model based on hybrid data mining methods," *International Conference on Artificial Intelligence and Big Data (ICAIBD)*, vol. 2018, pp. 57–61, Article ID 4989140, 2018.

[14] C.-L. Jan, "An effective financial statements fraud detection model for the sustainable development of financial markets: evidence from Taiwan," *Sustainability*, vol. 2018, no. 2, 14 pages, Article ID 8882253, 2018.

[15] K. M. Fanning and K. O. Cogger, "Neural network detection of management fraud using published financial data," *Intelligent Systems in Accounting Finance & Management*, vol. 7, no. 2, pp. 21–41, 1998.

[16] M. Pazarskis, G. Drogalas, and K. Baltzi, "Detecting false financial statements: evidence from Greece in the period of economic crisis," *Investment Management and Financial Innovations*, vol. 14, no. 3, pp. 102–112, 2017.

[17] G. S. Temponeras, S. N. Alexandropoulos, S. B. Kotsiantis, and M. N. Vrahatis, "Financial fraudulent statements detection through a deep dense artificial neural network," in *Proceedings of the 2019 10th International Conference on Information, Intelligence, Systems and Applications (IISA)*, pp. 1–5, Patras, Greece, 2019.

[18] E. Kirkos, C. Spathis, and Y. Manolopoulos, "Data mining techniques for the detection of fraudulent financial statements," *Expert Systems with Applications*, vol. 32, no. 8, pp. 995–1003, 2007.

[19] R. Gupta and N. S. Gill, "Prevention and detection of financial statement fraud – an implementation of data mining framework," *International Journal of Advanced Computer Science and Applications*, vol. 3, no. 8, pp. 150–156, 2012.

[20] S. Zionts, "MCDM-if not a roman numeral, then what?" *Interfaces*, vol. 9, no. 4, pp. 94–101, 1979.

[21] B. Roy, *Multicriteria Methodology for Decision Aiding*, Kluwer Academic Publishers, Dordrecht, Netherlands, 1996.

[22] E. Jacquet-Lagreze and J. Siskos, "Assessing a set of additive utility functions for multicriteria decision-making, the UTA method," *European Journal of Operational Research*, vol. 10, no. 2, pp. 151–164, 1982.

[23] Y. Siskos and D. Yannacopoulos, "UTASTAR: An ordinal regression method for building additive value functions," *Investigação Operacional*, vol. 5, pp. 39–53, 1985.

[24] S. Corrente, M. Doumpos, S. Greco, R. Słowiński, and C. Zopounidis, "Multiple criteria hierarchy process for sorting problems based on ordinal regression with additive value functions," *Annals of Operations Research*, vol. 251, no. 1-2, pp. 117–139, 2017.

[25] V. Mousseau, Ö. Özpeynirci, and S. Özpeynirci, "Inverse multiple criteria sorting problem," *Annals of Operations Research*, vol. 253, no. 1, pp. 1–34, 2017.

[26] C. M. D. M. Mota and A. T. de Almeida, "A multicriteria decision model for assigning priority classes to activities in project management," *Annals of Operations Research*, vol. 199, no. 1, pp. 361–372, 2012.

[27] C. Zopounidis and M. Doumpos, "A multicriteria decision aid methodology for sorting decision problems: the case of financial distress," *Computational Economics*, vol. 14, no. 3, pp. 197–218, 1999.

[28] K. Kosmidou, F. Pasiouras, M. Doumpos, and C. Zopounidis, "Assessing performance factors in the UK banking sector: a multicriteria methodology," *Central European Journal of Operations Research*, vol. 14, no. 1, pp. 25–44, 2006.

[29] M. M. Reza, S. M. M. Reza, and E. M. S. M. Mohsen, "Applying the clustering and UTADIS models to form an investment portfolio," *Financial Research*, vol. 20, no. 1, pp. 53–74, 2018.

[30] M. Doumpos, C. Zopounidis, and P. Fragiadakis, "Assessing the financial performance of European banks under stress testing scenarios: a multicriteria approach," *Operational Research*, vol. 16, no. 2, pp. 197–209, 2016.

[31] C. Spathis, M. Doumpos, and C. Zopounidis, "Detecting falsified financial statements: a comparative study using multicriteria analysis and multivariate statistical techniques," *European Accounting Review*, vol. 11, no. 3, pp. 509–535, 2002.

[32] S. Grigori, G. Alexander, G.-A. Helena, and P. David, "Soft similarity and soft cosine measure: similarity of features in vector space model," *Computacióny Sistemas*, vol. 18, no. 3, pp. 491–504, 2014.

[33] M. Mironiuc, I.-B. Robu, and M.-A. Robu, "The fraud auditing: empirical study concerning the identification of the financial dimensions of fraud," *Journal of Accounting and Auditing: Research & Practice*, vol. 2012, Article ID 391631, 13 pages, 2012.

[34] S. Y. Huang, R. H. Tsaih, and W. Y. Lin, "Unsupervised neural networks approach for understanding fraudulent financial reporting," *Industrial Management & Data Systems*, vol. 112, no. 2, pp. 224–244, 2012.

Hindawi
Discrete Dynamics in Nature and Society
Volume 2020, Article ID 1738279, 14 pages
https://doi.org/10.1155/2020/1738279

Research Article

Regional Credit, Technological Innovation, and Economic Growth in China: A Spatial Panel Analysis

Huan Zhou,[1] Shaojian Qu,[1,2,3] Xiaoguang Yang,[4] and Qinglu Yuan[5]

[1]*Business School, University of Shanghai for Science and Technology, Shanghai 200093, China*
[2]*School of Management Science and Engineering, Nanjing University of Information Science and Technology, Nanjing 210044, China*
[3]*National University of Singapore, Singapore*
[4]*Academy of Mathematics and Systems Science, CAS, Beijing 100190, China*
[5]*Institute of Disaster Prevention, Beijing 101601, China*

Correspondence should be addressed to Shaojian Qu; qushaojian@usst.edu.cn

Received 26 July 2020; Revised 30 August 2020; Accepted 5 October 2020; Published 3 November 2020

Academic Editor: Dehua Shen

Based on data of 31 provinces in China for the period 2007–2017, this paper establishes spatial models by means of a transcendental logarithmic production function and analyzes the impact of regional credit and technological innovation on regional economic growth. The Jenks natural breaks method, kernel density function, and Moran index are introduced for spatial statistical analysis. Spatial weight matrices are constructed from two aspects of geographical characteristics and innovative input characteristics. The empirical results show significant spatial heterogeneity and spatial autocorrelation in economic growth, regional credit, and technological innovation. Both regional credit and technological innovation are important impacts to economic growth, whereas the interaction of regional credit and technological innovation has a negative effect on provincial economic growth. Therefore, we argue that China should rationally allocate regional credit resources, strengthen technological innovation capabilities, and boost the integrated development of regional credit and technological innovation. It is a particularly important way to facilitate regional economic integration and sustainable development.

1. Introduction

Entering a new era, China is in a critical period of economic high-quality growth with the increase of uncertainties in the international economic situation and the competitive landscape. To successfully surmount this critical period, we must heighten the proportion of science and technology and knowledge-intensive industries, stimulate technical innovation as the "first driving force," and take the road of regional innovation-driven development. In the recent years, regional credit and technological innovation have brought into play more and more vital effect in the transformation and upgrading of China's economy [1,2]. In terms of the ranking of the World Intellectual Property Organization (WIPO), Chinese synthesize ranking of scientific and technological innovation was 14th in 2019. In addition, the value of contract deals in domestic technical markets by type of contracts of China increased by more than 26.56% in 2019. Furthermore, the contribution rate of scientific and technological progress to the GDP has risen to 58.5% in 2018. Accordingly, in the process of China's modernization, technological innovation as the main driving force of economic development should be placed at the core.

In this economic situation, having a solid financial system is essential to provide an effective financing, risk management, and the sustainable development of China's economy [3]. According to the National Bureau of Statistics of China, the outstanding loans in local and foreign currencies of all financial institutions in China reached 23 trillion dollar in 2019, an increase of 2.4 trillion dollar over 2018. Figure 1 serves as the trend of financial institution credit measured by the logarithm of loan-based metrics

(lnRC), technological innovation measured by the logarithm of patent-based metrics (lnRD), and total economic output measured by the logarithm of the GDP (lnGDP) of China from 2007 to 2018. As can be seen from Figure 1, lnGDP and lnRC maintained steady and rapid growth. Actually, reasonable credit supply creates a favorable financial environment for high-quality economic development. lnRD has remained high, mainly because of China's increasing emphasis on technological innovation in the recent years [4]. Meanwhile, technological innovation highly depends on the support of credit supply [2,5,6]. Credit supply has a direct impact on technological innovation and its transformation efficiency. Analyzing financial dependence and technological innovation [5] shows that firms in external finance-dependent industries generate a better patent portfolio. By comparing the trends of lnGDP, lnRC, and lnRD, it is also found that there is a certain correlation and similarity among them.

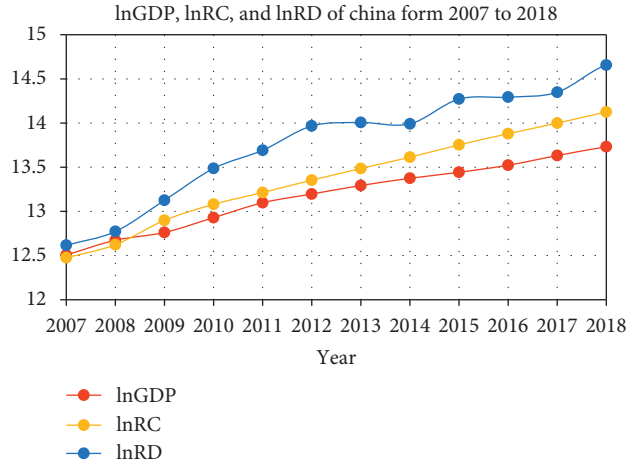

Figure 1: lnGDP, lnRC, and lnRD of China from 2007 to 2018.

Most researchers focus on the Chinese technological innovation surge, interestingly, while few have been known about the impact of regional credit and technological innovation on regional economic growth in China. From a regional perspective, is there spatial heterogeneity and a regional correlation in China's economic growth? Does China's regional credit level promote or restrain regional economic growth? How does regional credit affect regional economic growth through technological innovation? In the process of implementing an innovation-driven development strategy, exploring the influence of regional credit and technological innovation on economic growth is conducive to optimizing an innovation ecosystem and realizing the coordinated development of multiagent economy.

The following structure is arranged as follows. Section 2 is the literature review. Section 3 introduces the model specification and description of variables, including the spatial econometric model, variable selection, and spatial weight matrix construction. Section 4 uses spatial statistical analysis technology to analyze the dynamic evolution trend and spatial agglomeration effect of regional credit, technological innovation, and economic growth. Section 5 analyzes the empirical results of the static spatial model and dynamic spatial model. Section 6 draws the research conclusion and gives policy recommendations.

2. Literature Review

2.1. Regional Credit and Economic Growth. Finance is the core of modern economy and plays an important role in regulating the economy. The relationship between regional credit and economic growth has attracted great attention in the available theoretical and empirical literature. By comparing countries' economic growth performance, we summarize three main views on the relationship between regional credit and economic growth. First, financial credit has a positive effect on steady-state economic growth [7–10]. Diallo and Al-Titi [11] theoretically and empirically investigated the positive effect of bank credit on regional economic growth. Second, the link between regional credit and economic growth is not significant [12,13]. Zhang [13] explained that the contribution of bank credit development to economic growth was not significant in China. Third, financial credit has a negative effect on economic growth [14,15]. Sassi and Gasmi [14] explained the negative effect of credit on economic growth and the heterogeneity of the credit. Meanwhile, credit supply is unbalanced in the region [16], and it is not matched and not coordinated with the good situation of regional economic development, which restricts the development of regional economy to a certain extent. However, China's credit supply under the dominance of economic growth indicates that China is a puzzling example to the general financial credit literature.

2.2. Technological Innovation and Economic Growth. Statistical evaluation and quantitative analysis of technological innovation are the hot spots and trends of current scientific and technological research. Many studies focus on firms' capabilities for innovation [17], technological innovation output, the intensity of technological innovation [18], and sustainable innovation [19]. Innovation is the main engine of socioeconomic development for an increasing number of economic agents and countries. In particular, technological innovation is an important independent factor to reveal the change of economic growth [20,21]. Consequently, technological innovation has always been an intriguing research topic for scholars and policy makers. The existing literature has two main views on the impact of technological innovation on regional economic growth. First, an efficient regional innovation system plays a significant and positive role in promoting regional economic growth in China [22,23]. Zhou and Luo [24] analyzed that technological innovation had a delayed positive effect on economic growth. China hopes to stimulate the development of regional economy through the research of technological innovation. Second, there are significant regional differences in technological innovation [25,26]. Through econometric tools, Santana et al. [25] aimed to analyze the link between technological innovation and sustainable development in different countries and regions. The research indicated that technological innovation could produce

different types of impacts according to the analysis of the development stages of different regions. The improvement of technological innovation capability is of great significance to innovation-driven development, innovation ecology, and regional economic synergy.

2.3. Regional Credit, Technological Innovation, and Economic Growth. A region's short-term growth depends on capital accumulation, while its long-term growth depends on technological innovation. A proper allocation of credit funds in a region can easily reduce transaction costs and achieve economies of scale. A well-developed and perfect credit mechanism can facilitate the intertemporal and inter-regional turnover of funds for the real economy, which is conducive to the growth and innovation of regional technologies. Technological innovation is the main driving force of regional economic growth in the new era. The integration of regional credit and technological innovation is a double-edged sword for economic growth.

Firstly, regional credit and technological innovation coordinate and play a synergistic effect to jointly promote regional economic growth. On the one hand, the deep integration of credit resources and technological innovation promotes the emergence and development of new nonbank credit institutions, breaks the monopoly of bank credit funds, and effectively optimizes the credit market system. On the other hand, the deep integration promotes financial innovation and provides diversified financing channels for innovative small and medium-size enterprises (SMES). Simultaneously, it reduces the financing transaction costs of SMES, improves their market profitability, and creates new advantages for regional economic growth. Therefore, the interactive integration of regional credit and technological innovation plays a role in economic growth. For example, Amore et al. [6] believe that the growth of financial credit could accelerate the accumulation of regional capital, enhance the financing capacity of enterprises in the region, and effectively promote the output of technological innovation. Pradhan et al. [23] explore the panel unit root test, panel cointegration test, and vector correction model to study the interaction among financial credit, economic development, and technological innovation of 49 European countries from 1961 to 2014. The results verify that, in the long run, both financial development and innovation are the causative factors of economic growth. Jia et al. [27] believe that innovation is the intermediate variable of financial development promoting economic growth.

Secondly, there are potential risks in the process of integration of regional credit and technological innovation, which will have an inhibitory effect on regional economic growth. On the one hand, the incentive of regional innovation policy makes some innovative enterprises exaggerate the economic effect of enterprises and expand blindly in order to obtain funds. As a result, enterprises fall into a vicious circle of "repaying old debts with new debts," which eventually leads to the bankruptcy of enterprises and increases the nonperforming loan rate of credit institutions. On the other hand, there is serious information asymmetry between credit institutions and innovative enterprises. It is difficult for credit institutions to grasp the core production technology and market competitiveness of enterprises in time and completely. As a result, it is unable to accurately evaluate the business performance and market prospects of enterprises, resulting in the mismatch of credit resources and increasing the potential risk of credit funds. Jiang and Ding [28] considered that the ratio of total financial deposits and loans to the local gross national product (GNP) inhibited the improvement of the quality of economic growth and was not conducive to technological innovation and the increase of economic growth. Zhang [29] used the spatial econometric model of 30 regions of China to study the positive effect of credit funds and technological innovation on regional economic growth, but the interaction between credit funds and technological innovation had no significant effect on economic growth. The prosperity of the technological innovation is a new development paradigm of global economy, while Brown et al. [30] considered that credit markets did not play an important role in funding its development. Also, they found that credit market development was not a major impediment to the expansion of the high-tech sector. Distortions in financial sector lower economic growth by reducing the speed of technological innovation [31,32]. These research studies provide various evidences for the role of regional credit in the process of innovation-driven regional economic growth.

2.4. Summary of the Aforementioned Literature. The aforementioned literature shows a significant gap in the conclusion of previous studies. Compared with the available literature, this paper makes three primary contributions.

Firstly, although regional credit, technological innovation, and economic growth have attracted great attention theoretically and empirically in the existing literature, most of the literature only considers two aspects of them. For example, Önder and Özyildirim [10], Diallo and Al-Titi [11], and Ouyang and Li [15] only explore the relationship between regional credit and economic growth. Santana et al. [25], Pradhan et al. [23], and Zhou and Luo [24] only explore the nexus between technological innovation and economic growth. However, only few researchers have studied the nexus among regional credit, technological innovation, and economic growth, such as Amore et al. [6], Pradhan et al. [23], Jiang and Ding [28], and Brown et al. [30]. This paper considers the impact of regional credit and technological innovation and their integration (coordination) on economic growth of China from the national perspective.

Secondly, although many scholars have analyzed the imbalance and incoordination of regional economic distribution, they seldom introduce spatial factors. Traditional econometric models, such as the ordinary least squares estimation, panel unit root test, panel cointegration test, and vector correction model, ignore the spatial effects and may be considered biased [4]. The spatial effect is the essential characteristic of spatial econometric analysis. Only Zhang [29] and Li and Zhou [32] introduce spatial models, while Zhang [29] does not consider spatial heterogeneity and

dynamic evolution, and Li and Zhou [32] ignore the influence of other factors (institutional factors, open conditions, etc.) other than explanatory variables on the explained variables. This paper establishes static spatial panel models and dynamic spatial panel models by means of transcendental logarithmic production function and analyzes the impact of regional credit and technological innovation on regional economic growth in China. Simultaneously, the Jenks natural breaks method, kernel density function, and Moran index are introduced for spatial statistical analysis.

Thirdly, the spatial weight matrix setting form is limited. The spatial weight matrix is the main tool to abstract spatial and reflect a spatial effect. It is one of the core contents of the spatial econometric model. The setting and optimization of spatial weight matrices have always been the focus of attention. Li and Zhou [32] only constructed the weight matrix based on adjacency and geographical distance, and the spatial dependent structure of reaction variables had limitations. Spatial weight matrices are constructed from the spatial adjacency matrix, geographical distance weight matrix, and innovation capital input weight matrix in this paper.

3. Model Specification and Variables Description

3.1. Model Specification. Most of the existing literature is according to the Cobb–Douglas production function, which regards credit as an input factor. But, in the actual economic system, not only the input factors have an impact on output, but also the interaction of input factors will have an impact on output. Transcendental Logarithmic Production function is a variable substitution elastic production function model, which is generally used to analyze the interaction between input factors [33,34]. This paper establishes a transcendental logarithmic production function model to analyze the impact of regional credit, technological innovation, and their interaction on economic growth.

$$\begin{aligned}\ln \mathrm{GDP}_{it} &= \beta_1 \ln \mathrm{RC}_{it} + \beta_2 \ln \mathrm{RD}_{it} + \beta_3 \ln(\mathrm{RC}_{it}) * \ln(\mathrm{RD}_{it}) \\ &\quad + \gamma \ln X_{it} + \varepsilon_{it},\end{aligned} \tag{1}$$

where GDP denotes the gross domestic product, RC denotes the regional credit, and RD denotes technological innovation. The interaction term, $\ln(\mathrm{RC}) * \ln(\mathrm{RD})$, denotes the influence of the integration of regional credit and technological innovation on economic growth. X denotes other control variables affecting economic growth, $\beta_1, \beta_2, \beta_3, \gamma$ denote the coefficients of each variable, respectively, ε denotes the error perturbation term, i represents a certain region, and t represents a certain year ranging from 2007 to 2017.

The output elasticity of regional credit is as follows:

$$Z = \frac{\partial(\ln \mathrm{GDP}_{it})}{\partial(\ln \mathrm{RC}_{it})} = \beta_1 + \beta_3 \ln(\mathrm{RD}_{it}). \tag{2}$$

The impact of regional credit on economic growth is not only related to the scale and structure of regional credit but also to technological innovation. When $\beta_3 \ln(\mathrm{RD}) > 0$, it says that technological innovation enhanced the impact of regional credit on economic growth. When $\beta_3 \ln(\mathrm{RD}) < 0$, it says that technological innovation restrained the impact of regional credit on economic growth. When $\beta_3 \ln(\mathrm{RD}) = 0$, it says that the impact of regional credit on economic growth had nothing to do with technological innovation.

In addition to regional credit and technological innovation, regional economic growth will be affected by a series of other factors, such as provincial material capital (K_{it}), labor input (L_{it}), and consumption level (C_{it}). By incorporating these control variables into the equation, equation (1) can be transformed into

$$\begin{aligned}\ln \mathrm{GDP}_{it} &= \beta_1 \ln \mathrm{RC}_{it} + \beta_2 \ln \mathrm{RD}_{it} + \beta_3 \ln(\mathrm{RC}_{it}) * \ln(\mathrm{RD}_{it}) + \gamma_1 \ln K_{it} \\ &\quad + \gamma_2 \ln L_{it} + \gamma_3 \ln C_{it} + \varepsilon_{it}.\end{aligned} \tag{3}$$

Equation (3) is a traditional panel model. If the spatial effect of the gross domestic product is taken into consideration, the spatial lag is brought into equation (3) and the static spatial panel model is established. The basic models of static spatial panel models include spatial autoregressive models (SAR) and spatial error models (SEM). Equations (4) and (5) are the SAR and SEM.

$$\begin{aligned}\ln \mathrm{GDP}_{it} &= \rho W(\ln \mathrm{GDP}_{it}) + \beta_1 \ln(\mathrm{RC}_{it}) + \beta_2 \ln(\mathrm{RD}_{it}) \\ &\quad + \beta_3 \ln(\mathrm{RC}_{it}) * \ln(\mathrm{RD}_{it}) \\ &\quad + \gamma_1 \ln K_{it} + \gamma_2 \ln L_{it} + \gamma_3 \ln C_{it} + \varepsilon_{it},\end{aligned} \tag{4}$$

$$\begin{aligned}\ln \mathrm{GDP}_{it} &= \beta_1 \ln \mathrm{RC}_{it} + \beta_2 \ln \mathrm{RD}_{it} + \beta_3 \ln(\mathrm{RC}_{it}) * \ln(\mathrm{RD}_{it}) \\ &\quad + \gamma_1 \ln K_{it} + \gamma_2 \ln L_{it} + \gamma_3 \ln C_{it} + \lambda W \varepsilon_{it} + \mu_{it},\end{aligned} \tag{5}$$

where ρ and λ, reflecting the spatial spillover of gross domestic product, respectively, represent the estimated parameters of spatial lag and spatial error. W is a spatial weight matrix, which reflects the spatial relationships among the various regions. If the dynamic effect and the spatial effect of the gross domestic product are taken into consideration, the first-order lag and spatial lag are brought into equation (3). The dynamic spatial panel models are established as follows:

$$\begin{aligned}\ln \mathrm{GDP}_{it} &= \tau \ln \mathrm{GDP}_{i(t-1)} + \rho W(\ln \mathrm{GDP}_{it}) \\ &\quad + \beta_1 \ln(\mathrm{RC}_{it}) + \beta_2 \ln \mathrm{RD}_{it}(\mathrm{RD}_{it}) \\ &\quad + \beta_3 \ln(\mathrm{RC}_{it}) * \ln(\mathrm{RD}_{it}) \\ &\quad + \gamma_1 \ln K_{it} + \gamma_2 \ln L_{it} \\ &\quad + \gamma_3 \ln C_{it} + \varepsilon_{it}\varepsilon_{it} = \lambda W \varepsilon_{it} + \mu_{it},\end{aligned} \tag{6}$$

where τ denotes the estimated parameter of first-order lag of the gross domestic product, which reflects the impact of the past relevant factors on the current gross domestic product.

3.2. Selection of the Spatial Weight Matrix

3.2.1. Spatial Adjacency Matrix (W1). In order to establish a spatial econometric model, this paper firstly defines the

space distance. The distance here is generalized, and it can be geographic distance or can be other economic sense of the distance. The spatial data of n regions are expressed as $\{x_i\}_{i=1}^n$, where i denotes the region i. w_{ij} denotes the spatial distance between the region i and the region j, and then, the spatial weight matrix W can be defined as

$$W = \begin{bmatrix} w_{11} & \cdots & w_{1n} \\ \vdots & \ddots & \vdots \\ w_{n1} & \cdots & w_{nn} \end{bmatrix}, \tag{7}$$

where $w_{ii} = 0\,(i = 1, \ldots, n)$. Because the distance from region i to region j is the same as that from region j to region i, that is, $w_{ij} = w_{ji}$, the spatial weight matrix W is a symmetric matrix. The most commonly used spatial weight matrix is the adjacency matrix (W_1). Specifically, if regions i and j have a common boundary, the weight is 1; otherwise, it is 0.

3.2.2. Geographical Distance Weight Matrix (W2). In order to enhance the robustness of the results, this paper not only constructs the spatial adjacency matrix (W_1) but also considers the geographical distance weight matrix (W_2) and the innovation capital input weight matrix (W_3). The geographical distance weight matrix (W_2) is constructed by the reciprocal of the spherical distance between provincial capitals. Namely,

$$w_{ij} = \begin{cases} \dfrac{1}{d_{ij}}, & i \neq j, \\ 0, & i = j. \end{cases} \tag{8}$$

In formula (8), d_{ij} is the spherical distance between the provincial capital city of i province and that of j province, indicating that the closer the distance is, the closer the relationship between provinces is. The advantage of this approach is that it takes full account of the actual situation of interaction and interaction between provinces which are close but not adjacent in space.

3.2.3. Innovation Capital Input Weight Matrix (W3). The weight matrix based on spatial adjacency and geographical distance does not reflect the correlation of regional economic characteristics. Lin et al. [35] took the spatial correlation of social and economic characteristics into consideration and constructed the weight matrix of social and economic distance. Substantively, it mainly embodies the ability of transforming the research achievements of technological innovation into technologies and products, and it is the materialized achievement of technological innovation in promoting economic and social development. Naturally, we consider establishing the distance weight matrix (W_3) of innovation capital input. W_3 reflects the correlation between research and experimental development expenditure and geographical distance. Significantly, W_3 is beneficial to the robustness test of the results. The specific formula is as follows:

$$W_3 = W_1 \mathrm{diag}\left(\frac{\overline{T}_1}{\overline{T}}, \frac{\overline{T}_2}{\overline{T}}, \frac{\overline{T}_3}{\overline{T}}, \ldots, \frac{\overline{T}_n}{\overline{T}}\right), \tag{9}$$

where $\overline{T}_i = (1/(t_1 - t_0 + 1)) \sum_{t=t_0}^{t_1} T_{it}$ represents the average expenditure on research and experimental development (R&D) in Province i during the investigation period. $\overline{T} = (1/(n(t_1 - t_0 + 1))) \sum_{i=1}^{n} \sum_{t=t_0}^{t_1} T_{it}$ represents the average expenditure on total research and experimental development (R&D) during the investigation period, and t is in different periods.

3.3. Variables Description

3.3.1. Explained Variable: Economic Growth (GDP). In empirical analysis, there are generally two methods to measure regional economic growth. Firstly, the GDP of each region is adopted and converted into the real GDP expressed in terms of the base year constant price by the GDP index. Second is GDP per capita. GDP per capita can only approximate regional economic development. If regional growth is to be properly measured, the most direct measure is the real GDP at constant prices. Therefore, this paper uses the real GDP, expressed in constant prices on the basis of 2007, to reflect regional economic growth. Data source: China Statistical Yearbook (2007–2017).

3.3.2. Core Explanatory Variables. Regional credit (RC): in previous studies, credit supply is considered as an important financial service to promote economic growth and is often used as an important indicator of credit. Credit supply is the main source of enterprise financing, which can measure the important role of financial credit in economic growth. Because of considering the availability and validity of the data, the balance of credit funds of financial institutions is used to reflect regional credit development. Data sources: the Statistical Yearbook of each province, Statistical Bulletin of National Economic and Social Development of each province, and Regional Financial Operation Report of the People's Bank of China.

Technological innovation (RD): as for the measurement index of technological innovation, the research literature mainly selects the input index and output index of technological innovation. In practice, there is great uncertainty from R&D input to output. The patent data can reflect the application value of technological innovation and the provincial technological innovation information, so most literature adopts the number of patents granted as the measurement index of the technological innovation output, such as [6]. Following the general practice, this paper adopts the number of patents granted in each province as the measurement index of technological innovation in the province. Data source: China Statistical Yearbook (2007–2017).

3.3.3. Control Variables. According to economic theory and the availability and validity of data, the control variables are as follows: provincial capital investment (K) is expressed by

total investment in fixed assets in the whole country, labor input (L) is expressed by the number of employed persons in urban units, and consumption level (C) is expressed by total retail sales of regional social consumer goods. In order to reduce the influence of heteroscedasticity on the model, we take the logarithmic form of all variables to be dimensionless. Table 1 shows descriptive statistics of all the variables used. All variables have good statistical characteristics.

4. Spatial Feature Analysis

This section firstly describes geospatial distribution characteristics of regional credit, technological innovation, and economic growth from a macro perspective. Secondly, the kernel density function is used to reflect the dynamic evolution trend of regional credit, technology innovation, and economic growth. Finally, the Moran index and LISA are adopted to depict whether the spatial agglomeration phenomenon exists in the regional credit, technological innovation, and economic growth in Chinese provinces.

4.1. Geospatial Characteristics Analysis. The Jenks natural breaks classification is designed to place variable values into naturally occurring data categories [36]. We utilize the Jenks natural breaks method to distinguish logical breakpoints in economic datasets by grouping similar values of "minimizing differences in the sum of squares within a class and maximizing differences in the sum of squares between groups" [36,37]. We employ GeoDa to yield the geospatial distribution characteristics of regional credit, technological innovation, and economic growth of Chinese 31 provinces. The 31 provinces are itemized according to the Jenks natural breaks algorithm [38,39], which is shown in Figures 2–4. Different colors indicate different levels of geospatial distribution. As the color deepens, the level of development of regional credit, technological innovation, and economic growth increases gradually. If the classification value is superior to the average value, the development level of the region will have a spillover effect. Conversely, if the value is less than the average, the development level of this region has a weak impact on the development of neighboring provinces.

(1) Figure 2 shows the geospatial distribution of regional economic growth. As can be seen, the regions with high economic growth are mainly concentrated in the eastern and central regions of China. The lower economic growth is concentrated in northwest China. Also, this concentration is continuously changing in a ladder form from west to east, which shows that the economic growth of neighboring provinces influences each other. Furthermore, this proves the existence of the spatial spillover effect of economic growth.

(2) Figure 3 shows the geographic spatial distribution of regional credit. Clearly, the areas with large credit supply are mainly concentrated in the southeast coastal areas of China, where the economy is relatively developed, forming a financial cluster. In addition, Sichuan, Henan, and Hubei have higher credit level, but no obvious agglomeration area.

(3) Figure 4 shows the geospatial distribution of technological innovation levels. It can be seen that Shandong, Jiangsu, Shanghai, Zhejiang, Fujian, and Guangdong have higher technological innovation levels. The lower technological innovation levels are concentrated in the western and northern parts of China.

4.2. Spatiotemporal Dynamic Evolution. For the spatial heterogeneity feature measure, the existing literature usually uses the kernel density estimation method, Dagum Gini coefficient, Theil index, and coefficient of variation. Although the calculation methods and processes are different, the conclusions are not much different. The kernel density estimation method is the most popular method now. The main idea of kernel density estimation is to reflect its evolution trend by dynamic changes of specific graphical features such as kurtosis, skewness, and symmetry in the index distribution map. On the basis of the practice of Jiang et al. [40], Ma et al. [41], Yang et al. [42], and Zhao [43], taking 2007, 2009, 2011, 2013, 2015, and 2017 as measuring time points, this paper adopted the kernel density estimation method to comprehensively depict the spatial distribution characteristics and spatiotemporal dynamic evolution of regional credit, technology innovation, and economic growth. By comparing the kernel density estimation curves (Figures 5–7), we come to the following conclusion:

(1) The overall economic growth level of China's provinces has grown steadily. During the inspection period, the center of the distribution curve of real GDP logarithm showed a trend of gradually shifting to the right, indicating that China's provincial economic growth level is gradually increasing. This feature is consistent with the overall description. The peak value of the main peak increases gradually, and the width of the main peak shows a weak trend of narrowing, indicating that the gap of economic growth between provinces in China tends to be narrow. The density distribution curve always has a trailing phenomenon, and its distribution tends to extend to the right, indicating that the provinces with higher economic growth show an upward trend, and some provinces have a lower level of economic growth. From the shape of the curve, the unipolarization phenomenon of the distribution is obvious, and its peak value first increases and, then, decreases, but the decrease range is small, indicating that the economic growth level of each province is advancing smoothly as a whole.

(2) The spatial distribution of credit levels in various provinces in China tends to converge. During the inspection period, the center of the density distribution curve of the credit funds of 31 provincial financial institutions gradually shifted to the right, indicating that the overall credit level of China's

Table 1: Statistical description of variables.

Variables	Mean	Std. dev.	Min	Max
Economic growth (lnGDP)	9.289	1.051	5.833	11.293
Regional credit (lnRC)	9.568	1.104	5.390	11.886
Technological innovation (lnRD)	9.371	1.713	4.220	13.078
Intersection of regional credit and technological innovation (lnRC ∗ lnRD)	91.470	25.501	22.831	155.435
Capital investment of provinces (lnK)	9.068	1.019	5.600	10.959
Labor input (lnL)	5.907	0.926	2.178	7.947
Consumption level (lnC)	8.423	1.145	4.724	10.584

Data source: China Statistical Yearbook.

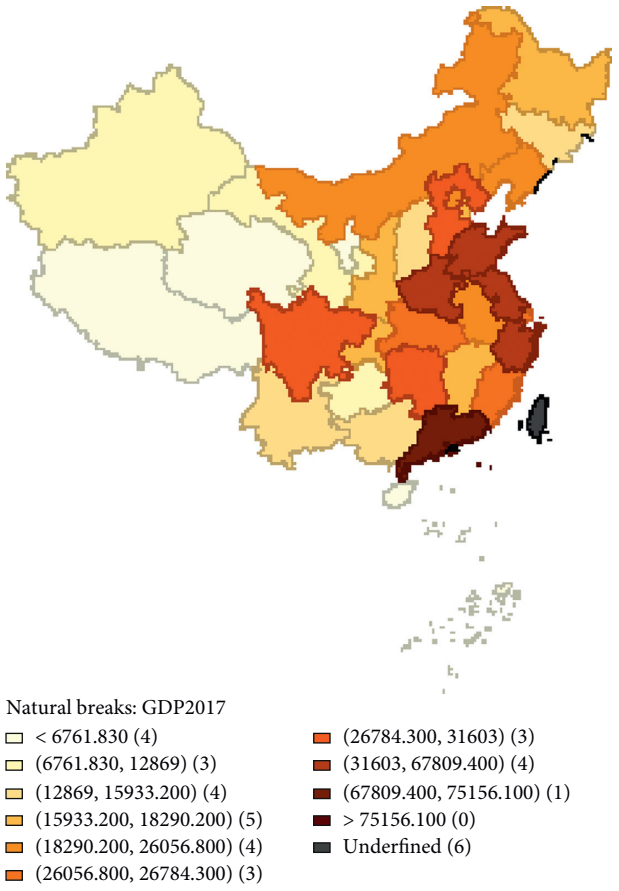

Figure 2: Geospatial distribution of economic growth in Chinese 31 provinces in 2017.

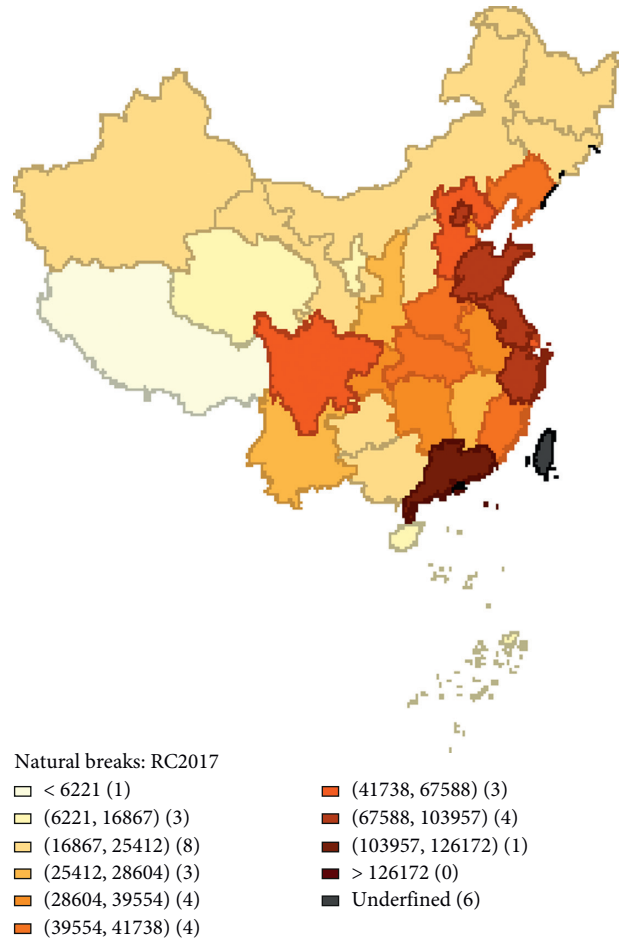

Figure 3: Geospatial distribution of regional credit in Chinese 31 provinces in 2017.

provinces showed a gradual upward trend. The main peak of the distribution curve showed a significant upward trend, and the main peak width decreased year by year. It shows that the absolute gap of credit levels in various provinces is shrinking. The distribution curve shows a tailing phenomenon to the left, and its distribution ductility tends to converge from broadening, indicating that the provinces with high credit levels are on the rise and the gap with the average level is shrinking year by year. The ductility gap has been shrinking year by year. The single polarization phenomenon of distribution has always existed, and its peak value rises stepwise, indicating that the polarization phenomenon of provincial credit level is gradually alleviated and controlled over time.

(3) China's provincial technological innovation capability has shown an overall upward trend year by year. During the inspection period, the center of the density distribution curve of the 31 provincial patent application grants gradually shifted to the right, indicating that the technological innovation capability of China's provinces showed an upward trend. The distribution curve had a tailing phenomenon, and the distribution curve always had a single polarization phenomenon. The peak value of the main

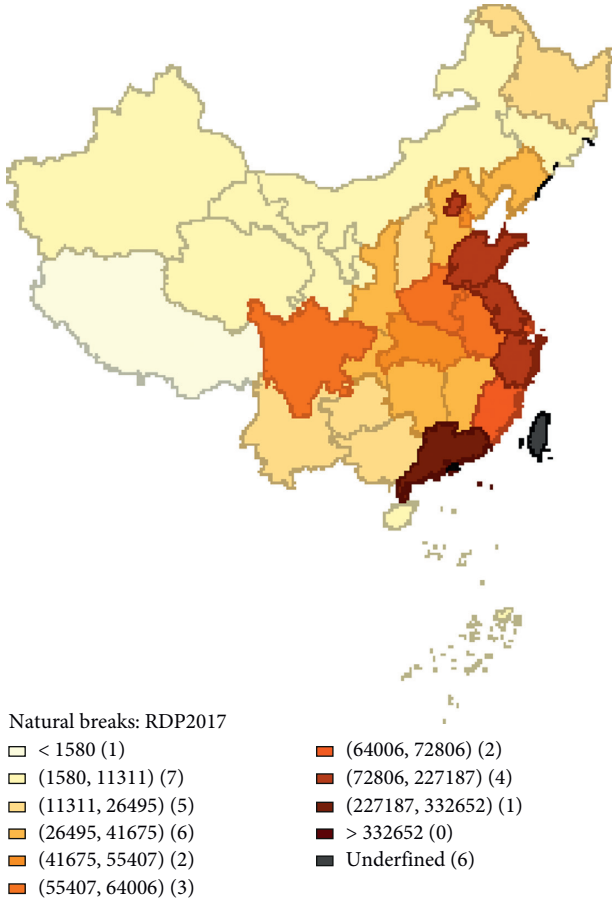

Figure 4: Geospatial distribution of technological innovation in Chinese 31 provinces in 2017.

peak first rises and then rises, and the width of the main peak does not change much, indicating that the technical innovation ability of each province has progressed smoothly.

4.3. Spatial Autocorrelation Analysis. Spatial heterogeneity (spatial structure) mainly examines the spatial imbalance of regional credit, technological innovation, and economic growth, while spatial autocorrelation (spatial interaction) mainly reflects the spatial agglomeration effect of regional credit, technological innovation, and economic growth. If the spatial characteristics of the data are strongly influenced by the observation location, the adjacent spatial units interact with each other, and the adjacent areas tend to have more similarities than the remote areas. The Moran index (*Moran's I*) [44] is the most popular method for estimating spatial autocorrelation in the literature.

4.3.1. Global Spatial Autocorrelation Analysis. For the purpose of testing the spatial correlation of economic growth, regional credit, and technological innovation, this paper uses the spatial adjacent weight matrix and global *Moran's I* to estimate. From Table 2, we find that *Moran's I* of economic

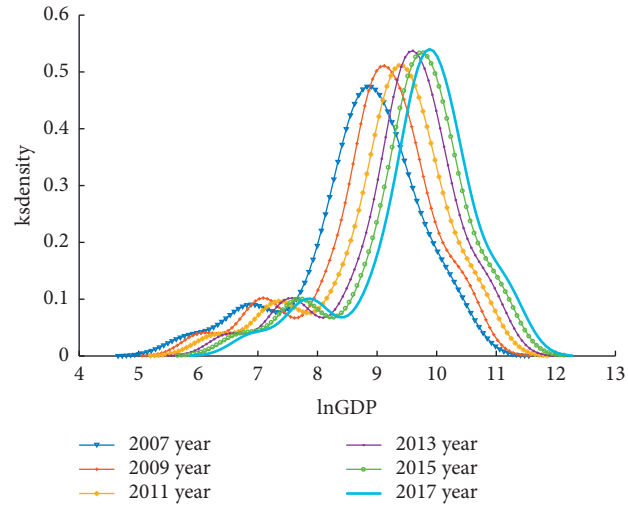

Figure 5: Kernel density distribution of 31 provincial lnGDP.

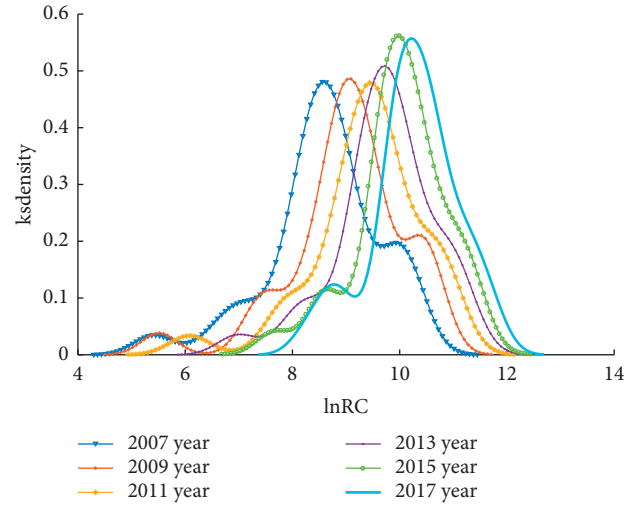

Figure 6: Kernel density distribution of 31 provincial lnRC.

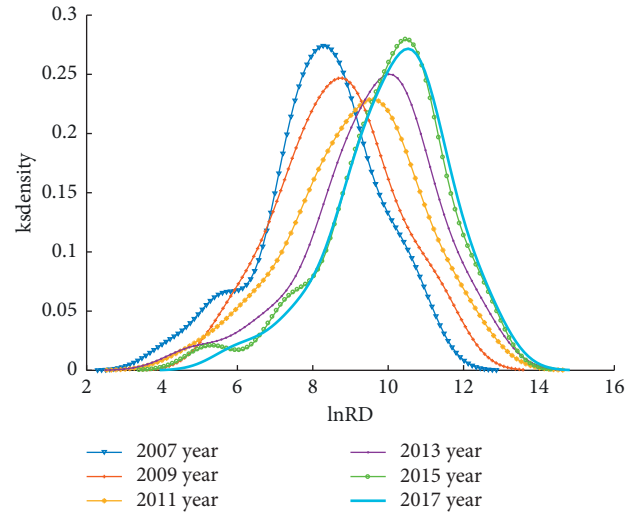

Figure 7: Kernel density distribution of 31 provincial lnRD.

Table 2: Global *Moran's I* in China from 2007 to 2017.

Year	2007	2008	2009	2010	2011	2012	2013	2014	2015	2016	2017
lnGDP	0.359***	0.358***	0.367***	0.362***	0.357***	0.350***	0.346***	0.346***	0.361***	0.378***	0.371***
lnRC	0.384***	0.380***	0.349***	0.350***	0.347***	0.353***	0.356***	0.353***	0.348***	0.367***	0.388***
lnRD	0.349***	0.362***	0.396***	0.397***	0.422***	0.415***	0.402***	0.420***	0.411***	0.430***	0.439***

***, **, and *denote statistical significance levels at 1%, 5%, and 10%, respectively.

growth in 2007–2017 is concentrated in 0.346–0.378 and passed the significance level test of 1%. In 2016, *Moran's I* of economic growth reached its highest value of 0.378. It shows that the economic growth of 31 provinces in China is not randomly distributed in space, but has positive autocorrelation in space and presents strong spatial agglomeration in geographical space. From 2007 to 2017, *Moran's I* of regional credit concentrated between 0.347 and 0.388 and passed the significance test under 1% level. It shows that a positive spatial autocorrelation exists in the credit of the provinces and regions. From 2007 to 2017, *Moran's I* of technological innovation concentrated between 0.349 and 0.464, and all of them passed the significance test at the level of 1%. The lowest *Moran's I* was 0.349 in 2007 and the highest was 0.464 in 2017. The results show that there is a strong positive autocorrelation in the space of technological innovation in 31 provinces in China, and the trend is strengthening year by year. Compared with economic growth and regional credit, technological innovation has the strongest positive spatial autocorrelation and shows stronger spatial agglomeration characteristics in geographic space.

By comparing *Moran's I* of the economic growth, regional credit, and technological innovation, we find that they have similar spatial agglomeration characteristics. That is to say, the provinces with the high *Moran's I* value are close to the provinces with high index value, and the provinces with low *Moran's I* value are close to the provinces with low index value. This agglomeration indirectly reflects the imbalance of economic growth, regional credit, and technological innovation in China's provinces. In addition, this paper also finds that there are certain correlations and similarities among the three trends of economic growth, regional credit, and technological innovation.

4.3.2. Local Spatial Autocorrelation Analysis. In order to further analyze the local agglomeration characteristics of economic growth, regional credit, and technological innovation in different provinces of China, this paper took the year of 2017 as an example and undertook a local indicator of spatial association (LISA) analysis [45]. The LISA agglomeration maps allowed us to explore the local spatial autocorrelation (Figures 8–10). Local *Moran's I* scatter plots were divided into four quadrants. The positive spatial correlation is distributed in the first and third quadrants, while the negative spatial correlation is distributed in the second and fourth quadrants.

From Figure 8, we can see that the high-high agglomeration, are mostly distributed in Shandong, Jiangsu, Shanghai, Anhui, and Fujian of eastern coastal areas of China. The provinces with low-low agglomeration are Xinjiang, Tibet, Qinghai, and Gansu provinces of northwest China. As can be seen from *Moran's I* scatter plots, the provinces in quadrants 1 and 3 account for the majority, which reflects that the level of technological innovation in China shows a strong positive spatial correlation. The differentiation of "high-high" and "low-low" basically conforms to the spatial pattern of China's economic development from east to west. It fully demonstrates that China's economy has obvious spatial autocorrelation and spatial heterogeneity in geographical spatial distribution. The spatial distribution of regional credit and technological innovation is similar to that of economic growth (Figures 9 and 10).

5. Spatial Econometric Analysis

5.1. Model Recognition. Traditional econometric models do not involve such spatial effects, and the estimates are biased. Upon the abovementioned analysis, we find that there are spatial autocorrelation among regional credit, technological innovation, and economic growth. This means that the geographic distance and spatial effect are both significant factors affecting regional economic growth.

According to the model discriminant criteria of Anselin et al. [46], the SLM model and the SEM model are tested by the Lagrange multiplier (LM). LM (error) and Robust-LM (error) are used to test the spatial correlation of the residual, while LM (lag) and Robust-LM (lag) are used to test the spatial lag of the model. Table 3 shows the results. The values of LM (lag) and Robust-LM (lag) were 9.886 and 9.804, respectively, and were significant; the values of LM (error) and Robust-LM (error) were 0.105 and 0.023, respectively, and were not significant. It shows that the SAR model is better than the SEM model.

Furthermore, the Hausman test shows that the Hausman statistic is 183.65 and has passed the significance test of 1%, indicating that the spatial fixed effect model is more applicable. In general, the fixed effect model works better when the subject is a specific individual. Compared with the random effect model, Lee and Yu [47] believe that the fixed effect model is more robust and simpler in calculation. According to the different control of space and time effect, the model of the spatial fixed effect can be divided into the time fixed effect, space fixed effect, mixed effect (that is, no space fixed effect and no time fixed effect), and both fixed effect. This paper also estimates the four spatial econometric models and finds that the model fits better under the dual fixed effect of space and time. In fact, there are obvious regional differences in China's economic growth. Mixed effects and time effects ignore these differences. Spatial both fixed effects take into account both temporal and regional impacts and also distinguish spatial correlation from spatial heterogeneity and missing variables [48]. Therefore, both

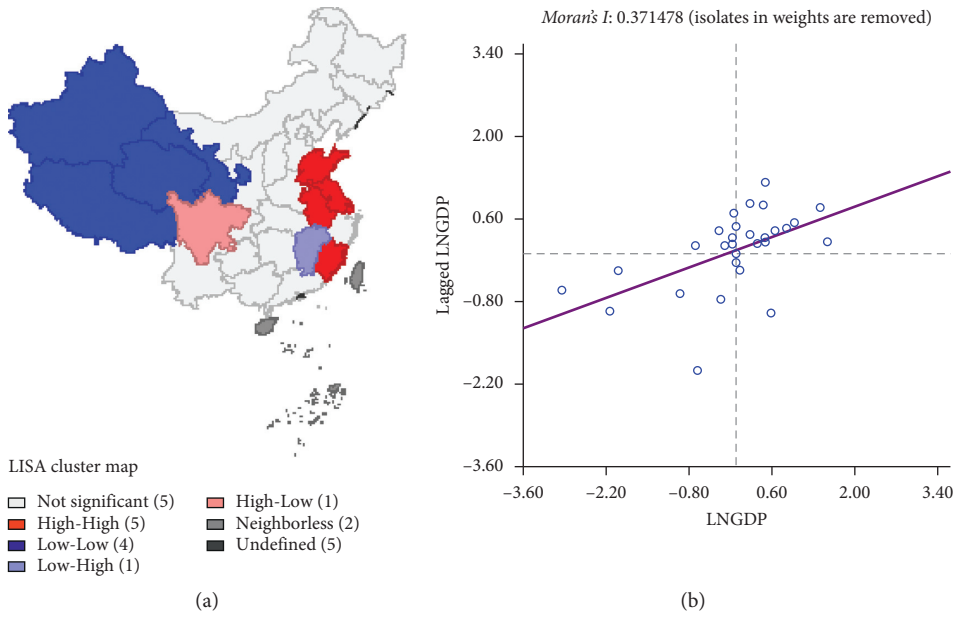

Figure 8: LISA agglomeration map and *Moran's I* scatter plot of economic growth in 2017.

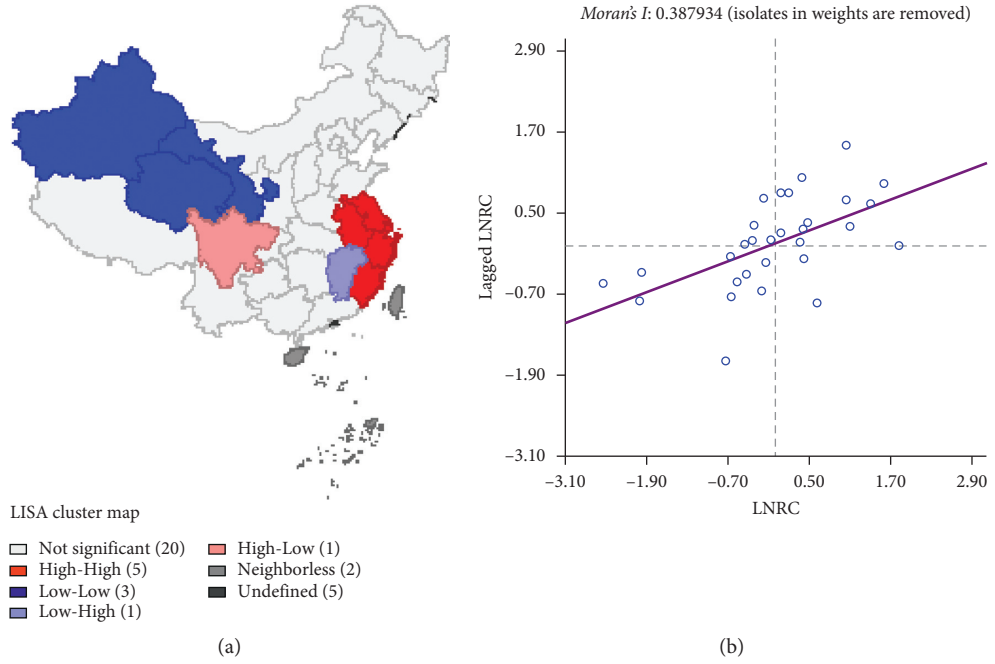

Figure 9: LISA agglomeration map and *Moran's I* scatter plot of regional credit in 2017.

fixed effects can more accurately reflect the actual situation of regional economic growth. Therefore, the both fixed effect model of SAR is adopted in this paper.

5.2. Estimation Results Analysis. To enhance the validity and robustness of spatial models, we simultaneously employ three kinds of weight matrices to estimate the static SAR models. The regression results are shown in the models (1), (2), and (3) in Table 4. The spatial weight matrices in static spatial panel model (1), (2), and (3) are the spatial adjacency matrix (W_1), spherical distance weight matrix (W_2), and innovation capital input weight matrix (W_3). The spatial correlation coefficient of model (1) is 0.229, which is significant at 1%, higher than that of model (2) and model (3). It shows that the economic growth of adjacent provinces affects each other, but that of nonadjacent provinces is not strong. According to the adjusted statistics of R^2, Sigma^2,

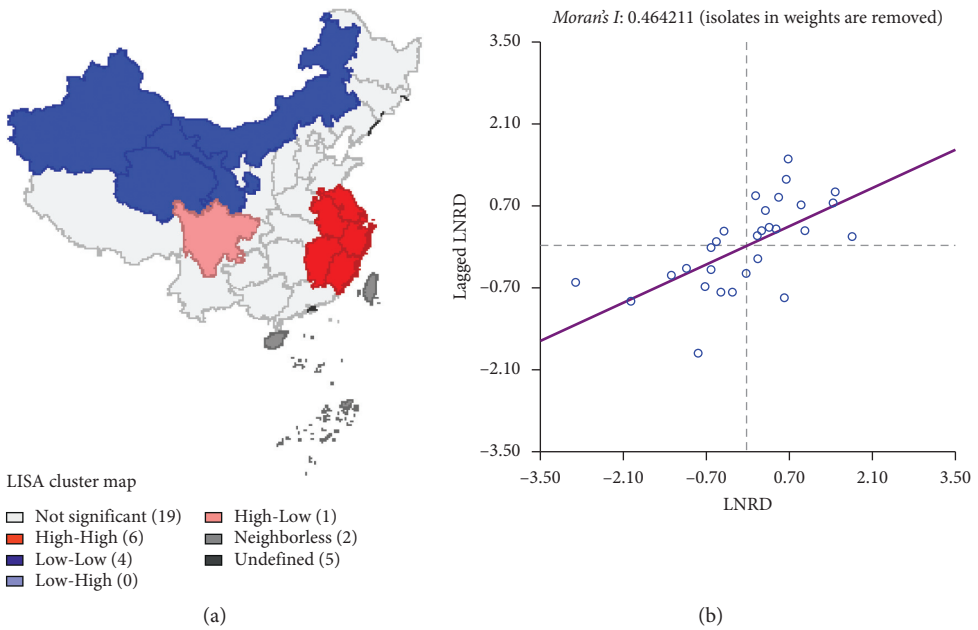

Figure 10: LISA agglomeration map and *Moran's I* scatter plot of technological innovation in 2017.

Table 3: The results of the LM test.

Test	Statistic
Lagrange multiplier (error)	0.105
Robust Lagrange multiplier (error)	0.023
Lagrange multiplier (lag)	9.886***
Robust Lagrange multiplier (lag)	9.804***

***, **, and *denote statistical significance levels at 1%, 5%, and 10%, respectively.

and Log-L, the models (1), (2), and (3) have goodness of fit. From the estimation results of explanatory variable coefficients in the model, there is little difference among explanatory variable coefficients and the significance test.

The static spatial panel model ignores the influence of other factors (institutional factors and open conditions) other than explanatory variables on the explained variables. Therefore, this paper uses the first-order lag of regional economic growth to represent other potential influencing factors of regional economic growth and establishes a dynamic spatial econometric model of SAR. The models (4), (5), and (6) in Table 4 give the estimation results of the dynamic spatial panel model established based on the weight matrices W_1, W_2, W_3. It can be seen from Table 4 that, in the dynamic spatial panel model, the spatial correlation coefficients of the three models are 0.001, 0.379, and 0.001, respectively, and all of them are significant at the level of 5%. The spatial correlation coefficient of spatial model (4) is lower than that of the static panel. The spatial correlation coefficients of dynamic model (5) and (6) are significantly positive, which is not consistent with the estimation of the spatial correlation in the static model. Compared with the spatial correlation coefficient of model (4) and model (5), the spatial correlation coefficient of model (6) is relatively higher, which explains to some extent that the economic growth of one region depends on other regions, not only because of the adjacent and adjacent geographical locations of the two regions. In the dynamic space panel, expressed in the dependent variable of first-order lag other potential factors and other potential factors impact on regional economic growth from the separated space structure factors, spatial correlation changed, regional economic growth as a dynamic, continuous economic system, and the potential factors of its influence is very important. Therefore, it is necessary to establish a dynamic spatial panel model. The regression coefficients of dynamic factors in models (4), (5), and (6) are, respectively, 0.897, 0.879, and 0.897, which are all significant at the level of 1%, further verifying the positive influence of other factors on regional economic growth.

In the dynamic spatial panel model, Sargan statistic, Log-L, and other statistics all have good fitness. From the estimation results of explanatory variable coefficients in the model, the estimation results of model (6) have passed the significance test, which is obviously superior to the estimation results of other models. Therefore, this paper chooses the estimation results of model (6) for discussion. The regional credit regression coefficient is 0.011, and the technological innovation regression coefficient is 0.052, which is significant at the level of 1%. That is to say, if the provincial credit level and technological innovation increase by one unit, the provincial economic growth level will increase by 1.1% and 5.2%, respectively. Therefore, the regional credit level and technological innovation have significant positive effects on provincial economic growth. In the recent years, with the gradual rise of China's financial market, the market system is becoming increasingly sound, the scale is expanding, the structure is becoming more reasonable, and the role of financial credit level in promoting economic growth is becoming increasingly obvious. People's

Table 4: Regression results of SAR.

Type	Static spatial panel model			Dynamic spatial panel model		
	Model (1)	Model (2)	Model (3)	Model (4)	Model (5)	Model (6)
lnRC	0.024**	0.022**	0.022**	0.005	0.001	0.011***
lnRD	0.026	0.028	0.027	0.053***	0.046***	0.052***
lnRC × lnRD	−0.001	−0.001	−0.001	−0.004***	−0.004***	−0.005***
lnK	0.061***	0.073***	0.069***	0.001*	0.008**	0.006**
lnL	0.074***	0.071***	0.070**	0.073***	0.057***	0.065**
lnC	0.347***	0.416***	0.400***	0.029**	0.062***	0.032***
T (dynamic factors)				0.897***	0.879***	0.897***
ρ (spatial factors)	0.229***	−0.540	−0.092	0.001**	0.379***	0.001***
Cons				0.157***	0.144***	0.125***
$Sigma^2$	0.001***	0.001***	0.001***			
Adj-R^2	0.898	0.981	0.993			
Obs.	341	341	341	310	310	310
Log-L	719.601	742.055	736.742	871.341	886.382	884.562
Sargan statistic				777.308***	761.571***	776.856***

***, **, and *denote statistical significance levels at 1%, 5%, and 10%, respectively. This paper makes a comparative analysis of the spatial models with "lnRC × lnRD" and without "lnRC × lnRD" and finds that the estimation results of models are robust. Limited to the length of the paper, the experimental results are omitted. Interested readers can obtain it from the authors.

understanding of technological innovation is deepening gradually, R&D funds are increasing everywhere, patent authorization is increasing day by day, and the level of technological innovation plays an increasingly important role in stimulating the economy.

The intersection of regional credit and technological innovation (lnRC ∗ lnRD) is −0.005 at the level of 1%. That is to say, the interaction between regional credit and technological innovation will reduce regional economic growth by 0.5% for each additional unit. This shows that, in the process of development, financial credit has a significant delayed effect on the support of technological innovation and inhibits the current economic growth. On the one hand, under the incentive of regional innovation policies, some innovation-oriented enterprises exaggerate their economic effects and implement blind expansion in order to raise funds. This will lead enterprises into a vicious circle of "borrowing new debt to repay old debt," which will eventually lead to the bankruptcy of enterprises and increase the nonperforming loan ratio of credit institutions. On the other hand, due to the serious information asymmetry between credit institutions and innovative enterprises, it is difficult for credit institutions to grasp the core production technology and market competitiveness of enterprises in a timely and complete manner. As a result, credit institutions are unable to accurately assess the business performance and market prospects of enterprises, leading to the mismatch of credit resources, thus increasing the potential risk of credit funds. In a word, the integration degree of financial credit to technological innovation in China is not enough. There are still many problems in technological finance to the economic growth of provinces.

In terms of control variables, the capital investment, labor input, and consumption level of every province are significantly positive in six models, which shows that the material capital, labor input, and consumption level of every province have a significant positive effect on provincial economic growth during the survey period. The higher the consumption level of each province, the stronger the consumption capacity of the province and the faster the economic growth. Capital investment and labor input are one of the important input factors of regional economic growth. The amount of capital investment and labor input directly affects the production of economic sectors. Speeding up the construction of regional human capital and education level plays an important role in regional economic growth.

6. Conclusions

Using panel data of 31 provinces in China from 2007 to 2017, this paper establishes static spatial panel models and dynamic spatial panel models based on transcendental logarithmic production function and empirically analyses the impact of regional credit and technological innovation on regional economic growth in China. The kernel density function and Moran index are introduced for spatial statistical analysis. Spatial weight matrices are constructed from two aspects of geographical characteristics and innovative capital input characteristics. Through spatial statistical analysis and spatial econometric analysis, the following conclusions are drawn: (1) There are spatial heterogeneity and spatial correlation in economic growth, regional credit, and technological innovation of China's provinces and regions. When studying the impact of regional credit and technological innovation on economic growth, we should not neglect the influence of geographical factors and spatial effects. (2) Regional credit and technological innovation have significant positive effects on provincial economic growth. (3) Regional credit has a significant delayed effect on the support of technological innovation and inhibits regional economic growth. In the process of increasing the level of financial credit and technological innovation, they lack more and deeper integration and interaction. Regional credit and technological innovation have not yet achieved coordinated development.

Based on the abovementioned conclusions, this paper provides policy recommendations for China heading for a sustainable economic growth. (1) China government departments should strengthen the free flow of credit between regions, which is conducive to the rational and optimal allocation of financial credit funds in multilevel regions. Accelerating the strategic layout of the multilevel regional financial credit center and regional credit cooperation is conducive to the integration of financial credit market and promoting the long-term stable growth of regional economy. (2) For regions with better economic development, the Chinese government has relaxed financial control, which is conducive to the integration of financial credit capital into technological innovation and the reduction of financing costs for technological innovation of enterprises. This is the institutional guarantee for innovative enterprises to build a sound financial environment. (3) Exploring the integration mode of technological innovation and regional credit is beneficial to improving the depth and breadth of technological innovation and financial credit integration and realizing the coordinated development of technological innovation and regional credit.

Data Availability

The data used to support the findings of this study are available from the corresponding author upon request.

Conflicts of Interest

The authors declare that there are no conflicts of interest regarding the publication of this paper.

Acknowledgments

This research was funded by the National Social Science Foundation of China (17BGL083).

References

[1] A. Hanley, W.-H. Liu, and A. Vaona, "Credit depth, government intervention and innovation in China: evidence from the provincial data," *Eurasian Business Review*, vol. 5, no. 1, pp. 73–98, 2015.

[2] F. Xin, J. Zhang, and W. Zheng, "Does credit market impede innovation? Based on the banking structure analysis," *International Review of Economics & Finance*, vol. 52, pp. 268–288, 2017.

[3] B. M. Eren, N. Taspinar, and K. K. Gokmenoglu, "The impact of financial development and economic growth on renewable energy consumption: empirical analysis of India," *Science of The Total Environment*, vol. 663, pp. 189–197, 2019.

[4] H. Zhou, S. Qu, Z. Wu, and Y. Ji, "A study of environmental regulation, technological innovation, and energy consumption in China based on spatial econometric models and panel threshold models," *Environmental Science and Pollution Research*, vol. 27, pp. 37894–37910, 2020.

[5] V. Acharya and Z. Xu, "Financial dependence and innovation: the case of public versus private firms," *Journal of Financial Economics*, vol. 124, pp. 223–243, 2017.

[6] M. D. Amore, C. Schneider, and A. Žaldokas, "Credit supply and corporate innovation," *Journal of Financial Economics*, vol. 109, no. 3, pp. 835–855, 2013.

[7] R. G. King and R. Levine, "Finance and growth: schumpeter might be right," *The Quarterly Journal of Economics*, vol. 108, no. 3, pp. 717–737, 1993a.

[8] H. Zhou, S. Qu, Q Yuan, and S Wang, "Spatial Effects and Nonlinear Analysis of Energy Consumption, Financial Development, and Economic Growth in China," *Energies*, vol. 13, no. 18, pp. 1–18, 2020.

[9] R. Levine, N. Loayza, and T. Beck, "Financial intermediation and growth: causality and causes," *Journal of Monetary Economics*, vol. 46, no. 1, pp. 31–77, 2000.

[10] Z. Önder and S. Özyıldırım, "Role of bank credit on local growth: do politics and crisis matter?" *Journal of Financial Stability*, vol. 9, no. 1, pp. 13–25, 2013.

[11] B. Diallo and O. Al-Titi, "Local growth and access to credit: theory and evidence," *Journal of Macroeconomics*, vol. 54, pp. 410–423, 2017.

[12] J. Andres, I. Hernando, and J. D. Lopez-Salido, "The role of the finance system in the growth-inflation link: the OECD experience," *European Journal of Political Economy*, vol. 20, pp. 941–961, 2004.

[13] J. Zhang, *Why China's Credit Increasing Contributes Little To Economic Growth*, Academic Monthly, no. 7, pp. 69–75, Bijing, China, 2006.

[14] S. Sassi and A. Gasmi, "The effect of enterprise and household credit on economic growth: new evidence from European Union countries," *Journal of Macroeconomics*, vol. 39, pp. 226–231, 2014.

[15] Y. Ouyang and P. Li, "On the nexus of financial development, economic growth, and energy consumption in China: new perspective from a GMM panel VAR approach," *Energy Economics*, vol. 71, pp. 238–252, 2018.

[16] A. V. Guender, "Credit prices vs. credit quantities as predictors of economic activity in Europe: which tell a better story?" *Journal of Macroeconomics*, vol. 57, pp. 380–399, 2018.

[17] S. Mousavi and B. A. Bossink, "Firms' capabilities for sustainable innovation: the case of biofuel for aviation," *Journal of Cleaner Production*, vol. 167, pp. 1263–1275, 2017.

[18] W. Jin, H.-q. Zhang, S.-s. Liu, and H.-b. Zhang, "Technological innovation, environmental regulation, and green total factor efficiency of industrial water resources," *Journal of Cleaner Production*, vol. 211, pp. 61–69, 2019.

[19] E. Rosca, M. Arnold, and J. C. Bendul, "Business models for sustainable innovation-an empirical analysis of frugal products and services," *Journal of Cleaner Production*, vol. 162, pp. S133–S145, 2017.

[20] N. Bloom, M. A. Schankerman, and J. Van Reenen, "Identifying technology spillovers and product market rivalry," *Econometrica*, vol. 7, pp. 1347–1393, 2013.

[21] M. Irandoust, "The renewable energy-growth nexus with carbon emissions and technological innovation: evidence from the Nordic countries," *Ecological Indicators*, vol. 69, pp. 118–125, 2016.

[22] M. W. Zafar, M. Shahbaz, F. Hou, and A. Sinha, "From nonrenewable to renewable energy and its impact on economic growth: the role of research & development expenditures in Asia-Pacific Economic Cooperation countries," *Journal of Cleaner Production*, vol. 212, pp. 1166–1178, 2019.

[23] R. P. Pradhan, M. B. Arvin, and S. Bahmani, "Are innovation and financial development causative factors in economic growth? Evidence from a panel granger causality test,"

Technological Forecasting and Social Change, vol. 132, pp. 130–142, 2018.

[24] G. Zhou and S. Luo, "Higher education input, technological innovation, and economic growth in China," *Sustainability*, vol. 10, pp. 2–15, 2018.

[25] N. B. Santana, D. Rebelatto, A. Périco, F. Herick, and W. Filho, "Technological innovation for sustainable development: an analysis of different types of impacts for countries in the BRICS and G7 groups," *International Journal of Sustainable Development & World Ecology*, vol. 22, no. 5, pp. 1–12, 2015.

[26] D. J. Teece, "Profiting from innovation in the digital economy: enabling technologies, standards, and licensing models in the wireless world," *Research Policy*, vol. 47, no. 8, pp. 1367–1387, 2018.

[27] J. Jia, X. Lun, and S. Lin, "Financial development, corporation innovation and economic growth: empirical analysis from the patent perspective," *Journal of Financial Research*, vol. 1, pp. 99–113, 2017.

[28] Q. Jiang and Q. Ding, "Financial development, technological innovation and regional economic development——based on both quantity and quality of economic growth in Shandong province," *Review of Economy and Management*, vol. 32, no. 2, pp. 145–153, 2016.

[29] L. Zhang, "Financial development, technological innovation and real economic growth-an empirical study based on spatial econometrics," *Journal of Finance and Economics*, vol. 31, no. 1, pp. 14–25, 2016.

[30] J. R. Brown, G. Martinsson, and B. C. Petersen, "Stock markets, credit markets, and technology-led growth," *Journal of Financial Intermediation*, vol. 32, no. 8, pp. 45–59, 2017.

[31] R. G. King and R. Levine, "Finance, entrepreneurship and growth," *Journal of Monetary Economics*, vol. 32, no. 3, pp. 513–542, 1993.

[32] Y. Li and H. Zhou, "Empirical analysis on the impact of regional credit and technological innovation on economic growth: based on the spatial panel perspective," *On Economic Problems*, vol. 11, pp. 26–35, 2018.

[33] L. R. Christensen and D. W. Jorgenson, "Transcendental logarithmic production frontiers," *The Review of Economics and Statistics*, vol. 55, no. 1, pp. 28–45, 1973.

[34] L. R. Lau and J. L. J. Lau, "Transcendental logarithmic utility functions," *The American Economic Review*, vol. 65, no. 3, pp. 367–383, 1975.

[35] G. Lin, Z. Long, and M. Wu, "A spatial analysis of regional economic convergence in China: 1978–2002," *China Economic Quarterly*, vol. 4, no. S1, pp. 67–82, 2005.

[36] G. F. Jenks, "The data model concept in statistical mapping," *International Yearbook of Cartography*, vol. 7, pp. 186–190, 1967.

[37] T. A. Slocum, R. B. McMaster, F. C. Kessler, and H. H. Howard, "Thematic cartography and geovisualization," *Prentice Hall Series in Geographic Information Science*, Prentice-Hall, Upper Saddle River, NJ, USA, 3rd edition, 2008.

[38] J. Michael, S. De, F. Michael, and P. A. Goodchild, *Longley. Geospatial Analysis: A Comprehensive Guide to Principles, Techniques and Software Tools*, Troubador Publishing Ltd., Kibworth, UK, 2007.

[39] C. Wang, X. Zhang, P. Ghadimi, Q. Liu, M. K. Lim, and H. E. Stanley, "The impact of regional financial development on economic growth in Beijing-Tianjin-Hebei region: a spatial econometric analysis," *Physica A: Statistical Mechanics and Its Applications*, vol. 521, pp. 635–648, 2019.

[40] L. Jiang, H. Folmer, M. Ji, and P. Zhou, "Revisiting cross-province energy intensity convergence in China: a spatial panel analysis," *Energy Policy*, vol. 121, pp. 252–263, 2018.

[41] D. Ma, W. Wu, and Z. Dong, "Industrial carbon emission performance and its influencing factors in China: based on an empirical study of spatial panel data model," *China Economic Studies*, vol. 1, pp. 121–135, 2017.

[42] M. Yang, H. Zhang, and Y. Sun, "Regional disparity and distributional dynamic evolution of the innovation ability in seven Chinese megalopolises," *The Journal of Quantitative & Technical Economics*, vol. 34, no. 3, pp. 21–39, 2017.

[43] Q. Zhao, Q. Yan, and H. Zhao, "Research on spatial characteristics and influencing factors of provincial carbon emissions in China," *Journal of Beijing Institute of Technology (Social Sciences Edition)*, vol. 20, no. 1, pp. 9–16, 2018.

[44] P. A. P. Moran, "Notes on continuous stochastic phenomena," *Biometrika*, vol. 37, no. 1-2, pp. 17–23, 1950.

[45] L. Anselin, "Local indicators of spatial association—LISA," *Geographical Analysis*, vol. 27, no. 2, pp. 93–115, 1995.

[46] L. Anselin, A. K. Bera, R. Florax, and M. J. Yoon, "Simple diagnostic tests for spatial dependence," *Regional Science and Urban Economics*, vol. 26, no. 1, pp. 77–104, 1996.

[47] L.-f. Lee and J. Yu, "Some recent developments in spatial panel data models," *Regional Science and Urban Economics*, vol. 40, no. 5, pp. 255–271, 2010.

[48] G. Arbia, R. Basile, and G. Piras, "Using spatial panel data in modelling regional growth and convergence," *Social Science Electronic*, vol. 55, 2006.

Hindawi
Discrete Dynamics in Nature and Society
Volume 2020, Article ID 8827440, 14 pages
https://doi.org/10.1155/2020/8827440

Research Article

Forecasting Carbon Emissions with Dynamic Model Averaging Approach: Time-Varying Evidence from China

Siqi Xu,[1] **Yifeng Zhang**,[2] **and Xiaodan Chen**[2]

[1]*School of Social Development, Xihua University, Chengdu, China*
[2]*School of Finance, Yunnan University of Finance and Economics, Kunming, China*

Correspondence should be addressed to Yifeng Zhang; zyf@ynufe.edu.cn

Received 22 September 2020; Revised 9 October 2020; Accepted 10 October 2020; Published 28 October 2020

Academic Editor: Dehua Shen

Although energy-related factors, such as energy intensity and energy consumption, are well recognized as major drivers of carbon dioxide emission in China, little is known about the time-varying impacts of other macrolevel nonenergy factors on carbon emission, especially those from macroeconomic, financial, household, and technology progress indicators in China. This paper contributes to the literature by investigating the time-varying predictive ability of 15 macrolevel indicators for China's carbon dioxide emission from 1982 to 2017 with a dynamic model averaging (DMA) method. The empirical results show that, firstly, the explanatory power of each nonenergy predictor changes significantly with time and no predictor has a stable positive/negative impact on China's carbon emissions throughout the whole sample period. Secondly, all these predictors present a distinct predictive ability for carbon emission in China. The proportion of industry production in GDP (IP) shows the greatest predictive power, while the proportion of FDI in GDP has the smallest forecasting ability. Interestingly, those Chinese household features, such as Engel's coefficient and household savings rate, play very important roles in the prediction of China's carbon emission. In addition, we find that IP are losing its predictive power in recent years, while the proportion of value-added of the service sector in GDP presents not only a leading forecasting weight, but a continuous increasing prediction power in recent years. Finally, the dynamic model averaging (DMA) method can produce the most accurate forecasts of carbon emission in China compared to other commonly used forecasting methods.

1. Introduction

As an important part of the atmosphere, greenhouse gases, i.e., carbon dioxide (CO_2), nitrous oxide, and methane, act just like a blanket, can absorb infrared radiation, and prevent it from escaping into outer space, maintaining the temperature of Earth's atmosphere and surface. However, since the beginning of the Industrial Revolution in the early 1800s, the concentration of greenhouse gases, especially CO_2, in the atmosphere, has greatly increased because of the great consumptions of fossil fuels. The level of CO_2 in the atmosphere has increased by more than 40 percent, from about 280 parts per million (ppm) in the 1800s to 400 ppm recently. The increase in CO_2 causes the gradual warming of the Earth's atmosphere and surface, which is known as global warming. The process of global warming would cause serious natural and societal effects such as extreme weather events, a rise in sea levels, and increasing ocean acidification.

In addition, China has become the largest CO_2 emissions country in the world, by the end of 2019, with a share as much as 28.8% of the total amount [1]. Thus, determining the major factors that would have an effect on the growth rate of China's carbon emissions is a key task for policymakers. Our research contributes to the literature on this issue in the following three points.

Firstly, many research studies have proved the impacts of energy-related factors, such as energy consumption per capita, total energy consumption, fossil fuel energy consumption, renewable energy consumption, nuclear energy consumption, and coal consumption, on CO_2 emission (see [2–9] and among many others). This paper, however, pays attention to those nonenergy indicators from

macroeconomy (especially from finance sectors), household wealth conditions, and technical progress level, which have not been investigated in a comprehensive framework in previous research studies. More specifically, the Chinese household features, such as household wealth or saving (consumption) behaviors, have not been investigated regarding their impacts on China's CO_2 emission in the previous literature. In addition, patent number is commonly used as a proxy of technical progress in extant research studies. However, these patent data are not available for China in the early 1980s. Therefore, in our research, we use the ratios of total R&D to GDP as well as the number of college students to China's population as the other two proxies to measure the technical progress condition in China.

Secondly, in terms of research methods, constant coefficient (CC) models, i.e., multivariate linear regression, cointegration, VECM, or ARDL, which have the advantages of providing simple and easy estimates, are widely used for investigating the impacts of different factors on the Chinese CO_2 emission. It is, however, well documented in economic and econometric researches that CC models have the obvious shortcoming that they cannot depict the time-varying effects of one variable on another. It is also well known that major policy switching, business cycle, and economy certainty may alter the dependence structure between CO_2 emission and its influential factors. Thus, it is very important and necessary to account for these time-varying effects by using models with time-varying parameter (TVP) setting. The TVP method is useful for exploring the time-varying connections between the explanatory variable and the explained variable because it can produce the time-varying parameters for explanatory variables. Thus, we utilize both traditional CC and TVP OLS models to forecast China's CO_2 emission in recent years and evaluate their performances within several evaluation criteria.

Lastly, many recent research studies use a large number of factors to detect their impacts on China's CO_2 emission (see [10, 11] and among many others). But using too many explanatory variables in an econometric model, no matter it is a CC or TVP model has some clear drawbacks. Koop and Korobilis [12] indicate that a model with too many explanatory variables often leads to overfitting in-sample and, thus, forecasting poorly out-of-sample. Besides, studies have shown that a fixed set of explanatory variables may not always be related to the explained variable throughout a long time period [3, 13–18]. In other words, during different time periods and/or under different policy conditions, the influence of each determinant on China's CO_2 emission may not be fixed. Research studies further indicate that a model with the fixed set of predictors may behave inconsistently over time [19–21]. These problems can be solved by performing a dynamic model selection process at each time point, while the computational burden of this process is huge. In the process of dynamic model selection, if n predictors are given, we need to evaluate $2n$ models at each time point, so throughout the evaluation period of T, the total number of models to be assessed will be as large as $2nT$. This computational task would be difficult to achieve when n and T are large. Therefore, the model averaging method, such as Bayesian model averaging (BMA) and forecast combination, is a preferred choice for improving the forecasting accuracy. Model averaging method is useful for achieving stable and accurate forecasts. However, either forecast combination or BMA method is difficult to capture each model's time-varying contribution because the weights they assigned for combining different models are fixed over time [19, 21, 22]. To address these problems, we further utilize a dynamic model averaging (DMA) method, which is proposed by Raftery et al. [23] and widely employed in recent researches [24–27], to carry out our task of forecasting China's CO_2 emission with many predictors. Using two forgetting factors, DMA combines different models in a dynamic way, allowing the coefficients of predictors and the sets of predictors to change over time. These two forecasting factors can also simplify the model selection process which has a huge computational task.

The remainder of this paper is organized as follows: Section 2 reviews the extant literature on the topic of impactors on China's carbon emission. Section 3 describes the data used in this paper. Methodologies are introduced in Section 4. Section 5 analyzes the empirical results and Section 6 concludes the paper.

2. Literature Review

Numerous studies have been trying to investigate the factors that would influence CO_2 emissions. Various variables, such as population activities, energy consumption patterns, economic growth, innovation and technology, urbanization process, and government policies, are used in these studies to explain their effects on carbon emissions. These impact factors can be summarized into three major categories.

Firstly, energy consumption is an output of human activities that produces carbon emission. From this perspective, population growth, population density, and urbanization process in an economy are supposed to play significant roles in carbon dioxide emissions. Zhang and Tan [28] investigate the connections between CO_2 emissions and population factors using the Stochastic Impacts by Regression on Population, Affluence, and Technology (STIRPAT) method. They found a positive connection between carbon emissions and population. STIRPAT method is also adopted by Guan et al. [29] to discuss the main drivers of China's CO_2 emissions. According to their results, CO_2 emission is negatively correlated with disposable income, population density, and development of tertiary industries, whereas positively correlated with GDP per capita, secondary industries, and urban employment. Employing four Chinese megacities (Beijing, Tianjin, Shanghai, and Chongqing) as cases, Shi et al. [30] conclude that the improvement of resident living standards and the development of manufacturing in these cities are the main drivers of carbon emission per capita from 2010 to 2015. Yao et al. [31] use the mediating effect model and the threshold regression model, finding that the urbanization in China helps to decline the carbon emission scale, carbon intensity, and carbon emission per capita in recent years. Based on the data

of consumption level, population size, and population structure in China from 1978 to 2008, Zhu and Peng [32] use the ridge regression method and find that the urbanization of population is the key driver for the growth of China's CO_2 emission. Moreover, population structure, population age, urbanization, and household size are also significantly associated with carbon emissions. Ma et al. [33] further note that wealth, economic structure, energy structure, population structure, and the development of technology are also major influential factors of China's carbon emission. Meng et al. [34] investigate the impact of local officials' promotion incentives on China's CO_2 emission. The results indicated the significant influence of age, tenure, and local officials' promotion sources on total CO_2 emissions.

Secondly, economic growth is regarded as another major driver of excessive energy consumption in China [28, 29, 35]. It is agreed that there are significant positive connections among China's CO_2 emission and economic growth and energy consumption. Based on China's energy consumption data from 2005 to 2016, Ma et al. [36] find that aggressive economic output and increasing energy consumption basically promote China's carbon emissions. More specifically, CO_2 emissions from China's energy consumption mainly come from industry, residential consumption sector, transportation industry, and tertiary industry. Using the structural decomposition analysis (SDA) approach, Chen et al. [37] measure the construction industry CO_2 emissions difference between the USA and China by the structural decomposition analysis (SDA) and found that the four largest contributors to the difference of China and USA construction carbon emissions are energy intensity, final demand ration effect, final demand effect, and the carbonization factor effect. These findings suggest the adverse interaction between construction carbon emissions and economic growth. Thus, they propose that the Chinese government should take efforts to change the economic development mode. By formulating the industrial subsector decomposition analysis in Tianjin province, China, Kang et al. [38] find that the economic growth is the most important influential factor for driving the growth of CO_2 emissions, while energy efficiency improvement is crucial to promote the decreases of CO_2 emissions. By using the LMDI method, Wang and Yang [39] show that the main influential factors for the industrial CO_2 emissions in Beijing–Tianjing–Hebei economic band including the rapid economic growth, energy structure, and energy intensity. Ma et al. [40] also employ the LMDI method to examine the connection between economic growth and household CO_2 emissions in China. Their results show that energy intensity and economic growth are the two primary drivers of carbon emission fluctuations. By using the DPSIR and PLS-SEM methods, Wei et al. [35] find that the economic development level and the urbanization are the two main drivers for CO_2 emissions. In summary, sustainable economic growth and long-term industrial transformation would lead to the continued growing for the total CO_2 emissions [41].

Lastly, financing activities can adjust the economic structure and improve economic efficiency, since finance sector is generally considered to be of low resource consumption and high value-added. So many researchers suggest that improving finance sector is an effective way to reduce carbon dioxide intensity. Jalil and Feridun [42] explore the influence of energy consumption, economic growth, and financial development on China's CO_2 emissions from 1953 to 2006 and prove that a decrease in carbon emissions can be caused by financial development. Other empirical analysis also confirms that the development of tertiary industries, including finance sector development, is the key influential factor for CO_2 emission decreases [29, 43]. By applying spatial econometric analysis, Xu et al. [44] reach a conclusion that China's financial structure is negatively related to the carbon emission, meaning that optimizing financial structure is an effective strategy for reducing CO_2 emissions. The research of Zhang et al. [45] shows that carbon emission trading (CET) market, which is one of the promising financial market, has a significant impact on the decrease of China's CO_2 emissions in recent years. This conclusion is consistent with Zhou et al. [46] but quite different from the study of Mo et al. [47], which reveals that China's carbon emissions trading program cannot support low carbon energy consumption, and other policies are necessary to complete China's CET trading mechanism. Except for the factors listed above, foreign direct investment (FDI) is another significant contributor to carbon emission reduction [31, 48, 49], implying that financial development can attract more FDI inflow and evolve superior technology to reduce carbon emission [50]. However, other researchers debate that due to economy globalization, financing activities are conducive to the expansion of industrialization, which may bring more FDI, faster economic growth, and thus larger CO_2 emissions [51–54]. Recently, the results of [36] show that China's tertiary industries account for an increasing proportion of energy consumption. Using the Granger causality test and ARDL bound test, Zhang and Zhang [11] investigate the short-term and long-term dynamic and casual relationship between China's CO_2 emissions and GDP, exchange rate, FDI, and trade structure from 1982 to 2016. They find the negative effects of the exchange rate and the trade in services on China's carbon emissions and the positive impact of FDI inflows on it. These results come to a consensus with Zhang [55], indicating that the financial industry in China is an important factor for promoting CO_2 emissions. Zhang [55] examines the impact of China's financial development on CO_2 emissions by various econometric techniques, including the Granger causality test, cointegration test, and variance decomposition. The empirical results show that the financial development of China, especially the financial intermediation scale, is an important influential factor for the increase of CO_2 emissions. In addition, even though the results show that FDI has the least impact on CO_2 emission in China among the concerned financial development indicators because it only accounts for a small proportion in the GDP of China (see also in [49]), Zhang [55] also insists that FDI is an important CO_2 emission influential factor due to the utilization of China's FDI in carbon-intensive sectors. In summary, it can be seen from the above literature that financial sectors have

important effects on carbon emission in China, but there are no widely accepted relationships between them.

3. Data

To account for both changes in China's carbon emission and total population, we use carbon emission per capita to measure the carbon emission levels in China (see also in [11, 45]). Furthermore, as explained above, we do not focus on those predictors directly related to energy sectors, such as energy consumption per capita, total energy consumption, fossil fuel energy consumption, renewable energy consumption, nuclear energy consumption, and coal consumption. In contrast, we utilize 15 indicators from three nonenergy categories: (1) *China's macroeconomic indices*, especially those from financial sectors (see [11, 45, 55] and among many others). (2) *Indicators on China's household wealth conditions and saving behaviors*: we think that these indicators are key bases for a family to decide what kinds of energy and how much energy it will consume within a time period, which will influence the carbon emissions in China consequently. (3) *Technical progress indices*: as documented in many studies [10, 35], technology development can not only improve the energy production and consumption with lower carbon emission but also promote better methods for energy conservation and environment protection. To account for both data available and data matching, we collect the data we need covering a time period from 1982 to 2017. All data are recorded in annual frequency with 36 observations for each of them. Table 1 presents the detailed definitions of these indicators.

Table 1 reveals that the 15 nonenergy predictors are selected from three general categories: macroeconomic, household feature, and technical progress indicators. In addition, macroeconomic indicators are further divided into four specific sorts from macroeconomic aggregate, macroeconomic structure, financial market, and international trade. Table 2 then shows the descriptive statistics for these variables.

To ensure stationary, all data are transformed in the forms of natural logarithm growth rate, which is a method commonly used in time series analysis. Table 2 indicates that the growth rates vary greatly among them, indicating some interesting macroeconomic overviews in China. For example, firstly, in terms of macroeconomic structure, the proportions of both agriculture and industry productions to GDP of China have negative means, but the share of value-added of the service sector in the GDP keeps a positive mean of 2.4 percent. That is to say, the service sector in GDP is becoming more and more important in determining the GDP growth of China. However, the industry and agriculture sectors are losing this power. Additionally, we can also see that the Chinese public finance revenue maintains a negative 0.2 percent annual growth rate, and the public expenditure, however, keeps a positive 0.2 percent growth rate. These two numbers further reveal that the Chinese government is trying to lower down the tax and other financial burdens in the real economy and increase the public welfare in the past few decades. Secondly, as far as the Chinese household features are concerned, we find that Engel's coefficient continues to decrease, while the saving rate is increasing, which together imply that the Chinese family is becoming more and more affluent with more money being saved since 1982. Finally, with regard to the technical progress indices, we can see that both R&D and college students keep a positive growth rate in China, indicating the continuous improvement in the innovation capabilities and scientific research strength in China.

In addition, we find that almost all the variables are skewed distributed with excess kurtosis. Considering this, most of the variables reject the null hypotheses of normality distribution based on the Jarque–Bera statistics. However, most results in Ljung–Box Q test indicate no rejections for the null hypotheses of no autocorrelation up to 5th lag order. The most important results are that all the variables considered here reject the null hypotheses of one unit root according to the ADF and/or P-P statistics, implying that all the time series are stationary and can be modeled directly without further transforms.

4. Methodology

4.1. TVP Model and Dynamic Model Averaging (DMA) Forecasts. Although the constant coefficient (CC) models such as autoregression (AR) or multivariable regression have the advantages of providing simple estimation and straightforward explanations, they also possess the drawbacks that the regressor coefficients of the CC model are fixed. In contrast, the time-varying parameter (TVP) approach is a very natural way to depict the time-varying relationships between explanatory variables and explained variable because it allows the parameters of explanatory variables to be time-varying. As mentioned by Primiceri [56], Koop et al. [57], and Wei and Cao [24], a basic TVP model can be defined as follows:

$$y_t = x_{t-1}'\beta_t + \varepsilon_t, \tag{1}$$

$$\beta_t = \beta_{t-1} + \eta_t, \tag{2}$$

where y_t is the target variable to be forecasted at time t. x_{t-1} is a $1 \times m$ vector of predictors, in which the lagged dependent variable y_t is usually included besides other exogenous variables. β_t is an $m \times 1$ vector of coefficients, $\varepsilon_t \sim i.i.d.N(0, V_t)$, and $\eta_t \sim i.i.d.N(0, W_t)$.

For the TVP model defined in equations (1) and (2), the predictors in x_{t-1} are assumed to be fixed throughout the whole forecasting time period, which may cause the over-parameterization problem and a loss of forecasting precision. However, the dynamic model averaging (DMA) and dynamic model selection (DMS) can facilitate the problem of the TVP model because they allow both the predictor sets (forecasting models) and the coefficients of predictors to be time-varying. Therefore, following Raftery et al. [23], Koop and Korobilis [12], Wei and Cao [24], and Wei et al., [25], we utilize DMA and DMS methods to forecast China's carbon emission. The DMA (DMS) method can be written as follows:

Table 1: Definitions of the explained variable and various nonenergy predictors.

Category (frequency)	Variable	Definition	Calculation	Unit
Explained variable (annual)	Carbon	CO_2 emission per capita	Total CO_2 emission divided by the total population in China	Tons per capita
Predictors (annual)				
Macroeconomic aggregate	GDP	Nominal GDP per capita	Nominal GDP divided by the total population in China	Yuan per capita
Macroeconomic structure	Agriculture	Proportion of agriculture production to total GDP	Agriculture production divided by GDP in China	%
	Industry	Proportion of industry production to total GDP	Industry production divided by total GDP in China	%
	Service added	Proportion of value-added of the service sector to total GDP	Value-added of the service sector divided by GDP in China	%
Financial market	FDI	Proportion of foreign direct investment in China to total GDP	FDI divided by GDP in China	%
	Total loan	Proportion of total loan by financial intermediation in China to total GDP	Total loan divided by GDP in China	%
	Public revenue	Proportion of total public revenue in China to total GDP	Total public revenue divided by GDP in China	%
	Public expenditure	Proportion of total public expenditure in China to total GDP	Total public expenditure divided by total GDP	%
	M_0	Proportion of M_0 in China to total GDP	M_0 divided by GDP in China	%
International trade	Exchange rate	The exchange rate of RMB against US dollar	Nominal exchange rate of RMB against US dollar	Yuan/ dollar
	Service trade	Proportion of service trade to total trade in China	Service trade divided by total international trade in China	%
Household feature	Engel's coefficient	Proportion of income spent on food	Food expenditure of China's family divided by family's income	%
	Total saving	Proportion of family saving to GDP	China's family saving divided by GDP	%
Technical progress	R&D	Proportion of total research & development (R&D) expenditure to GDP in China	Total research & development (R&D) expenditure divided by GDP in China	%
	College student	Proportion of college student number to population in China	College student number divided by total population in China	%

Table 2: Descriptive statistics for energy returns.

	Mean	St. deviation	Skewness	Kurtosis	Jarque–Bera	Q (5)	ADF	P-P
Carbon	0.043	0.043	1.138***	1.518*	10.910***	31.304***	−2.998**	−2.958**
GDP	0.135	0.060	0.843*	0.327	4.299	26.065***	−3.257**	−2.867*
Agriculture	−0.041	0.044	0.299	0.581	1.013	5.622	−5.405***	−5.208***
Industry	−0.003	0.023	0.632	1.521*	5.708*	7.783	−3.741***	−3.738***
Service added	0.024	0.033	1.336***	3.510***	28.374***	7.828	−3.965***	−3.990***
FDI	0.021	0.221	2.254***	4.726***	62.208***	7.876	−5.487***	−4.507***
Total loan	0.017	0.108	−2.173***	9.359***	155.310***	3.502	−2.625*	−6.299***
Public revenue	−0.002	0.062	−0.794*	0.130	3.701	39.392	−2.692*	−2.599*
Public expenditure	0.002	0.065	−0.156	−0.156	0.177	27.427	−2.618*	−2.628*
M_0	0.001	0.073	0.821*	1.457	7.024**	8.349	−4.102***	−4.040***
Exchange rate	0.036	0.097	2.172***	5.338***	69.084***	16.384***	−5.047***	−4.219***
Service trade	0.012	0.109	−0.516	1.831**	6.443**	6.985	−2.625*	−5.967***
Engel's coefficient	−0.020	0.036	−0.824*	3.051***	17.539***	1.974	−4.148***	−5.500***
Total saving	0.008	0.037	0.231	−0.258	0.410	7.547	−2.399*	−3.925***
R&D	0.016	0.105	1.163***	3.965***	30.830***	14.908**	−3.435**	−3.516**
College student	0.081	0.080	1.053**	0.357	6.652**	36.586	−2.710*	−2.110

Notes: the Jarque–Bera statistic tests the null hypothesis of normal distribution. Q (5) is the Ljung–Box statistics that test the null hypothesis of no serial correlation for up to 5 orders. ADF are the statistics of Augmented Dickey–Fuller unit root test. P-P refers to the statistics of Phillips–Perron unit root tests. Symbols ***, **, and * indicate the rejections of null hypothesis at 1%, 5%, and 10% significance levels, respectively.

$$y_t = x_{t-1}^{(k)'}\beta_t^{(k)} + \varepsilon_t^{(k)},$$
$$\beta_t^{(k)} = \beta_{t-1}^{(k)} + \eta_t^{(k)}, \tag{3}$$

where $x_{t-1}^{(k)'} \subseteq x_{t-1}'$ for $k = 1, 2, \ldots, K$ indicates a set of predictors, $\varepsilon_t \sim i.i.d.N(0, V_t^{(k)})$, and $\eta_t \sim i.i.d.N(0, W_t^{(k)})$. For the set x_{t-1}' with m predictors, there would be $K = 2^m$ possible

combinations of these predictors. The uncertain factors in these K models can then be incorporated by DMA and DMS in a dynamic way:

$$\begin{aligned}\widehat{y}_t^{\mathrm{DMA}} &= \sum_{k=1}^{K} \pi_{(t|t-1,k)} x_{t-1}^{(k)'} \beta_{t-1}^{(k)},\\ \widehat{y}_t^{\mathrm{DMS}} &= x_{t-1}^{(k^*)'} \beta_{t-1}^{(k^*)},\end{aligned} \tag{4}$$

where $Y^{t-1} = \{y_1, \ldots, y_{t-1}\}$, $\pi_{(t|t-1,k)} = \Pr(L_t = k|Y^{t-1})$ is the probability (or weight) assigned to model k, and the equation $L_t = k$ denotes that model k is chosen at time t. DMA approach obtains its forecasts by averaging all the K models in terms of their historical forecasting performances, calculated by the probability, $\pi_{(t|t-1,k)}$. However, DMS selects the model which has the highest probability, $\pi_{(t|t-1,k^*)}$.

The DMA and DMS methods discussed above have the drawback of heavy computational when the sample length is long or the number of predictors is large. So Raftery et al. [23] propose a Kalman filter method which involves two forgetting factors, λ and α, to simplify the estimation process without loss of forecast accuracy. λ, which is a forgetting factor with $0 < \lambda \leq 1$, can simplify the covariance matrix of $\beta_{t-1}^{(k)}$, which is important for the calculation of $\beta_{t-1}^{(k)}$. This simplified process is given as follows:

$$\beta_{t|t-1}^{(k)} = \beta_{t-1|t-1}^{(k)}, \tag{5}$$

$$\Sigma_{t|t-1}^{(k)} = \frac{1}{\lambda} \Sigma_{t-1|t-1}^{(k)}, \tag{6}$$

where $\Sigma_{t|t-1}^{(k)}$ is the covariance matrix of $\beta_{t-1}^{(k)}$. Then, the parameter estimation is achieved by the following updating equations:

$$\widehat{\beta}_{t|t}^{(k)} = \widehat{\beta}_{t-1|t-1}^{(k)} + \Sigma_{t|t-1}^{(k)} x_{t-1}^{(k)'} \left(V_t^{(k)} + x_{t-1}^{(k)'} \Sigma_{t|t-1}^{(k)} x_{t-1}^{(k)} \right)^{-1} \left(y_t - x_{t-1}^{(k)'} \widehat{\beta}_{t-1}^{(k)} \right), \tag{7}$$

$$\Sigma_{t|t}^{(k)} = \Sigma_{t|t-1}^{(k)} - \Sigma_{t|t-1}^{(k)} x_{t-1}^{(k)'} \left(V_t^{(k)} + x_{t-1}^{(k)'} \Sigma_{t|t-1}^{(k)} x_{t-1}^{(k)} \right)^{-1} x_{t-1}^{(k)} \Sigma_{t|t-1}^{(k)}. \tag{8}$$

For the probability, $\pi_{(t|t-1,k)}$, if a transition probability matrix is used, $K = 2^m$ model combinations should be considered at each time in point. m is the number of predictors, and if the sample period is long or m is large, it is computationally infeasible to operate the Markov switching in the $K \times K$ matrix. However, the use of the forgetting factor, α $(0 < \alpha \leq 1)$, provides an effective way for reducing the calculation error and time. Based on this forgetting factor, the probability for the forecasting model k is defined as follows:

$$\pi_{(t|t-1,k)} = \frac{\pi_{(t-1|t-1,k)}^{\alpha}}{\sum_{\ell=1}^{K} \pi_{(t-1|t-1,\ell)}^{\alpha}}, \tag{9}$$

and the updating equation is defined as follows:

$$\pi_{(t|t,k)} = \frac{\pi_{(t|t-1,k)} f_k\left(y_t|Y^{t-1}\right)}{\sum_{y_t|Y^{t-1}}^{K} \pi_{(t|t-1,k)} f_\ell\left(y_t|Y^{t-1}\right)}, \tag{10}$$

where $f_\ell(y_t|Y^{t-1})$ is the predictive density of model ℓ. In summary, the steps through equations (5)–(10) consist of a complete process of Kalman filter updating and prediction method. Furthermore, Raftery et al. [23] indicate that a BMA (Bayesian model averaging) method can be regarded as a special case of the DMA model with $\lambda = \alpha = 1$.

4.2. Model Evaluation. Various statistical criteria can be used to quantitatively assess the forecasting performance of different models. Following the mainstream of literature in this field, two loss functions, mean squared forecast error (MSFE) and mean absolute forecast error (MAFE), are used in this paper. MSFE and MSAE are simply defined as follows:

$$\begin{aligned}\mathrm{MSFE} &= M^{-1} \sum_{t=1}^{M} \left(y_t - \widehat{y}_t\right)^2,\\ \mathrm{MAFE} &= M^{-1} \sum_{t=1}^{M} \left|y_t - \widehat{y}_t\right|,\end{aligned} \tag{11}$$

where M is the total number of forecasting methods, y_t denotes the true observation, and $\widehat{y}_t$ is the forecast set achieved by different forecasting methods.

However, the two loss functions discussed above can hardly offer us the significance levels of forecasting difference among various models. Therefore, this paper utilizes the model confidence set (MCS) test which is proposed by Hansen et al. [58] and widely used in recent research studies [24, 25, 59], to achieve this goal and to determine the superior models. The MCS test is developed from several traditional and standard model evaluation methods [60–63] but with more obvious advantages over these traditional ones. Firstly, the MCS test uses a bootstrap method to obtain the test statistics, reducing the influence of outliers in the data. Secondly, it does not have to specify a benchmark mode. Finally, this test does not limit the number of the "best" model to be one. The MCS process is as follows.

Suppose that we have a model set, $M_0 = \{1, \ldots, m_0\}$ which includes a finite number of objects (models). These models are evaluated over the sample, $t = 1, \ldots, n$, and under a loss function i. The purpose of MCS is to select a model set, M^*, which consists of the best models from M_0. The set of superior models can be defined as follows:

$$M^* \equiv \left\{u \in M_0 \colon E\left(d_{i,uv,t}\right) \leq 0, \quad \text{for all } v \in M_0\right\}, \tag{12}$$

where $d_{uv,t} \equiv L_{u,t} - L_{v,t}$ is the relative performance of model u and model v, for any u, $v \in M_0$, in which $L_{u,t}$ is the loss of model u in period t, and $E(d_{i,uv,t})$ is the mathematical expectation of $d_{uv,t}$. MCS test is performed by a series of

significance tests, in which the models that are found to be significantly worse than other elements of M_0 are eliminated. The null hypothesis of this test can be identified as follows:

$$H_{0,M}: E\left(d_{i.uv,t}\right) = 0, \quad \text{for all } u, v \in M \subset M_0. \tag{13}$$

The MCS process consists of an *equivalence test*, δ_M, and an *elimination rule*, e_M. δ_M examines the hypothesis H_0 for any two models in M_0. When H_0 is rejected, e_M is used to identify the model that is to be removed from M_0. A model set, $\widehat{M}^*_{1-\alpha}$, which consists of the set of "surviving" models, and which are named as the MCS, can be obtained by repeating these two tests. The significance level, α, of the MCS test is generally set to be 0.1 by Hansen et al. [58] and among many others. If the p value of one MCS test is larger than 0.1, the corresponding model is a "surviving" model and it has the forecasting accuracy that is superior to other competitive models.

In the MCS test, two statistics, the range statistic (T_R) and the semiquadratic statistic (T_{SQ}), are commonly utilized. They are calculated as follows:

$$\begin{aligned} T_R &= \max_{u,v\in M} \frac{\left|\overline{d}_{i,uv}\right|}{\sqrt{\operatorname{var}\left(d_{i,uv}\right)}}, \\ T_{SQ} &= \max_{u,v\in M} \frac{\left(\overline{d}_{i,uv}\right)^2}{\operatorname{var}\left(\overline{d}_{i,uv}\right)}, \end{aligned} \tag{14}$$

where $\overline{d}_{i,uv} = (1/n)\sum_{t=1}^{n} d_{i,uv,t}$. The null hypothesis in equation (13) cannot be rejected when the p values of T_R and T_{SQ} are larger than 0.1. The asymptotic distributions of these two test statistics depend on nuisance parameters, so they are nonstandard. However, these conditions do not pose any obstacles because the distribution of these two statistics can be easily estimated by the bootstrap methods and thus implicitly solve the problem of nuisance parameter. To get more robust conclusions, except for T_R and T_{SQ}, four more test statistics, i.e., $T_{\max}$, T_Q, T_F, and T_D, are used in our research. A more detailed discussion of these test statistics can be found in Hansen et al. [58].

5. Empirical Results

5.1. Time-Varying Contributions of Single Explanatory Variable to Carbon Emission. In this section, we firstly examine the time-varying effects of individual predictors on China's carbon emission by using the simple univariate TVP regression model denoted in equations (1) and (2). For clarity, Figure 1 represents the time-varying coefficients for only 9 predictors in the univariate TVP regression.

Figure 1 shows that the explanatory power of each predictor really changes significantly with time. In general, no predictors always have positive or negative impacts on carbon emissions in China throughout the estimation time period. For example, through 1985 to 1990, the proportion of industry production to GDP (IP) offers negative effects, while from 1991 to 2017 it has large positive impacts on China's carbon emission. GDP per capita has a positive impact on carbon emission in most years, but experiences an obvious decreasing explanatory power from 2004 and ends up with a small negative effect in 2017. Similar results can also be evidenced for other predictors in Figure 1. Moreover, we can see that the impacts of different predictors vary greatly with time. In particular, IP seems to provide the largest positive impact in recent years. The proportion of value-added of the service sector to total GDP (service added), however, has the largest negative effects on China's carbon emission from 2000.

In summary, it is interesting but difficult to quantify the overall contributions of various predictors on China's carbon emission in a time-varying way. The empirical findings in this section only give us the in-sample fitting results of time-varying effects of explanatory variables on carbon emission within a univariate TVP model. Thus, to obtain the out-of-sample forecasting evaluations, we have to seek helps from various forecasting results in multivariate TVP models and model combination methods.

5.2. Forecasting Results of Different Models. In the extant literature, to identify what factors are important for determining carbon emission in China is usually investigated by multivariate constant coefficient (CC) OLS regression models. Nevertheless, as discussed above, a better way to solve this problem is to seek help from TVP models. Furthermore, to take the different contributions of various explanatory variables at different time periods or market conditions into account, we further employ several commonly used combination forecasting approaches in this paper. In summary, nine models are considered here: CC OLS, TVP OLS, equal weighted, BMA, BMS, DMA95, DMS95, DMA99, and DMS99. The recursive out-of-sample forecasting approach is applied to all the nine models. The descriptions of these models in details are as follows:

(1) CC OLS: a constant coefficient multivariate regression model with all the 15 explanatory variables

(2) TVP OLS: a time-varying parameter multivariate regression model with all the 15 explanatory variables

(3) Equal weighted: the equal-weighted averaging of K OLS models, i.e., the equal-weighted DMA model. In this paper, we have 15 explanatory variables, which means that we have $K = 2^{15} = 32{,}768$ models to combine

(4) BMA: DMA forecasting with $\lambda = \alpha = 1$

(5) BMS: DMS forecasting with $\lambda = \alpha = 1$

(6) DMA95: dynamic model averaging with $\lambda = \alpha = 0.95$

(7) DMS95: dynamic model selection with $\lambda = \alpha = 0.95$

(8) DMA95: dynamic model averaging with $\lambda = \alpha = 0.99$

(9) DMS95: dynamic model selection with $\lambda = \alpha = 0.99$

To get a visible overview of the performances for these forecasting models, Figure 2 shows the predictive results through 1985 to 2017. The blue line with circles denotes the true growth rate of carbon emission per capita in China,

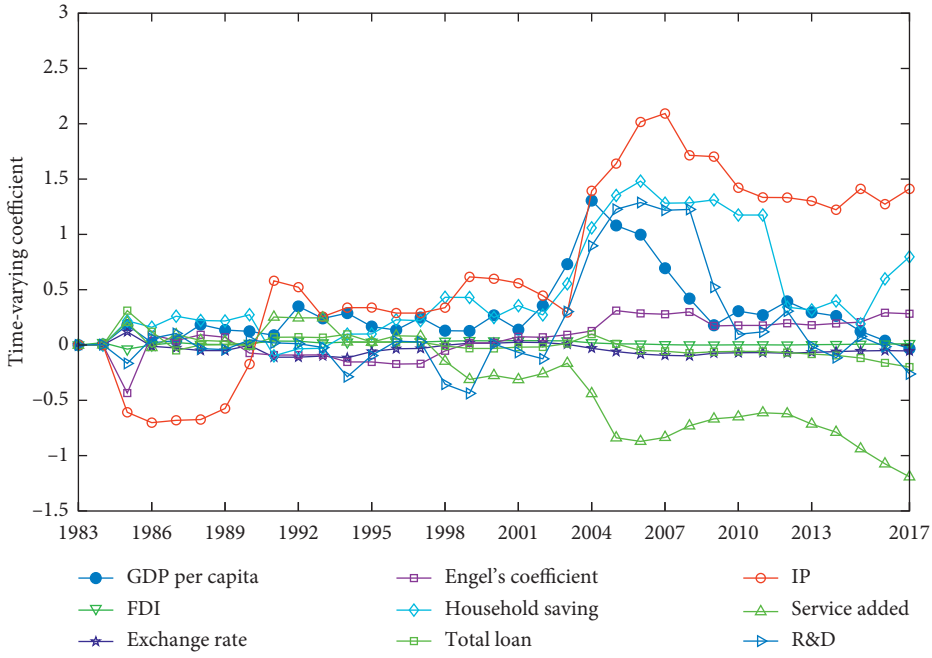

Figure 1: Estimations of time-varying coefficients of univariate TVP regression models.

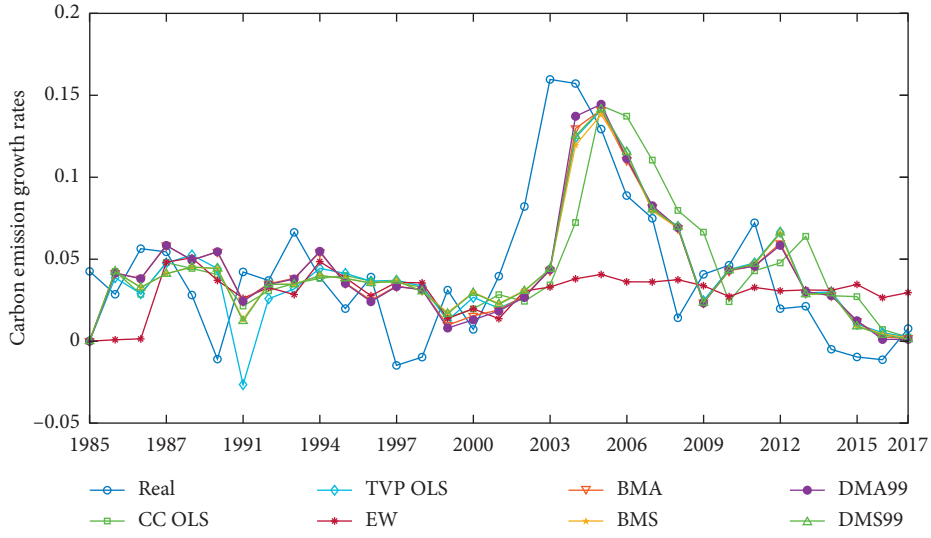

Figure 2: Carbon emission forecasting results by various models.

while other lines with different colors and markers are the forecasting results made by various models. We can see in Figure 2 that, in general, most models can produce similar forecasts to the real observations. In particular, during the period of 2000 to 2009, the growth rate of carbon emission experiences large fluctuations. We can see that those combination methods, such as BMA, BMS, DMA, and DMS, make more accurate predictions than others. In addition, we also find that the equal-weighted averaging model seems to offer too "mild" forecasts to follow the changing trend of real carbon emissions. Tables 3 and 4 report the results of forecasting errors and MCS test, respectively.

Table 3 shows the MSFE and MAFE of various models. Moreover, the R^2 of a Mincer–Zarnowitz regression is also reported in this table [64]. The Mincer–Zarnowitz approach is a regression of the real dependent variable against its fitted values produced by a forecasting model, which is also a commonly accepted approach to assess the forecast accuracy of a model. Like the meaning of ordinary adjusted R^2 in a multivariate regression, a larger R^2 of a Mincer–Zarnowitz regression indicates a better forecasting accuracy for a model.

Table 3 shows that, in general, dynamic combination (selection) methods, i.e., DMA, DMS, BMA, and BMS,

Table 3: Results of loss functions for different forecasting models.

	Loss functions		
Models	MSFE	MAFE	Mincer–Zarnowitz
CC OLS	0.00164	0.03140	0.20793
TVP OLS	0.00135	0.02807	0.32244
Equal weighted	0.00211	0.03553	−0.02215
BMA	0.00117	0.02554	0.39684
BMS	0.00118	0.02579	0.38466
DMA95	0.00117	0.02588	**0.43213**
DMS95	0.00119	0.02606	0.40760
DMA99	**0.00116**	**0.02552**	0.40446
DMS99	0.00118	0.02589	0.38941

Note: the bold numbers in this table indicate the smallest MSFE and MAFE and the largest R^2 of a Mincer–Zarnowitz regression, respectively.

Table 4: Results of the MCS test.

	MSFE						MAFE					
Models	T_R	T_{SQ}	T_{Max}	T_Q	T_F	T_D	T_R	T_{SQ}	T_{Max}	T_Q	T_F	T_D
CC OLS	0.0532	0.1836	0.0421	0.0190	0.1068	0.0557	0.0228	0.1081	0.0253	0.0107	0.0967	0.0185
TVP OLS	0.1092	0.5285	0.4836	0.4916	0.6097	0.4238	0.1343	0.4919	0.6017	0.0717	0.1814	0.4870
Equal weighted	0.0992	0.3116	0.0604	0.0006	0.0309	0.0683	0.0511	0.2200	0.0696	0.0094	0.0967	0.0336
BMA	0.9511	0.9700	0.9242	0.9280	0.9335	0.9495	0.9386	0.9386	0.9419	0.9701	0.9711	0.9419
BMS	0.9153	0.9700	0.9242	0.8302	0.8526	0.9495	0.9034	0.9277	0.8650	0.9701	0.9711	0.8950
DMA95	0.9511	0.9700	0.9251	0.9280	0.9335	0.9495	0.9034	0.9099	0.8386	0.6742	0.6997	0.8950
DMS95	0.9153	0.9664	0.9242	0.4916	0.6097	0.9495	0.8443	0.9099	0.8386	0.2473	0.3541	0.8950
DMA99	**1.0000**	**1.0000**	**1.0000**	**1.0000**	**1.0000**	**1.0000**	**1.0000**	**1.0000**	**1.0000**	**1.0000**	**1.0000**	**1.0000**
DMS99	0.9153	0.9700	0.9242	0.9280	0.9335	0.9495	0.8443	0.9099	0.8386	0.4055	0.4750	0.8950

Notes: the underlined numbers indicate those p values smaller than 0.1, implying that the corresponding prediction models cannot survive the MCS tests. The bold numbers indicate p values of 1.000, showing that the corresponding prediction models perform better than all other competitive models. MSFE and MAFE denote mean squared forecast error and mean absolute forecast error, respectively.

produce close forecasting errors. In particular, under the MSFE and MAFE criteria, the DMA method with forgetting factors $\lambda = \alpha = 0.99$ (DMA99) produces the smallest prediction errors of 0.00116 and 0.02552, respectively. The equal-weighted averaging method, however, obtains the largest forecasting errors of 0.00211 and 0.03553, respectively. With regard to Mincer–Zarnowitz regression, the DMA method with forgetting factors $\lambda = \alpha = 0.95$ (DMA95) gets the largest R^2 of 0.43213, implying again the superiority of DMA approach to individual CC or TVP models, as well as other combination methods.

In addition, to obtain a statistically robust conclusion about the forecasting accuracy of all the competitive models, we further conduct the MCS test on the forecasting results. Table 4 offers us a clearer picture of the performances of various prediction models. Firstly, no matter under MSFE or MAFE criteria with various statistics, the DMA method with forgetting factors $\lambda = \alpha = 0.99$ (DMA99) can definitely survive with the largest p values of 1.0, revealing its dominance over other models. Secondly, we find that the CC OLS and equal-weighted averaging models cannot survive in the MCS tests under many statistical criteria with p values smaller than 0.1. This means that, on the one hand, constant coefficient (CC) model can rarely describe the true relationships between carbon emission in China and those commonly used explanatory variables and thus cannot provide accurate predictions for it. On the other hand, even if the equal-weighted averaging method is applied, it also lacks the ability to depict the time-varying contributions of different predictors in different time periods.

In summary, the empirical results in both Tables 3 and 4 supply strong evidence that the dynamic model averaging method (DMA) can produce better forecasting accuracy than other predictive models. This finding also verifies the rationality of considering both the TVP models and a model averaging (selection) procedure in forecasting the carbon emissions in China.

5.3. Contributions of Various Predictors in Forecasting China's Carbon Emission. In this section, we are to understand how much each predictor contributes to explaining the growth rate of carbon emission in China in the past few decades. This question is answered through a measurement called "inclusion probability," which measures the total weights obtained by one predictor through all the $K = 2^m$ combinations of models in a DMA forecasting process. To be more formal, the inclusion probability for a predictor x_i is the sum of the probabilities ($\pi_{(t|tt-n1q,hk)}$) that a given predictor would be included in the forecasting model k ($k = 1, 2, \ldots, K$) of DMA at time t. In this paper, as we have 15 predictors, the inclusion probability of predictor x_i ($i = 1, 2, \ldots, 15$) will be a

number summed through $K = 2^{15} = 32{,}768$ combinations of forecasting models. A predictor with a higher inclusion probability would be assigned more prediction weights, thus contributing more important predictive power.

Figure 3 presents the overall picture of the time-varying contributions (inclusion probabilities) of the 15 nonenergy predictors in forecasting growth rate of carbon emission in China. Firstly, we find that all the 15 indicators present a steady but distinct predictive ability for carbon emission in China over the past few decades. At the beginning of the prediction period, i.e., 1985 to 1994, the DMA method needs to calculate the historical performance of different model (predictor) combinations, and thus, the inclusion probabilities for different predictors show small dispersions with similar time-varying trends. In particular, at the first prediction time point in 1985, the DMA method assigns all the predictors with the same inclusion probability of 0.5. As time goes by, however, with the different performances of various predictors, we can see that the inclusion probabilities begin to split up.

Secondly, predictors with major or minor contributions to predict carbon emissions in China are identified. It is clear that the proportion of industry production in GDP (IP) shows the greatest predictive power than others, while the growth rate of FDI to GDP (FDI) in China has the smallest forecasting ability. Interestingly, those Chinese household features, such as Engel's coefficient and household savings rate, are observed as the second and third important factors in explaining carbon emission in China. They provide more contributions than other factors from financial market, international trade, and technical progress sectors. That is to say, the household wealth and saving behavior are extremely important elements to determine China's family energy consumptions and thus have great predictive power for the carbon emission in China. Moreover, we also find that the proportion of value-added of the service sector to GDP (service added) has a large prediction ability to carbon emission in China. However, GDP per capita in China, an important index of macroeconomic development level, just makes moderate explanatory ability. Additionally, other factors except for those mentioned above, supply relatively small and similar forecasting power to carbon emission in China.

Finally, taking the time-varying trends for various inclusion probabilities into account, we get several interesting results as follows: first, although the IP index holds the largest forecasting weight among all the predictors, it clearly experiences a declining trend in its predictive power especially in recent years. Similarly, we also find the decreasing prediction power of the two household factors, i.e., Engel's coefficient and household saving since the year 2009. Then, it is worth mentioning that the proportion of value-added of the service sector to GDP (service added) presents not only a leading forecasting weight, but a continuous increasing prediction power in recent years. Notably, in 2016 and 2017, the inclusion probabilities assigned to service added becomes the second largest one among all the factors, implying its emerging status in explaining the carbon emission in China. In addition, other factors from financial markets, international trade, and technical progress have relatively small but increasing weights in recent years.

5.4. Robustness Checks of Model Forecasting Results. In this section, we utilize two alternative model evaluation methods to further check the forecasting performances of various predictive models. On the one hand, the forecasting directional accuracy of a model is also very important for investors and regulators' decision making. Degiannakis and Filis [65] opine that Direction-of-Change (DoC) is the core of market timing and portfolio trading strategies. Thus, following Degiannakis and Filis [65] and Zhang et al. [59], we adopt the Direction-of-Change (DoC) test as another model evaluation approach. In detail, DoC is a ratio that accounts for the accurate predictions to the total predictions in the direction of a forecasted variable by a model. Assuming that p_t is a dummy variable, it takes the value of 1 if the prediction model correctly forecasts the direction of carbon emission growth rate at time t, and 0 otherwise. It is defined as follows:

$$p_t = \begin{cases} 1, & \text{if } y_t > y_{t-1} \text{ and } \widehat{y}_t > y_{t-1}, \\ 1, & \text{if } y_t < y_{t-1} \text{ and } \widehat{y}_t < y_{t-1}, \\ 0, & \text{otherwise}, \end{cases} \tag{15}$$

where y_t and $\widehat{y}_t$ are the actual growth rate of carbon emission and the forecasted growth rate of carbon emission made by a specific model, respectively. Mathematically, the DoC ratio is $1/q \sum_{t=1}^{q} p_t$, where q is the length of the out-of-sample forecasting period. A larger DoC rate, e.g., close to 1, indicates a better forecasting of directional changes by a model. In order to investigate the statistical significance of directional accuracy, we also use PT statistic proposed by Pesaran and Timmermann [66]. The null hypothesis of PT tests is that the DoC rate of a prediction model is smaller than or equal to the DoC rate of random walk forecasts.

Table 5 reveals similar results to those reported in Tables 3 and 4: DMA and DMS methods, as well as the BMA and BMS, show very close DoC rates from 0.742 to 0.774, indicating that dynamic model combination (selection) methods can beat traditional TVP OLS and equal-weighted combination approaches in predicting the directional changes in the Chinese carbon emission growth rate. The constant coefficient (CC OLS) model, however, fails to pass the PT test with the lowest DoC rate of 0.548.

In addition, we employ the out-of-sample R^2 (R^2_{OOS}) criterion proposed by Campbell and Thompson [67] to assess prediction accuracy. The out-of-sample R^2 of a forecasting model is defined as follows:

$$R^2_{\text{OOS}} = 1 - \frac{\sum_{k=1}^{q} (y_k - \widehat{y}_k)^2}{\sum_{k=1}^{q} \left(y_k - \widehat{y}_{k,\text{bench}}\right)^2}, \tag{16}$$

where y_k, $\widehat{y}_k$, and $\widehat{y}_{k,\text{bench}}$ are, respectively, the actual growth rate of carbon emission, the forecasted growth rate of carbon emission made by a specific model, and the

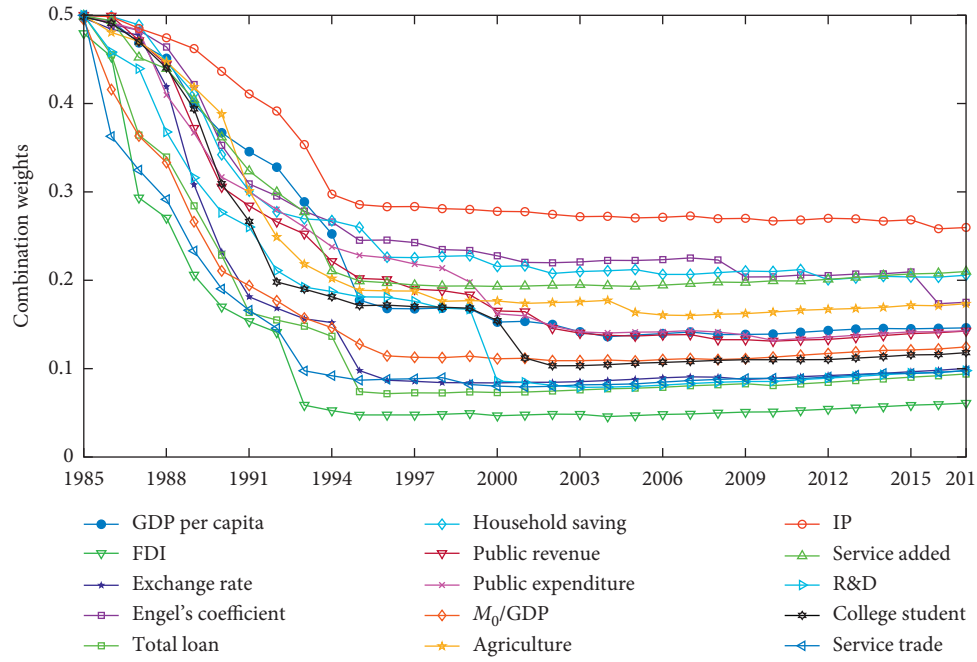

Figure 3: Inclusion probability (forecasting weights) for various nonenergy predictors.

Table 5: Results of Direction-of-Change test.

Models	DoC rate	PT statistic	p value
CC OLS	0.548	0.568	0.285
TVP OLS	0.710***	2.368	0.009
Equal weighted	0.677**	1.944	0.026
BMA	0.742***	2.771	0.003
BMS	0.774***	3.102	0.001
DMA95	0.677**	2.037	0.021
DMS95	0.774***	3.102	0.001
DMA99	0.742***	2.771	0.003
DMS99	0.774***	3.102	0.001

Notes: this table reports the Direction-of-Change (DoC) rates and the PT statistics of Pesaran and Timmermann [66] test for all forecasting approaches. Statistical significance for DoC rate is based on the p values of the PT statistic. Symbols *, **, and *** indicate the rejection of the null hypothesis at the 10%, 5%, and 1% significance level, respectively.

Table 6: Results of out-of-sample R-square test.

Models	R^2_{OOS} (%)	MSFE-adjusted	p value
TVP OLS	17.557**	1.952	0.025
Equal weighted	−28.813*	1.455	0.073
BMA	28.796**	2.323	0.010
BMS	27.980***	2.492	0.006
DMA95	28.869**	1.907	0.028
DMS95	27.569**	1.918	0.028
DMA99	29.102**	2.195	0.014
DMS99	28.140***	2.350	0.009

Notes: this table presents the out-of-sample prediction performance based on the out-of-sample R^2 test. The benchmark model is the CC OLS model. A positive value of out-of-sample R^2 implies that the forecasting model of interest has higher prediction accuracy than the benchmark model. Symbols *, **, and *** indicate the rejection of the null hypothesis at the 10%, 5%, and 1% significance level, respectively.

forecasted growth rate of carbon emission made by the benchmark model on time k and q represents the length of the out-of-sample period. In this paper, we set CC OLS as the benchmark model and compare its performance with others. The R^2_{OOS} statistic evaluates the percent reduction in mean squared forecast error (MSFE) of a forecasting model relative to the benchmark. A positive value of R^2_{OOS} indicates a superior forecasting accuracy of a specific model to the benchmark. To estimate the significance of improvement in MSFE obtained by one model, we use the Clark and West [68] statistic, which implies the null hypothesis that the MSFE of the benchmark model is not larger than the MSFE of the interested model. The Clark and West [68] statistic is defined as follows:

$$f_t = \left(y_k - \widehat{y}_{k,\text{bench}}\right)^2 - \left(y_k - \widehat{y}_k\right)^2 + \left(\widehat{y}_{k,\text{bench}} - \widehat{y}_k\right)^2, \quad (17)$$

where y_k, $\widehat{y}_k$, and $\widehat{y}_{k,\text{bench}}$ are, respectively, the actual growth rate of carbon emission, the forecasted growth rate of carbon emission made by a specific model, and the forecasted growth rate of carbon emission made by the benchmark model on time k, respectively. The MSFE-adjusted statistic is the t-statistic from the regression of f_t on a constant term. In addition, the p value of the statistic can be obtained from the standard normal distribution [68].

Table 6 also shows quite similar outcomes presented in Tables 3 to 5. On the one hand, DMA and DMS methods, as well as the BMA and BMS, exhibit alike out-of-sample R^2 ranging from about 27% to 29%, implying again the superior performances of dynamic model averaging (selection) models to the benchmark CC OLS. Among them, DMA99 and DMA95 are the best ones in all these methods. On the other hand, TVP OLS has better performance than the CC

OLS, while the equal-weighted combination method fails to beat the benchmark model.

6. Conclusions

A large amount of literature pays close attention to those energy-related factors regarding their roles in explaining or forecasting carbon emission in China. It is no surprise that those energy-related factors, such as energy consumption and energy intensity, have significantly great impacts on the China's carbon emission. This paper, in contrast, focuses on the prediction power of nonenergy factors from macroeconomy, financial markets, household features, and technical progress sectors in China from a time-varying perspective. This research may offer us a new viewpoint to identify the underlying determinants of China's carbon emission and help the policymakers to introduce innovative and effective regulations to reduce carbon emission in China.

The major findings are listed as follows. Firstly, the explanatory power of each predictor changes significantly with time and no predictors always keep positive or negative effects on China's carbon emissions throughout the sample period. Secondly, the proportion of industry production in GDP (IP) presents the largest prediction power among all the 15 predictors, but with a decreasing weight in recent years. Similarly, two indices from household features, i.e., Engel's coefficient and household savings rate are observed as the second and third important factors in forecasting carbon emission in China. Thirdly, the proportion of value-added of the service sector to GDP (service added) presents not only a leading forecasting weight, but a continuous increasing prediction power in recent years, especially since the year 2016. This result reveals that the development of service sector may bring significant changes in economic structure and energy consumption in China and thus gives more predictive power to future carbon emissions. Finally, in terms of forecasting methods, we find that individual constant coefficient (CC) and TVP models, as well as equal-weighted averaging method, cannot provide satisfactory forecasting accuracy for the growth rate of carbon emission in China. However, the dynamic model averaging method (DMA) can dominate other individual and combination methods no matter in two simple evaluation criteria of MSFE and MAFE or other rigorous statistical tests.

The empirical results obtained in this paper have several important policy implications for the Chinese policymakers. For example, first of all, the time-varying positive or negative impacts of various predictors on China's carbon emission suggest that policymakers should not make fixed administrative policies to the factors that have effects on China's carbon emission considered in this paper. Then, both the decreasing prediction power of IP and the increasing weight of service added reveal that the Chinese government should persist in promoting the development of service sector in economy, especially those modern service industries, such as communication, information technology, finance, logistics, education, and medical care. The sustainable developments in these industries may be effective ways to reduce carbon emission in China. We think that the Chinese regulators do right efforts in this direction with the evidence that the IP/GDP ratio decreases from about 44.6% in 1982 to about 40.4% in 2017, while the service added/GDP ratio increases sharply from about 22.6% in 1982 to about 51.6% in 2017. Finally, the household features measuring family wealth should also be concerned for their important roles in influencing the energy consumption behavior in Chinese families. The increasing wealth in China's family can accelerate more consumption in clean energy, i.e., solar, wind, and nuclear energy and thus reduce the carbon emission in China. Fortunately, in 2018, the Chinese government begins to massively cut taxes and administrative fees nationwide, which should have an optimistic impact on the reduction of China's carbon emission in the following years.

Data Availability

The data used in this paper are all confidential and are available by subscribers of the Wind database.

Conflicts of Interest

The authors declare no conflicts of interest.

Authors' Contributions

S.-Q. X. prepared the initial manuscript and the data collection. Y.-F. Z. made the empirical model estimations. X.-D. C. provided the pivotal idea of this research and the literature review. All authors have read and agreed to the published version of the manuscript.

Acknowledgments

This research was funded by the National Natural Science Foundation of China (71671145 and 71971191), Humanities and Social Science Fund of Ministry of Education of China (17YJA790015, 17XJA790002, 18YJC790132, and 18XJA790002), Science and Technology Innovation Team of Yunnan Provincial Universities (2019014), and Yunnan Fundamental Research Projects (202001AS070018).

References

[1] BP, *Statistical Review of World Energy 2020*, 2020, http://www.bp.com/statisticalreview, 69th edition.

[2] H. Iwata, K. Okada, and S. Samreth, "Empirical study on the determinants of CO_2 emissions: evidence from OECD countries," *Applied Economics*, vol. 44, no. 27, pp. 3513–3519, 2012.

[3] N. Apergis and J. E. Payne, "Renewable energy, output, CO_2 emissions, and fossil fuel prices in Central America: evidence from a nonlinear panel smooth transition vector error correction model," *Energy Economics*, vol. 42, pp. 226–232, 2014.

[4] C. F. Tang and B. W. Tan, "The impact of energy consumption, income and foreign direct investment on carbon dioxide emissions in Vietnam," *Energy*, vol. 79, pp. 447–454, 2015.

[5] E. M. Bildirici and T. Bakirtas, "The relationship among oil and coal consumption, carbon dioxide emissions, and

economic growth in BRICTS countries," *Journal of Renewable and Sustainable Energy*, vol. 8, Article ID 045903, 2016.

[6] K. Dong, R. Sun, H. Jiang, and X. Zeng, "CO_2 emissions, economic growth, and the environmental Kuznets curve in China: what roles can nuclear energy and renewable energy play?" *Journal of Cleaner Production*, vol. 196, pp. 51–63, 2018.

[7] S. A. Raza, N. Shah, and A. Sharif, "Time frequency relationship between energy consumption, economic growth and environmental degradation in the United States: evidence from transportation sector," *Energy*, vol. 173, pp. 706–720, 2019.

[8] Z. D. Shabani and R. Shahnazi, "Energy consumption, carbon dioxide emissions, information and communications technology, and gross domestic product in Iranian economic sectors: a panel causality analysis," *Energy*, vol. 169, pp. 1064–1078, 2019.

[9] A. Valadkhani, R. Smyth, and J. Nguyen, "Effects of primary energy consumption on CO_2 emissions under optimal thresholds: evidence from sixty countries over the last half century," *Energy Economics*, vol. 80, pp. 680–690, 2019.

[10] X.-t. Jiang, Q. Wang, and R. Li, "Investigating factors affecting carbon emission in China and the USA: a perspective of stratified heterogeneity," *Journal of Cleaner Production*, vol. 199, pp. 85–92, 2018.

[11] Y. Zhang and S. Zhang, "The impacts of GDP, trade structure, exchange rate and FDI inflows on China's carbon emissions," *Energy Policy*, vol. 120, pp. 347–353, 2018.

[12] G. Koop and D. Korobilis, "Forecasting inflation using dynamic model averaging," *International Economic Review*, vol. 53, no. 3, pp. 867–886, 2012.

[13] D. E. Rapach and J. K. Strauss, "Differences in housing price forecastability across US states," *International Journal of Forecasting*, vol. 25, no. 2, pp. 351–372, 2009.

[14] L. Kristoufek, K. Janda, and D. Zilberman, "Correlations between biofuels and related commodities before and during the food crisis: a taxonomy perspective," *Energy Economics*, vol. 34, no. 5, pp. 1380–1391, 2012.

[15] E. Ghysels, A. Plazzi, R. Valkanov, and W. Torous, "Forecasting real estate prices," in *Handbook of Economic Forecasting*, G. Elliott and A. Timmermann, Eds., Elsevier, Amsterdam, Netherlands, 2013.

[16] O. Nneji, C. Brooks, and C. W. R. Ward, "House price dynamics and their reaction to macroeconomic changes," *Economic Modelling*, vol. 32, pp. 172–178, 2013.

[17] V. Plakandaras, R. Gupta, P. Gogas, and T. Papadimitriou, "Forecasting the U.S. real house price index," *Economic Modelling*, vol. 45, pp. 259–267, 2015.

[18] F. Collingro and M. Frenkel, "On the financial market impact of euro area monetary policy: a comparative study before and after the Global Financial Crisis," *Global Finance Journal*, 2019.

[19] M. Próchniak and B. Witkowski, "Time stability of the beta convergence among EU countries: Bayesian model averaging perspective," *Economic Modelling*, vol. 30, pp. 322–333, 2013.

[20] A. Vasnev, M. Skirtun, and L. Pauwels, "Forecasting monetary policy decisions in Australia: a forecast combinations approach," *Journal of Forecasting*, vol. 32, no. 2, pp. 151–166, 2013.

[21] G. Man, "Competition and the growth of nations: international evidence from Bayesian model averaging," *Economic Modelling*, vol. 51, pp. 491–501, 2015.

[22] J. Nowotarski, E. Raviv, S. Trück, and R. Weron, "An empirical comparison of alternative schemes for combining electricity spot price forecasts," *Energy Economics*, vol. 46, pp. 395–412, 2014.

[23] A. E. Raftery, M. Kárný, and P. Ettler, "Online prediction under model uncertainty via dynamic model averaging: application to a cold rolling mill," *Technometrics*, vol. 52, no. 1, pp. 52–66, 2010.

[24] Y. Wei and Y. Cao, "Forecasting house prices using dynamic model averaging approach: evidence from China," *Economic Modelling*, vol. 61, pp. 147–155, 2017.

[25] Y. Wei, J. Liu, X. Lai, and Y. Hu, "Which determinant is the most informative in forecasting crude oil market volatility: fundamental, speculation, or uncertainty?" *Energy Economics*, vol. 68, pp. 141–150, 2017.

[26] H. Naser and F. Alaali, "Can oil prices help predict US stock market returns? Evidence using a dynamic model averaging (DMA) approach," *Empirical Economics*, vol. 55, no. 4, pp. 1757–1777, 2018.

[27] V. Plakandaras, R. Gupta, and W.-K. Wong, "Point and density forecasts of oil returns: the role of geopolitical risks," *Resources Policy*, vol. 62, pp. 580–587, 2019.

[28] C. Zhang and Z. Tan, "The relationships between population factors and China's carbon emissions: does population aging matter?" *Renewable and Sustainable Energy Reviews*, vol. 65, pp. 1018–1025, 2016.

[29] Y. Guan, L. Kang, C. Shao, P. Wang, and M. Ju, "Measuring county-level heterogeneity of CO_2 emissions attributed to energy consumption: a case study in Ningxia Hui Autonomous Region, China," *Journal of Cleaner Production*, vol. 142, pp. 3471–3481, 2017.

[30] L. Shi, J. Sun, J. Lin, and Y. Zhao, "Factor decomposition of carbon emissions in Chinese megacities," *Journal of Environmental Sciences*, vol. 75, pp. 209–215, 2019.

[31] X. Yao, D. Kou, S. Shao, X. Li, W. Wang, and C. Zhang, "Can urbanization process and carbon emission abatement be harmonious? new evidence from China," *Environmental Impact Assessment Review*, vol. 71, pp. 70–83, 2018.

[32] Q. Zhu and X. Peng, "The impacts of population change on carbon emissions in China during 1978–2008," *Environmental Impact Assessment Review*, vol. 36, pp. 1–8, 2012.

[33] S.-C. Ma, Y. Fan, and L. Feng, "An evaluation of government incentives for new energy vehicles in China focusing on vehicle purchasing restrictions," *Energy Policy*, vol. 110, pp. 609–618, 2017.

[34] H. Meng, X. Huang, H. Yang et al., "The influence of local officials' promotion incentives on carbon emission in Yangtze River Delta, China," *Journal of Cleaner Production*, vol. 213, pp. 1337–1345, 2019.

[35] Y. Wei, X. Zhu, Y. Li, T. Yao, and Y. Tao, "Influential factors of national and regional CO_2 emission in China based on combined model of DPSIR and PLS-SEM," *Journal of Cleaner Production*, vol. 212, pp. 698–712, 2019.

[36] X. Ma, C. Wang, B. Dong et al., "Carbon emissions from energy consumption in China: its measurement and driving factors," *Science of the Total Environment*, vol. 648, pp. 1411–1420, 2019.

[37] J. Chen, Q. Shi, L. Shen, Y. Huang, and Y. Wu, "What makes the difference in construction carbon emissions between China and USA?" *Sustainable Cities and Society*, vol. 44, pp. 604–613, 2019.

[38] J. Kang, T. Zhao, N. Liu, X. Zhang, X. Xu, and T. Lin, "A multi-sectoral decomposition analysis of city-level greenhouse gas emissions: case study of Tianjin, China," *Energy*, vol. 68, pp. 562–571, 2014.

[39] Z. Wang and L. Yang, "Delinking indicators on regional industry development and carbon emissions: Beijing-Tianjin-Hebei economic band case," *Ecological Indicators*, vol. 48, pp. 41–48, 2015.

[40] X.-W. Ma, Y. Ye, X.-Q. Shi, and L.-L. Zou, "Decoupling economic growth from CO_2 emissions: a decomposition analysis of China's household energy consumption," *Advances in Climate Change Research*, vol. 7, no. 3, pp. 192–200, 2016.

[41] C. Shuai, X. Chen, Y. Wu, Y. Tan, Y. Zhang, and L. Shen, "Identifying the key impact factors of carbon emission in China: results from a largely expanded pool of potential impact factors," *Journal of Cleaner Production*, vol. 175, pp. 612–623, 2018.

[42] A. Jalil and M. Feridun, "The impact of growth, energy and financial development on the environment in China: a cointegration analysis," *Energy Economics*, vol. 33, no. 2, pp. 284–291, 2011.

[43] M. Liao and T. Wu, "The empirical analysis of the impact of industrial structure on carbon emissions," in *Communication Systems and Information Technology*, Springer, Berlin, Germany, 2011.

[44] H. Xu, Y. Li, and H. Huang, "Spatial research on the effect of financial structure on CO_2 emission," *Energy Procedia*, vol. 118, pp. 179–183, 2017.

[45] Y.-J. Zhang, Y.-L. Peng, C.-Q. Ma, and B. Shen, "Can environmental innovation facilitate carbon emissions reduction? Evidence from China," *Energy Policy*, vol. 100, pp. 18–28, 2017.

[46] Z. Zhou, C. Liu, X. Zeng, Y. Jiang, and W. Liu, "Carbon emission performance evaluation and allocation in Chinese cities," *Journal of Cleaner Production*, vol. 172, pp. 1254–1272, 2018.

[47] J.-L. Mo, P. Agnolucci, M.-R. Jiang, and Y. Fan, "The impact of Chinese carbon emission trading scheme (ETS) on low carbon energy (LCE) investment," *Energy Policy*, vol. 89, pp. 271–283, 2016.

[48] R. J. R. Elliott, P. Sun, and S. Chen, "Energy intensity and foreign direct investment: a Chinese city-level study," *Energy Economics*, vol. 40, pp. 484–494, 2013.

[49] J. W. Lee, "The contribution of foreign direct investment to clean energy use, carbon emissions and economic growth," *Energy Policy*, vol. 55, pp. 483–489, 2013.

[50] A. Omri, S. Daly, C. Rault, and A. Chaibi, "Financial development, environmental quality, trade and economic growth: what causes what in MENA countries," *Energy Economics*, vol. 48, pp. 242–252, 2015.

[51] J. A. Frankel and D. Romer, "Does trade cause growth?" *American Economic Review*, vol. 89, no. 3, pp. 379–399, 1999.

[52] P. Sadorsky, "Financial development and energy consumption in Central and Eastern European frontier economies," *Energy Policy*, vol. 39, no. 2, pp. 999–1006, 2011.

[53] S. Iamsiraroj, "The foreign direct investment-economic growth nexus," *International Review of Economics & Finance*, vol. 42, pp. 116–133, 2016.

[54] H. Nasir, S. Majeed, and A. Aleem, "Does financial development leads economic growth? Evidence from emerging asian markets," *Asian Economic and Financial Review*, vol. 8, no. 5, pp. 599–617, 2018.

[55] Y.-J. Zhang, "The impact of financial development on carbon emissions: an empirical analysis in China," *Energy Policy*, vol. 39, no. 4, pp. 2197–2203, 2011.

[56] G. E. Primiceri, "Time varying structural vector autoregressions and monetary policy," *The Review of Economic Studies*, vol. 72, no. 3, pp. 821–852, 2005.

[57] G. Koop, R. Leon-Gonzalez, and R. W. Strachan, "On the evolution of the monetary policy transmission mechanism," *Journal of Economic Dynamics and Control*, vol. 33, no. 4, pp. 997–1017, 2009.

[58] P. R. Hansen, A. Lunde, and J. M. Nason, "The model confidence set," *Econometrica*, vol. 79, pp. 453–497, 2011.

[59] Y. Zhang, Y. Wei, Y. Zhang, and D. Jin, "Forecasting oil price volatility: forecast combination versus shrinkage method," *Energy Economics*, vol. 80, pp. 423–433, 2019.

[60] F. X. Diebold and R. S. Mariano, "Comparing predictive accuracy," *Journal of Business & Economic Statistics*, vol. 13, no. 3, pp. 253–263, 1995.

[61] K. D. West, "Asymptotic inference about predictive ability," *Econometrica*, vol. 64, no. 5, pp. 1067–1084, 1996.

[62] H. White, "A reality check for data snooping," *Econometrica*, vol. 68, no. 5, pp. 1097–1126, 2000.

[63] P. R. Hansen, "A test for superior predictive ability," *Journal of Business & Economic Statistics*, vol. 23, no. 4, pp. 365–380, 2005.

[64] M. L. Higgins and S. Mishra, "Testing forecast rationality under asymmetric loss with the Mincer-Zarnowitz regression," *Journal of Quantitative Economics*, vol. 7, pp. 59–72, 2009.

[65] S. Degiannakis and G. Filis, "Forecasting oil price realized volatility using information channels from other asset classes," *Journal of International Money and Finance*, vol. 76, pp. 28–49, 2017.

[66] M. H. Pesaran and A. Timmermann, "A simple nonparametric test of predictive performance," *Journal of Business & Economic Statistics*, vol. 10, no. 4, pp. 461–465, 1992.

[67] J. Y. Campbell and S. B. Thompson, "Predicting excess stock returns out of sample: can anything beat the historical average?" *Review of Financial Studies*, vol. 21, no. 4, pp. 1509–1531, 2008.

[68] T. E. Clark and K. D. West, "Approximately normal tests for equal predictive accuracy in nested models," *Journal of Econometrics*, vol. 138, no. 1, pp. 291–311, 2007.

Hindawi
Discrete Dynamics in Nature and Society
Volume 2020, Article ID 9673623, 23 pages
https://doi.org/10.1155/2020/9673623

Research Article

A Time-Varying Multivariate Noncentral Contaminated Normal Copula Model and Its Application to the Visualized Dependence Analysis of Hong Kong Stock Markets

Zhenyu Xiao,[1] Jie Wang,[2] Teng Yuan Cheng,[1] and Kuiran Shi[1]

[1]*School of Finance, Nanjing Audit University, Jiangsu, Nanjing 211815, China*
[2]*School of Business, Shaoxing University, Shaoxing, Zhejiang 312000, China*

Correspondence should be addressed to Teng Yuan Cheng; tybrian@gmail.com

Received 27 July 2020; Revised 18 September 2020; Accepted 29 September 2020; Published 22 October 2020

Academic Editor: Dehua Shen

Financial data usually have the features of complexity and interdependence structure, such as asymmetric, tail, and time-varying dependence. This study constructs a new multivariate skewed fat-tailed copula, namely, noncentral contaminated normal (NCCN) copula, to analyze the dependent structure of financial market data. The dynamic conditional correlation (DCC) model is also incorporated into constructing the time-varying NCCN copula model. This study comprehensively examines the effects of the DCC-NCCN copula and related models on fitting dependence structures of Hong Kong stock markets. The results show that the DCC-NCCN copula model can better depict the dependence structures of returns. Considering the flexibility and complexity, the DCC-NCCN copula model is a relatively ideal, time-varying, multivariate skewed fat-tailed copula model.

1. Introduction

After suffering from loss in the stock market, Isaac Newton ever said that "I can calculate the motions of the heavenly bodies, but not the madness of people." This reflects the complexity of financial markets. In general, the financial asset return series have relatively complex interdependence structural features, such as asymmetric dependence, tail dependence, and time-varying dependence. According to whether it can depict asymmetric dependence and fat-tailed dependence, copula can be divided into four categories: symmetric thin-tailed copula, symmetric fat-tailed copula, skewed thin-tailed copula, and skewed fat-tailed copula. The examples above are normal copula, t-copula, skew-normal copula, and skew-t-copula. The multivariate skew-normal copula is the copula of the multivariate skew-normal distribution, such as Wei et al. [1] proposed the copula of the multivariate skew-normal distribution of Azzalini and Valle [2]. The multivariate skew-t-copula is the copula of the multivariate skew-t distribution, such as Demarta and McNeil [3] proposed the copula of the multivariate generalized hyperbolic skew-t (GHST) distribution of Barndorff-Nielsen [4]. Kollo and Pettere [5] propose the copula of the multivariate skew-t distribution of Azzalini and Capitanio [6]; Smith et al. [7] put forth the copula of the multivariate skew-t distribution of Sahu et al. [8]; and Liu et al. [9] advanced the copula of the multivariate extended skew-t (EST) distribution by Arellano-Valle and Genton [10].

Although these multivariate skew-t copulas are very flexible, they are also highly complex and challenging to apply. Considering both flexibility and complexity, these multivariate skew-t copulas may not be very ideal. This study constructs a new multivariate skewed fat-tailed distribution, namely, the multivariate noncentral contaminated normal (NCCN) distribution. The multivariate NCCN distribution can be interpreted as a multivariate noncentral normal scale mixture distribution, which is similar to the multivariate normal variance-mean mixture distribution and multivariate skew-normal scale mixture distribution. The multivariate NCCN distribution can also be interpreted as a simplified mixture of two multivariate normal distributions.

Then, the copula of the multivariate NCCN distribution can be called the multivariate NCCN copula. Note that the multivariate NCCN copula cannot be interpreted as a mixture of two multivariate normal copulas. The NCCN copula may be relatively ideal. The advantages are shown as follows. First, the NCCN copula can flexibly describe positive and negative dependence. Second, according to Mardia's kurtosis, the NCCN copula has stronger tail dependence than the normal copula. Third, the NCCN copula can flexibly describe asymmetric dependence. Fourth, the subclasses of the NCCN copula include normal copula and contaminated normal (CN) copula. Note that the flexibility of the CN copula is similar to the t-copula, but the complexity of the CN copula is significantly lower than that of the t-copula. Fifth, NCCN copula is suitable for two- and higher-dimensional dependence structure modeling. Sixth and the last, the flexibility of the NCCN copula is similar to that of skew-t copulas, but the complexity of the NCCN copula is significantly lower than that of skew-t copulas.

According to whether it can delineate the time-varying dependence, the copula can be divided into two classes: static copula and dynamic one. There are many options in modeling dynamic structures, including the time-varying parameter model [11], the dynamic conditional correlation (DCC) model [12] and the dynamic condition-related improvement (DCC-Student-t) model [13], the time-varying correlation (TVC) model [14], the asymmetric DCC (ADCC) model [15,16], and the generalized autoregressive score (GAS) model [17]. These dynamic models have pros and cons, and we compare them as follows. The advantage of the Patton model is that it does not limit the type of time-varying parameters, and the dynamic structure is relatively simple; the disadvantage is that the dimension is limited to two dimensions, and the meaning to interpret the dynamic structure is not very clear. The advantages of the DCC model and TVC model are as follows: dimension is unlimited, the dynamic structure is simple, and the interpretation meaning of the dynamic structure is clear; the disadvantage is to limit the type of time-varying parameters to the linear correlation matrix. The advantage of the ADCC model is that it further considers asymmetric dynamics based on the DCC model. For the GAS model, the advantages are unlimited dimension and time-varying parameter type. The interpretation of the dynamic structure is relatively definite. The disadvantage is that the dynamic structure is generally quite complex. There are only a few studies on the dynamic multivariate skewed fat-tailed copula, mainly including the dynamic asymmetric copula (DAC) model given by Christoffersen et al. [18], GAS-GHST copula model [19], and dynamic double asymmetric copula (DDAC) model [20]. The above dynamic structures provide ample potential options for building the time-varying NCCN copula.

The contributions of this paper are as follows. First, a new multivariate skewed fat-tailed distribution, namely, multivariate NCCN distribution, is constructed. Second, the copula of the multivariate NCCN distribution, namely, multivariate NCCN copula, is proposed. Third, we adopt the DCC model to construct a new time-varying copula model, namely, DCC-NCCN copula model. The last, employing the Hang Seng Index (HSI), Hang Seng China Enterprises Index (CEI), and Hang Seng China-Affiliated Corporations Index (CCI) as our sample data, we compare the fitting effects of the DCC-NCCN copula model with some other copula models and perform the visualized dependence analysis of Hong Kong stock markets.

2. Model Development

2.1. Fundamental Theory of the Copula. A copula is a multivariate cumulative distribution function (cdf) with uniform univariate margins and can be used to link univariate margins to a joint cdf. According to Sklar's theorem, for a d-dimensional random vector $(X_1, \ldots, X_d)$ with joint cdf $F(x_1, \ldots, x_d)$ and marginal cdfs $F_1(x_1), \ldots, F_d(x_d)$, there exists a copula function C: $[0,1]^d \longrightarrow [0,1]$ such that

$$F(x_1, \ldots, x_d) = C(F_1(x_1), \ldots, F_d(x_d)). \tag{1}$$

The copula is unique if the random vector is continuous. For a continuous random vector $(X_1, \ldots, X_d)$ with joint cdf $F(x_1, \ldots, x_d)$, joint probability density function (pdf) $f(x_1, \ldots, x_d)$, marginal cdfs $F_1(x_1), \ldots, F_d(x_d)$, marginal pdfs $f_1(x_1), \ldots, f_d(x_d)$, and marginal quantile functions $F_1^{-1}(u_1), \ldots, F_d^{-1}(u_d)$, the copula function and its pdf are, respectively, given by

$$C(u_1, \ldots, u_d) = F\left(F_1^{-1}(u_1), \ldots, F_d^{-1}(u_d)\right),$$

$$c(u_1, \ldots, u_d) = \frac{\partial^d C(u_1, \ldots, u_d)}{\partial u_1, \ldots, \partial u_d} = \frac{f\left(F_1^{-1}(u_1), \ldots, F_d^{-1}(u_d)\right)}{\prod_{i=1}^{d} f_i\left(F_i^{-1}(u_i)\right)}, \tag{2}$$

where $(u_1, \ldots, u_d) \in [0,1]^d$. According to Sklar's theorem, we can quickly get the copula of a given multivariate distribution. In particular, $F_1(X_1), \ldots, F_d(X_d)$ can be called the uniform scores of the random variables $X_1, \ldots, X_d$, and $\Phi^{-1}(F_1(X_1)), \ldots, \Phi^{-1}(F_d(X_d))$ can be called the normal scores of the random variables $X_1, \ldots, X_d$, where Φ^{-1} is the quantile function of the univariate standard normal distribution. Clearly, the uniform score follows the univariate uniform distribution on $[0,1]$, and the normal score follows the univariate standard normal distribution.

The copula function is closely related to many dependence measures, such as Kendall's tau, quantile dependence (QD) coefficient, and Mardia's skewness and kurtosis of normal scores. These dependence measures are briefly described in the following.

Kendall's tau is also called Kendall's rank correlation coefficient. It can be utilized to measure global dependence. Let (X_1, X_2) and (Y_1, Y_2) be independent and identically distributed random vectors. For the bivariate continuous random vector (X_1, X_2) with joint cdf $F(x_1, x_2)$, copula function $C(u_1, u_2)$, and uniform scores (U_1, U_2), bivariate Kendall's tau is given by

$$\begin{aligned}\tau(X_1, X_2) &= P[(X_1 - Y_1)(X_2 - Y_2) > 0] \\ &\quad - P[(X_1 - Y_1)(X_2 - Y_2) < 0] \\ &= 2P[(X_1 - Y_1)(X_2 - Y_2) > 0] \\ &\quad - 1 = 4P(X_1 < Y_1, X_2 < Y_2) - 1 \\ &= 4E[F(X_1, X_2)] - 1 = 4E[C(U_1, U_2)] - 1.\end{aligned} \tag{3}$$

The value range of bivariate Kendall's tau is $[-1, 1]$. Bivariate Kendall's tau can be interpreted as the probability of concordance minus the probability of discordance.

The quantile dependence coefficient can be used to measure local dependence. For a bivariate continuous random vector (X_1, X_2) with copula function $C(u_1, u_2)$ and uniform scores (U_1, U_2), the bivariate lower-lower (lower), upper-upper (upper), upper-lower, and lower-upper quantile dependence coefficients (LLQD, UUQD, ULQD, and LUQD) are, respectively, given by

$$\begin{aligned}\lambda_{00}(X_1, X_2) &= P(U_2 \le q | U_1 \le q) = \frac{C(q, q)}{q}, \\ \lambda_{11}(X_1, X_2) &= P(1 - U_2 \le q | 1 - U_1 \le q) \\ &= \frac{[2q - 1 + C(1 - q, 1 - q)]}{q}, \\ \lambda_{10}(X_1, X_2) &= P(U_2 \le q | 1 - U_1 \le q) = \frac{[q - C(1 - q, q)]}{q}, \\ \lambda_{01}(X_1, X_2) &= P(1 - U_2 \le q | U_1 \le q) = \frac{[q - C(q, 1 - q)]}{q},\end{aligned} \tag{4}$$

where $q \in [0, 1]$ is the quantile level. The value range of bivariate quantile dependence coefficients is $[0, 1]$. If $q = 1$, then $\lambda_{00} = \lambda_{11} = \lambda_{10} = \lambda_{01} = 1$. If $q = (1/2)$, then $\lambda_{00} = \lambda_{11} = 2C(1/2), (1/2)$ and $\lambda_{10} = \lambda_{01} = 1 - 2C(1/2), (1/2)$. If $q \longrightarrow 0$, we can get the bivariate tail dependence coefficients (LLTD, UUTD, ULTD, and LUTD).

Mardia [21] proposed Mardia's skewness and kurtosis. For a multivariate continuous random vector X with mean vector μ and covariance matrix Σ, Mardia's skewness and kurtosis are, respectively, given by

$$\begin{aligned}\beta_1(X) &= E\left\{\left[(X - \mu)\prime\Sigma^{-1}(Y - \mu)\right]^3\right\}, \\ \beta_2(X) &= E\left\{\left[(X - \mu)\prime\Sigma^{-1}(X - \mu)\right]^2\right\},\end{aligned} \tag{5}$$

where Y and X are independent identically distributed random vectors. For a multivariate continuous random vector with the multivariate normal distribution, multivariate Mardia's skewness and kurtosis are 0 and $d(d + 2)$, respectively. Mardia's skewness and kurtosis of normal scores can also be called Gaussian skewness and kurtosis. Gaussian skewness and kurtosis can be used to measure the asymmetric dependence and tail dependence, respectively. Note that the Gaussian skewness cannot measure the direction of asymmetric dependence. For a multivariate random vector with the multivariate normal copula, Mardia's skewness and kurtosis are not clear, but the Gaussian skewness and kurtosis are 0 and $d(d + 2)$, respectively. Note that the tail dependence coefficients cannot reasonably distinguish the strength of tail dependence. The two copulas with the same tail dependence coefficients may have different Gaussian kurtosis.

2.2. Nonlinear Asymmetric GARCH (NAGARCH) Model. Before modeling the dependence structure, we need to model the marginal distribution. This study adopts the NAGARCH model of Engle and Ng [22] to describe the dynamics of financial asset return series. The parameterization form of the NAGARCH model is not unique, and the distribution assumption is not unique. To easily explain the parameter of the NAGARCH model, this paper adopts a variance targeting (VT) form. To avoid the distribution specification error, this paper does not assume a specific distribution. We set the NAGARCH model:

$$\begin{cases} y_t = \mu + \varepsilon_t = \mu + \sigma_t z_t, \\ \mu = \dfrac{1}{T}\displaystyle\sum_{t=1}^{T} y_t, \\ \sigma_1^2 = \sigma^2 = \dfrac{1}{T}\displaystyle\sum_{t=1}^{T} \varepsilon_t^2, \\ \sigma_{t+1}^2 = (1 - \beta)\sigma^2 + \beta\sigma_t^2 + \alpha\left(\varepsilon_t^2 - \sigma_t^2 + 2\gamma\sigma_t\varepsilon_t\right), \\ \widehat{\theta} = \arg\max\limits_{\theta} \displaystyle\sum_{t=1}^{T}\left(-\ln\sigma_t - \frac{1}{2}z_t^2\right), \quad \theta = (\alpha, \beta, \gamma), \\ \alpha \ge 0, \\ \beta \in (0, 1), \\ \gamma \in \mathbb{R}, \\ \alpha\left(1 + \gamma^2\right) \le \beta, \end{cases} \tag{6}$$

where y_t is the return, μ is the unconditional mean, σ is the unconditional standard deviation, σ_t is the conditional standard deviation, ε_t is the residual with mean 0, and z_t is the standardized residual with mean 0 and variance 1.

The conditional variance σ_{t+1}^2 can be interpreted as the asymmetric information shock item $(\varepsilon_t^2 - \sigma_t^2 + 2\gamma\sigma_t\varepsilon_t)$ plus

the weighted average of unconditional variance σ^2 and lagged conditional variance σ_t^2. This equation makes the parameter representation clearer. Parameter α can control the dynamics of the conditional variance: the larger α, the stronger the dynamics of the conditional variance. In particular, when $\alpha = 0$, the model is a constant volatility model. Parameter β can control the clustering and mean reversion of the conditional variance: when β is close to 1, the conditional variance shows stronger clustering and weaker mean reversion; when β is close to 0, the conditional variance shows weaker clustering and stronger mean reversion. Parameter γ can control the asymmetric dynamics of the conditional variance: when $\gamma > 0$, the conditional variance has a positive asymmetry; when $\gamma < 0$, the conditional variance has a negative asymmetry, and the negative value impacts more on the conditional variance than the same degree of a positive one. In particular, when $\gamma = 0$, the model is the GARCH model. The conditional variance equation can also be expressed as

$$\sigma_{t+1}^2 = (1-\beta)\sigma^2 + \left[\beta - \alpha\left(1+\gamma^2\right)\right]\sigma_t^2 + \alpha\left(\varepsilon_t + \gamma\sigma_t\right)^2. \quad (7)$$

Clearly, all conditional variances can be insured to be greater than 0 under given parameter constraints.

In terms of parameter estimation, we adopt the quasi-maximum likelihood (QML) method to estimate the parameters of the NAGARCH model, that is, to apply the maximum likelihood (ML) method to conduct the estimation of the parameters of the NAGARCH-normal model.

The NAGARCH model is used to filter the return series to obtain the standardized residual series. Then, using the empirical cdf, we transform the standardized residual series into the uniform scores. For a standardized residual series $\{z_t\}_{t=1}^T$, the empirical cdf is

$$F_E(z) = \frac{1}{T+1}\sum_{t=1}^{T} I\left(z_t \le z\right), \quad (8)$$

where $I(\cdot)$ is the indicator function. The uniform scores can be applied to further model the dependence structures.

2.3. Multivariate NCCN Distribution and Multivariate NCCN Copula. We firstly introduce the multivariate NCCN distribution. Because the location and scale parameters of the multivariate NCCN distribution cannot influence the multivariate NCCN copula [23], this paper does not take the location and scale parameters into account when defining the multivariate NCCN distribution.

Let $\phi(x)$ and $\Phi(x)$ be the pdf and cdf of the univariate standard normal distribution $N(0,1)$, $\phi_2(x,y;\rho)$ and $\Phi_2(x,y;\rho)$ be joint the pdf and joint cdf of the bivariate standard normal distribution $N_2(0,0,1,1,\rho)$ with the linear correlation coefficient ρ, and $\phi_d(x;R)$ and $\Phi_d(x;R)$ be the joint pdf and joint cdf of the multivariate standard normal distribution $N_d(0,R)$ with the linear correlation matrix R. $\phi(x)$, $\phi_2(x,y;\rho)$, and $\phi_d(x;R)$ can be expressed as:

$$\begin{aligned}
\phi(x) &= \frac{1}{\sqrt{2\pi}}\exp\left(-\frac{1}{2}x^2\right), \quad x \in \mathbb{R},\\
\phi_2(x,y;\rho) &= \frac{1}{2\pi\sqrt{1-\rho^2}}\exp\left(-\frac{x^2 - 2\rho xy + y^2}{2\left(1-\rho^2\right)}\right), \quad (x,y) \in \mathbb{R}^2,\\
\phi_d(x;R) &= \frac{1}{(2\pi)^{d/2}|R|^{1/2}}\exp\left(-\frac{1}{2}x' R^{-1} x\right), \quad x \in \mathbb{R}^d.
\end{aligned} \quad (9)$$

The multivariate NCCN distribution can be interpreted as a multivariate noncentral normal scale mixture distribution [24]. The stochastic representation of the multivariate NCCN distribution can be given by

$$\begin{cases}
X = (X_1, \ldots, X_d)' = \sqrt{W}\, Z,\\
Z = (Z_1, \ldots, Z_d)' \sim N_d(\gamma, R),\\
P(W = a) = 1 - p,\\
P(W = b) = p,\\
a \in (0,1),\\
p \in (0,1),\\
\gamma = (\gamma_1, \ldots, \gamma_d)' \in \mathbb{R}^d,\\
(1-p)a + pb = 1,
\end{cases} \quad (10)$$

where the random vector X follows the NCCN distribution. The random vector Z follows the multivariate noncentral normal distribution with correlation matrix R and noncentral parameter vector γ. The random variable W is a two-point distribution with probability parameter p, shape parameter a, and mean 1. Z and W are independent of each other.

The multivariate NCCN distribution can also be interpreted as a simplified mixture of two multivariate normal distributions [25]. The stochastic representation of the multivariate NCCN distribution can also be given by

$$\begin{cases}
X = (X_1, \ldots, X_d)\prime,\\
P\left[\dfrac{X}{\sqrt{a}} \sim N_d(\gamma, R)\right] = 1 - p,\\
P\left[\dfrac{X}{\sqrt{b}} \sim N_d(\gamma, R)\right] = p,\\
a \in (0,1),\\
p \in (0,1),\\
\gamma = (\gamma_1, \ldots, \gamma_d)\prime \in \mathbb{R}^d,\\
(1-p)a + pb = 1.
\end{cases} \quad (11)$$

The parameters of the multivariate NCCN distribution can be divided into three parts: (1) a correlation matrix R, (2) two tail parameters a and p, and (3) a skewness vector γ. According to the two stochastic representations, the joint cdf and pdf of the multivariate NCCN distribution can be easily given by

$$\begin{aligned}\mathrm{NCCN}_d(x;R,a,p,\gamma) &= (1-p)\Phi_d\left(\frac{x}{\sqrt{a}}-\gamma;R\right)\\ &\quad + p\Phi_d\left(\frac{x}{\sqrt{b}}-\gamma;R\right),\\ \mathrm{nccn}_d(x;R,a,p,\gamma) &= \frac{1-p}{a^{d/2}}\phi_d\left(\frac{x}{\sqrt{a}}-\gamma;R\right)\\ &\quad + \frac{p}{b^{d/2}}\phi_d\left(\frac{x}{\sqrt{b}}-\gamma;R\right),\end{aligned} \tag{12}$$

where $x=(x_1,\ldots,x_d)\prime\in\mathbb{R}^d$, $(1-p)a+pb=1$, R is a correlation matrix, $a\in(0,1)$, $p\in(0,1)$, and $\gamma=(\gamma_1,\ldots,\gamma_d)\prime\in\mathbb{R}^d$. The multivariate NCCN distribution family includes multivariate contaminated normal (CN) distribution when $\gamma=0$ and multivariate normal distribution $N_d(\gamma,R)$ when $a\longrightarrow 1$ or $p\longrightarrow 1$.

The mean vector, covariance matrix, and linear correlation matrix of the multivariate NCCN distribution are, respectively, given as equations (13)–(15):

$$E(X)=E(\sqrt{W})\gamma=[(1-p)\sqrt{a}+p\sqrt{b}\,]\gamma, \tag{13}$$

$$\mathrm{Cov}(X)=E(XX\prime)-E(X)E(X)\prime=R+D(\sqrt{W})\gamma\gamma\prime, \tag{14}$$

$$\mathrm{Corr}(X)=\mathrm{diag}(\mathrm{Cov}(X))^{-(1/2)}\mathrm{Cov}(X)\mathrm{diag}(\mathrm{Cov}(X))^{-(1/2)}. \tag{15}$$

Obviously, matrix R is not the linear correlation matrix of the multivariate NCCN distribution. For the multivariate CN distribution, $E(X)=0$, $\mathrm{Cov}(X)=\mathrm{Corr}(X)=R$, Mardia's skewness is 0 and Mardia's kurtosis is $d(d+2)\,E(W^2)=d(d+2)[1+(1-a)^2((1/p)-1)]\in(d(d+2),+\infty)$.

As to the two stochastic representations, any bivariate marginal distribution of the multivariate NCCN distribution is a bivariate NCCN distribution. The joint cdf and pdf of the bivariate NCCN distribution can be easily given by

$$\begin{aligned}\mathrm{NCCN}_2(x_1,x_2;\rho,a,p,\gamma_1,\gamma_2) &= (1-p)\Phi_2\left(\frac{x_1}{\sqrt{a}}-\gamma_1,\frac{x_2}{\sqrt{a}}-\gamma_2;\rho\right)+p\Phi_2\left(\frac{x_1}{\sqrt{b}}-\gamma_1,\frac{x_2}{\sqrt{b}}-\gamma_2;\rho\right),\\ \mathrm{nccn}_2(x_1,x_2;\rho,a,p,\gamma_1,\gamma_2) &= \frac{1-p}{a}\phi_2\left(\frac{x_1}{\sqrt{a}}-\gamma_1,\frac{x_2}{\sqrt{a}}-\gamma_2;\rho\right)+\frac{p}{b}\phi_2\left(\frac{x_1}{\sqrt{b}}-\gamma_1,\frac{x_2}{\sqrt{b}}-\gamma_2;\rho\right),\end{aligned} \tag{16}$$

where $(x_1,x_2)\in\mathbb{R}^2$, $(1-p)a+pb=1$, $\rho\in(-1,1)$, $a\in(0,1)$, $p\in(0,1)$, and $(\gamma_1,\gamma_2)\in\mathbb{R}^2$. Note that this bivariate NCCN distribution can be regarded as the simplified bivariate mixed-normal distribution.

The linear correlation coefficient of the bivariate NCCN distribution is

$$\mathrm{Corr}(X_1,X_2)=\frac{\rho+D(\sqrt{W})\gamma_1\gamma_2}{\sqrt{1+D(\sqrt{W})\gamma_1^2}\sqrt{1+D(\sqrt{W})\gamma_2^2}}. \tag{17}$$

Although the correlation parameter ρ is not equal to the linear correlation coefficient of the bivariate NCCN distribution, it changes in the same direction as the linear correlation coefficient. The two skewness parameters have a substantial influence on the linear correlation coefficient: when $\gamma_1=\gamma_2\to\pm\infty$, $\mathrm{Corr}(X_1,X_2)=1$; when $\gamma_1=\gamma_2=0$, $\mathrm{Corr}(X_1,X_2)=\rho$; and when $\gamma_1=-\gamma_2\to\pm\infty$, $\mathrm{Corr}(X_1,X_2)=-1$. The two tail parameters have a substantial influence on the linear correlation coefficient: when $a\to 1$ or $p\to 1$, $\mathrm{Corr}(X_1,X_2)=\rho$.

Each univariate marginal distribution of the multivariate NCCN distribution obviously follows the univariate NCCN distribution. The cdf and pdf of the univariate NCCN distribution are, respectively,

$$\begin{aligned}\mathrm{NCCN}(x;a,p,\gamma) &= (1-p)\Phi\left(\frac{x}{\sqrt{a}}-\gamma\right)+p\Phi\left(\frac{x}{\sqrt{b}}-\gamma\right),\\ \mathrm{nccn}(x;a,p,\gamma) &= \frac{1-p}{\sqrt{a}}\phi\left(\frac{x}{\sqrt{a}}-\gamma\right)+\frac{p}{\sqrt{b}}\phi\left(\frac{x}{\sqrt{b}}-\gamma\right),\end{aligned} \tag{18}$$

where $x\in\mathbb{R}$, $(1-p)a+pb=1$, $a\in(0,1)$, $p\in(0,1)$, and $\gamma\in\mathbb{R}$. It is difficult to simplify the quantile function of the univariate NCCN distribution, $\mathrm{NCCN}^{-1}(u;a,p,\gamma)$, $u\in[0,1]$. According to the cdf and pdf of the univariate NCCN distribution, the quantile function can be calculated by Newton's method. Note that this univariate NCCN distribution can be regarded as the univariate mixed-normal distribution without location and scale parameters.

The mean, variance, skewness, and kurtosis of the univariate NCCN distribution are

$$
\begin{aligned}
E(X) &= [(1-p)\sqrt{a} + p\sqrt{b}\,]\gamma,\\
E\left(X^2\right) &= 1+\gamma^2,\\
E\left(X^3\right) &= \left(3\gamma+\gamma^3\right)\left[(1-p)a^{3/2}+pb^{3/2}\right],\\
E\left(X^4\right) &= \left(3+6\gamma^2+\gamma^4\right)\left[(1-p)a^2+pb^2\right],\\
D(X) &= E\left(X^2\right)-E(X)^2,\\
\text{skewness}(X) &= \frac{\left[E\left(X^3\right)-3E(X)E\left(X^2\right)+2E(X)^3\right]}{D(X)^{3/2}},\\
\text{kurtosis}(X) &= \frac{\left[E\left(X^4\right)-4E(X)E\left(X^3\right)+6E(X)^2E\left(X^2\right)-3E(X)^4\right]}{D(X)^2}.
\end{aligned}
\tag{19}
$$

For the univariate CN distribution, $E(X)=0$, $D(X)=1$, $\text{skewness}(X)=0$, and $\text{kurtosis}(X)=3+3(1-a)^2\ ((1/p)-1)\in(3,+\infty)$. Clearly, the two tail parameters a and p inversely change with the kurtosis.

According to the above description, the flexibility of the univariate, bivariate, and multivariate CN distributions are similar to that of the univariate, bivariate, and multivariate t-distributions, respectively. The flexibility of the univariate, bivariate, and multivariate NCCN distributions are similar to that of the univariate, bivariate, and multivariate skew-t distributions, respectively.

According to Sklar's theorem, the multivariate NCCN copula function and its pdf can be easily expressed as

$$
\begin{aligned}
C(u_1,\ldots,u_d;R,a,p,\gamma) &= \text{NCCN}_d\left(\text{NCCN}^{-1}(u_1;a,p,\gamma_1),\ldots,\text{NCCN}^{-1}(u_d;a,p,\gamma_d);R,a,p,\gamma\right),\\
c(u_1,\ldots,u_d;R,a,p,\gamma) &= \frac{\text{nccn}_d\left(\text{NCCN}^{-1}(u_1;a,p,\gamma_1),\ldots,\text{NCCN}^{-1}(u_d;a,p,\gamma_d);R,a,p,\gamma\right)}{\prod_{i=1}^{d}\text{nccn}\left(\text{NCCN}^{-1}(u_i;a,p,\gamma_i);a,p,\gamma_i\right)},
\end{aligned}
\tag{20}
$$

where $(u_1,\ldots,u_d)\in[0,1]^d$, R is a correlation matrix, $a\in(0,1)$, $p\in(0,1)$, and $\gamma=(\gamma_1,\ldots,\gamma_d)\prime\in\mathbb{R}^d$. Similar to the multivariate NCCN distribution, subclasses of the multivariate NCCN copula include multivariate normal copula and multivariate CN copula. Clearly, the multivariate NCCN copula cannot be regarded as a mixture of two multivariate normal copulas.

The bivariate NCCN copula function and its pdf can be expressed as

$$
\begin{aligned}
C(u_1,u_2;\rho,a,p,\gamma_1,\gamma_2) &= \text{NCCN}_2\left(\text{NCCN}^{-1}(u_1;a,p,\gamma_1),\text{NCCN}^{-1}(u_2;a,p,\gamma_2);\rho,a,p,\gamma_1,\gamma_2\right),\\
c(u_1,u_2;\rho,a,p,\gamma_1,\gamma_2) &= \frac{\text{nccn}_2\left(\text{NCCN}^{-1}(u_1;a,p,\gamma_1),\text{NCCN}^{-1}(u_2;a,p,\gamma_2);\rho,a,p,\gamma_1,\gamma_2\right)}{\text{nccn}\left(\text{NCCN}^{-1}(u_1;a,p,\gamma_1);a,p,\gamma_1\right)\text{nccn}\left(\text{NCCN}^{-1}(u_2;a,p,\gamma_2);a,p,\gamma_2\right)},
\end{aligned}
\tag{21}
$$

where $(u_1,u_2)\in[0,1]^2$, $\rho\in(-1,1)$, $a\in(0,1)$, $p\in(0,1)$, and $(\gamma_1,\gamma_2)\in\mathbb{R}^2$. The bivariate NCCN copula density function diagrams are given in Figures 1 and 2.

According to the bivariate NCCN copula density function diagrams, the meaning of parameters can be easily understood. The correlation parameter ρ can affect global dependence: when ρ is larger, the negative dependence is weaker, and the positive dependence is stronger. The two tail parameters a and p can affect the tail dependence: when they are smaller, the tail dependence is stronger. The two skewness parameters can affect the asymmetric dependence: when $\gamma_1<0$ and $\gamma_2<0$, the lower-lower tail dependence is stronger than the upper-upper tail dependence; when $\gamma_1>0$ and $\gamma_2>0$, the upper-upper tail dependence is stronger than the lower-lower tail dependence; when $\gamma_1<0$ and $\gamma_2>0$, the lower-upper tail dependence is stronger than the upper-lower tail dependence; and when $\gamma_1>0$ and $\gamma_2<0$, the upper-lower tail dependence is stronger than the lower-upper tail dependence.

2.4. Time-Varying NCCN Copula. For the multivariate NCCN copula, this paper further considers that the correlation matrix may change over time and does not consider the dynamics of other parameters.

The DCC model is a basic dynamic correlation model. This study presents the DCC model as

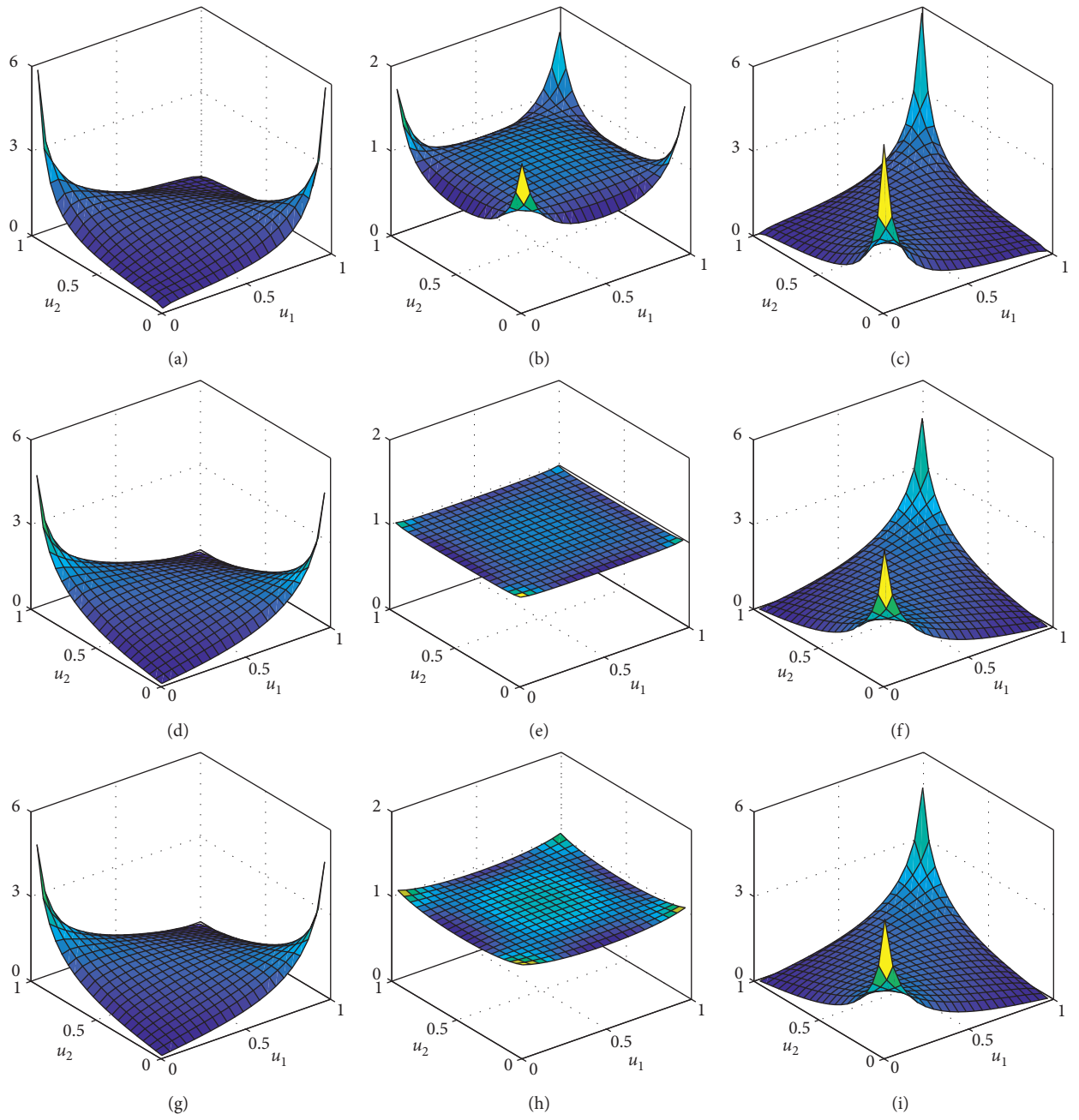

FIGURE 1: The bivariate NCCN copula density function. (a) $\rho = -0.5$, $a = 0.5$, and $p = 0.5$. (b) $\rho = 0.5$, $a = 0.5$, and $p = 0.5$. (c) $\rho = 0.5$, $a = 0.5$, and $p = 0.5$. (d) $\rho = -0.5$, $a = 0.9$, and $p = 0.5$. (e) $\rho = 0$, $a = 0.9$, and $p = 0.5$. (f) $\rho = 0.5$, $a = 0.9$, and $p = 0.5$. (g) $\rho = -0.5$, $a = 0.5$, and $p = 0.9$. (h) $\rho = 0$, $a = 0.5$, and $p = 0.9$. (i) $\rho = 0.5$, $a = 0.5$, and $p = 0.5$.

$$\begin{cases} Q_1 = Q = \dfrac{1}{T}\displaystyle\sum_{t=1}^{T} z_t z_t', \\ Q_{t+1} = (1-\beta)Q + \beta Q_t + \alpha\left(z_t z_t' - Q_t\right), \\ R_t = \operatorname{diag}\left(Q_t\right)^{-(1/2)} Q_t \operatorname{diag}\left(Q_t\right)^{-(1/2)}, \\ \alpha \geq 0, \beta \in (0,1), \alpha \leq \beta, \end{cases} \tag{22}$$

where T is the sample size, $z_t = (z_{1t}, \ldots, z_{dt})\prime$ is the standardized residual vector, R_t is the conditional correlation matrix of z_t, Q_t is similar to the conditional covariance matrix, and Q is similar to the unconditional covariance matrix and can be estimated by using the sample mean of $z_t z_t'$. Note that Q_{t+1} can be interpreted as an information shock term plus the weighted average of Q and Q_t.

Parameter α controls the dynamics of the conditional correlation matrix: when α is large, the dynamics of the conditional correlation matrix are strong. In particular, when $\alpha = 0$, the model degenerates into the constant conditional correlation (CCC) model. Parameter β controls the clustering and mean reversion of the

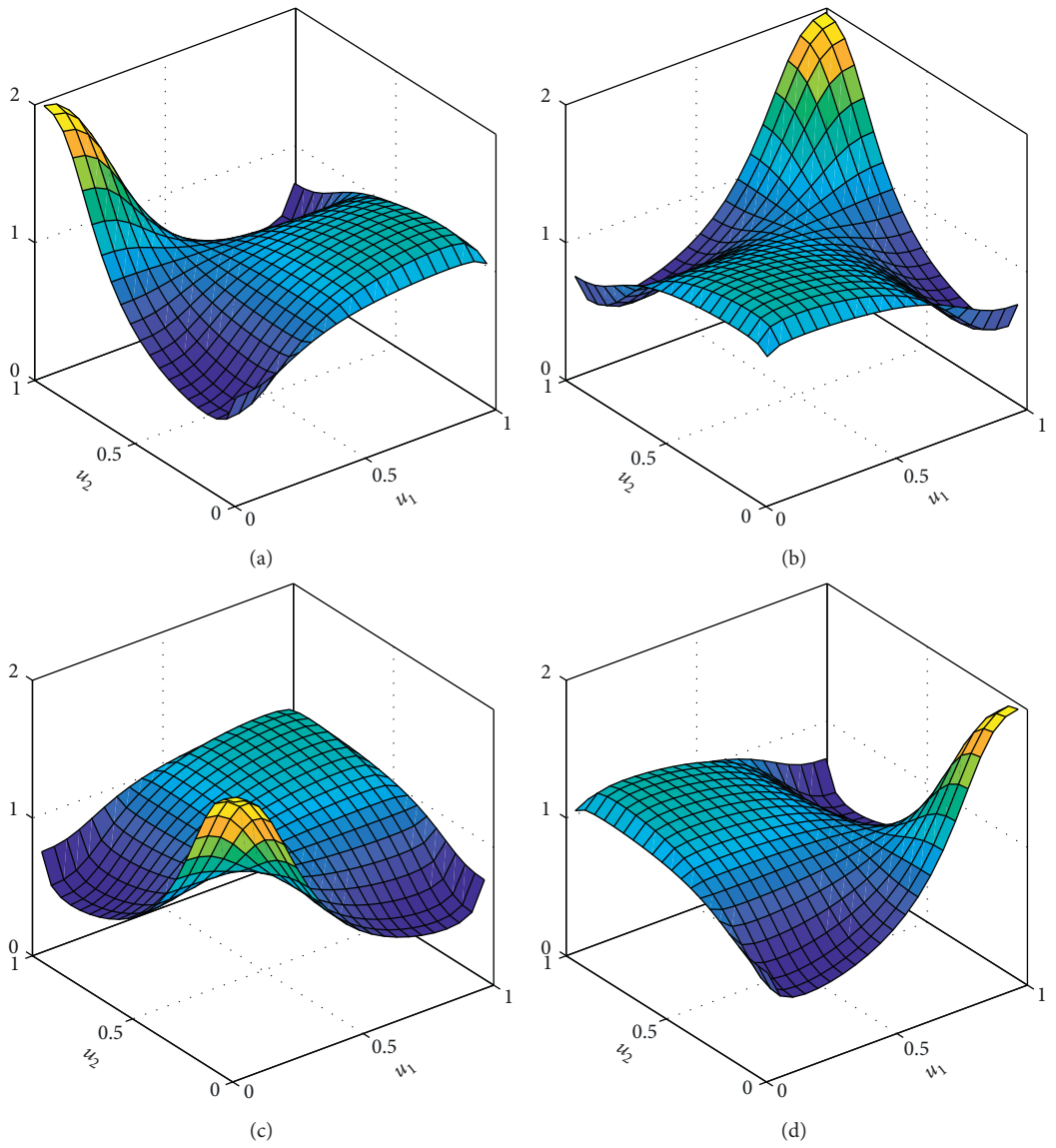

Figure 2: The bivariate NCCN copula density function. (a) $\gamma_1 = -2$; $\gamma_2 = 2$. (b) $\gamma_1 = 2$; $\gamma_2 = 2$. (c) $\gamma_1 = -2$; $\gamma_2 = -2$. (d) $\gamma_1 = 2$; $\gamma_2 = -2$.

conditional correlation matrix: when β is close to 1, the conditional correlation matrix shows strong clustering and weak mean reversion; when β is close to 0, the conditional correlation matrix shows weak clustering and strong mean reversion. The renewal equation of Q_t can also be expressed as

$$Q_{t+1} = (1-\beta)Q + (\beta-\alpha)Q_t + \alpha z_t z_t'. \tag{23}$$

In this renewal equation, Q_{t+1} can be interpreted as the weighted average of Q, Q_t, and $z_t z_t'$. Under the given parameter constraints, R_t can be guaranteed to be a true correlation matrix.

The common DCC-normal copula model can be given by

$$\begin{cases} u_t = (u_{1t}, \ldots, u_{dt})' \sim C(u_t; R_t), \\ z_t = (z_{1t}, \ldots, z_{dt})', z_{it} = \Phi^{-1}(u_{it}), \\ Q_1 = Q = \dfrac{1}{T}\displaystyle\sum_{t=1}^{T} z_t z_t', \\ Q_{t+1} = (1-\beta)Q + \beta Q_t + \alpha(z_t z_t' - Q_t), \\ R_t = \operatorname{diag}(Q_t)^{-(1/2)} Q_t \operatorname{diag}(Q_t)^{-(1/2)}, \\ \widehat{\theta} = \arg\max\limits_{\theta} \displaystyle\sum_{t=1}^{T}\left(\ln \phi_d(z_t; R_t) - \sum_{i=1}^{d} \ln \phi(z_{it}) \right), \\ \theta = (\alpha, \beta), \alpha \geq 0, \beta \in (0,1), \alpha \leq \beta, \end{cases} \tag{24}$$

where u_t follows the multivariate normal copula with time-varying parameter matrix R_t and z_t follows the standardized multivariate normal distribution with time-varying linear correlation matrix R_t. For a sample of uniform scores $\{u_t\}_{t=1}^{T}$, we can employ the ML method to estimate the parameter set θ.

Similar to the DCC-normal copula model, the DCC-NCCN copula model can be given by

$$\begin{cases} u_t = (u_{1t}, \ldots, u_{dt})' \sim C(u_t; R_t, a, p, \gamma), x_t = (x_{1t}, \ldots, x_{dt})', \\ x_{it} = \mathrm{NCCN}^{-1}(u_{it}; a, p, \gamma_i), \\ z_t = s^{-1}(x_t - m), \\ Q_1 = Q = \dfrac{1}{T}\sum_{t=1}^{T} z_t z_t', \\ Q_{t+1} = (1-\beta)Q + \beta Q_t + \alpha(z_t z_t' - Q_t), \\ R_t^* = \mathrm{diag}(Q_t)^{-(1/2)} Q_t \,\mathrm{diag}(Q_t)^{-(1/2)}, \\ R_t = s R_t^* s + mm' - \gamma\gamma', \\ \widehat{\theta} = \underset{\theta}{\mathrm{argmax}} \sum_{t=1}^{T} \left(\ln \mathrm{nccn}_d(x_t; R_t, a, p, \gamma) - \sum_{i=1}^{d} \ln \mathrm{nccn}(x_{it}; a, p, \gamma_i) \right), \\ m = [(1-p)\sqrt{a} + p\sqrt{b}\,]\gamma, s = \left[I_d + \mathrm{diag}(\gamma\gamma' - mm')\right]^{1/2}, (1-p)a + pb = 1, \\ \theta = (a, p, \gamma, \alpha, \beta), \\ a \in (0,1), \\ p \in (0,1), \\ \gamma = (\gamma_1, \ldots, \gamma_d)' \in \mathbb{R}^d, \\ \alpha \geq 0, \beta \in (0,1), \alpha \leq \beta, \end{cases} \tag{25}$$

where I_d is an identity matrix, u_t follows the multivariate NCCN copula with time-varying parameter matrix R_t, x_t follows the multivariate NCCN distribution, and z_t follows the standardized multivariate NCCN distribution with time-varying linear correlation matrix R_t^*. Because the meaning of R_t is not very clear, we first portray time-varying R_t^* and then get time-varying R_t.

Akaike information criterion (AIC) and Bayesian information criterion (BIC) can be used to compare the fitting effect of different models. The expressions for AIC and BIC are

$$\begin{aligned} \mathrm{AIC} &= -2\mathrm{LL} + 2k, \\ \mathrm{BIC} &= -2\mathrm{LL} + k\ln n, \end{aligned} \tag{26}$$

where LL is the log-likelihood, k is the number of parameters, and n is the sample size. The smaller the AIC and BIC are, the better the model is when we compare the models.

3. Empirical Results

3.1. Descriptive Statistics. This study employs the Hang Seng Index (HSI), Hang Seng China Enterprises Index (CEI), and Hang Seng China-Affiliated Corporations Index (CCI) from the Hong Kong stock market as our sample, abbreviated as HSI, CEI, and CCI thereafter, respectively. We obtained three daily closing price series from the period from Jan 1, 2005, to Dec 31, 2018, with 3451 data, respectively. The data source can be found at https://cn.investing.com, and we calculate the daily logarithmic return, $y_t = 100 \times (\ln P_t - \ln P_{t-1})$, where P_t is the daily closing price at time t, and we have 3 return series, with 3450 observations each.

The relative price (P_t/P_1) series are given in Figure 3.

The graph shows that all price series have strong dynamics and an upward trend. Considering long-term investment, CCI is the best choice, and HSI is the worst choice. The return series are given in Figure 4.

Return series have significant dynamic characteristics, and the dynamic process shows significant mean reversion.

The univariate descriptive statistics of returns are presented in Table 1.

As expected, the minimum values are negative, and the maximum values are positive. The range of all returns is large. The median and mean values are close to zero, where the mean values are less than the median values. The standard deviation values are greater than 1. According to skewness, HSI is skewed to the left, and CEI and CCI are

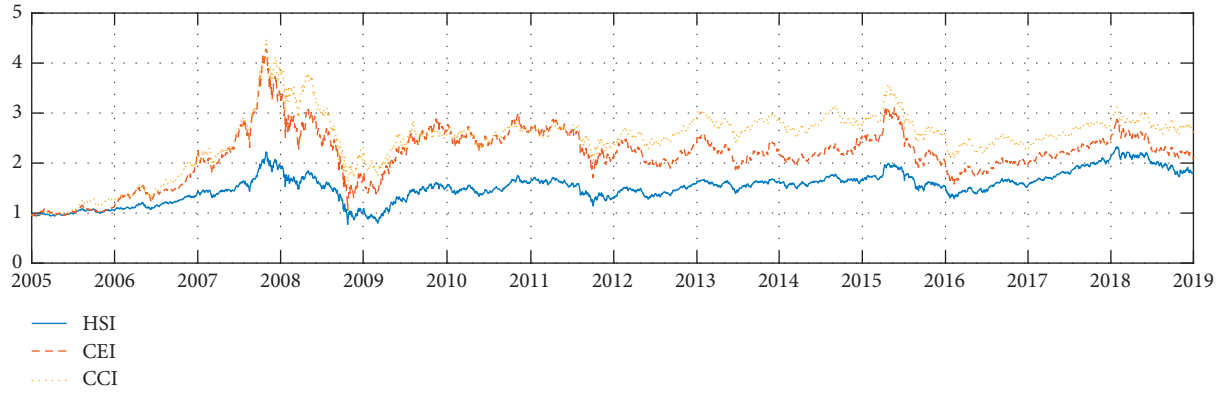

Figure 3: Relative price series.

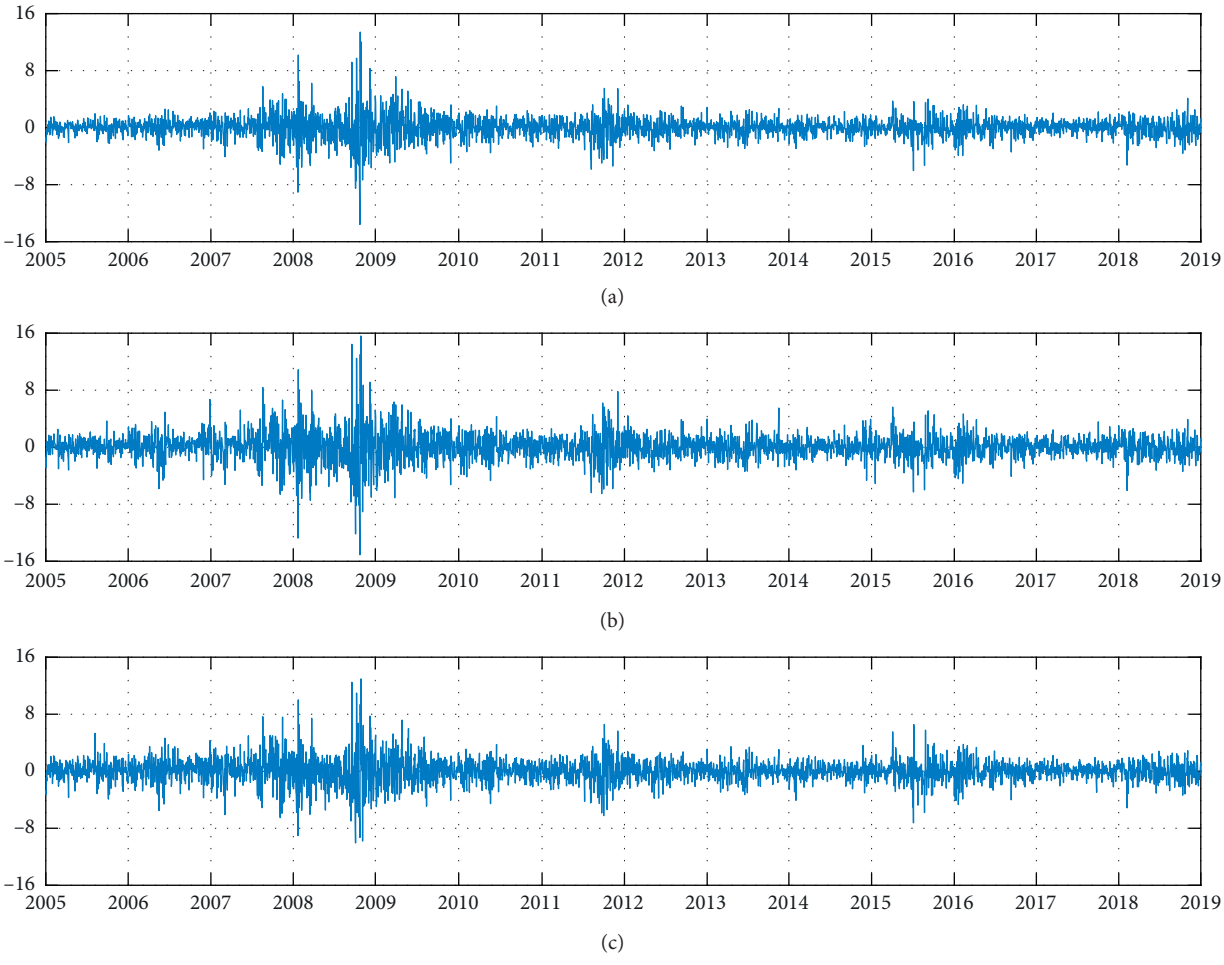

Figure 4: Return series. (a) HSI. (b) CEI. (c) CCI.

skewed to the right. The kurtosis values are significantly larger than 3, implying that returns have fatter tails than the normal distribution. The skewness and kurtosis tests show that the returns cannot follow the normal distribution.

Using the Ljung-Box Q(5) test method, the autocorrelation tests of the first four moments of returns are reported in Table 2.

As for the tests, the autocorrelation of returns is weak, but the autocorrelation of second-order, third-order, and fourth-order moments of returns is strong, indicating that the returns cannot have serial independence. The autocorrelation of squared returns is particularly prominent, indicating that the dynamic of volatility (variance or standard deviation) is the most important.

Table 1: Univariate descriptive statistics of returns.

	Min	Max	Median	Mean	Std.	Skewness	p value	Kurtosis	p value
HSI	−13.582	13.407	0.067	0.017	1.483	−0.009	0.829	12.571	≤0.001
CEI	−15.087	15.606	0.032	0.022	1.893	0.026	0.535	10.805	≤0.001
CCI	−10.059	12.953	0.058	0.028	1.693	0.103	0.014	8.691	≤0.001

Table 2: Autocorrelation tests of the first four moments of returns.

	Statistics				p value			
	$Q^1(5)$	$Q^2(5)$	$Q^3(5)$	$Q^4(5)$	$Q^1(5)$	$Q^2(5)$	$Q^3(5)$	$Q^4(5)$
HSI	7.85	1838.73	534.72	1304.44	0.165	≤0.001	≤0.001	≤0.001
CEI	9.18	1725.55	385.99	848.21	0.102	≤0.001	≤0.001	≤0.001
CCI	11.01	1446.67	241.22	386.80	0.051	≤0.001	≤0.001	≤0.001

Using window length $2 \times 30 + 1 = 61$, the moving sample standard deviation series of returns are given in Figure 5.

For each return series, the time-varying volatility can be easily observed.

3.2. Fitting of the Marginal Distribution. We employ the NAGARCH model to describe the dynamics of the return series. Table 3 shows the estimation results of the NAGARCH model.

The values of parameter α are greater than 0.05, indicating significant time-varying volatility. The values of parameter β are close to 1, showing strong clustering and weak mean reversion. The values of parameter γ are less than 0, exhibiting volatility asymmetry. The standard deviation series of the NAGARCH model are given in Figure 6.

The standard deviation series of the NAGARCH model are consistent with the moving sample standard deviation series, indicating that the NAGARCH model can effectively describe the time-varying volatility. Based on the NAGARCH model, we can obtain the standardized residual series. The univariate descriptive statistics of standardized residuals are given in Table 4.

Compared with the return series, the range of standardized residual series is significantly reduced. The sample mean values of standardized residuals are almost equal to 0, and the sample standard deviation is almost equal to 1, which can meet the theoretical requirements. The skewness values of standardized residuals are quite different from returns. The kurtosis values of standardized residuals are smaller than returns. Based on the skewness and kurtosis tests, standardized residuals cannot follow a normal distribution.

Using the Ljung-Box Q(5) test method, the autocorrelation tests of the first four moments of standardized residuals are reported in Table 5.

Based on the tests, the autocorrelation of the first four moments of standardized residuals is not strong. The standardized residual series can basically meet the serial independence. In general, the NAGARCH model can effectively portray the dynamics of each return series.

Using the empirical cdf to transform standardized residuals into uniform scores, uniform scores satisfy the serial independence and follow a uniform distribution on [0,1].

3.3. Descriptive Analysis of Dependence Structures. To perform some sample analyses of the bivariate dependence structures, the sample bivariate dependence measures of uniform scores are reported in Table 6.

The bivariate global dependence measures are positive. The bivariate global dependence is the smallest for CEI-CCI and largest for HSI-CEI. The bivariate lower tail dependence measures are larger than the upper ones, implying that the bivariate dependence structures have stronger lower tail dependence. The upper-lower and lower-upper tail dependence measures are very close to zero. The Gaussian skewness tests show that the bivariate dependence structures are significantly asymmetric. The Gaussian skewness is the smallest for HSI-CCI and largest for HSI-CEI. The Gaussian kurtosis values are larger than 8, implying that the bivariate dependence structures have stronger tail dependence than the bivariate normal copula. The Gaussian kurtosis is the smallest for HSI-CCI and largest for HSI-CEI. The Gaussian skewness and kurtosis tests show that the bivariate dependence structures cannot follow the normal copula.

The bivariate scatter plots of uniform scores are given in Figure 7.

The points are mainly concentrated around the main diagonal. The points in the lower-lower and upper-upper tail regions are dense, but the points in the lower-upper and upper-lower tail regions are sparse.

To understand the bivariate local dependence of uniform scores, the sample quantile dependence curves of uniform scores are given in Figure 8. The horizontal axis shows quantile levels, and the vertical axis shows bivariate quantile dependence coefficients.

The sample quantile dependence curves show the following features: (1) LLQD and UUQD curves are significantly higher than ULQD and LUQD curves, indicating that all bivariate dependence structures have a strong positive dependence. (2) LLQD and UUQD curves are obviously not coincident, and the LLQD curve is significantly higher than

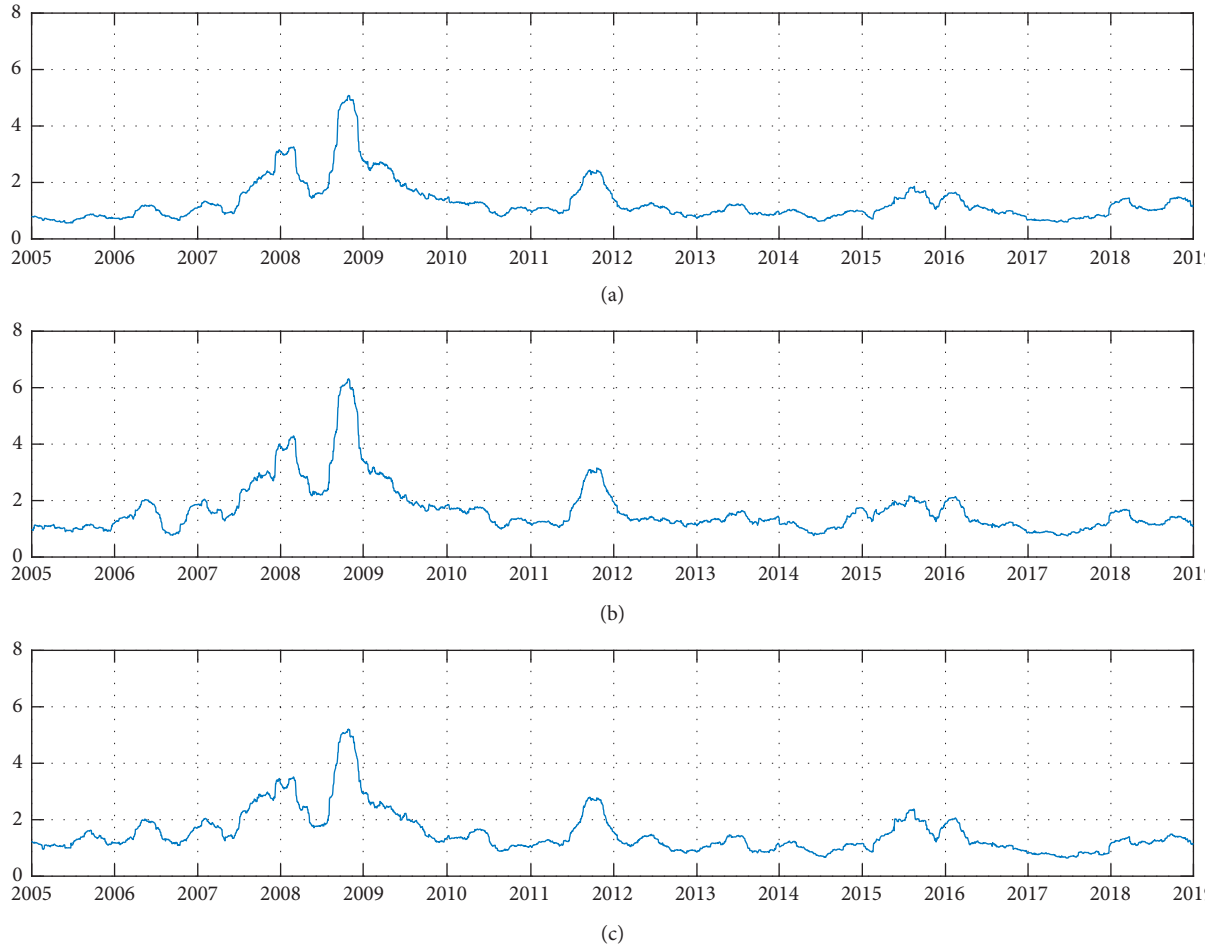

Figure 5: Moving sample standard deviation series. (a) HSI. (b) CEI. (c) CCI.

Table 3: Parameter estimation of the NAGARCH model.

	α	β	γ	LL	AIC	BIC
HSI	0.0704	0.9877	−0.6550	−5479.13	10964.27	10982.71
CEI	0.0813	0.9875	−0.3187	−6407.51	12821.01	12839.45
CCI	0.0664	0.9894	−0.4152	−6093.35	12192.7	12211.14

the UUQD curve at the low quantile levels, indicating that all bivariate dependence structures are asymmetric, and the lower tail dependence is significantly higher than the upper tail dependence. (3) ULQD and LUQD curves are almost coincident.

Using window length $2 \times 30 + 1 = 61$, moving sample bivariate Kendall's tau series of uniform scores are given in Figure 9.

The time-varying bivariate global dependence can be easily observed. From 2005 to 2007, the global dependence of HSI-CCI is the largest. However, since 2008, the global dependence of HSI-CEI is the largest.

3.4. Fitting of Dependence Structures. This paper considers CCC-N, CCC-CN, CCC-NCCN, DCC-N, DCC-CN, and DCC-NCCN copula models. Considering that the asymmetric dependence between uniform scores is mainly in the upper and lower tail, we can constrain all skewness parameters of the NCCN copula to be equal. In addition, we consider three common Archimedean copulas, namely, Clayton, Gumbel, and Frank copulas.

(1) Clayton copula function:

$$C(u, v; \theta) = \left(u^{-\theta} + v^{-\theta} - 1\right)^{-(1/\theta)}, \tag{27}$$

where $\theta > 0$. Kendall's tau of Clayton copula is $(\theta/(\theta + 2))$.

(2) Gumbel copula function:

$$C(u, v; \theta) = \exp\left\{-\left[(-\ln u)^{\theta} + (-\ln v)^{\theta}\right]^{1/\theta}\right\}, \tag{28}$$

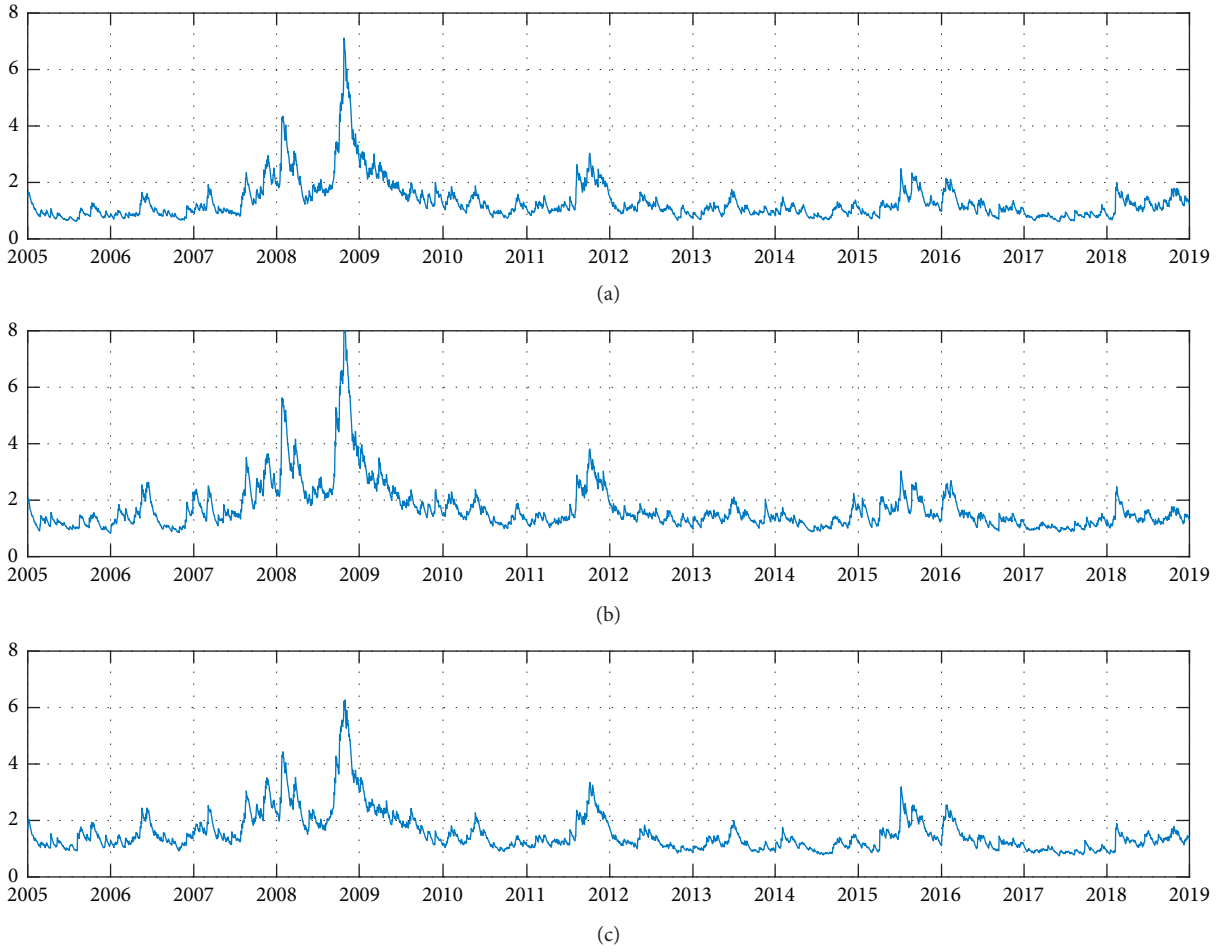

Figure 6: Standard deviation series of NAGARCH model. (a) HSI. (b) CEI. (c) CCI.

Table 4: Univariate descriptive statistics of standardized residuals.

	Min	Max	Median	Mean	Std.	Skewness	p value	Kurtosis	p value
HSI	−5.423	5.153	0.044	0.003	0.987	−0.241	≤0.001	4.072	≤0.001
CEI	−4.619	4.466	0.007	0.004	0.989	−0.036	0.391	3.967	≤0.001
CCI	−5.719	5.736	0.022	−0.001	0.991	−0.108	0.010	4.402	≤0.001

Table 5: Autocorrelation tests of the first four moments of standardized residuals.

	Statistics				p value			
	$Q^1(5)$	$Q^2(5)$	$Q^3(5)$	$Q^4(5)$	$Q^1(5)$	$Q^2(5)$	$Q^3(5)$	$Q^4(5)$
HSI	7.29	15.38	7.24	0.70	0.200	0.009	0.204	0.983
CEI	16.22	16.38	3.86	7.69	0.006	0.006	0.570	0.174
CCI	11.46	6.33	3.44	0.06	0.043	0.275	0.633	1.000

Table 6: Sample bivariate dependence measures of uniform scores.

	Kendall's tau	10% LLQD	10% UUQD	10% ULQD	10% LUQD	Gaussian skewness	p value	Gaussian kurtosis	p value
HSI-CEI	0.747	0.809	0.701	≤0.001	≤0.001	0.155	≤0.001	10.439	≤0.001
HSI-CCI	0.728	0.780	0.655	≤0.001	≤0.001	0.083	≤0.001	8.759	≤0.001
CEI-CCI	0.672	0.728	0.609	≤0.001	≤0.001	0.101	≤0.001	9.160	≤0.001

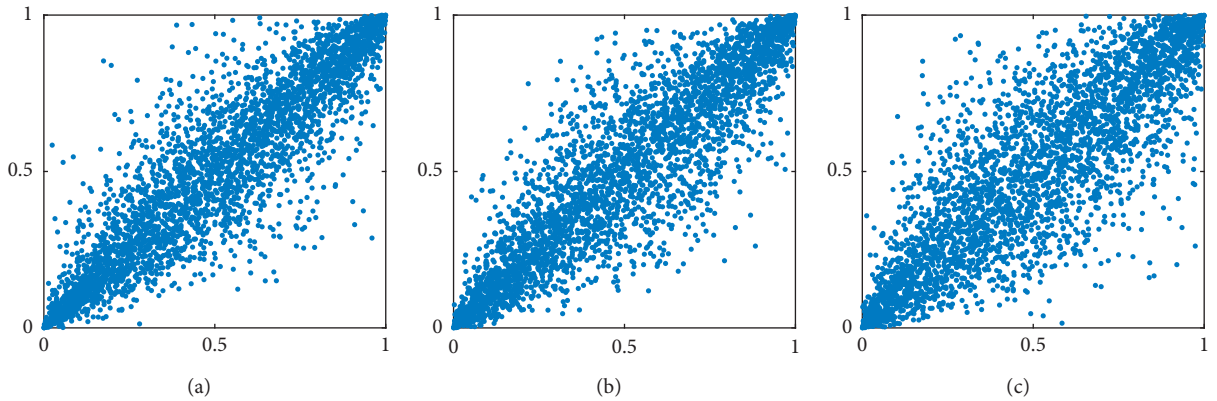

Figure 7: Bivariate scatter plots of uniform scores. (a) HSI-CEI. (b) HSI-CCI. (c) CEI-CCI.

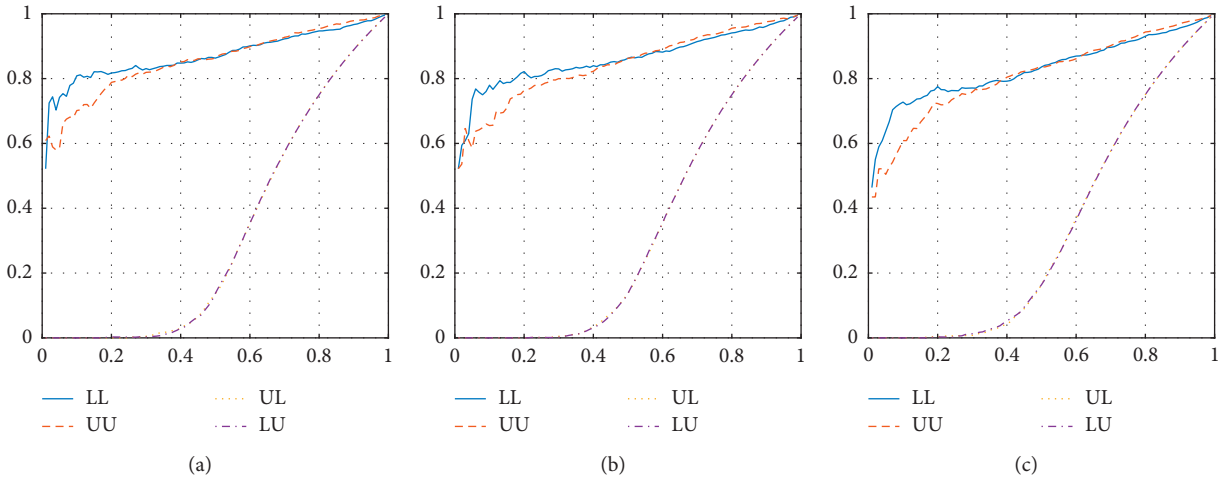

Figure 8: Sample quantile dependence curves of uniform scores. (a) HSI-CEI. (b) HSI-CCI. (c) CEI-CCI.

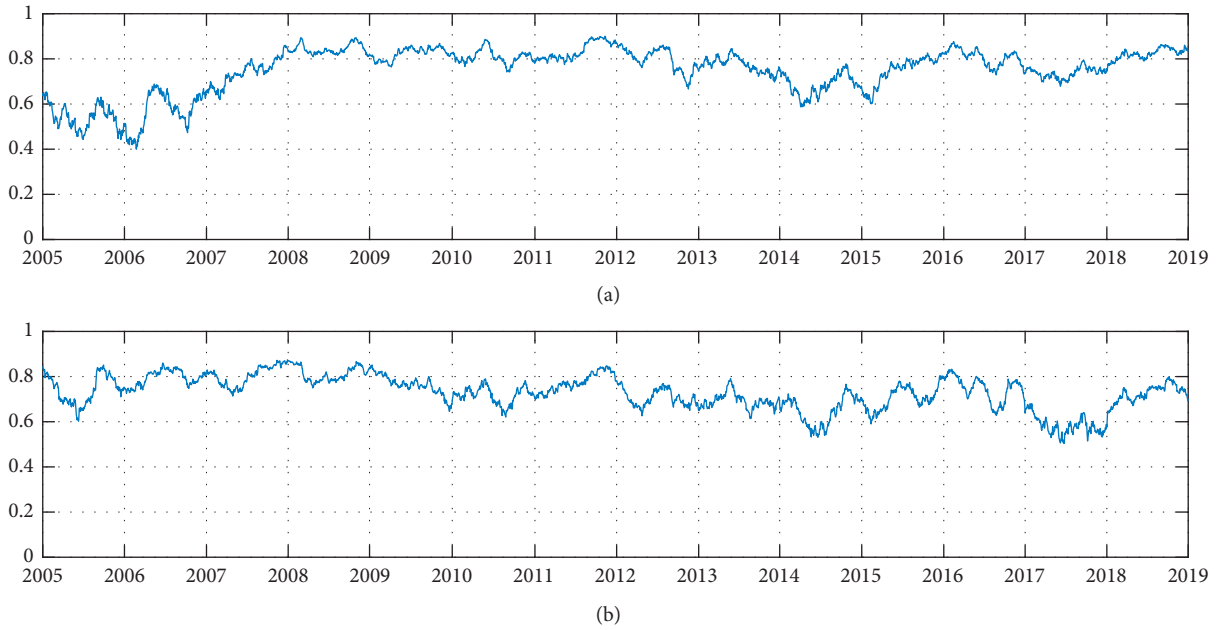

Figure 9: Continued.

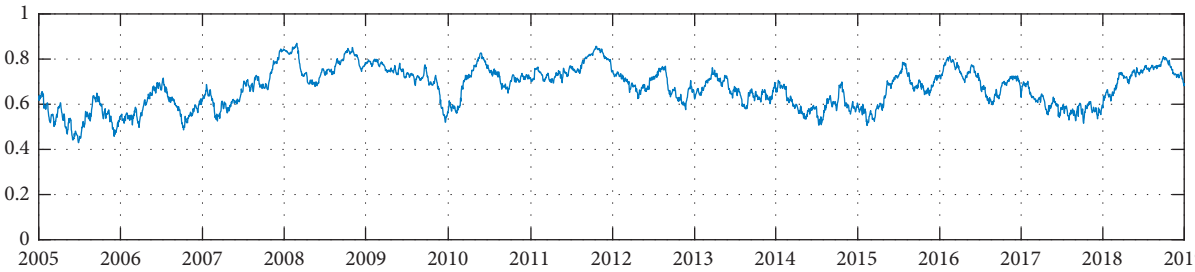

(c)

Figure 9: Moving sample Kendall's tau series of uniform scores. (a) HSI-CEI. (b) HSI-CCI. (c) CEI-CCI.

Table 7: Fitting results of bivariate copula models (HSI-CEI).

Copula model	α	β	a	p	γ	ΔP	ΔLL	LL	AIC	BIC
Clayton						0	−542.16	9	9	9
Gumbel						0	−198.62	8	8	8
Frank						0	−159.71	7	7	7
CCC-N						0	0	6	6	6
CCC-CN			0.4569	0.3015		2	127.49	5	5	5
CCC-NCCN			0.4325	0.3197	−0.9133	3	162.49	4	4	4
DCC-N	0.0365	0.9955				2	375.83	3	3	3
DCC-CN	0.0374	0.9960	0.5593	0.4275		4	405.52	2	2	2
DCC-NCCN	0.0359	0.9962	0.7094	0.2338	−1.8581	5	428.98	1	1	1

where $\theta \geq 1$. Kendall's tau of Gumbel copula is $1 - (1/\theta)$.

(3) Frank copula function:

$$C(u, v; \theta) = -\frac{1}{\theta}\ln\left[1 + \frac{\left(e^{-\theta u} - 1\right)\left(e^{-\theta v} - 1\right)}{e^{-\theta} - 1}\right], \quad (29)$$

where $\theta \neq 0$. Kendall's tau of Frank copula is $1 - (4/\theta)[1 - (1/\theta)\int_0^\theta (t/(e^t - 1))dt]$.

For the Clayton, Gumbel, and Frank copulas, sample Kendall's tau can be used to estimate their parameters. For other copulas, the maximum likelihood estimation (MLE) can be used.

To compare the fitting effect, the CCC-N copula model can be used as the benchmark model. Then, the parameter increment ΔP and LL increment ΔLL of each copula model can be calculated. Also, the models can be ranked by LL, AIC, and BIC, respectively. The fitting results of bivariate copula models are given in Tables 7–9.

The values of parameter α are greater than 0.02, and the values of parameter β are close to 1. The values of two tail parameters are not close to 1, implying that all bivariate dependence structures have stronger tail dependence than the normal copula. The values of the skewness parameter are negative, implying the lower tail dependence is stronger than the upper tail dependence for each bivariate dependence structure. The ΔLL values show that the fitting of Clayton, Gumbel, Frank, CCC-N, CCC-CN, CCC-NCCN, DCC-N, DCC-CN, and DCC-NCCN copula models is improved in turn. In terms of ranking, the DCC-NCCN copula model is the best.

To easily understand the fitting effect of the bivariate local dependence, the quantile dependence curves of bivariate copula models are given in Figures 10–15.

Compared with the sample QD curves, the bivariate Clayton copula model overestimates the degree of asymmetric dependence in the upper and lower tails. The bivariate Gumbel copula model has a wrong asymmetric direction on the upper and lower tail dependence, and it overestimates the strength of the asymmetric tail dependence. The bivariate Frank copula model cannot describe the asymmetric dependence and seriously underestimates the strength of the upper and lower tail dependence. The bivariate CCC-N copula model cannot describe the asymmetric dependence and significantly underestimates the degree of the lower tail dependence. The bivariate CCC-CN copula model cannot describe the asymmetric dependence. The bivariate CCC-NCCN copula model is basically correct.

To easily understand the fitting effect of the bivariate time-varying global dependence, Kendall's tau series of the bivariate DCC-NCCN copula model are given in Figure 16.

Kendall's tau series of the bivariate DCC-NCCN copula model is basically consistent with moving sample Kendall's tau series. The results illustrate that the bivariate DCC-NCCN copula model can better depict the bivariate time-varying global dependence.

The 10% QD coefficient series of the bivariate DCC-NCCN copula model are given in Figure 17. Note that the 10% ULQD and 10% LUQD coefficient series are omitted because their values are very close to 0.

Table 8: Fitting results of bivariate copula models (HSI-CCI).

Copula model	α	β	a	p	γ	ΔP	ΔLL	LL	AIC	BIC
Clayton						0	−670.24	9	9	9
Gumbel						0	−264.77	8	8	8
Frank						0	−231.43	7	7	7
CCC-N						0	0	6	6	6
CCC-CN			0.3845	0.6094		2	41.47	5	5	5
CCC-NCCN			0.5012	0.4108	−1.3943	3	68.54	4	4	4
DCC-N	0.0283	0.9885				2	94.51	3	3	3
DCC-CN	0.0303	0.9892	0.4162	0.6339		4	123.37	2	2	2
DCC-NCCN	0.0312	0.9893	0.5994	0.3433	−1.9381	5	153.51	1	1	1

Table 9: Fitting results of bivariate copula models (CEI-CCI).

Copula model	α	β	a	p	γ	ΔP	ΔLL	LL	AIC	BIC
Clayton						0	−504.67	9	9	9
Gumbel						0	−222.81	8	8	8
Frank						0	−153.91	7	7	7
CCC-N						0	0	6	6	6
CCC-CN			0.6251	0.2729		2	47.38	5	5	5
CCC-NCCN			0.5638	0.3176	−1.5486	3	78.63	4	4	4
DCC-N	0.0357	0.9921				2	146.24	3	3	3
DCC-CN	0.0357	0.9926	0.7740	0.1827		4	167.95	2	2	2
DCC-NCCN	0.0358	0.9919	0.6832	0.2964	−2.0066	5	191.36	1	1	1

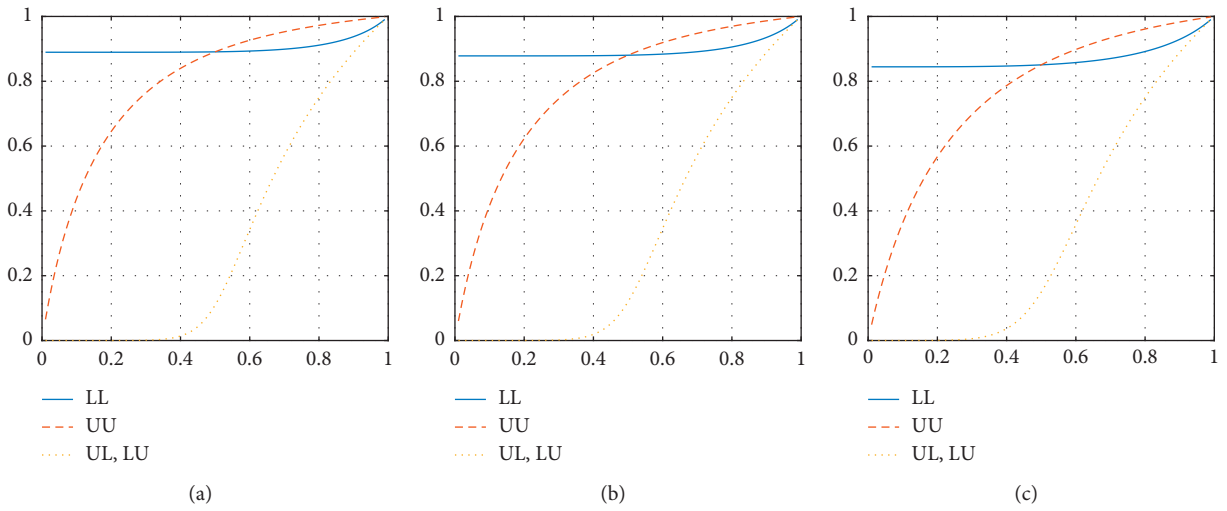

Figure 10: QD curves of bivariate Clayton copula model. (a) HSI-CEI. (b) HSI-CCI. (c) CEI-CCI.

The dynamic characteristics of 10% LLQD and 10% UUQD coefficient series are consistent with Kendall's tau series. For each bivariate dependence structure, the time-varying lower and upper tail dependence can be easily observed.

In comparison with the fitting effects of the multivariate copula models, the fitting results of multivariate copula models are given in Table 10.

The fitting results of the multivariate copula models are consistent with the fitting results of the bivariate copula models. Based on LL values, the time-varying dependence, tail dependence, and asymmetric dependence all play an important role in improving the fitting effect of a multivariate dependence structure. The multivariate DCC-NCCN copula model is the best choice.

Some diagrams of the multivariate CCC-NCCN copula and DCC-NCCN copula models are given in Figures 18–20. Compared with bivariate CCC-NCCN and

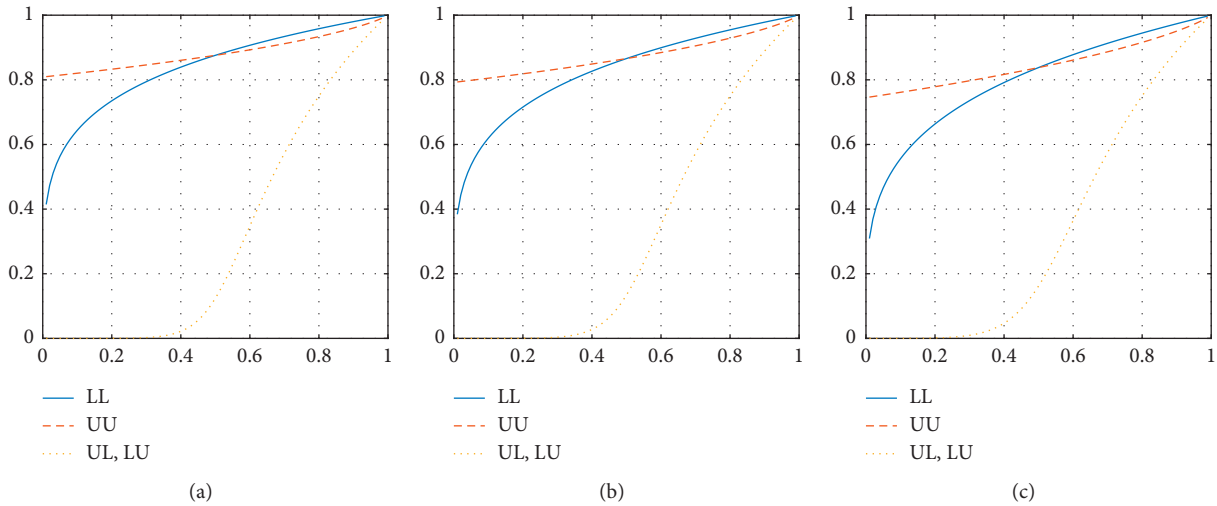

Figure 11: QD curves of bivariate Gumbel copula model. (a) HSI-CEI. (b) HSI-CCI. (c) CEI-CCI.

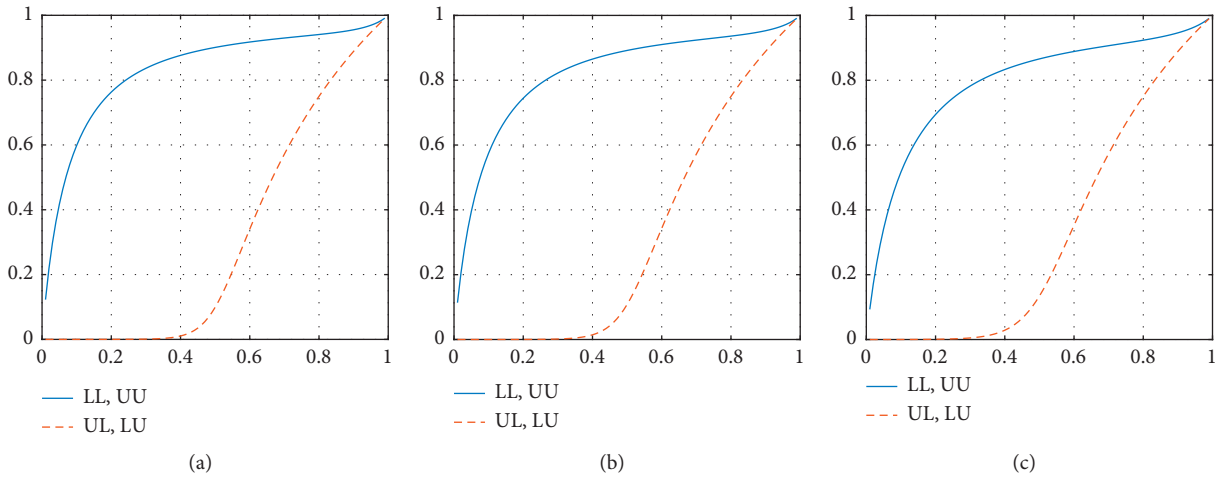

Figure 12: QD curves of bivariate Frank copula model. (a) HSI-CEI. (b) HSI-CCI. (c) CEI-CCI.

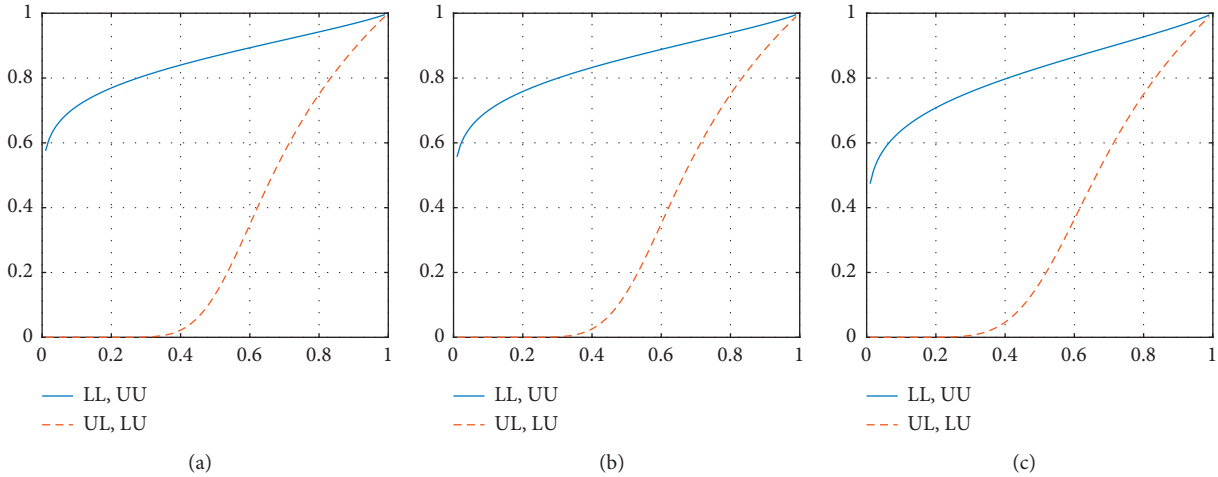

Figure 13: QD curves of the bivariate CCC-N copula model. (a) HSI-CEI. (b) HSI-CCI. (c) CEI-CCI.

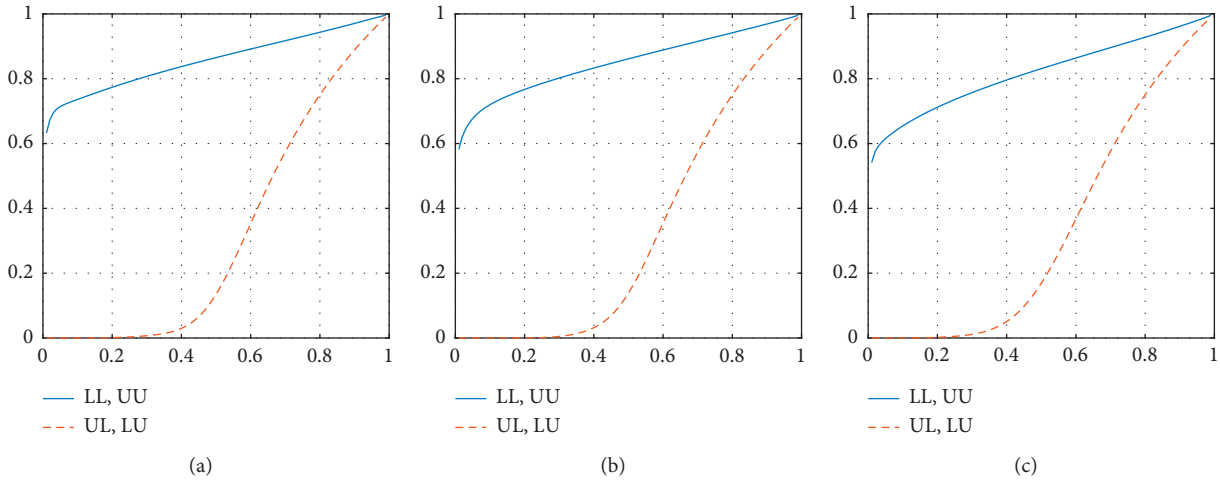

Figure 14: QD curves of bivariate CCC-CN copula model. (a) HSI-CEI. (b) HSI-CCI. (c) CEI-CCI.

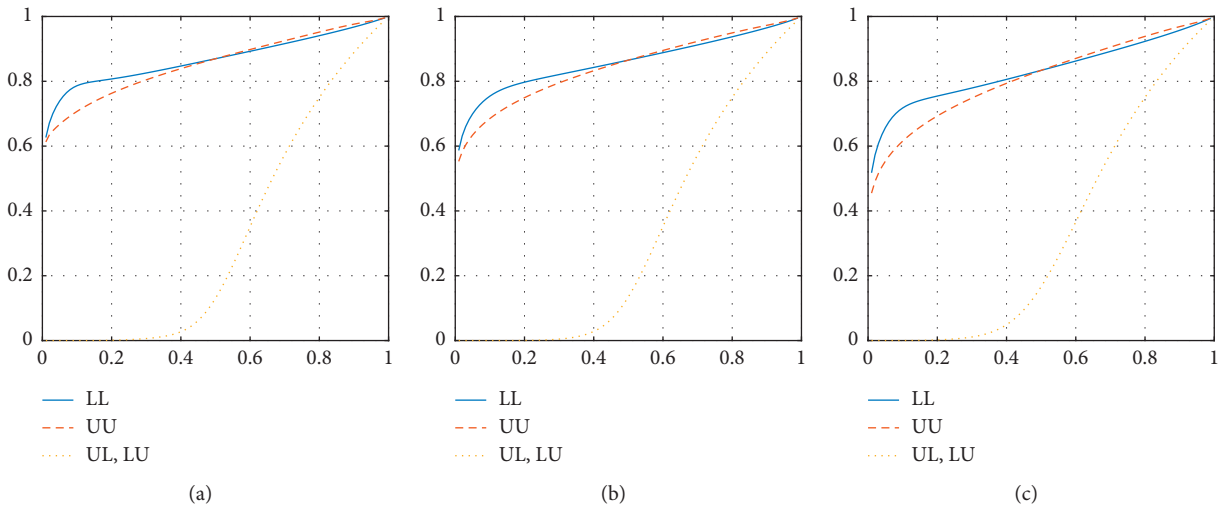

Figure 15: QD curves of bivariate CCC-NCCN copula model. (a) HSI-CEI. (b) HSI-CCI. (c) CEI-CCI.

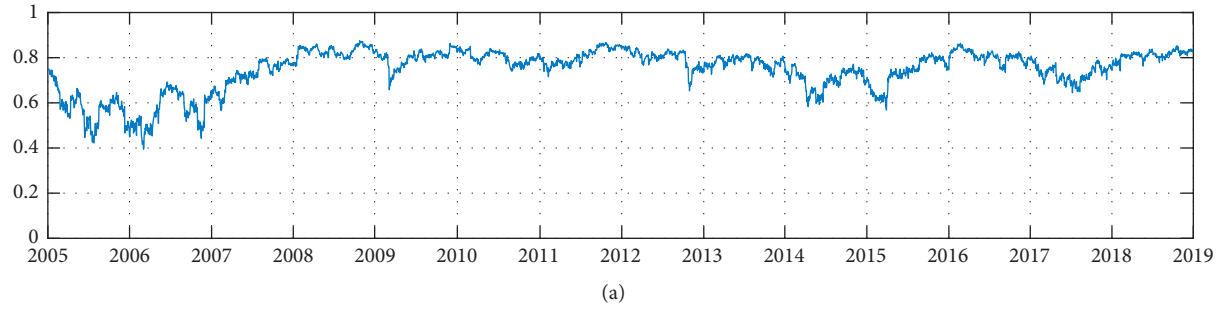

Figure 16: Continued.

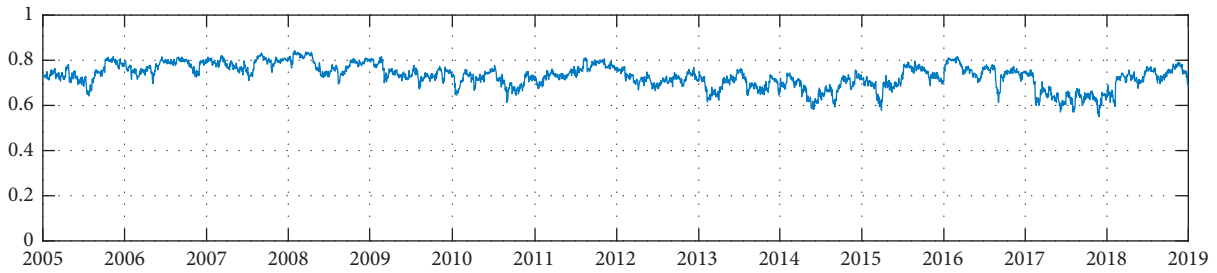

(b)

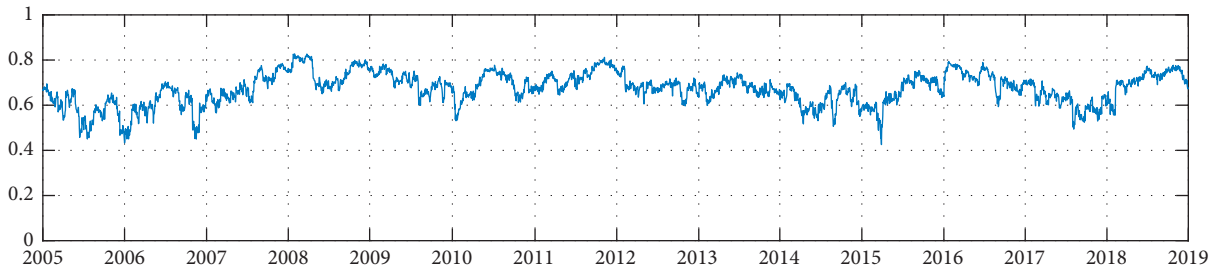

(c)

Figure 16: Kendall's tau series of the bivariate DCC-NCCN copula model. (a) HSI-CEI. (b) HSI-CCI. (c) CEI-CCI.

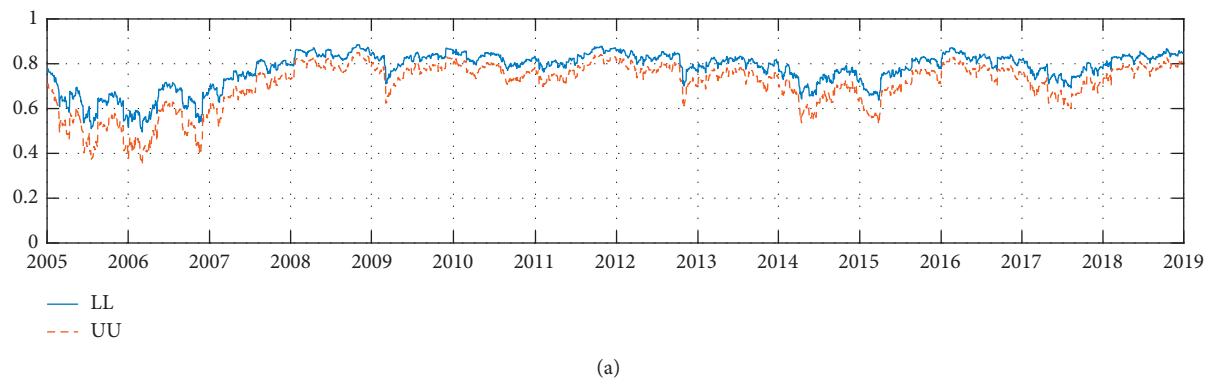

(a)

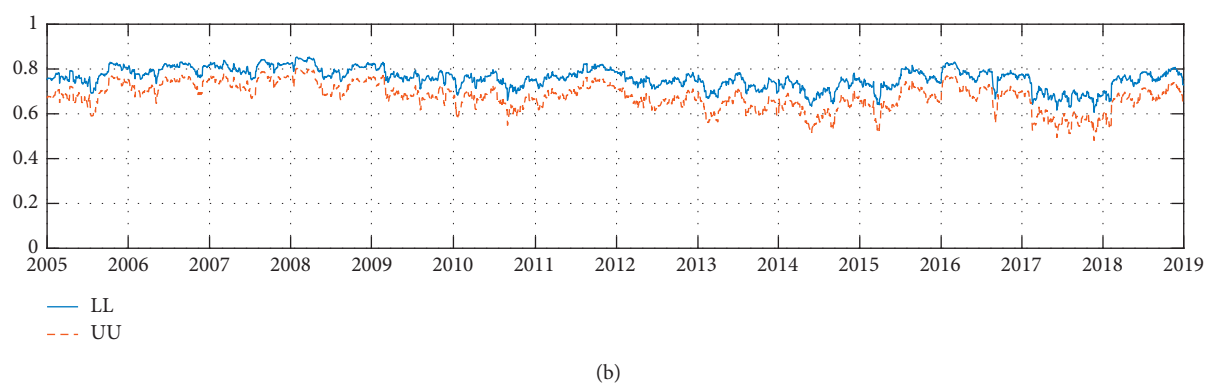

(b)

Figure 17: Continued.

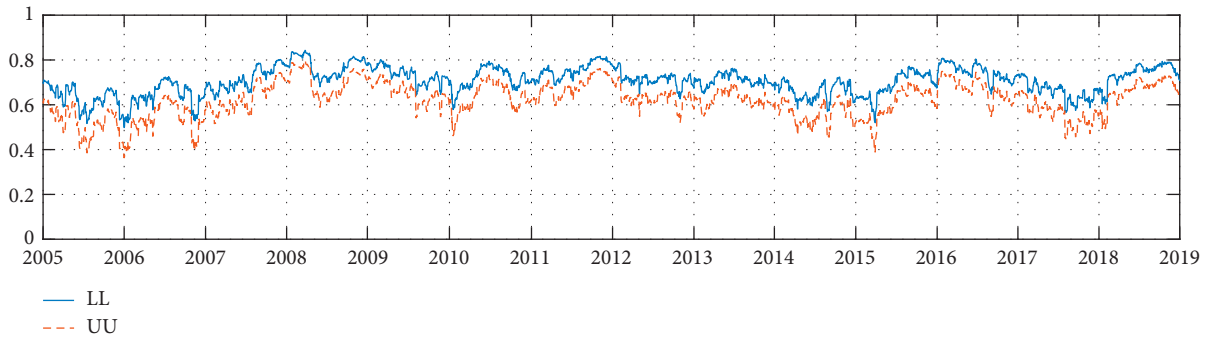

(c)

Figure 17: 10% QD coefficient series of the bivariate DCC-NCCN copula model. (a) HSI-CEI. (b) HSI-CCI. (c) CEI-CCI.

Table 10: Fitting results of multivariate copula models (HSI-CEI-CCI).

Copula model	α	β	a	p	γ	ΔP	ΔLL	LL	AIC	BIC
CCC-N						0	0	6	6	6
CCC-CN			0.5206	0.3727		2	152.02	5	5	5
CCC-NCCN			0.5139	0.3564	−1.3371	3	217.24	4	4	4
DCC-N	0.0310	0.9936				2	485.46	3	3	3
DCC-CN	0.0315	0.9943	0.5892	0.4450		4	546.89	2	2	2
DCC-NCCN	0.0314	0.9938	0.6669	0.3115	−2.0710	5	601.18	1	1	1

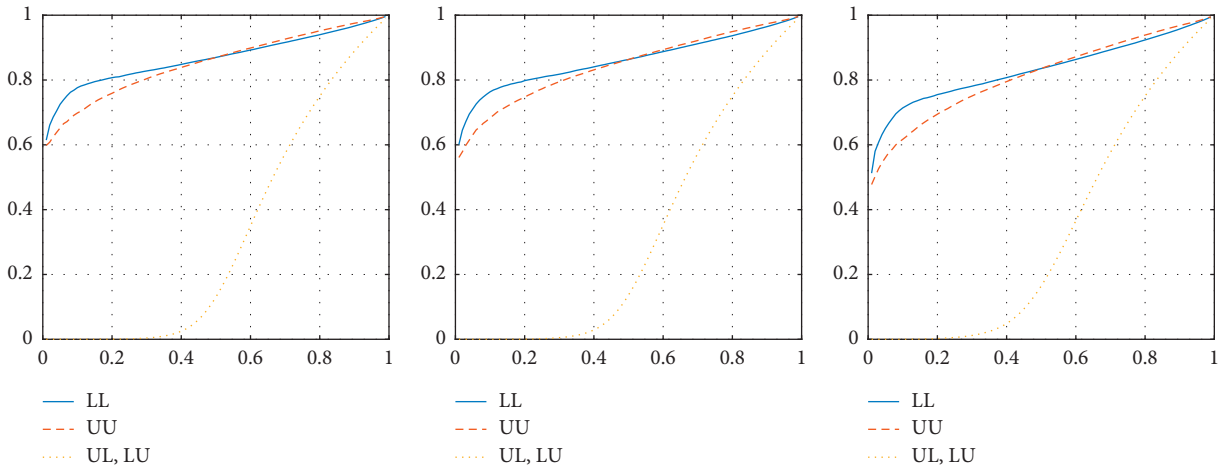

(a) (b) (c)

Figure 18: QD curves of multivariate CCC-NCCN copula model. (a) HSI-CEI. (b) HSI-CCI. (c) CEI-CCI.

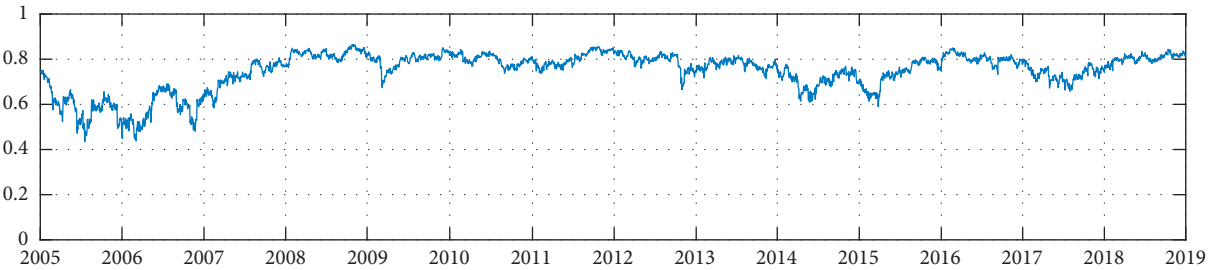

(a)

Figure 19: Continued.

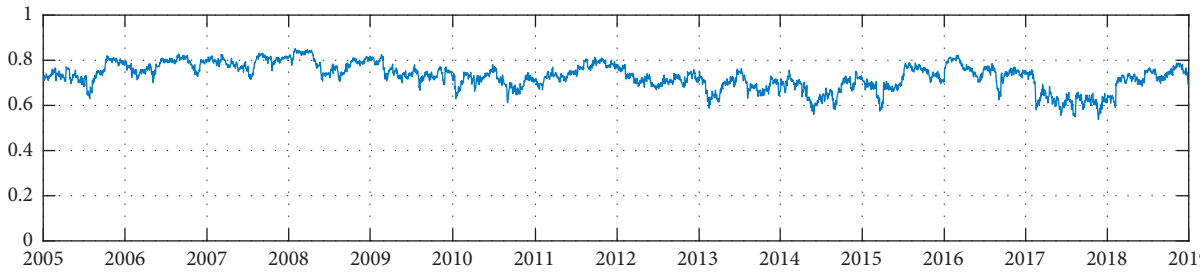

(b)

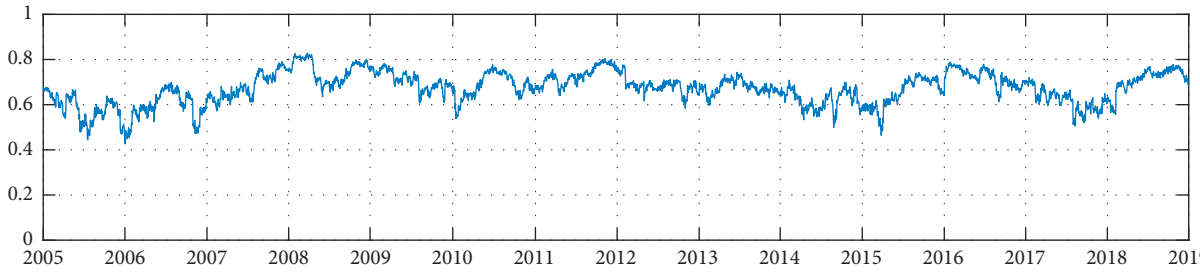

(c)

Figure 19: Kendall's tau series of the multivariate DCC-NCCN copula model. (a) HSI-CEI. (b) HSI-CCI. (c) CEI-CCI.

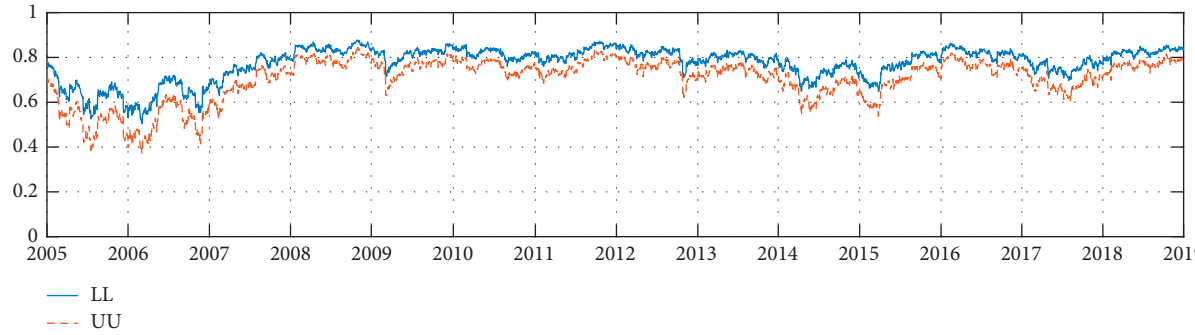

(a)

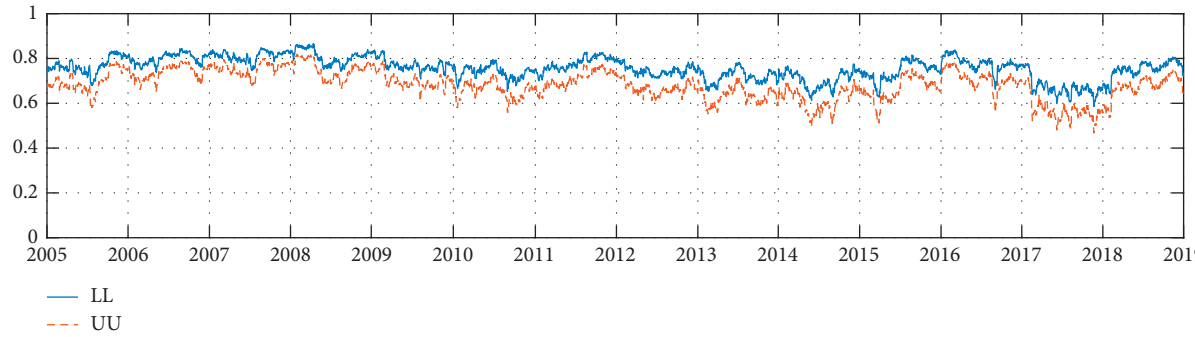

(b)

Figure 20: Continued.

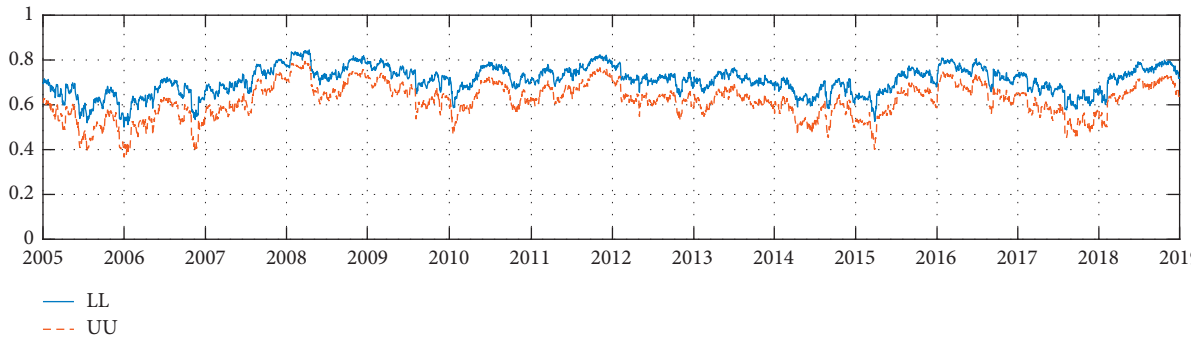

(c)

Figure 20: 10% QD coefficient series of the multivariate DCC-NCCN copula model. (a) HSI-CEI. (b) HSI-CCI. (c) CEI-CCI.

DCC-NCCN copula models, the effects of the multivariate CCC-NCCN copula and DCC-NCCN copula models have no significant differences.

4. Conclusion

This study examines the effects of the DCC-NCCN copula model and some other copula models on fitting dependence structures of Hong Kong stock markets. The main conclusions in this paper are as follows:

First, according to descriptive statistics and fitting results of the marginal distribution, return series of HSI, CEI, and CCI all reveal significant time-varying volatility. NAGARCH model can well depict the dynamic characteristics of returns.

Second, descriptive statistics and fitting results show that the bivariate dependence structures have strong positive dependence, asymmetric dependence, tail dependence, and time-varying dependence. For each bivariate dependence structure, the lower tail dependence is higher than the upper tail dependence.

Third, through the comparison of the DCC-NCCN copula model and some other copula models, the DCC-NCCN copula model can well describe the bivariate dependence structures, but other copula models are not good. Considering the flexibility and complexity, the DCC-NCCN copula model is a relatively ideal copula model.

Data Availability

The data used to support the findings of this study are public and available on HK stock exchange or database.

Conflicts of Interest

The authors declare that there are no conflicts of interest regarding the publication of this study.

Acknowledgments

This research was supported by the Key Program of National Social Science Foundation of China under Grant 18AGL001.

References

[1] Z. Wei, S. Kim, and D. Kim, "Multivariate skew normal copula for non-exchangeable dependence," *Procedia Computer Science*, vol. 91, pp. 141–150, 2016.

[2] A. Azzalini and A. D. Valle, "The multivariate skew-normal distribution," *Biometrika*, vol. 83, no. 4, pp. 715–726, 1996.

[3] S. Demarta and A. J. McNeil, "The *t* copula and related copulas," *International Statistical Review*, vol. 73, no. 1, pp. 111–129, 2005.

[4] O. E. Barndorff-Nielsen, "Exponentially decreasing distributions for the logarithm of particle size," *Proceedings of the Royal Society of London*, vol. 353, no. 1674, pp. 401–419, 1977.

[5] T. Kollo and G. Pettere, "Parameter estimation and application of the multivariate skew *t*-copula," in *Copula Theory and Its Applications*, pp. 289–298, Springer, Berlin, Germany, 2010.

[6] A. Azzalini and A. Capitanio, "Distributions generated by perturbation of symmetry with emphasis on a multivariate skew *t*-distribution," *Journal of the Royal Statistical Society: Series B (Statistical Methodology)*, vol. 65, no. 2, pp. 367–389, 2003.

[7] M. S. Smith, Q. Gan, and R. J. Kohn, "Modelling dependence using skew *t* copulas: bayesian inference and applications," *Journal of Applied Econometrics*, vol. 27, no. 3, pp. 500–522, 2012.

[8] S. K. Sahu, D. K. Dey, and M. D. Branco, "A new class of multivariate skew distributions with applications to Bayesian regression models," *Canadian Journal of Statistics*, vol. 31, no. 2, pp. 129–150, 2003.

[9] C.-S. Liu, M.-S. Chang, X. Wu, and C. M. Chui, "Hedges or safe havens-revisit the role of gold and USD against stock: a multivariate extended skew-*t* copula approach," *Quantitative Finance*, vol. 16, no. 11, pp. 1763–1789, 2016.

[10] R. B. Arellano-Valle and M. G. Genton, "Multivariate extended skew-*t* distributions and related families," *Metron*, vol. 68, no. 3, pp. 201–234, 2010.

[11] A. J. Patton, "Modelling asymmetric exchange rate dependence," *International Economic Review*, vol. 47, no. 2, pp. 527–556, 2006.

[12] R. Engle, "Dynamic conditional correlation: a simple class of multivariate generalized autoregressive conditional heteroskedasticity models," *Journal of Business & Economic Statistics*, vol. 20, no. 3, pp. 339–350, 2002.

[13] M. Yahya, A. Oglend, and R. E. Dahl, "Temporal and spectral dependence between crude oil and agricultural commodities:

a wavelet-based copula approach," *Energy Economics*, vol. 80, pp. 277–296, 2019.

[14] Y. K. Tse and A. K. C. Tsui, "A multivariate generalized autoregressive conditional heteroscedasticity model with time-varying correlations," *Journal of Business & Economic Statistics*, vol. 20, no. 3, pp. 351–362, 2002.

[15] L. Cappiello, R. F. Engle, and K. Sheppard, "Asymmetric dynamics in the correlations of global equity and bond returns," *Journal of Financial Econometrics*, vol. 4, no. 4, pp. 537–572, 2006.

[16] Y. Cui and Y. Feng, "Composite hedge and utility maximization for optimal futures hedging," *International Review of Economics & Finance*, vol. 68, pp. 15–32, 2020.

[17] D. Creal, S. J. Koopman, and A. Lucas, "Generalized autoregressive score models with applications," *Journal of Applied Econometrics*, vol. 28, no. 5, pp. 777–795, 2013.

[18] P. Christoffersen, V. Errunza, K. Jacobs, and H. Langlois, "Is the potential for international diversification disappearing? A dynamic copula approach," *Review of Financial Studies*, vol. 25, no. 12, pp. 3711–3751, 2012.

[19] A. Lucas, B. Schwaab, and X. Zhang, "Conditional euro area sovereign default risk," *Journal of Business & Economic Statistics*, vol. 32, no. 2, pp. 271–284, 2014.

[20] Y. Fang, L. Liu, and J. Liu, "A dynamic double asymmetric copula generalized autoregressive conditional heteroskedasticity model: application to China's and US stock market," *Journal of Applied Statistics*, vol. 42, no. 2, pp. 327–346, 2015.

[21] K. V. Mardia, "Measures of multivariate skewness and kurtosis with applications," *Biometrika*, vol. 57, no. 3, pp. 519–530, 1970.

[22] R. F. Engle and V. K. Ng, "Measuring and testing the impact of news on volatility," *The Journal of Finance*, vol. 48, no. 5, pp. 1749–1778, 1993.

[23] J. W. Tukey, "A survey of sampling from contaminated distributions," *Contributions to Probability and Statistics*, pp. 448–485, Princeton University, Princeton, NJ, USA, 1960.

[24] G. Celeux and G. Govaert, "Gaussian parsimonious clustering models," *Pattern Recognition*, vol. 28, no. 5, pp. 781–793, 1995.

[25] A. Punzo and P. D. McNicholas, "Parsimonious mixtures of multivariate contaminated normal distributions," *Biometrical Journal*, vol. 58, no. 6, pp. 1506–1537, 2016.